ERWEITERUNG DER TESTPLATTFORM ZUR CHARAKTERISIERUNG VON ALDOSTERONSYNTHASE-INHIBITOREN UNTER BESONDERER BERÜCKSICHTIGUNG VON SPEZIESUNTERSCHIEDEN

Dissertation

zur Erlangung des Grades des Doktors der Naturwissenschaften
der Naturwissenschaftlich-Technischen Fakultät III
Chemie, Pharmazie, Bio- und Werkstoffwissenschaften
der Universität des Saarlandes

von

Dipl. Biol. Christina Zimmer

Saarbrücken
2010

Tag des Kolloquiums:	19. November 2010
Dekan:	Prof. Dr. Stefan Diebels
Berichterstatter:	Prof. Dr. Rolf W. Hartmann Prof. Dr. Hans H. Maurer
Vorsitz:	Prof. Dr. Manfred J. Schmitt
Akad. Mitarbeiter:	Dr. Michael Heydel

Die vorliegende Arbeit wurde von April 2005 bis August 2009 unter Anleitung von Herrn Prof. Dr. Rolf W. Hartmann am Institut für Pharmazeutische und Medizinische Chemie der Naturwissenschaftlich-Technischen Fakultät III der Universität des Saarlandes angefertigt.

„Inmitten der Schwierigkeiten liegt die Möglichkeit.“

Albert Einstein

FÜR MEINEN MANN

UND

MEINE FAMILIE

ABSTRACT

The enzyme aldosterone synthase (CYP11B2) is an innovative target, that could improve the treatment of aldosterone-mediated disorders significantly compared to standard therapy. 3-Pyridine substituted naphthalenes were identified as potent lead compounds, which are *in vitro* highly potent CYP11B2 inhibitors with a pronounced selectivity against the highly homologous CYP11B1 enzyme. These early leads exhibit several major pharmacological drawbacks, above all undesirable hepatic CYP interactions and lacking *in vivo* activity in rats. The optimization process described in this thesis yielded more than 100 new compounds, developed in a combined ligand- and structure-based approach. Further *in vitro* test systems were established in order to identify potential candidates to investigate the *Proof of Principle* and the *Proof of Concept* in a rat model. Most of the herein described compounds are highly potent CYP11B2 inhibitors with IC_{50} values in the low nanomolar to picomolar range and an excellent selectivity against other steroidogenic CYP enzymes. The most promising compounds of the present study show an improved pharmacological profile compared to the corresponding naphthalene derivatives. Furthermore a "rat-active" compound was identified *in vitro* and evaluated for its ability to decrease plasma aldosterone levels in rats. The compound of the dihydro-1*H*-quinolin-2-one series exerts potent aldosterone-lowering effects *in vivo* using an ACTH stimulated rat model. In conclusion, after further optimization and pharmacological evaluation the current work might give rise to a drug candidate for preclinical testing.

ZUSAMMENFASSUNG

Das Enzym Aldosteronsynthase (CYP11B2) stellt ein innovatives Target dar, durch dessen Beeinflussung die Behandlung Aldosteron-abhängiger Erkrankungen, im Vergleich zur derzeit verfügbaren Therapie, deutlich verbessert werden könnte. 3-Pyridin substituierte Naphthalene konnten als potente Leitverbindungen identifiziert werden, die CYP11B2 *in vitro* effektiv inhibieren und die Aktivität des hoch homologen CYP11B1-Enzyms deutlich weniger beeinflussen. Diese Substanzen weisen jedoch unerwünschte Wechselwirkungen mit hepatischen CYP-Enzymen auf und sind nicht in der Lage die Aldosteronbiosynthese *in vivo* in der Ratte zu hemmen. In der vorliegenden Arbeit wurden mehr als 100 neuartige Hemmstoffe durch Ligand- und Struktur-basiertes Design entwickelt, synthetisiert und auf biologische Aktivität und Selektivität getestet. Darüber hinaus wurden weitere *in vitro* Testsysteme etabliert, die es erlauben potentielle Kandidaten zur Erbringung des *Proof of Principle* und des *Proof of Concept* im Rattenmodell zu identifizieren. Die meisten der hierin vorgestellten Verbindungen sind hochpotente CYP11B2-Inhibitoren mit IC_{50}-Werten im nano- bis picomolaren Bereich mit hoher Selektivität gegenüber anderen steroidogenen CYP-Enzymen. Außerdem weisen die vielversprechenden Hemmstoffe ein deutlich verbessertes pharmakologisches Gesamtprofil gegenüber den entsprechenden Naphthalenderivaten auf. Des Weiteren konnte eine „rattenaktive“ Substanz *in vitro* identifiziert und eine signifikante Absenkung der Plasma-Aldosteronspiegel *in vivo* gezeigt werden. Nach erweiterten pharmakologischen Untersuchungen und gegebenenfalls erforderlichen strukturellen Optimierungen sollen aus den vorgestellten Substanzklassen Wirkstoffkandidaten für die präklinische Prüfung hervorgehen.

LISTE DER PUBLIKATIONEN

Diese wissenschaftliche Arbeit basiert auf folgenden sieben Publikationen, auf die sich im Text durch Nennung ihrer Römischen Ziffern bezogen wird:

I **Overcoming Undesirable CYP1A2 Inhibition of Pyridylnaphthalene Type Aldosterone Synthase Inhibitors: Influence of Heteroaryl Derivatization on Potency and Selectivity**
Ralf Heim, Simon Lucas, Cornelia M. Grombein, **Christina Ries**, Katarzyna E. Schewe, Matthias Negri, Ursula Müller-Vieira, Barbara Birk and Rolf W. Hartmann
J. Med. Chem. **2008**, *51*, 5064–5074

II **Novel Aldosterone Synthase Inhibitors with Extended Carbocyclic Skeleton by a Combined Ligand-Based and Structure-Based Drug Design Approach**
Simon Lucas, Ralf Heim, Matthias Negri, Iris Antes, **Christina Ries**, Katarzyna E. Schewe, Alessandra Bisi, Silvia Gobbi and Rolf W. Hartmann
J. Med. Chem. **2008**, *51*, 6138-6149

III ***In Vivo* Active Aldosterone Synthase Inhibitors with Improved Selectivity: Lead Optimization Providing a Series of Pyridine Substituted 3,4-Dihydro-1*H*-quinolin-2-one Derivatives**
Simon Lucas, Ralf Heim, **Christina Ries**, Katarzyna E. Schewe, Barbara Birk and Rolf W. Hartmann
J. Med. Chem. **2008**, *51*, 8077-8087

IV **Fine-Tuning the Selectivity of Aldosterone Synthase Inhibitors: SAR Insights from Studies of Heteroaryl Substituted 1,2,5,6-Tetrahydropyrrolo[3,2,1-*ij*]quinolin-4-one Derivatives**
Simon Lucas, **Christina Ries**, Ralf Heim and Rolf W. Hartmann
J. Med. Chem. **2010**, manuscript finalized, for patent reasons not yet submitted

V **Selective Aldosterone Synthase Inhibitors Reduce Aldosterone Formation *in vitro* and *in vivo***
Christina Ries, Simon Lucas, Ralf Heim, Barbara Birk and Rolf W. Hartmann
J. Steroid Biochem. Mol. Biol. **2009**, *116*, 121-126

VI ***N*-(Pyridin-3-yl)benzamides as Selective Inhibitors of Human Aldosterone Synthase (CYP11B2)**

Christina Zimmer, Marieke Hafner, Michael Zender, Dominic Ammann, Rolf W. Hartmann and Carsten A. Vock

Bioorg. Med. Chem. Lett. **2010**, manuscript finalized, for patent reasons not yet submitted

VII **First Selective CYP11B1 Inhibitors for the Treatment of Cortisol-Dependent Diseases**

Ulrike E. Hille[†], **Christina Zimmer**[†], Carsten A. Vock and Rolf W. Hartmann

[†]**These authors contributed equally to this work.**

Med. Chem. Lett. **2010**, accepted

Der Verfasser dieser Dissertation war als Co-Author an der Erstellung weiterer Publikationen beteiligt, die thematisch jedoch vom Hauptinhalt der Arbeit abweichen. Diese Veröffentlichungen werden hier genannt, ihr Inhalt ist jedoch nicht Bestandteil der Diskussion.

VIII **Optimization of the First Selective Steroid-11β-hydroxylase (CYP11B1) Inhibitors for the Treatment of Cortisol-Dependent Diseases**

Ulrike E. Hille, **Christina Zimmer**, Jörg Haupenthal and Rolf W. Hartmann

Med. Chem. Lett. **2010**, manuscript finalized, for patent reasons not yet submitted

IX **Novel Highly Potent and Selective Nonsteroidal Aromatase Inhibitors: Synthesis, Biological Evaluation and Structure-Activity Relationships Investigation**

Silvia Gobbi, **Christina Zimmer**, Federica Belluti, Angela Rampa, Rolf W. Hartmann, Maurizio Recanatini and Alessandra Bisi

J. Med. Chem. **2010**, *53*, 5347-5351

X **Synthesis and Antineoplastic Activity of O-Alkylated Derivatives of 7-Hydroximinoandrost-5-ene Steroids**

Ranju Bansal, Sheetal Guleria, **Christina Ries** and Rolf W. Hartmann

Arch. Pharm. **2010**, *343*, 377-383.

XI **Synthesis of some Imidazolyl Substituted 2-Benzylidene Indanone Derivatives as Potent Aromatase Inhibitors for Breast Cancer Therapy**

Ranju Bansal, Gaurav Narang, **Christina Zimmer** and Rolf W. Hartmann

Med. Chem. Res. **2010**, submitted

XII Synthesis of Some Novel Androstanes as Potential Aromatase Inhibitors

Mange Ram Yadav, Prafulla M. Sabale, Rajani Giridhar, **Christina Zimmer** and Rolf W. Hartmann

Steroids **2010**, submitted

XIII Design, Synthesis, and Biological Evaluation of Imidazolyl Derivatives of 4,7-Disubstituted Coumarins as Selective Aromatase Inhibitors

Angela Stefanachi, Angelo D. Favia, Orazio Nicolotti, Francesco Leonetti, Saverio Cellamare, Leonardo Pisani, Marco Catto, **Christina Zimmer**, Rolf W. Hartmann and Angelo Carotti

J. Med Chem. **2010**, soon to be submitted

XIV PET-Radiopharmaka für die Differenzialdiagnose zwischen bilateraler oder unilateraler Erkrankung beim primären Hyperaldosteronismus

Dr. Stefanie Hahner, Dr. Andreas Schirbel, Prof. Bruno Allolio, **Christina Ries**, Prof. Rolf W. Hartmann

Erfindungsanmeldung der Julius-Maximilians-Universität Würzburg

XV First Selective CYP11B1 Inhibitors for the Treatment of Cushing's Syndrome and Metabolic Syndrome

Prof. Dr. Rolf W. Hartmann, Ulrike E. Hille, **Christina Zimmer**, Qingzhong Hu

Erfindgunsanmeldung der Universität des Saarlandes

CONTRIBUTION REPORT

Dem Verfasser dieser Dissertation ist es ein Anliegen seine Beteiligung an der Entstehung der Publikationen I-VII darzustellen:

I Der Verfasser hat maßgeblichen Anteil am Aufbau des Testsystems und hat die biologische Testung koordiniert. Darüber hinaus war er an der Interpretation der Hemmdaten beteiligt und hat an der Erstellung des Manuskriptes mitgewirkt. Die Synthese der Hemmstoffe **2**, **2a**–**g**, **5**, **12**, **13**, **29** and **30** wurde von Cornelia M. Grombein im Rahmen ihrer Diplomarbeit durchgeführt. Die Verbindungen **6**, **6a**–**b**, **8**, **8a** and **27** wurden von Dr. Ralf Heim synthetisiert. Die Synthese aller weiteren Hemmstoffe wurde von Dr. Simon Lucas durchgeführt.

II Der Verfasser hat maßgeblichen Anteil am Aufbau des Testsystems und hat die biologische Testung koordiniert. Darüber hinaus war er an der Interpretation der Hemmdaten beteiligt und hat an der Erstellung des Manuskriptes mitgewirkt. Die Synthese der Hemmstoffe wurde von Dr. Simon Lucas durchgeführt.

III Der Verfasser hat maßgeblichen Anteil am Aufbau des Testsystems, hat die biologische Testung koordiniert und die Plasma-Aldosteron-Spiegel der Pharmakodynamik-Studie gemessen. Darüber hinaus war er an der Interpretation der Hemmdaten beteiligt und hat an der Erstellung des Manuskriptes mitgewirkt. Die Synthese der Hemmstoffe wurde von Dr. Simon Lucas durchgeführt (mit Ausnahme von Verbindung **1**, synthetisiert von Dr. Ralf Heim).

IV Der Verfasser hat maßgeblichen Anteil am Aufbau des Testsystems und hat die biologische Testung koordiniert. Darüber hinaus war er an der Interpretation der Hemmdaten beteiligt und hat an der Erstellung des Manuskriptes mitgewirkt. Die Synthese der Hemmstoffe wurde von Dr. Simon Lucas durchgeführt.

V Der Verfasser hat den zellbasierten Ratten-CYP11B2-Enzym-Assay und den Nebennieren-Organ-Assay etabliert. Er hat die biologischen Tests durchgeführt und war maßgeblich an der Interpretation der Ergebnisse beteiligt. Die Synthese der Hemmstoffe wurde von Dr. Simon Lucas durchgeführt. Der Verfasser hat das Manuskript zu dieser Publikation geschrieben.

VI Der Verfasser hat maßgeblichen Anteil am Aufbau des Testsystems und hat die biologische Testung koordiniert. Darüber hinaus war er an der Interpretation der Hemmdaten beteiligt und hat an der Erstellung des Manuskriptes mitgewirkt. Die Synthese der Hemmstoffe **3c, d, f, i, j, l, q, r** und **u** wurde von Dr. Carsten Vock durchgeführt. Die Verbindungen **3g, h, k, m-p** und **s** wurden von Marieke Hafner, die Inhibitoren **3a, b** und **e** von Michael Zender und Verbindung **3t** von Dominic Ammann synthetisiert.

VII Der Verfasser hat maßgeblichen Anteil am Aufbau des Testsystems und hat die biologische Testung koordiniert. Darüber hinaus war er an der Interpretation der Hemmdaten beteiligt und hat an der Erstellung des Manuskriptes mitgewirkt. Die Synthese der Hemmstoffe wurde von Ulrike Hille durchgeführt.

ABKÜRZUNGSVERZEICHNIS

11β-HSD1	11β-Hydroxysteroid Dehydrogenase Typ 1
11β-HSD2	11β-Hydroxysteroid Dehydrogenase Typ 2
18-EP	18-Ethynylprogesteron
18-VDOC	18-Vinyldeoxycorticosteron
18-VP	18-Vinylprogesteron
3β-HSD	3β-Hydroxysteroid Dehydrogenase
ACE	Angiotensin Converting Enzyme
ACTH	Adrenocorticotrophes Hormon
Ang I	Angiotensin I
Ang II	Angiotensin II
AT_1	Angiotensin II-Rezeptor Typ 1
AUC	Area under the curve
cAMP	cyclisches Adenosinmonophosphat
cDNA	komplementäre Deoxyribonukleinsäure
CGS 16949A	Fadrozol (Racemat)
CHF	kongestive Herzinsuffizienz
Ci	Curie, 1 Ci = 3,7 x 10^{10} Becquerel (Anzahl radioaktiver Zerfälle pro Zeiteinheit)
CNS	Zentrales Nervensystem
CONSENSUS	Cooperative north scandinavian enalapril survival study
CRH	Corticotrophin Releasing Hormone
CYP	Cytochrome P450
CYP1A2	hepatisches CYP-Enzym, unspezifische Monooxygenase
CYP2B6	hepatisches CYP-Enzym, unspezifische Monooxygenase
CYP2C9	hepatisches CYP-Enzym, unspezifische Monooxygenase
CYP2C19	hepatisches CYP-Enzym, unspezifische Monooxygenase
CYP2D6	hepatisches CYP-Enzym, unspezifische Monooxygenase
CYP3A4	hepatisches CYP-Enzym, unspezifische Monooxygenase
CYP11A1	Cholesteroldesmolase
CYP11B1	Steroid-11β-hydroxylase
CYP11B2	Aldosteronsynthase
CYP17	17α-Hydroxylase-17,20-lyase
CYP19	Aromatase

DMEM	Dulbecco’s Modified Eagle Medium
dNTP	Deoxynukleosidtriphosphat
EnaC	Epithelialer Natriumkanal
EPHESUS	Eplerenone post-acute myocardial infarction heart failure efficacy and survival study
ER	Endoplasmatisches Retikulum
Et	Ethyl
ETO	Etomidat
FAD 286A	*R*(+)-Enantiomer von Fadrozol
FCS	Fetales Kälberserum
G418	Geneticin
GR	Glucocorticoidrezeptor
HPA	Hypothalamic-Pituitary-Adrenal
HPTLC	Hochleistungsdünnschichtchromatographie
Het	Heteroaryl
HSD	Hydroxysteroiddehydrogenase
IC_{50}	Benötigte Konzentration für 50 % Hemmung
IE	Internationale Einheit
*i*Pr	Isopropyl
kB	Kilobase
kDa	Kilodalton
KTZ	Ketoconazol
MCS	Multiple Cloning Site
Me	Methyl
MetS	Metabolisches Syndrom
MMP1	Matrixmetalloproteinase 1
MR	Mineralocorticoidrezeptor
mRNA	messenger Ribonukleinsäure
MTP	Metyrapon
μg	Mikrogramm
μM	Mikromolar
NADP	Nikotinamid Adenin Dinukleotid Phosphat
nm	Nanometer
nM	Nanomolar
PCR	Polymerase-Ketten-Reaktion
PEG	Polyethylenglykol
Ph	Phenyl

PK	Pharmakokinetik
pM	Picomolar
POC	Proof of Concept
QSAR	Quantitative Struktur-Wirkungs-Beziehungen
RAAS	Renin-Angiotensin-Aldosteron-System
RALES	Randomized aldactone evaluation study
RIA	Radioimmunoassay
RNA	Ribonukleinsäure
SAR	Struktur-Wirkungs-Beziehung
SEM	Standard error of the mean
Å	Ångström

INHALTSVERZEICHNIS

1 Einleitung

1.1 Physiologie der Mineralo- und Glucocorticoide

1.1.1 Biosynthese der Mineralo- und Glucocorticoide

Die Corticoide sind eine Gruppe von Hormonen, die sich strukturell vom Steranmolekül herleiten. Ihre Biosynthese findet in den Nebennieren statt. Diese setzen sich aus zwei funktionell und embryologisch unterschiedlichen Anteilen, dem Nebennierenmark (Medulla) und der Nebennierenrinde (Cortex), zusammen. Sie liegen retroperitoneal in unmittelbarer Beziehung zu den oberen Nierenpolen. Die rechte Nebenniere ist dreieckig, die linke halbmondförmig. Die humanen Nebennieren sind ca. 3 cm lang und 5-10 g schwer. Das Nebennierenmark gehört zum vegetativen Nervensystem und bildet die Hormone Adrenalin und Noradrenalin. Die Zellen der Nebennierenrinde sind zur *de novo*-Synthese von Steroidhormonen aus Cholesterol befähigt. Die adulte Nebennierenrinde wird unterteilt in drei radiär angeordnete Zonen, die sich funktionell wie morphologisch unterscheiden (Abbildung 1). Durch ein zonenspezifisches Expressionsmuster der Enzyme der Steroidbiosynthese ergibt sich ein funktionelles Sekretionsprofil.

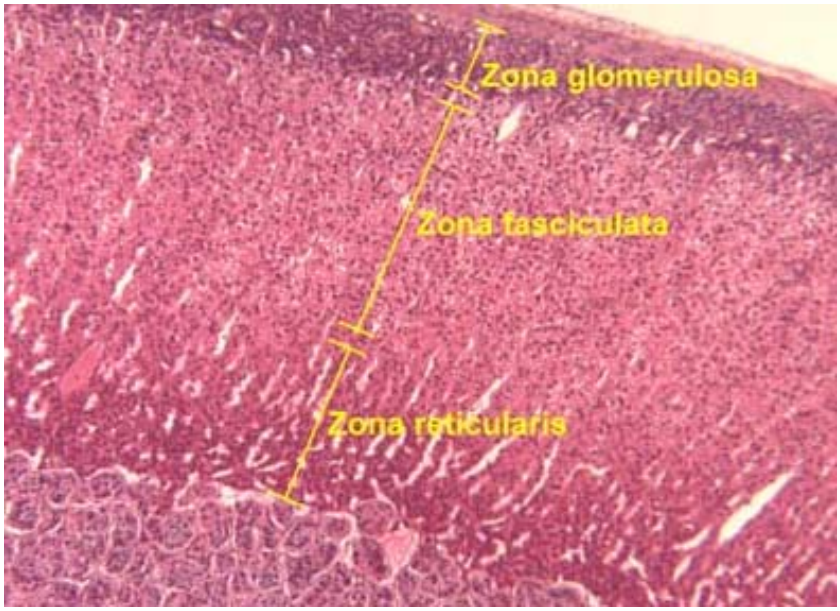

Abbildung 1: Zonierung der Nebennierenrinde [http://w3.ouhse.edu/histology]

Das physiologisch wirksamste Mineralocorticoid Aldosteron wird in den *Zona glomerulosa*-Zellen, der äußersten Schicht der Nebennierenrinde (Abbildung 1), gebildet. Seine Funktion besteht in der Regulation des Elektrolyt- und Wasserhaushaltes, indem es hauptsächlich die Retention von Natriumionen (Na^+) und Wasser bewirkt und gleichzeitig die Ausscheidung von Kaliumionen (K^+) fördert. Somit ist es maßgeblich an der Regulation des Blutvolumens und folglich des Blutdrucks beteiligt. Der initiale Schritt der Aldosteronbiosynthese ist die Umwandlung von Cholesterol zu Pregnenolon, katalysiert durch die Cholesteroldesmolase CYP11A1 (Cholesterol side chain cleavage enzyme) an der inneren Mitochondrienmembran (Abbildung 2). Hierbei erfolgen zwei Hydroxylierungen in 20α- und 22-Position und anschließende Spaltung der Kohlenstoff-Kohlenstoff-Bindung zwischen C_{20} und C_{22}.[1] Im Folgenden wird Pregnenolon in Position 3 oxidiert mit anschließender Isomerisierung der Doppelbindung an C_5, es entsteht Progesteron. Diese Reaktion wird katalysiert durch das Enzym 3β-Hydroxysteroiddehydrogenase (3β-HSD, lokalisiert im Endoplasmatischen Retikulum). Durch Hydroxylierung in Position 21, vermittelt durch CYP21, wird Deoxycorticosteron gebildet, welches bereits mineralocorticoide Wirkung besitzt und das Substrat für das Schlüsselenzym der Aldosteronbiosynthese, das Cytochrom P450-Enzym CYP11B2 (Aldosteronsynthase) darstellt. Durch drei Oxidationsreaktionen in 11β- und 18-Position wird Aldosteron über die Zwischenstufen Corticosteron und 18-Hydroxycorticosteron synthetisiert.[2]

Die Glucocorticoide werden in der mittleren Schicht der Nebennierenrinde von den *Zona fasciculata*-Zellen gebildet. Mit Cortisol als wichtigstem Vertreter fördern sie die Gluconeogenese und hemmen gleichzeitig den Glucosetransport und die Glucoseverwertung. Somit wirken sie regulierend auf den Blutzuckerspiegel. Darüber hinaus zeigen Glucocorticoide antiinflammatorische und immunmodulatorische Wirkungen, sowie zahlreiche permissive Effekte. Die Cortisolbiosynthese geht ebenfalls vom Cholesterol aus. In den *Zona fasciculata*-Zellen wird im Gegensatz zu den *Zona glomerulosa*-Zellen das Enzym 17α-Hydroxylase-C17,20-Lyase (CYP17) exprimiert, das eine Hydroxylierung des Pregnenolons in Position 17 katalysiert. Es entsteht 17-Hydroxypregnenolon. Dieses wird durch 3β-HSD zu 17-Hydroxyprogesteron umgewandelt und schließlich von CYP21 zu Deoxycortisol umgesetzt. Hierbei handelt es sich um das Substrat der Steroid-11β-hydroxylase (CYP11B1), dem Schlüsselenzym der Cortisolbiosynthese. Es bildet durch einfache Oxidation in 11β-Position Cortisol aus Deoxycortisol. Im Gegensatz zur Aldosteronsynthase (CYP11B2) besitzt es nicht die Fähigkeit zur Oxidation in 18-Position.

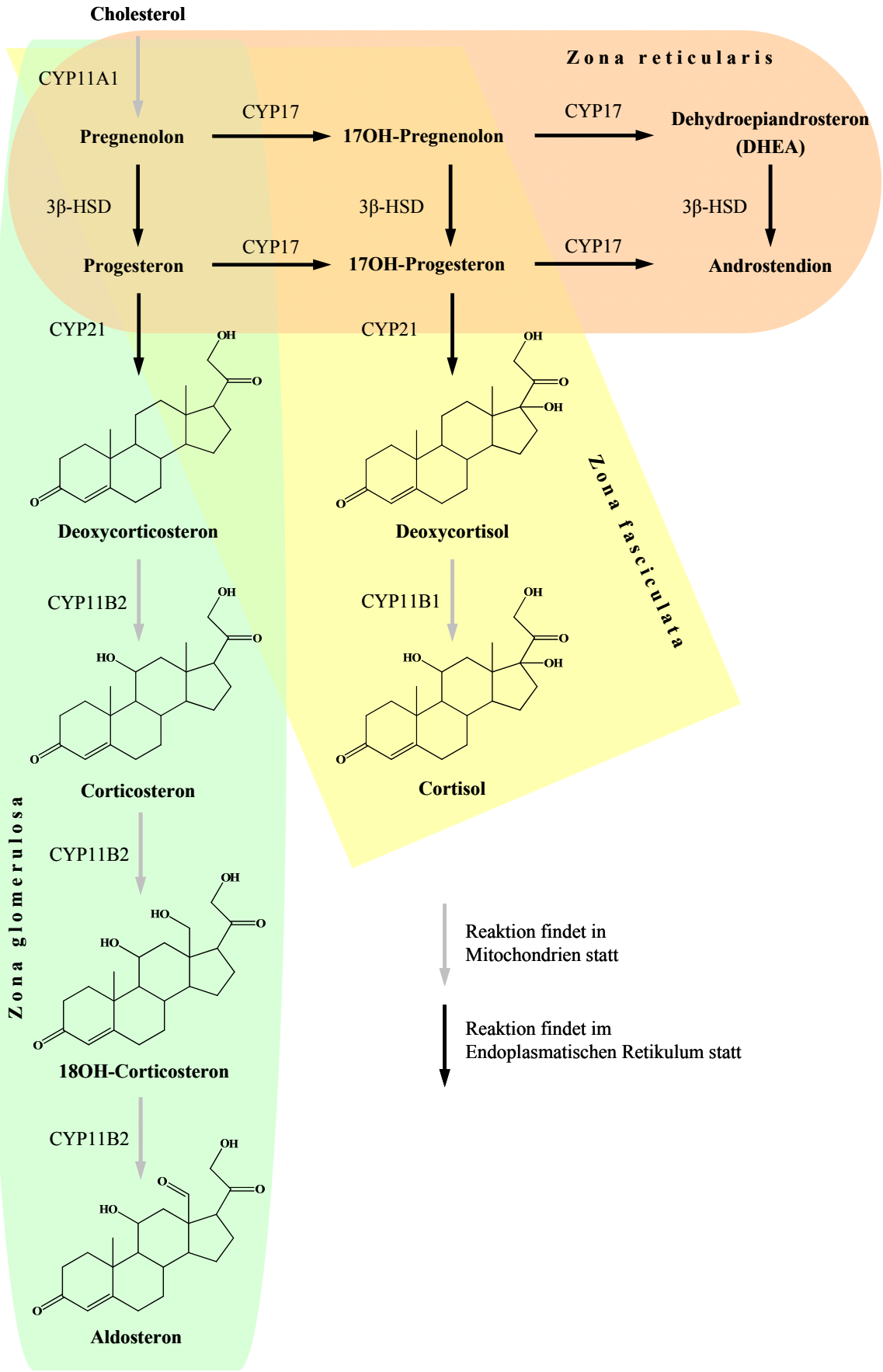

Abbildung 2: Biosynthese der Mineralo- und Glucocorticoide in der Nebennierenrinde

1.1.2 Regulation und physiologische Wirkung der Mineralocorticoide

Die Sekretion von Aldosteron untersteht der Kontrolle diverser Regulationsmechanismen. Von großer Bedeutung ist hierbei das Renin-Angiotensin-Aldosteron-System (RAAS)[3], das in entscheidender Weise an der Konstanterhaltung bzw. Normalisierung des Blutdrucks beteiligt ist. Es reguliert die Aldosteronausschüttung über einen Feedback-Mechanismus. Bei Natriummangel im Blut oder unzureichender Nierenperfusion durch Volumen- oder Druckverminderung wird im juxtaglomerulären Apparat der Niere vermehrt Renin freigesetzt (Abbildung 3). Dieses proteolytische Enzym initiiert eine Reaktionskaskade, indem es im Blut das in der Leber gebildete α_2-Globulin Angiotensinogen in das biologisch unwirksame Dekapeptid Angiotensin I spaltet, welches durch das Angiotensin-Converting-Enzyme (ACE) in das vasopressiv wirksame Oktapeptid Angiotensin II umgewandelt wird. ACE ist eine Dipeptidylcarboxypeptidase, die hauptsächlich in der Lunge gebildet wird. Angiotensin II bindet an seinen membranständigen Rezeptor (Angiotensin II-Rezeptor Typ 1) der *Zona glomerulosa*-Zellen und führt zur Synthese und Sekretion von Aldosteron aus der Nebennierenrinde.

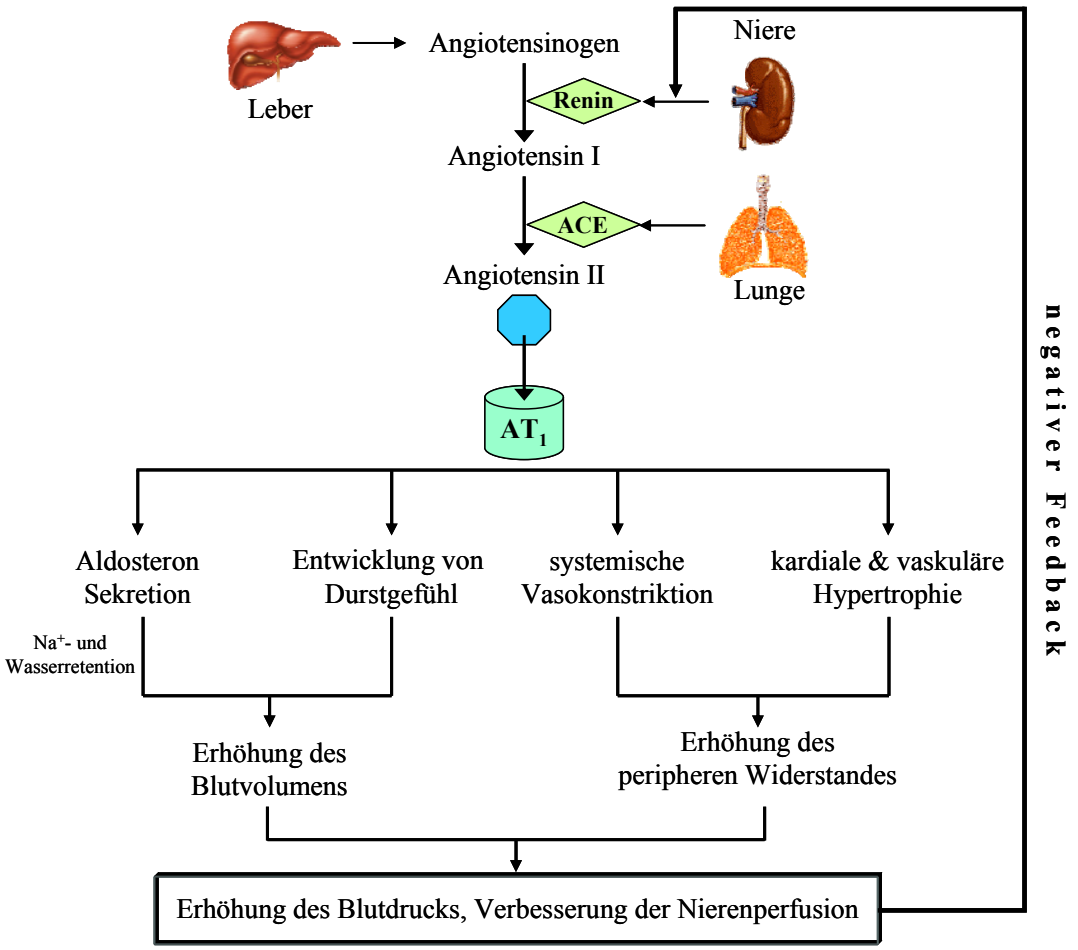

Abbildung 3: Schematische Darstellung des Renin-Angiotensin-Aldosteron-Systems (RAAS)

Zusätzlich hat Angiotensin II starke vasokonstriktorische Wirkung und erhöht systemisch den peripheren Widerstand. Des Weiteren bewirkt es im Hypothalamus die Bildung von Vasopressin, das neben seiner vasopressorischen auch antidiuretische Wirkung zeigt und infolgedessen auch antidiuretisches Hormon (ADH) genannt wird. Dieser Effekt kommt durch eine Erhöhung der Anzahl an Wasserkanal-Molekülen (Aquaporine) in den Epithelzellen der Sammelrohre zustande. Somit wird die Wasserrückresorption an den Sammelrohrepithelien verstärkt. Darüber hinaus löst Angiotensin II im Gehirn ein Durstgefühl aus, sodass es durch gesteigerte Flüssigkeitsaufnahme zu einer Erhöhung des Blutvolumens kommt. Die gesteigerte Natrium- und Wasserretention führt zu einer Expansion des extrazellulären Volumens. Alle diese Mechanismen führen zu einer Erhöhung des Blutdrucks, was unmittelbar durch Barorezeptoren in der Niere registriert wird und die Ausschüttung von Renin in einem negativen Feedbackmechanismus unterbindet (Abbildung 3). Die normalisierten Kalium- und Natriumkonzentrationen wirken ebenfalls regulierend auf die Aldosteronbiosynthese. So beeinflusst Natrium offenbar die Affinität und Anzahl der auf den *Zona glomerulosa*-Zellen lokalisierten Angiotensin II-Rezeptoren. Angiotensin II ist der stärkste bekannte biologische Stimulator der adrenalen Aldosteronbiosynthese. Des Weiteren wird diese durch die extrazelluläre K^+-Konzentration und das Adrenocorticotrope Hormon (ACTH) reguliert. Bereits geringe Schwankungen der Kalium-Konzentrationen führen zu einer Steigerung oder Hemmung der Aldosteronbiosynthese. Hyperkaliämie führt zu einer direkten Stimulation der *Zona glomerulosa*-Zellen, während bei einer Hypokaliämie die Aldosteronbildung reduziert wird. ACTH ist der Hauptregulator der Glucocorticoidbiosynthese (s. u.) und führt zu einer akuten und kurzfristigen Stimulation der Aldosteronsekretion. Bei chronischem ACTH-Überschuss nähern sich die Aldosteron-Plasmakonzentrationen wieder den Normwerten an.

Aldosteron ist das finale endokrine Signal im RAAS. Nach Bindung an den Mineralocorticoid-Rezeptor (MR) löst der Steroid-Rezeptor-Komplex in seinen Zielzellen als Transkriptionsfaktor die Expression verschiedener Proteine aus. Beim MR handelt es sich um einen zytosolischen Steroidrezeptor, der in den Epithelien verschiedener Gewebe vorkommt. Eine besonders hohe Anzahl von Aldosteronrezeptoren findet sich in den proximalen und distalen Abschnitten der Nierentubuli und in den Sammelrohren. Durch deren Aktivierung kommt es zur verstärkten Expression eines epithelialen apikalen Natriumkanalproteins (ENaC)[4] sowie einer basolateralen Na^+/K^+-ATPase.[5] Diese Strukturen dienen den Natriumionen als Transportwege vom Tubuluslumen in die Blutkapillaren (Abbildung 4). Die Erhöhung der Anzahl von Natriumkanälen führt zu einer gesteigerten Rückresorption von Na^+-Ionen. Dieser Vorgang erfolgt passiv durch die höhere Konzentration der Natriumionen im Urin im Verhältnis zum Zellinneren. Verantwortlich dafür ist die Natrium-Kalium-Pumpe, die unter Verwendung von ATP, Natriumionen aus der Zelle hinaus und Kaliumionen in die Zelle hinein pumpt. Gleichzeitig zur Natriumretention kommt es aus osmotischen Gründen zu einer verstärkten Wasserretention und zu einer passiven Rückresorption von Cl^--Ionen. Da die Kaliumkonzentration in der Zelle relativ zum Urin erhöht ist, strömen die Kaliumionen durch Kanäle

in den Urin. Begleitet wird dieser Vorgang von einer erhöhten Ausscheidung von Wasserstoff- und Ammoniumionen.

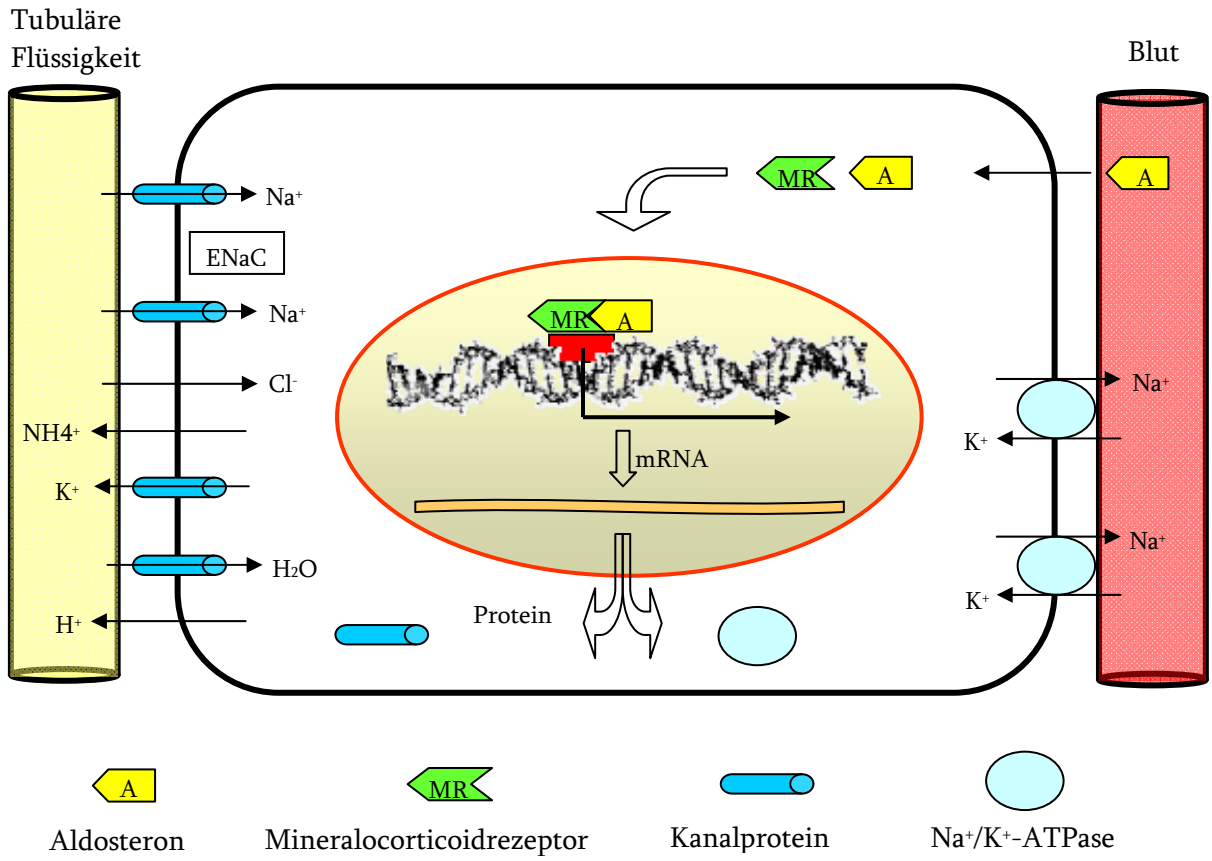

Abbildung 4: Molekularer Mechanismus der Aldosteronwirkung

Die „klassischen" Aldosteronzielzellen sind die Epithelien von Niere, Darm, Schweiß- und Speicheldrüsen. Es konnten jedoch weitere nichtepitheliale Gewebe des ZNS[6] und des kardiovaskulären Systems[7] als aldosteronsensitiv identifiziert werden. Für diese Gewebe wird darüber hinaus eine lokale, extra-adrenale Aldosteronbiosynthese kontrovers diskutiert. Silvestre *et al.* konnten in Rattenherzgewebe CYP11B2-mRNA nachweisen.[8] Sowohl in Homogenat als auch im Perfusat von Rattenherzen konnte Aldosteron in 17-fach höherer Konzentration als im Plasma gemessen werden.[9] Im Gegensatz dazu konnte die Gruppe um Ye *et al.* die CYP11B2-Expression im Rattenherz nicht bestätigen.[10] In einer anderen Studie konnte gezeigt werden, dass Herzgewebe die Fähigkeit besitzt aus der Zirkulation stammendes Aldosteron zu akkumulieren. Nach Adrenalektomie der Ratten sanken sowohl die kardialen als auch die Plasmaaldosteronlevel um 99,5 %,[11] was darauf schließen lässt, dass scheinbar kardial gebildetes Aldosteron doch aus der Nebenniere stammt und über die Zirkulation zum Herz gelangt.[12]

Über 50 Jahre nach der Entdeckung und Charakterisierung von Aldosteron durch Tait *et al.*[13] ist seine MR-vermittelte Wirkung weitestgehend aufgeklärt. Durch Bindung des Aldosterons an seinen Rezeptor kann nach einer gewissen Latenzzeit von 30 bis 60 min, wie oben beschrieben, die Expression verschiedener Proteine nachgewiesen werden. Durch Inhibitoren von Transkription oder Translation, Hemmstoffe der Steroidrezeptor-Translokation und MR-Antagonisten können diese genomischen Effekte gehemmt werden. In neueren Studien konnte gezeigt werden, dass es weitere, schnell eintretende (< 15 min) Aldosteronwirkungen gibt, die nicht durch Inhibitoren der Transkription (Actinomycin D) oder der Proteinsynthese (Cycloheximid) unterdrückt werden können und somit unabhängig von Gentranskription und Translation sind.[14] Diese Effekte wurden erstmals in Erythrozyten beobachtet. Aufgrund des fehlenden Zellkerns kann es sich hierbei nicht um genomische Effekte handeln.[15] Nicht genomische Aldosteronwirkungen konnten sowohl in Epithelzellen als auch in nicht epithelialem Gewebe nachgewiesen werden. Bei Untersuchungen an kultivierten Hautzellen einer MR-knockout-Maus konnte durch Zugabe von 10 nM Aldosteron innerhalb weniger Minuten ein starker Anstieg der intrazellulären Ca^{2+}- und cAMP-Konzentrationen beobachtet werden.[16] In humanen mononukleären Leukozyten führt eine Aldosteronexposition zu einem schnellen Anstieg der intrazellulären Na^{+}-, K^{+}- und Ca^{2+}-Level, die mit einer Vergrößerung des Zellvolumens einhergehen.[17] Darüber hinaus wurde in weiteren Studien die Aktivierung eines Na^{+}/H^{+}-Antiporters nachgewiesen, was zu einer schnellen Aldosteron-induzierten pH-Wert-Änderung in Zellen arterieller Blutgefäße und des distalen Tubulus führt.[18] Da diese Aldosteronwirkungen nicht durch MR-Antagonisten inhibiert werden können,[19] liegt die Vermutung nahe, dass diese Effekte über einen anderen Rezeptor vermittelt werden. In diesem Zusammenhang konnte durch cross-linking-Experimente ein 50 kDa großes Membranprotein gefunden werden, das eine hohe Affinität zu Aldosteron, nicht aber zu Cortisol aufweist.[20] Seine Struktur und Funktion konnten bisher aber nicht vollständig aufgeklärt werden.

1.1.3 Regulation und physiologische Wirkung der Glucocorticoide

Die Glucocorticoidsekretion wird über das hypothalamisch-hypophysäre-System reguliert. Nimmt die freie Cortisolkonzentration im Blut ab, wird im Hypothalamus das Corticotropin Releasing Hormon (CRH) ausgeschüttet, das in der Hypophyse eine Freisetzung des Adrenocorticotropen Hormons (ACTH) bewirkt (Abbildung 5). Durch Wechselwirkung von ACTH mit seinen Zellmembranrezeptoren auf den *Zona fasciculata*-Zellen der Nebennierenrinde stimuliert es die Biosynthese und Sekretion von Cortisol (siehe Abschnitt 1.1), welches dann, ähnlich wie beim RAAS durch einen negativen Feedbackmechanismus, die weitere CRH- und ACTH-Bildung steuert. Seine physiologische Wirkung erzielt Cortisol durch Bindung an den Glucocorticoidrezeptor (GR) im Zytosol seiner Zielzellen. Es kommt zur Translokation des Steroid-Rezeptor-Komplexes in den Zellkern, wo er als Transkriptionsfaktor die Transkription verschiedener Gene auslöst. Während der Mineralocorticoidrezeptor nur in bestimmten Geweben vorkommt, zeigt der Glucocorticoidrezeptor ubiquitäre Präsenz in praktisch allen Zellen des Organismus. Dies erklärt die vielfältigen Wirkungen

von Cortisol. Synergistisch mit Glukagon und den Katecholaminen wirkt es als Gegenspieler des Insulins bei der Regulation des Glukoseplasmaspiegels. Das Glucocorticoid fördert die Glukoneogenese und die Glykogenbildung in der Leber bei gleichzeitiger Hemmung der Glukoseaufnahme im peripheren Gewebe, was zu einer Erhöhung des Blutzuckerspiegels führt. Dies erfolgt unter anderem durch eine Induktion der Phosphoenolpyruvat-Carboxykinase und einer vermehrten Bereitstellung von Substraten für die Glukoneogenese aus peripheren Geweben. Des Weiteren zeigt Cortisol antiinflammatorische und immunmodulatorische Wirkungen, indem es die Funktion immunokompetenter Zellen hemmt und zu einer Verringerung der Zytokinbildung führt. Außerdem beeinflusst es die Bewegung von Leukozyten in entzündliche Gewebe.

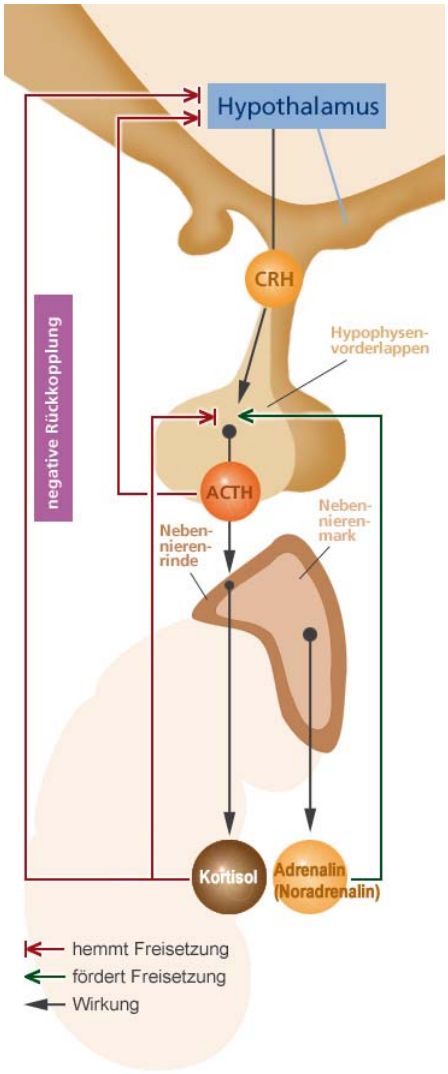

Abbildung 5: Regulation der Glucocorticoid-Freisetzung über die Hypothalamus-Hypophysen-Nebennierenrinden-Achse

[http://www.internisten-im-netz.de/media/orig/iin/grafiken/regulation-der-kortisolfreisetzung.jpg]

Cortisol bindet bemerkenswerter Weise mit einer ähnlich hohen Affinität an den Mineralocorticoidrezeptor wie Aldosteron. Dabei ist die Affinität des Glucocorticoids zum MR sogar höher als die zum eigenen Rezeptormolekül.[21] Um eine unspezifische Aktivierung des MR durch Cortisol, das im Vergleich zu Aldosteron in einem 100-1000fachen Überschuss vorliegt, zu verhindern wird in den aldosteronsensitiven Geweben ein weiteres Enzym coexprimiert.[22] Es handelt sich hierbei um die 11β-Hydroxysteroiddehydrogenase Typ 2 (11β-HSD2), eine NAD^+-abhängige Short-Chain-Dehydrogenase, die Cortisol in Position 11 zu Cortison oxidiert, welches aufgrund der Ketogruppe keine Affinität zum MR aufweist. Aldosteron liegt unter physiologischen Bedingungen als Halbacetal vor und kann daher nicht von 11β-HSD2 umgesetzt werden. Im Gegensatz dazu agiert das Isoenzym 1 der 11β-HSD NADPH-abhängig als Reduktase und regeneriert in glucocorticoidempfindlichen Geweben Cortisol aus inaktivem Cortison. Liegt ein krankheitsbedingter Mangel an 11β-Hydroxysteroiddehydrogenase Typ 2 vor, wird der Mineralocorticoidrezeptor von Cortisol gleichsam überschwemmt und es kommt zu dem Syndrom des scheinbaren Mineralocorticoidüberschusses mit schwerem Bluthochdruck, Hypokaliämie und Alkalose, sekundär gefolgt von Arrhythmien.[23]

1.1.4 Aldosteronsynthase (CYP11B2) und Steroid-11β-hydroxylase (CYP11B1), die Schlüsselenzyme der Corticoidbiosynthese

Die funktionelle Zonierung der Nebennierenrinde beruht unter anderem auf der Zonen-spezifischen Expression der beiden Isoenzyme Aldosteronsynthase (CYP11B2) und Steroid-11β-hydroxylase (CYP11B1), die jeweils die finalen Schritte der Aldosteron- bzw. Cortisolbiosynthese katalysieren (Abbildung 2). Die Notwendigkeit dieser Kompartimentierung wird klar, wenn man bedenkt, dass die zur Elektrolyt- und Wasserhomöostase benötigte Aldosteronkonzentration 100-1000mal niedriger ist als die Cortisolkonzentration, die zur Ausübung seiner physiologischen Wirkungen notwendig ist. Die Konzentrationen, der in der anteilsmäßig viel größeren *Zona fasciculata* synthetisierten Aldosteronvorstufen würden zu einem Mineralocorticoid-Exzess führen, würden sie weiter zu Aldosteron umgesetzt.

Die Schlüsselenzyme der Mineralo- und Glucocorticoidbiosynthese CYP11B2 und CYP11B1 zeigen eine sehr hohe strukturelle Identität und weisen eine große funktionelle Ähnlichkeit auf (siehe Abschnitt 1.1). Die für CYP11B2 und CYP11B1 kodierenden humanen Gene sind auf Chromosom 8q21-22 lokalisiert[24], etwa 45 kb voneinander entfernt.[25] Beide Enzyme bestehen aus 503 Aminosäuren einschließlich einer 24 Aminosäuren langen N-terminalen Signalsequenz, die nach Translokation der Proteine in die innere Mitochondrienmembran abgespalten wird. Die kodierenden DNA-Sequenzen beider Gene zeigen eine Identität von 95 %.[26] Die resultierenden Proteine unterscheiden sich lediglich in 34 der 503 Aminosäuren und weisen eine Proteinsequenz-Identität von 93% auf.[27] Die beiden humanen Enzyme CYP11B2 und CYP11B1 stehen evolutionär enger zueinander als zu den Corticoid-bildenden Enzymen anderer Spezies. Bei Rind, Schwein, Schaf und

Ochsenfrosch werden sowohl die Oxidation in 11β-Position als auch die beiden Oxidationsschritte in 18-Position des Sterangerüstes von nur einem Enzym (CYP11B) katalysiert.[28] Die Proteinsequenz-Identität zwischen humanem CYP11B2 bzw. CYP11B1 und dem CYP11B-Enzym von Rind, Schwein oder Schaf beträgt jeweils ca. 75 %.[29] Andere Spezies wie Ratte, Maus, Hamster, Meerschweinchen, Kaninchen oder Hund besitzen wie der Mensch zwei Enzyme für die Corticoidsynthese. Jedoch sind Ratten, Mäuse und Kaninchen aufgrund fehlender 17α-Hydroxylase-Aktivität in der Nebennierenrinde nicht in der Lage Cortisol zu produzieren. In diesen Nagerspezies stellt Corticosteron das wirksamste Glucocorticoid dar, das in den *Zona fasciculata*-Zellen durch CYP11B1 aus Deoxycorticosteron gebildet wird. Die Proteinsequenz-Identitäten und -Homologien zwischen den humanen corticoidproduzierenden Enzymen und den entsprechenden Enzymen einiger Nager sind sehr ähnlich und in Tabelle 1 dargestellt. Hierbei kann festgestellt werden, dass sowohl die Sequenz-Identitäten als auch die -Homologien zwischen den CYP11B2-Enzymen stets größer sind als zwischen den CYP11B1-Enzymen.

Tabelle 1: Proteinsequenz-Identitäten und -Homologien zwischen den humanen und verschiedenen Nager-CYP11B2 bzw. -CYP11B1-Enzymen

	CYP11B2 human-Nager		**CYP11B1 human-Nager**	
	Proteinsequenz-Identität	Proteinsequenz-Homologie	Proteinsequenz-Identität	Proteinsequenz-Homologie
Maus	68%	82%	63%	78%
Ratte	69%	83%	63%	79%
Hamster	69%	83%	61%	78%
Meerschweinchen	71%	84%	63%	76%

1.2 Aldosteronsynthase als potentielles Drug Target

1.2.1 Pathophysiologie von Aldosteron

Aldosteron erfüllt als Hauptmineralocorticoid wie oben beschrieben wichtige Funktionen in der Regulation der Elektrolyt- und Wasserhomöostase und ist entscheidend an der Blutdruckregulation beteiligt. Aldosteronkonzentrationen, die physiologische Level weit übersteigen, können jedoch für die Entstehung und Progression diverser Erkrankungen verantwortlich gemacht werden. Die pathologisch erhöhte Aldosteronbildung, verursacht durch eine strukturelle Veränderung der Nebenniere wird als Primärer (adrenaler) Hyperaldosteronismus bezeichnet. Dieses Syndrom wurde erstmals 1956 von Jerome Conn beschrieben, der von einem Patienten mit unbehandelbarem Bluthochdruck und Hypokaliämie berichtete.[30] Dieses Krankheitsbild konnte auf ein unilaterales aldosteronproduzierendes Nebennieren-Adenom zurückgeführt werden, welches die häufigste Ursache

(70-80 %) des Primären Hyperaldosteronismus darstellt. Bei 20-30 % der Patienten ist eine bilaterale Hyperplasie der Nebennierenrinde verantwortlich, eher selten ist ein Nebennierenrinden-Karzinom. Kommt es aufgrund einer Dysfunktion des regulierenden RAAS in Folge einer primären Erkrankung zu einer verstärkten Aldosteronbildung spricht man von Sekundärem (extraadrenalem) Hyperaldosteronismus. Eine mögliche Ursache hierfür sind deutlich erhöhte Plasma-Renin-Konzentrationen, die die Nebennierenrinde zu einer exzessiven Aldosteronbildung stimulieren. Bei Erkrankungen wie einer Leberzirrhose, Herzinsuffizienz, dem nephrotischen Syndrom oder einer Nierenarterienstenose kann die ursprünglich homöostatische Funktion des RAAS zu einer pathophysiologischen Form konvertieren. Bei einer bestehenden Herzinsuffizienz, z. B. in Folge eines Myokardinfarktes, einer primären Herzmuskelschwäche oder einer langjährigen Hypertonie, nimmt das Herzzeitvolumen ab, was zu einer Minderperfusion der Organe führt. Die unzureichende Durchblutung wird in der Niere registriert und durch Ausschüttung von Renin werden Gegenmaßnahmen zur Erhöhung des Blutdrucks und somit zur Verbesserung der Durchblutung eingeleitet. Das so aktivierte RAAS (Abbildung 3) verursacht eine verstärkte Wasserretention, um den Blutdruck trotz schwacher Herzleistung aufrecht zu erhalten. Es kommt zu einer progredienten Volumenüberladung des insuffizienten Herzens, das schon primär nicht in der Lage ist, das angebotene Blutvolumen mit einem adäquaten Schlagvolumen zu bewältigen. Des Weiteren konnte gezeigt werden, dass erhöhte Aldosteronlevel stimulierend auf kardiale Fibroblasten wirken.[31] Diese synthetisieren die Strukturproteine der Kollagenmatrix, Kollagen Typ I und Typ III und produzieren das Schlüsselenzym der interstitiellen Kollagendegradation, die Matrixmetalloproteinase 1 (MMP-1). Durch verstärkte Bildung und Einlagerung von Kollagenfasern kommt es zu einer fibrotischen Strukturveränderung der extrazellulären Matrix im interstitiellen und perivaskulären Raum des Myokards. Während Aldosteron die Kollagendegradation nicht beeinflusst, senkt Angiotensin II die MMP-1-Aktivität, was die Kollagenakkumulation im Interstitium des Myokards in synergistischer Weise noch verstärkt.[32] Die so entstehende Myokardfibrose führt zu einer zunehmenden Versteifung des Herzmuskels, der sich aufgrund mangelnder Elastizität in der diastolischen Phase nicht mehr ausreichend mit Blut füllen kann. Dieser Umstand bedingt eine weitere Verschlechterung der Pumpleistung. Als Gegenreaktion nimmt das Herz an Größe zu. Diese Größenzunahme schwächt das Herz noch weiter, weil die Blutgefäße des Herzmuskels nicht im gleichen Umfang mitwachsen, eine Minderversorgung des Myokards mit Sauerstoff ist die Folge. Die durch Angiotensin II vermittelte vasokonstriktorische Wirkung führt zu einer zusätzlichen Druckerhöhung in den Blutgefäßen. Durch die anhaltende Druckbelastung kommt es zu einer Hypertrophie der Gefäßwände, die ihrerseits weiter den peripheren Widerstand erhöht. Alle diese Faktoren führen zu einer zusätzlichen Mehrbelastung des primär schon insuffizienten Herzens, wodurch es zu einer weiteren Verminderung des Herzzeitvolumens kommt. Dieser Zustand manifestiert sich im Sinne eines *Circulus vitiosus* (Abbildung 6) in einer weiteren Verschlechterung der renalen Perfusion und chronischer Aktivierung des RAAS. Infolge dessen findet man im Plasma von Herzinsuffizienz-Patienten stark erhöhte

Aldosteronkonzentrationen (300 ng/dl) im Vergleich zu Gesunden, die Aldosteronspiegel von 5-15 ng/dl aufweisen.[33] Ein verlangsamter Abbau des Mineralocorticoids durch eine verminderte Leberperfusion verstärkt die Aldosteronakkumulation noch zusätzlich.[34]

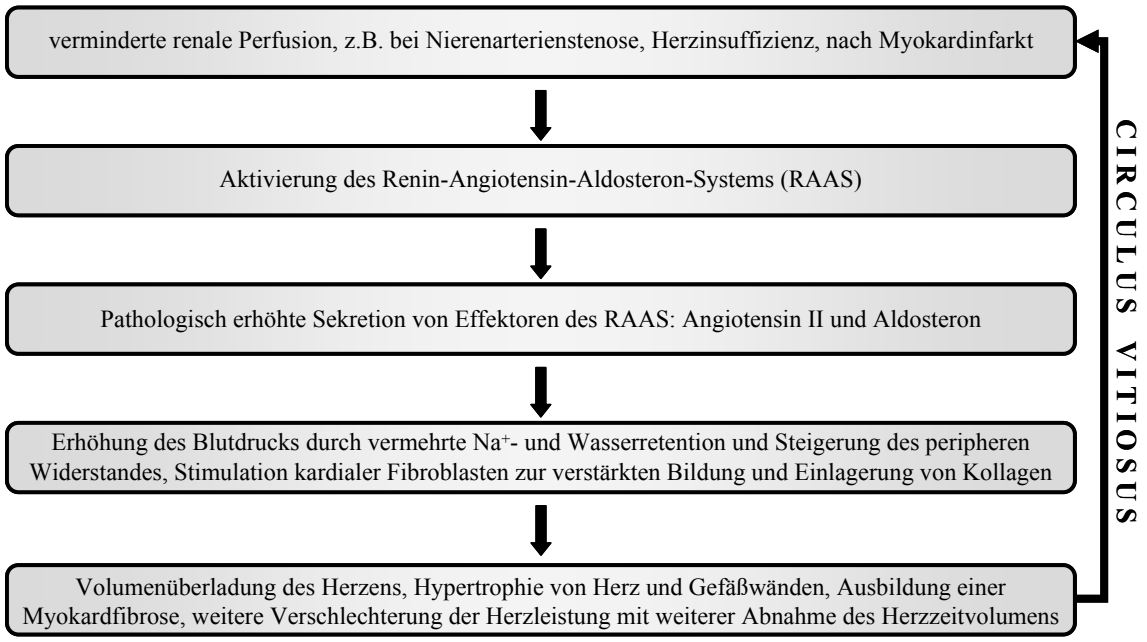

Abbildung 6: Manifestierung der pathophysiologischen Aldosteronwirkung im Sinne eines Circulus vitiosus

Mittlerweile nimmt man an, dass bei geschätzten 5-10 % aller Patienten mit Bluthochdruck als Ursache ein *Conn*-Syndrom (Primärer Hyperaldosteronismus) vorliegt. Somit sind auf Deutschland bezogen etwa 0,8 bis 1,6 Millionen Personen von dieser Erkrankung betroffen.[35] Häufiger als andere Bluthochdruckformen führt das *Conn*-Syndrom zu Folgeerkrankungen an Herz, Nieren (Proteinurie und eingeschränkte Nierenfunktion), Gefäßen (Arteriosklerose, Schlaganfall, Hirnmassenblutung) und Augen (Veränderungen des Augenhintergrunds). Ein bedeutender Teil aller Patienten stirbt an den Folgen koronarer Herzerkrankung, Herzinfarkt oder Herzinsuffizienz, was den schädigenden Effekt des Hormons auf das Herz-Kreislauf-System zusätzlich zur blutdrucksteigernden Wirkung deutlich macht. Darüber hinaus war in den letzten Jahren die Rolle von Aldosteron bei der Progression von Nierenerkrankungen Gegenstand zahlreicher Studien.[36] Dabei konnte die Induktion entzündlicher Prozesse und fibrotischer Strukturveränderungen an verschiedenen Organen einschließlich der Niere gezeigt werden, die deren Funktion in entscheidender Weise beeinträchtigen.[37]

1.2.2 Benefit von Mineralocorticoidrezeptor-Antagonisten bei der Therapie von Aldosteron-abhängigen Erkrankungen

Die zunehmende Alterung der Bevölkerung sowie die verbesserten Überlebenschancen von Personen mit einem akuten Herzinfarkt, Herzklappenerkrankungen, Kardiomyopathien und mit sekundären Myokarderkrankungen werden in den nächsten Jahren zu einem starken Anstieg der Zahl an Herzinsuffizienz-Patienten führen. Eine symptomatische Herzinsuffizienz ist in Bezug auf die Prognose mit einer malignen Krankheit vergleichbar und geht mit einer miserablen Lebensqualität und häufigen Krankenhausaufenthalten einher. Nach Diagnose beträgt die durchschnittliche Überlebenszeit bei Männern 1,7 Jahre, bei Frauen 3,2 Jahre. Nur 25 % der Männer und 38 % der Frauen mit Herzinsuffizienz überleben länger als 5 Jahre.[38] Selbst bei einer leichten Insuffizienz beträgt die Mortalität 10-20 %. Die derzeitig verfügbaren therapeutischen Strategien, die Herzglykoside, Diuretika, ACE-Hemmer und AT-II-Rezeptor Antagonisten beinhalten, haben limitierte Wirksamkeit und gravierende Nachteile. Viele zeigen bei längerer Anwendung einen deutlichen Aktivitätsverlust. Obwohl die positiven Effekte des ACE-Hemmers Enalapril auf Herz-Kreislauf-Erkrankungen durch Hemmung der Angiotensin II-Biosynthese im Rahmen der CONSENSUS-Studie sehr überzeugend waren (Verringerung der Mortalität um 50 % nach 6 Monaten und 46 % nach 12 Monaten Therapie),[39] wird bei einer Langzeittherapie mit ACE-Hemmern nach einer anfänglichen Reduktion der Plasma-Aldosteronkonzentrationen eine erhöhte Freisetzung des Mineralocorticoids aus der Nebennierenrinde beobachtet. Dieses Phänomen wird als „Aldosteron-Escape“ bezeichnet und wird möglicherweise durch erhöhte Serumkaliumspiegel verursacht.[40] Die o.g. Medikamente beeinflussen nicht den pathologisch erhöhten Aldosteronspiegel und verringern somit nicht die Stimulation der kardialen Fibrose, die einen großen Einfluss auf die Progression der Herzinsuffizienz aufweist.

Eine weitere therapeutische Option stellt der Einsatz von Aldosteron-Antagonisten dar. In zwei klinischen Studien (RALES, 1999; EPHESUS, 2003) konnte eindrucksvoll gezeigt werden, dass die Behandlung von kardiovaskulären Erkrankungen mit den Aldosteron-Antagonisten Spironolacton und Eplerenon, zusätzlich zur oben genannten Basistherapie, die Hospitalisationsrate deutlich absenken konnte und die Mortalität von Herzinsuffizienz-Patienten bis zu 30 % verringerte.[41] Weiterführende Studien ergaben, dass beide MR-Blocker in der Lage sind die Herzleistung zu verbessern und die Hypertrophie des linken Ventrikels sowie die Entwicklung bzw. das Fortschreiten der Myokardfibrose zu verhindern.[42,43] Auch bei Primärem Hyperaldosteronismus wird Spironolacton als Standardtherapie eingesetzt. Während bei Patienten mit einem unilateralen Adenom dessen chirurgische Entfernung das Mittel der Wahl ist, muss bei einer bilateralen Nebennierenrindenhyperplasie ein MR-Blocker eingesetzt werden, um die rezeptorvermittelten negativen Aldosteronwirkungen bestmöglich zu inhibieren. Auch im Zusammenhang mit fibrotischen Strukturveränderungen der Niere konnte die protektive Wirkung der Aldosteron-Antagonisten in verschiedenen Studien nachgewiesen werden.[37,44]

Jedoch ist die Anwendung von Spironolacton mit diversen, teilweise gravierenden Nebenwirkungen verbunden. Aufgrund seiner steroidalen Struktur zeigt es nur geringe Selektivität gegenüber anderen Steroidrezeptoren, was zu Gynäkomastie, Impotenz und Störungen der Menstruation führt. *In vitro* Studien ergaben nur einen Selektivitätsfaktor von sechs zwischen Androgenrezeptor und MR, darüber hinaus wird auch der Progesteronrezeptor aktiviert.[45] Eplerenon hingegen zeigt keine nennenswerten Affinitäten zu anderen Steroidrezeptoren. Seine Aktivität am Aldosteronrezeptor ist zwar um Faktor 40 geringer, aber es besitzt im Vergleich zu Spironolacton ein deutlich verbessertes Nebenwirkungsprofil. Eine weitere schwerwiegende Folgeerscheinung von beiden MR-Blockern ist das Auftreten von Hyperkaliämien. Diese führen zu Herzrhythmusstörungen und erhöhen das Risiko eines plötzlichen Herztodes. Nach Veröffentlichung der RALES-Studie kam es zu einem sprunghaften Anstieg von Spironolacton-Verordnungen. Dies korrelierte laut einer von Juurlink *et al.* publizierten Studie mit einer Zunahme an Klinikeinweisungen und Todesfällen aufgrund von Hyperkaliämien.[46] Deshalb ist bei Einnahme eines MR-Antagonisten eine engmaschige Kontrolle der Serumkaliumspiegel unerlässlich.

1.2.3 Inhibition von CYP11B2 als vielversprechende Therapieoption bei der Behandlung kardiovaskulärer Erkrankungen

Die positive Wirkung von Mineralocorticoid-Antagonisten auf die Progression Aldosteron-abhängiger Erkrankungen ist weitreichend belegt. Ihr Einsatz birgt jedoch nicht zu unterschätzende Nachteile. Hier sind die teilweise gravierenden Nebenwirkungen zu nennen und die Tatsache, dass MR-Blocker keinen reduzierenden Einfluss auf die pathologisch erhöhten Plasma-Aldosteronspiegel nehmen. Die Gabe von Spironolacton verursacht sogar noch einen weiteren Anstieg der Aldosteronlevel.[47] Zudem konnte beobachtet werden, dass hohe Aldosteronkonzentrationen nicht wie erwartet zu einer homologen Down-Regulation des Aldosteronrezeptors führen, sondern ganz im Gegenteil zu einer Up-Regulation.[48] Deshalb muss davon ausgegangen werden, dass es bei einer Langzeittherapie mit Aldosteron-Antagonisten zu einem Wirkverlust kommen kann. Darüber hinaus können die in Abschnitt 1.1.2 beschrieben nicht genomischen Aldosteronwirkungen auf diese Weise nicht inhibiert werden. Die Blockierung der rezeptorvermittelten Wirkung stellt jedoch nicht die einzige therapeutische Option dar, um den negativen Effekten erhöhter Aldosteronkonzentrationen entgegenzuwirken. Die Reduktion der Plasma-Aldosteronspiegel durch Hemmung der Aldosteronbiosynthese, genauer gesagt ihres Schlüsselenzyms CYP11B2, sollte ähnlich günstige Effekte aufweisen. Bei Patienten mit Hyperaldosteronismus, Herzinsuffizienz und Myokardfibrose könnte der in Abbildung 6 dargestellte *Circulus vitiosus*, der zu schweren kardiovaskulären Komplikationen führt, möglicherweise unterbrochen werden.

Da die Aldosteronsynthase CYP11B2 nach heutigem Wissenstand ausschließlich in die Aldosteronbiosynthese involviert ist, stellt sie den optimalen Angriffspunkt für die Entwicklung selektiver Hemmstoffe dar. Dieses Target wird bereits seit 1994 von unserer Arbeitsgruppe

propagiert,[49] ebenso wie die mögliche Anwendung selektiver CYP11B2-Inhibitoren bei der Behandlung von Hyperaldosteronismus, Herzinsuffizienz und Myokardfibrose.[50,51] Hinsichtlich potentieller Nebenwirkungen wird hierbei die Entwicklung nichtsteroidaler Inhibitoren bevorzugt. Diese Strategie weist Vorteile im Vergleich zur Rezeptorblockade auf. Zum einen kann von geringeren endokrinen Wechselwirkungen ausgegangen werden, da es keinen bekannten nichtsteroidalen Inhibitor eines steroidogenen CYP-Enzyms gibt, der Affinität zu einem Steroidrezeptor aufweist. Zum anderen können die erhöhten Aldosteronkonzentrationen im Plasma durch CYP11B2-Hemmung gesenkt werden.

Das *Proof of Concept* für Aldosteronsynthase konnte bereits mit der Substanz FAD286A erbracht werden. Hierbei handelt es sich um das *R*(+)-Enantiomer von Fadrozol, einem unselektiven Aromatase (CYP19)-Inhibitor, der zur Therapie von hormonabhängigem Brustkrebs eingesetzt wird.[52] Aufgrund mangelnder Selektivität wird bei seiner Applikation eine Hemmung der Corticoidbiosynthese beobachtet.[53,54] Im Jahre 2005 bestätigte eine Studie von Fiebeler *et al.* den potentiellen therapeutischen Nutzen eines Aldosteronsynthase-Inhibitors.[11] In transgenen Ratten, die die humanen Renin- und Angiotensinogen-Gene überexprimieren, kommt es zur Ausbildung eines Bluthochdrucks mit schweren kardialen und renalen Schäden. Nach der 7. Lebenswoche betrug die Mortalität der unbehandelten Tiere 40 % (5/13). Durch Applikation von FAD286A wurde die Angiotensin II induzierte Entwicklung fibrotischer Gewebsveränderungen an Herz und Nieren abgeschwächt, was deren Funktionalität verbesserte. Darüber hinaus konnte die kardiale Hypertrophie reduziert und die Sterblichkeit auf 10 % (1/10) gesenkt werden. Ähnliche Ergebnisse zeigten sich nach Durchführung einer Adrenalektomie, wobei die Glucocorticoide durch Dexamethason substituiert wurden. Hierauf folgten weitere Studien, die FAD286A als Aldosteronsynthase-Inhibitor einsetzten und seine Wirkungen direkt mit denen von den MR-Antagonisten Spironolacton und Kaliumcanrenoate verglichen. Ménard *et al*. untersuchten die Dosis-abhängige Wirkung von FAD286A und Spironolacton an Ratten, in welchen die Urin-Aldosteronlevel durch eine „low-salt"-Diät (0,05 % Natrium und 2 % Kalium) um das 40-fache erhöht waren im Vergleich zu einer „high-salt"-Diät (2 % Natrium und 0,9 % Kalium).[55] In beiden Versuchsgruppen konnte durch Applikation von 30 mg/kg FAD286A der Aldosterongehalt im Urin deutlich abgesenkt werden (um 87 % bei „low-salt"-Diät und um 75 % bei „high-salt"-Diät). Die gleiche Dosis Spironolacton führte zu einem Anstieg der Aldosteronkonzentration im Urin um 125 %. Die durch die „low-salt"-Diät ebenfalls erhöhten Plasma-Aldosteronspiegel konnten von 2877 pM um 64 % auf 1045 pM gesenkt werden. Durch die Verabreichung des Aldosteronsynthase-Inhibitors konnte keine vollständige Hemmung der Aldosteronbiosynthese erreicht werden und es zeigte sich kein signifikanter Anstieg der Plasma-Kaliumkonzentration. Somit konnte die schwerste Komplikation Hyperkaliämie, die bei der Therapie mit MR-Antagonisten auftritt, nicht beobachtet werden. In einer Studie von Minnaard-Huiban *et al*. mit spontan hypertensiven Ratten, die eine Herzinsuffizienz ausbilden (SHHF-Ratten), wurde die Wirksamkeit von FAD286A mit der des Rezeptorblockers Kaliumcanrenoate verglichen.[56] Hierbei

konnten die Urin- und Plasma-Aldosteronspiegel ebenfalls durch das *R*(+)-Enantiomer von Fadrozol gesenkt werden. Darüber hinaus war es in der Lage den Kollagengehalt im Gewebe des linken Ventrikels im gleichen Maße zu reduzieren wie der MR-Antagonist. Somit konnte gezeigt werden, dass die Hemmung von CYP11B2 eine bestehende Myokardfibrose im gleichen Umfang reduzieren kann wie die Blockierung des Aldosteronrezeptors. Auch in dieser Studie wurde keine Erhöhung der Plasma-Kaliumkonzentration festgestellt. In einer weiteren vergleichenden Studie zwischen FAD286A und Spironolacton wurden Ratten eingesetzt, in denen durch Ligation der linken Koronararterie ein Herzinfarkt erzeugt wurde. Diese Tiere entwickeln daraufhin eine Herzinsuffizienz mit Merkmalen, die die Situation im Menschen weitgehend repräsentiert.[57] In dieser Studie wurden die Effekte einer Langzeittherapie (90 Tage) des CYP11B2-Inhibitors und des MR-Blockers untersucht. Auch hier konnten die Ergebnisse vorangegangener Arbeiten bestätigt werden. Beide Wirkstoffe waren in der Lage die Herzfunktion zu verbessern, indem sie sowohl die linksventrikuläre Hypertrophie als auch die Kollagenakkumulation verringerten. Dabei waren die positiven Effekte bei Hemmung der Aldosteronbiosynthese ausgeprägter als bei Blockierung des Mineralocorticoidrezeptors, was die Autoren auf die zusätzliche Inhibition MR-unabhängiger Prozesse zurückführten. In einer erst kürzlich publizierten Studie wurde ebenfalls mit Spironolacton und FAD286A untersucht, ob MR-Antagonismus und Aldosteronsynthase-Hemmung ähnliche Wirkung auf Ang II/Salz-induzierte Organschäden in uninephrektomierten Ratten haben.[58] Dabei zeigte sich, dass FAD286A, aber nicht Spironolacton, in der Lage war, den durch Ang II/Salz-Behandlung signifikant erhöhten Plasma-Aldosteronspiegel abzusenken. Beide Wirkstoffe konnten jedoch die durch Ang II/Salz-induzierten fibrotischen Strukturveränderungen in Herz- und Nierengewebe vermindern. Dabei wurde im Myokard sowohl eine Hypertrophie als auch die Entwicklung einer interstitiellen Fibrose verhindert, nicht jedoch die Entstehung einer perivaskulären Fibrose. Die im Nierengewebe durch Ang II/Salz-verursachten Organschäden, Hypertrophie, Glomerulosklerose, tubulointerstitielle Fibrose sowie renale arterielle Hypertrophie, wurden von beiden Wirkstoffen in gleichem Maße reduziert.

Von den bisher auf dem Markt befindlichen Arzneistoffen ermöglicht nach gegenwärtigen Erkenntnissen nur die Anwendung von MR-Antagonisten die Möglichkeit den schädigenden Auswirkungen erhöhter Aldosteronkonzentrationen entgegenzuwirken. Ob die MR-Blockade ein besseres Konzept darstellt als die Hemmung der Aldosteronbiosynthese wird in der Literatur kontrovers diskutiert.[59] Die positiven Ergebnisse aus ersten Studien mit dem *R*(+)-Enantiomer des Aromatase-Inhibitors Fadrozol bezüglich der Evaluierung verschiedener Parameter (Hypertrophie, Fibrose, etc.) in Folge einer Aldosteronabsenkung in Krankheitsmodellen belegen das klinische Potential der CYP11B2-Hemmung. Da FAD286A jedoch kein selektiver Inhibitor der Mineralocorticoidsynthese darstellt und die angewendeten Dosierungen die therapeutisch relevanten Dosen für die Aromatase-Hemmung weit übersteigen, sollten die positiven Effekte der reduzierten Aldosteronaktivität durch Inhibition von CYP11B2 mit einem selektiven Aldosteronsynthase-Hemmstoff in einem Tiermodell gezeigt werden.

1.3 Steroid-11β-hydroxylase als potentielles Drug Target

1.3.1 Pathophysiologie von Cortisol und Therapie von Cortisol-abhängigen Erkrankungen

Cortisol ist ein lebenswichtiges Hormon, das der Adaption an physische und psychische Stresssituationen dient. Neben seiner regulatorischen Funktion vieler Stoffwechselprozesse hat es hauptsächlich immunmodulatorische und antiinflammatorische Wirkung. Zustände mit zu hohen oder zu niedrigen Plasmacortisolspiegeln sind mit schweren Krankheitsbildern assoziiert, die zum Tode führen können. Zu einem Hypocortisolismus kommt es beispielsweise bei der Zerstörung beider Nebennieren, was meist durch Autoimmunprozesse hervorgerufen wird. Es handelt sich hierbei um eine Primäre Nebenniereninsuffizienz, die auch als Morbus Addison (wurde 1855 erstmals von dem englischen Arzt Thomas Addison beschrieben) bezeichnet wird. Dabei kommt es aufgrund der Degeneration der Nebennierenrinde zu einem Ausfall der Corticoidproduktion, was unbehandelt tödlich verläuft. Diese Erkrankung kann heute gut durch synthetische Cortisolpräparate und eventuell zusätzlicher Gabe eines Mineralocorticoids behandelt werden. Die Substitution muss lebenslang erfolgen. Pathophysiologisch erhöhte Cortisolspiegel sind mit einer Vielzahl von Symptomen assoziiert, die unter dem Begriff des *Cushing*-Syndroms zusammengefasst sind, welches erstmals 1912 von Harvey Cushing beschrieben wurde. Durch die verstärkte Sekretion von Cortisol kommt es zur pathologischen Ausprägung der physiologischen Glucocorticoidwirkungen. Die katabolen Effekte von Cortisol führen zu Muskelschwund, atrophischer Haut und Osteoporose, sowie zu einer Mobilisation von Lipiddepots mit atyischer Redisposition, was zu dem charakteristischen Phänotyp eines *Cushing*-Patienten mit Vollmondgesicht, Stiernacken und Stammfettsucht führt. Aufgrund der gesteigerten Gluconeogenese kommt es zu einer schlecht auf Insulin ansprechenden Hyperglykämie („Steroiddiabetes“). Bei den Ursachen eines chronischen Hypercortisolismus unterscheidet man eine ACTH-abhängige (ca. 80 %) von einer ACTH-unabhängigen (ca. 20 %) Form. In vielen Fällen wird dieses Krankheitsbild durch Adenome oder Tumore der Hirnanhangdrüse oder der Nebennierenrinde verursacht, die zu einer verstärkten Cortisolproduktion führen. Es sind aber auch tumorunabhängige Formen des *Cushing*-Syndroms bekannt, ausgelöst z. B. durch Hyperplasie der Nebenniere. Für die tumorabhängigen Formen bietet sich als Mittel der Wahl die operative Entfernung des Tumors an. Dieses Verfahren ist in über 90 % der Fälle erfolgreich. Bei vollständiger Entfernung ist meist die medikamentöse Gabe von Cortisol notwendig. Bei unvollständiger Resektion des Adenoms (etwa 10 %) kann es zu einem Rückfall kommen, der eine weitere Operation erforderlich macht. Bleibt auch hier der Erfolg aus, kann die Bildung der Glucocorticoide durch bestimmte Medikamente (z. B. Ketoconazol) gehemmt werden. Die Entfernung der Nebennieren (Adrenalektomie) wird nur noch angewandt, wenn eine zweite Operation nicht erfolgreich ist oder ein ACTH-produzierender Tumor außerhalb der Hirnanhangdrüse vorliegt. Eine Alternative stellt die Bestrahlung der Hypophyse dar, deren Wirkung in der Regel aber erst nach 1-2 Jahren eintritt. Tumoren der Nebennieren werden

operativ entfernt. Bei gutartigen Adenomen ist die Prognose günstig, bei bösartigen Tumoren der Nebenniere hängt sie vom Zeitpunkt der Diagnose ab. Eine medikamentöse Therapie ist als Vorbereitung der operativen Versorgung, als Unterstützung beim Einsatz von Strahlentherapie, in der palliativen Versorgung sowie in kritischen nicht-operablen Fällen indiziert. Hierbei werden Arzneistoffe, die zu einer Reduzierung der erhöhten Cortisolspiegel führen oder die Glucocorticoid-Wirkung am Rezeptor blockieren als Mittel der Wahl angesehen. Jedoch führt die Gabe des Glucocorticoidrezeptor-Antagonisten Mifepriston zu einer massiven Cortisolsekretion, die wahrscheinlich durch die fehlende negative Rückkopplung innerhalb des hypothalamisch-hypophysären-Systems ausgelöst wird.[60]

Das Krankheitsbild des Metabolischen Syndroms (MetS) geht ebenfalls mit Hypercortisolismus einher. Unter MetS versteht man das gemeinsame Auftreten verschiedener Risikofaktoren, die mit schweren Herz- und Gefäßerkrankungen sowie mit der Entstehung von Diabetes mellitus Typ 2 assoziiert sind. Dazu gehören unter anderem Hyperglykämie, Stammfettsucht, Bluthochdruck und Fettstoffwechselstörungen. Es wird geschätzt, dass etwa ein Viertel der erwachsenen Weltbevölkerung vom Metabolischen Syndrom betroffen ist.[61-63] Aufgrund der sowohl beim *Cushing*- als auch beim Metabolischen Syndrom gemeinsam auftretenden charakteristischen Symptome liegt die Vermutung nahe, dass eine chronische Übersekretion von Cortisol für die Pathogenese beider Krankheitsbilder ursächlich ist, wobei der Hypercortisolismus bei MetS-Patienten im Vergleich zum *Cushing*-Syndrom deutlich weniger stark ausgeprägt ist.[64,65] Es konnte jedoch gezeigt werden, dass die Plasmacortisolspiegel bei Patienten mit Metabolischem Syndrom sowohl unter Basalbedingungen als auch nach Stimulation höher sind als bei Gesunden.[66] Des Weiteren konnte bei Patienten mit zentraler Fettleibigkeit und MetS eine Überexpression von 11β-HSD1 in Adipozyten nachgewiesen werden. Daraus ergibt sich eine verstärkte Umsetzung von Cortison in Cortisol und damit eine erhöhte Cortisolaktivität im peripheren Gewebe.[65,67] Die Teilerkrankungen des Metabolischen Syndroms müssen unabhängig voneinander behandelt werden. Zwei wesentliche Bestandteile der Therapie eines Metabolischen Syndroms sind Gewichtsreduktion und Blutdrucksenkung. Die Behandlungsansätze stützen sich vor allem auf eine Änderung der Lebensweise mit mehr Bewegung und einer ausgewogenen fettarmen Ernährung. Ändert sich die Stoffwechselsituation des Patienten nach drei bis sechs Monaten nicht, müssen die Komponenten des Syndroms medikamentös behandelt werden.

1.3.2 Inhibition von CYP11B1 als vielversprechende Therapieoption bei der Behandlung Cortisol-abhängiger Erkrankungen

Ein momentan intensiv verfolgter Ansatz zur Behandlung des Metabolischen Syndroms ist die Entwicklung selektiver Hemmstoffe der 11β-Hydroxysteroiddehydrogenase Typ 1.[68] Durch die Hemmung des im Fettgewebe überexprimierten Enzyms wird die Umwandlung von Cortison in Cortisol blockiert und so die lokalen Konzentrationen des wirksamen Hormons erniedrigt

(intrakriner Ansatz). Die Hemmung der Cortisolbiosynthese sollte eine bessere Therapieoption darstellen (endokriner Ansatz), da so die Gesamtmenge an Cortisol und Cortison reduziert werden könnte. Das ideale Target für einen solchen Ansatz ist das Schlüsselenzym der Cortisolbiosynthese CYP11B1 (Steroid-11β-hydroxylase), da es bei der Bildung von Cortisol den finalen Schritt, nämlich die Oxidation von Deoxycortisol in 11β-Position zu Cortisol katalysiert (siehe Abschnitt 1.1). Analog dem Konzept zur selektiven CYP11B2-Hemmung, besteht durch spezifische Inhibition von CYP11B1 die Möglichkeit, selektiv die Biosynthese von Glucocorticoiden zu hemmen, ohne gleichzeitig die Bildung von Mineralocorticoiden und Sexualhormonen zu beeinflussen. Ebenso wie bei der Hemmung von CYP11B2 wird auch bei diesem Target die Entwicklung nichtsteroidaler Inhibitoren hinsichtlich potentieller Nebenwirkungen bevorzugt.

Die bislang klinisch eingesetzten adrenostatischen Wirkstoffe (u. a. Ketoconazol, Etomidat und Metyrapon)[69] weisen aufgrund mangelnder Selektivität gegenüber zahlreichen CYP-Enzymen erhebliche Nebenwirkungen auf. Das Imidazolderivat Ketoconazol hemmt neben CYP11B1 und CYP11B2 das Cholesterol side chain cleavage enzyme (SCC, CYP11A1) und das Schlüsselenzym der Androgenbiosynthese CYP17. Des Weiteren trat unter der Anwendung von oral verabreichtem Ketoconazol in Einzelfällen eine sehr schwere Hepatotoxizität auf. Das Anästhetikum Etomidat befindet sich seit 1972 in der klinischen Anwendung und wurde im Wesentlichen zur Narkoseeinleitung und zur Sedierung von Intensivpatienten eingesetzt. Dabei kam es durch die damals noch unbekannte adrenostatische Wirkung zu einem Anstieg der Mortalität aufgrund einer akuten Nebenniereninsuffizienz. Bei Etomidat handelt es sich ebenfalls um eine substituierte Imidazolverbindung, die in der kurzfristigen Therapie bei Patienten mit schwerem Hypercortisolismus Anwendung findet und ebenfalls neben CYP11B1 auch CYP11B2 und CYP11A1 hemmt. Gleiches gilt für das Pyridinderivat Metyrapon, das sowohl diagnostisch zur Prüfung der Funktion der Hypophysenvorderlappen-Nebennierenrinden-Achse als auch therapeutisch zur Reduktion der Cortisolspiegel eingesetzt wird. In einer kürzlich erschienenen Arbeit berichten die Autoren über die Entwicklung selektiver Inhibitoren der Steroid-11β-Hydroxylierung ausgehend von Etomidat, wobei die neuen Substanzen jedoch weniger aktiv waren als die Ausgangsverbindung.[70] Über Selektivitäten wird in der vorliegenden Arbeit nicht berichtet. Selektive Steroid-11β-hydroxylase-Inhibitoren sollten wesentlich bessere Therapeutika zur Behandlung des *Cushing*-Syndroms als die zur Zeit eingesetzten sein, zur Behandlung des mit Hypercortisolismus einhergehenden Metabolischen Syndroms sind sie völlig neuartige Pharmaka.

2 Ziel der vorliegenden Dissertation

Das Enzym Aldosteronsynthase (CYP11B2) stellt ein vielversprechendes Target bei der Behandlung Aldosteron-abhängiger Erkrankungen dar. Durch Reduzierung der Aldosteronbiosynthese sollte es möglich sein Hypertrophien und fibrotische Strukturveränderungen an Herz und Nieren zu verhindern oder wenigsten zu minimieren und damit die Funktionalität der Organe zu erhalten. Neben der verringerten Aktivierung des Mineralocorticoidrezeptors und der damit verbundenen Wirkungen, sollte durch die Verminderung der Aldosteronsekretion aus der Nebennierenrinde zusätzlich ein diuretischer Effekt eintreten, der sich positiv auf die pathologisch induzierte Hypervolämie auswirken kann. Somit könnte es gelingen, den durch chronische RAAS-Aktivierung bestehenden *Circulus vitiosus* zu durchbrechen. Erste Studien mit dem unselektiven CYP11B2-Inhibitor FAD286A zeigten diesbezüglich vielversprechende Ergebnisse.

Das in der Arbeitsgruppe angewendete Screening-System zur Identifizierung potentieller Aldosteronsynthase-Hemmstoffe wurde in einem kontinuierlichen Prozess stetig weiter verbessert und erweitert. Erste Tests zur Bewertung von CYP11B2-Inhibitoren wurden an Präparationen boviner adrenaler Mitochondrien und an Nebennieren-Stücken der Ratte durchgeführt.[71,72] Im Hinblick auf die unter 1.1.4 beschriebenen Unterschiede in der Proteinsequenz zwischen den menschlichen CYP11B-Enzymen und denen anderer Spezies war die Entwicklung eines Testsystems mit humanem CYP11B2 unerlässlich. Deshalb wurde im Rahmen der Dissertation von Peter B. Ehmer in der Arbeitsgruppe ein Screening-Assay mit transgenen Hefen des Stammes *Schizosaccharomyces pombe* entwickelt, die das humane CYP11B2-Enzym rekombinant exprimieren.[49] Somit bestand zum ersten Mal die Möglichkeit potentielle CYP11B2-Inhibitoren am humanen Enzym zu untersuchen. Aufgrund der enorm hohen Sequenzidentität zwischen humanem CYP11B2 und CYP11B1 ist die Evaluierung der Selektivität der Inhibitoren zum Schlüsselenzym der Cortisolbiosynthese essentiell und sollte in einem sehr frühen Stadium der Hemmstoffentwicklung erfolgen. Zu diesem Zweck wurde ein weiterer Test entwickelt, der den Hefe-Assay schließlich abgelöst hat. Es erfolgte die Exprimierung der humanen CYP11B2- und CYP11B1-Gene, getrennt voneinander, in einer Säugerzelllinie, den V79MZ-Zellen. Diese besitzen keine endogene CYP-Aktivität, wodurch unspezifische Wechselwirkungen der getesteten Inhibitoren mit anderen CYP-Enzymen ausgeschlossen werden können. Es handelt sich bei diesen Zelllinien um einfache Modelle, die neben der Affinität zum Targetenzym lediglich die Membranpassage berücksichtigen. Die Miniaturisierung dieses Assays, sowie die Optimierung verschiedener Testparameter wurde von Ursula Müller-Vieira als Bestandteil ihrer Dissertation

durchgeführt. Dies diente der Anpassung an ein serielles Screening mit dem neue Leitverbindungen identifiziert werden konnten.[50,73] Diese nichtsteroidalen Inhibitoren mit einem Pyridin substituierten Naphthalen-Grundgerüst und strukturell verwandte Verbindungen stellten eine Klasse potenter Aldosteronsynthase-Hemmstoffe dar, die die Aktivität des hoch homologen CYP11B1-Enzyms deutlich weniger beeinflussen (Selektivitätsfaktoren bis zu 1500). Darüber hinaus zeigten diese Verbindungen gute pharmakokinetische Eigenschaften in Ratten nach per oraler Applikation. Weitergehende Untersuchungen ergaben jedoch entscheidende pharmakologische Nachteile dieser Inhibitoren. Zum einen stellte sich heraus, dass sie starke Inhibitoren des hepatischen CYP1A2-Enzyms darstellen, welches in entscheidender Weise am oxidativen Metabolismus von Xenobiotika beteiligt ist. Die Hemmung dieses Enzyms kann bei gleichzeitiger Gabe weiterer Medikamente zu schweren Arzneistoff-Wechselwirkungen führen, was in jedem Fall verhindert werden muss. Zum anderen waren die Inhibitoren *in vivo* in einem von Häusler *et al*.[74] publizierten Rattenmodell nicht in der Lage den Plasma-Aldosteronspiegel abzusenken, obwohl hohe Substanz-Plasmaspiegel gemessen werden konnten.

Die offensichtlich fehlende CYP11B2-Aktivität in der Ratte wurde auf Speziesunterschiede zurückgeführt, da die Proteinsequenz-Identität zwischen humanem und Ratten-Enzym lediglich 69 % beträgt. Da es unter ethischen und ökonomischen Gesichtspunkten nicht vertretbar war, viele weitere potente CYP11B2-Inhibitoren an Ratten zu testen, ohne ihre Aktivität am Rattenenzym zu kennen, sollte im Rahmen dieser Arbeit ein *in vitro*-Assay entwickelt werden, der eine zuverlässige Vorhersage bezüglich der Ratten-CYP11B2-Aktivität zulässt. Um gleichzeitig die Selektivität der Hemmstoffe im Rattenmodell abzuschätzen, sollten sowohl das CYP11B2- als auch das CYP11B1-Gen aus Rattennebennieren isoliert und in V79MZ-Zellen rekombinant exprimiert werden, um einen Test zu etablieren der analog dem Test mit den humanen Enzymen durchgeführt werden kann. Darüber hinaus sollte ein weiterer Assay entwickelt werden, bei dem die Enzyme in ihrer natürlichen Umgebung, nämlich den Nebennierenzellen, verbleiben. In Anlehnung an bereits in der Arbeitsgruppe vorgenommene Versuche an Rattennebennieren (Dissertation Gertrud Grün, 1994; Dissertation Christiane B. A. Scherer, 2007), sollten Tests an Organkulturen durchgeführt werden, bei welchen die Enzymaktivität von CYP11B2 durch Umsatz eines radioaktivmarkierten Substrates in Gegenwart bzw. Abwesenheit eines Inhibitors untersucht werden kann. Dieser Organ-Assay sollte bei Inaktivität der Hemmstoffe am Rattenenzym auch auf andere Spezies, wie z.B. Hamster oder Meerschweinchen, übertragen werden, um eine alternative Spezies für *in vivo*-Versuche zu identifizieren. Für den Fall, dass aus den neu etablierten *in vitro*-Assays „Hit"-Verbindungen mit nachgewiesener Ratten-CYP11B2-Aktivität hervorgehen, sollte im nächsten Schritt in dem Rattenmodell von Häusler *et al.* die Plasma-Aldosteronabsenkung durch einen Aldosteronsynthase-Hemmstoff im Sinne eines *Proof of Principle* gezeigt werden. Dieses *in vivo*-Modell wurde zur Bewertung von Nebenwirkungen des Aromatase-Inhibitors Fadrozol auf die Corticoid-Biosynthese von Ratten entwickelt und beinhaltet

eine ACTH-Stimulation der Mineralo- und Glucocorticoidbiosynthese 16 Stunden vor Applikation des Inhibitors um natürliche Schwankungen der Corticoidspiegel zu eliminieren.

Im Einzelnen sollten folgende Ziele im Rahmen dieser Dissertation erreicht werden:

- Strukturoptimierungen an bereits identifizierten Leitverbindungen mit Pyridin substituiertem Naphthalen-Grundgerüst zur Verbesserung der Selektivität gegenüber dem hepatischen CYP1A2-Enzyms
- Identifikation neuer Leitverbindungen mit verbessertem pharmakologischen Profil und Aktivität am Ratten-CYP11B2-Enzym
- Klonierung der Rattengene CYP11B2 und CYP11B1 in einen Vektor zur stabilen Expression in einer Säugerzelllinie
- Transfektion des Ratten-CYP11B2- bzw. Ratten-CYP11B1-Gens in V79MZ-Zellen und Isolierung monoklonaler Zelllinien mit Ratten-Aldosteronsynthase- bzw. Ratten-11β-Hydroxylase-Aktivität
- Etablierung eines zellbasierten Screening-Assays zur Identifikation von Hemmstoffen, die inhibitorische Aktivität am Ratten-CYP11B2-Enzym zeigen und deshalb für *in vivo*-Versuche zur Erbringung des *Proof of Principle* in der Ratte in Frage kommen
- Organkulturen von Rattennebennieren oder Nebennieren anderer Nager zur Evaluierung der CYP11B2-Aktivität in der jeweiligen Spezies als weiterer *in vitro*-Vorversuch zur Identifikation eines geeigneten Tiermodells

3 Ergebnisse

3.1 Overcoming Undesirable CYP1A2 Inhibition of Pyridyl-naphthalene Type Aldosterone Synthase Inhibitors: Influence of Heteroaryl Derivatization on Potency and Selectivity

Ralf Heim, Simon Lucas, Cornelia M. Grombein, Christina Ries, Katarzyna E. Schewe, Matthias Negri, Ursula Müller-Vieira, Barbara Birk and Rolf W. Hartmann

This manuscript has been published as an article in the

Journal of Medicinal Chemistry **2008**, *51*, 5064–5074.

Paper I

Abstract: Recently, we reported on the development of potent and selective inhibitors of aldosterone synthase (CYP11B2) for the treatment of congestive heart failure and myocardial fibrosis. A major drawback of these non-steroidal compounds was a strong inhibition of the hepatic drug-metabolizing enzyme CYP1A2. In the present study, we examined the influence of substituents in the heterocycle of lead structures with a naphthalene molecular scaffold to overcome this unwanted side effect. With respect to CYP11B2 inhibition, some substituents induced a dramatic increase in inhibitory potency. The methoxyalkyl derivatives **22** and **26** are the most potent CYP11B2 inhibitors up to now (IC_{50} = 0.2 nM). Most compounds also clearly discriminated between CYP11B2 and CYP11B1 and the CYP1A2 potency significantly decreased in some cases (e.g., isoquinoline derivative **30** displayed only 6 % CYP1A2 inhibition at 2 μM concentration). Furthermore, isoquinoline derivative **28** proved to be capable of passing the gastrointestinal tract and reached the general circulation after peroral administration to male Wistar rats.

Introduction

The most important circulating mineralocorticoid aldosterone is secreted by the zona glomerulosa of the adrenal gland and is to a minor extent also synthesized in the cardiovascular system.[1] The hormone plays a key role in the electrolyte and fluid homeostasis and thus for the regulation of blood pressure. Its biosynthesis is accomplished by the mitochondrial cytochrome P450 enzyme aldosterone synthase (CYP11B2) and proceeds via catalytic oxidation of the substrate 11-deoxycorticosterone to corticosterone and subsequently to aldosterone.[2] The adrenal aldosterone synthesis is regulated by several physiological parameters such as the renin-angiotensin-aldosterone system (RAAS) and the plasma potassium concentration. Chronically elevated plasma aldosterone levels increase the blood pressure and are closely associated with certain forms of myocardial fibrosis and congestive heart failure.[3] An insufficient renal flow chronically activates the RAAS and aldosterone is excessively released. The therapeutic benefit of reducing aldosterone effects by use of the mineralocorticoid receptor (MR) antagonists spironolactone and eplerenone has been reported in two recent clinical studies (RALES and EPHESUS).[4,5] The studies showed that treatment with these antagonists reduces mortality in patients with chronic congestive heart failure and in patients after myocardial infarction, respectively. Spironolactone, however, showed severe side effects presumably due to its steroidal structure.[4,6] Although the development of non-steroidal aldosterone receptor antagonists has been reported recently,[7] several issues associated with the unaffected and pathophysiologically elevated plasma aldosterone levels remain unsolved by this therapeutic strategy such as the up-regulation of the mineralocorticoid receptor expression[8] and non-genomic aldosterone effects.[9] A novel approach for the treatment of diseases affected by elevated aldosterone levels is the blockade of aldosterone biosynthesis by inhibition of CYP11B2.[10,11] Aldosterone synthase has previously been proposed as a potential pharmacological target,[12] and preliminary work focused on the development of steroidal inhibitors, i.e., progesterone[13] and deoxycorticosterone[14] derivatives with unsaturated C_{18}-substituents. These compounds were found to be mechanism-based inhibitors binding covalently to the active site of bovine CYP11B, however, data on inhibitory action towards human enzyme are essentially absent in these studies. The strategy of inhibiting the aldosterone formation has two main advantages compared to MR antagonism. First, there is no non-steroidal inhibitor of a steroidogenic CYP enzyme known to have affinity to a steroid receptor. For this reason, fewer side effects on the endocrine system should be expected. Furthermore, CYP11B2 inhibition can reduce the pathologically elevated aldosterone levels whereas the latter remain unaffected by interfering one step later at the receptor level. By this approach, however, it is a challenge to reach selectivity versus other CYP enzymes. Taking into consideration that the key enzyme of glucocorticoid biosynthesis, 11β-hydroxylase (CYP11B1), and CYP11B2 have a sequence homology of more than 93 %,[15] the selectivity issue becomes especially critical for the design of CYP11B2 inhibitors.

The aromatase (CYP19) inhibitor fadrozole (**I**, Chart 1) which is used in the therapy of breast cancer was found to significantly reduce the corticoid formation.[16] This compound is a potent inhibitor of CYP11B2 displaying an IC_{50} value of 1 nM (Table 1). The R(+)-enantiomer of fadrozole (FAD 286)

was recently shown to reduce mortality and to ameliorate angiotensin II-induced organ damage in transgenic rats overexpressing both the human renin and angiotensinogen genes.[17] These findings underline the potential therapeutic utility of aldosterone synthase inhibition, and up to now, several structurally modified fadrozole derivatives are investigated as CYP11B2 inhibitors.[18,19] Recently, the development of imidazolyl- and pyridylmethylenetetrahydronaphthalenes and -indanes as highly active and in some cases selective CYP11B2 inhibitors has been described by our group.[20,21] By keeping the pharmacophore and rigidization of the core structure, pyridine substituted naphthalenes[22] **II** and dihydronaphthalenes[23] **III** were shown to be potent and selective CYP11B2 inhibitors (Chart 1). Combining the structural features of these substance classes to a hybrid core structure led to pyridine substituted acenaphthenes as potent CYP11B2 inhibitors with remarkable selectivity.[24] Furthermore, most of the naphthalene and dihydronaphthalene type compounds exhibited a favorable selectivity profile versus selected hepatic CYP enzymes. However, they turned out to be potent inhibitors of the hepatic CYP1A2 enzyme (see examples **1**, **3**, and **4** in Table 1). CYP1A2 makes up about 10 % of the overall cytochrome P450 content in the liver and metabolizes aromatic and heterocyclic amines as well as polycyclic aromatic hydrocarbons.[25] This experimental result turned these naphthalene type aldosterone synthase inhibitors into unsuitable drug candidates since adverse drug-drug interactions are mainly caused by inhibition of hepatic cytochrome P450 enzymes and have to be avoided in either case. In our preceding studies, the attention was focused on the optimization of the naphthalene skeleton, the substitution pattern of the heme complexing 3-pyridine moiety, however, was not investigated in detail. Herein, we describe the synthesis of a series of naphthalenes and dihydronaphthalenes with various substituents in the pyridine heterocycle to examine their influence on potency and selectivity (Table 1). The biological activity of the synthesized compounds was determined *in vitro* on human CYP11B2 for potency and human CYP11B1 and CYP1A2 for selectivity. In addition, selected compounds were tested for inhibitory activity at human CYP17 (17α-hydroxylase-C17,20-lyase), CYP19, and selected hepatic CYP enzymes (CYP2B6, CYP2C9, CYP2C19, CYP2D6, CYP3A4). The *in vivo* pharmacokinetic profile of two promising compounds was determined in a cassette dosing experiment using male Wistar rats.

Chart 1. Non-steroidal inhibitors of CYP11B2

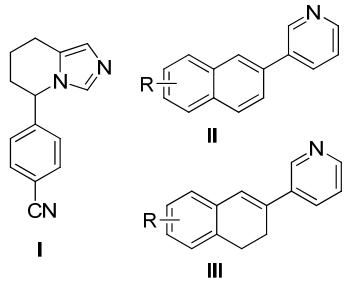

Results

Chemistry

The key step for the synthesis of pyridine substituted naphthalenes was a Suzuki cross coupling (Scheme 1).[26] A microwave enhanced method developed by van der Eycken et al. was chosen for this purpose.[27] By applying this method, various substituted bromopyridines were coupled with 6-methoxy-2-naphthaleneboronic acid to afford compounds **7**, **9**–**11**, **14**, **15**, **17**–**19**, **21**, **23**, **27**, and **28**. Compound **8** was obtained by coupling of 4-methyl-3-pyridineboronic acid with triflate **8a** which was accessible by treating 6-cyano-2-naphthol with Tf_2NPh and K_2CO_3 in THF under microwave irradiation.[28] The bromopyridines could be derivatized prior to Suzuki coupling according to Scheme 2 to provide heterocycles bearing a hydroxy, ethoxy or hydroxymethyl substituent (**10a**, **14a**, **21a**, and **23a**).[29]

Scheme 1[a]

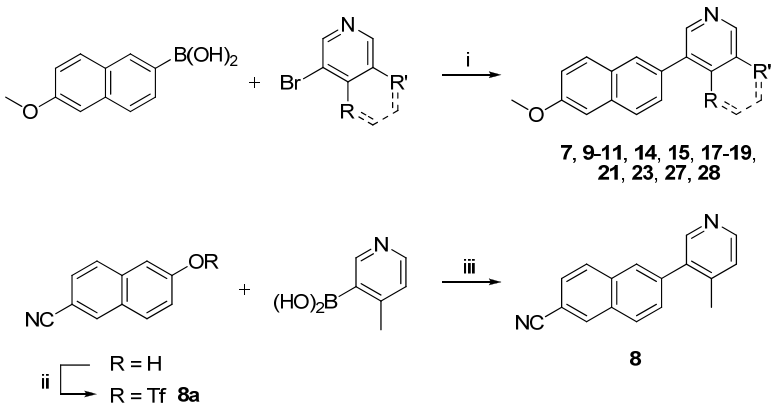

[a] Reagents and conditions: i) $Pd(PPh_3)_4$, DMF, aq. $NaHCO_3$, μw, 150 °C; ii) Tf_2NPh, K_2CO_3, THF, μw, 120 °C; iii) $Pd(dppf)Cl_2$, toluene/acetone, aq. Na_2CO_3, μw, 150 °C.

Scheme 2[a]

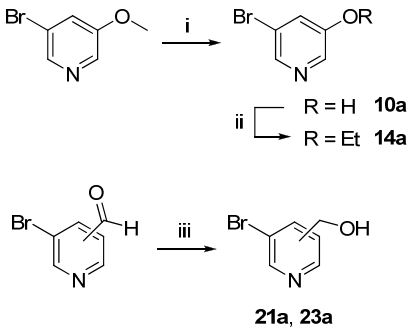

[a] Reagents and conditions: i) conc. HBr, reflux; ii) EtBr, K_2CO_3, DMF, rt; iii) $NaBH_4$, methanol, 0 °C.

For compounds **21**–**26**, the substitution pattern was modified after the cross-coupling reaction as shown in Scheme 3 by sodium borohydride reduction and optional methylation. Esterification of the carboxylic acids **15** and **19** by refluxing in methanol under acid catalysis afforded the corresponding

methyl esters **16** and **20**. The synthesis of 6-cyanodihydronaphthalene **6** was accomplished by the sequence shown in Scheme 4. Using 6-bromo-2-tetralone, Pd-catalyzed cyanation[30] led to intermediate **6b** which was transformed into the alkenyltriflate **6a** by deprotonation with KHMDS and subsequent treatment with Tf_2NPh.[31] Compound **6a** underwent Suzuki coupling with 3-pyridineboronic acid to afford **6**.

Scheme 3[a]

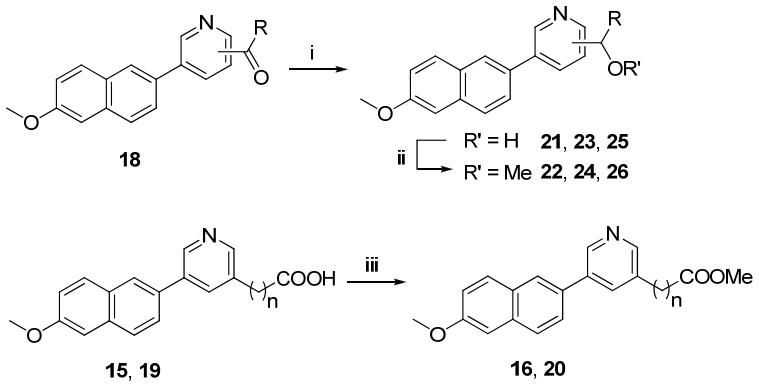

[a] Reagents and conditions: i) $NaBH_4$, methanol, 0 °C; ii) MeI, NaH, THF, rt; iii) methanol, H_2SO_4, reflux.

Scheme 4[a]

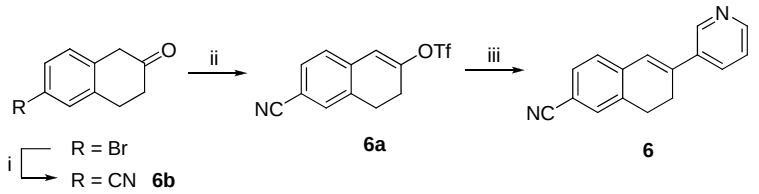

[a] Reagents and conditions: i) $Zn(CN)_2$, $Pd(PPh_3)_4$, DMF, 100 °C; ii) Tf_2NPh, KHMDS, THF/toluene, –78 °C; iii) 3-pyridineboronic acid, $Pd(PPh_3)_4$, DMF, aq. $NaHCO_3$, μw, 150 °C.

The naphthalenes **2**, **12**, **29** and the dihydronaphthalenes **5**, **13**, **30** were obtained as shown in Scheme 5. The sequence for the synthesis of intermediate **2e** was described previously and was only slightly modified by us (see supplementary material).[32] Regioselective α-bromination was accomplished by treating **2e** with $CuBr_2$ in refluxing ethyl acetate/$CHCl_3$.[33] After a subsequent reduction/elimination step,[23] the intermediate alkenylbromide **2b** underwent Suzuki coupling[34] with the appropriate boronic acid to afford the dihydronaphthalenes **5**, **13**, and **30**. The corresponding naphthalenes **2**, **12**, and **29** were obtained by aromatization of **2b** with DDQ in refluxing toluene[35] followed by Suzuki coupling.[27] The synthesis of compounds **1**, **3**, and **4** has been reported previously by our group.[22,23]

Scheme 5[a]

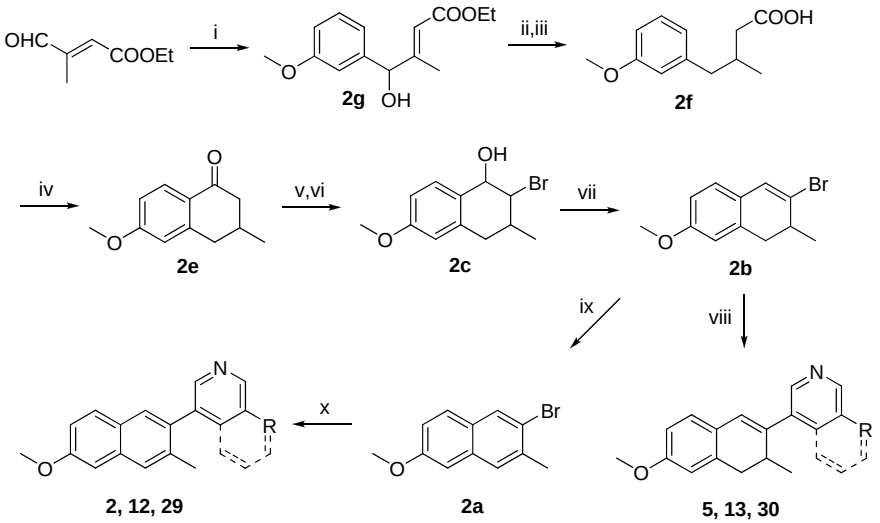

[a] Reagents and conditions: i) 3-methoxyphenylmagnesium bromide, THF, –5 °C; ii) KOH, NaOH/water, reflux; iii) H_2, Pd/C, AcOH, 60 °C; iv) $(COCl)_2$, CH_2Cl_2, rt, then $AlCl_3$, CH_2Cl_2, –10 °C; v) $CuBr_2$, ethyl acetate/$CHCl_3$, reflux; vi) $NaBH_4$, methanol, 0 °C; vii) *p*-toluenesulfonic acid, toluene, reflux; viii) boronic acid, $Pd(OAc)_2$, TBAB, acetone, aq. Na_2CO_3, µw, 150 °C; ix) DDQ, toluene, reflux; x) boronic acid, $Pd(PPh_3)_4$, DMF, aq. $NaHCO_3$, µw, 150 °C.

Biological Results

Inhibition of Human Adrenal Corticoid Producing CYP11B2 and CYP11B1 *In Vitro* (Table 1). The inhibitory activities of the compounds were determined in V79 MZh cells expressing either human CYP11B2 or CYP11B1.[10,36] The V79 MZh cells were incubated with [^{14}C]-deoxycorticosterone as substrate and the inhibitor at different concentrations. The product formation was monitored by HPTLC using a phosphoimager. Fadrozole, an aromatase (CYP19) inhibitor with proven ability to reduce corticoid formation *in vitro* and *in vivo* was used as a reference compound (CYP11B2, IC_{50} =1 nM; CYP11B1, IC_{50} = 10 nM).[16]

Most of the substituted pyridylnaphthalenes showed a high inhibitory activity at the target enzyme CYP11B2 with IC_{50} values in the low nanomolar range (Table 1). Some of the compounds displayed subnanomolar potency (IC_{50} < 1 nM) and turned out to be even stronger aldosterone synthase inhibitors than the reference substance fadrozole. The methoxyalkyl substituted compounds **22** and **26** exhibited IC_{50} values of 0.2 nM each. Hence, they are 5-fold more active than fadrozole (IC_{50} = 1 nM) and 30-fold more active than the unsubstituted parent compound **1** (IC_{50} = 6.2 nM). However, derivatization by polar and acidic residues in 5'-position resulted in a decrease in potency. This particularly applies to the carboxylic acids **15** and **19** showing no or only low inhibitory activity and to a minor extent also to the phenolic compound **10** and the carboxamide **17** with IC_{50} values of 94 nM each.

Table 1. Inhibition of human adrenal CYP11B2, CYP11B1 and human CYP1A2 *in vitro*

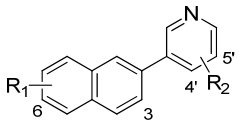

1-3, **7-12**, **14-27**

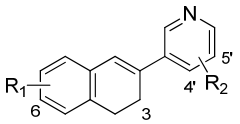

4-6, **13**

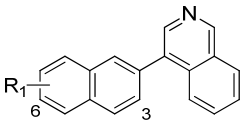

28, **29**

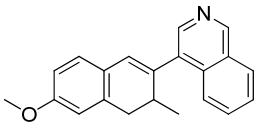

30

			IC_{50} value[a] (nM)			
			V79 11B2[b]	V79 11B1[c]	selectivity	% inhibition[e]
compd	R_1	R_2	hCYP11B2	hCYP11B1	factor[d]	CYP1A2[f]
1[g]	6-OMe	H	6.2	1577	254	98
2	6-OMe-3-Me	H	7.0	1047	150	93
3[g]	6-CN	H	2.9	691	239	97
4[g]	6-OMe	H	2.1	578	275	98
5	6-OMe-3-Me	H	3.3	248	79	73
6	6-CN	H	4.5	461	103	91
7	6-OMe	4'-Me	0.8	114	143	98
8	6-CN	4'-Me	0.6	52	87	86
9	6-OMe	4'-NH_2	13	1521	117	58
10	6-OMe	5'-OH	94	8925	95	93
11	6-OMe	5'-OMe	4.2	238	57	91
12	6-OMe-3-Me	5'-OMe	3.8	875	230	91
13	6-OMe-3-Me	5'-OMe	1.2	100	83	18
14	6-OMe	5'-OEt	5.1	373	73	85
15	6-OMe	5'-COOH	n.a.[h]	n.d.	n.d.	n.d.
16	6-OMe	5'-COOMe	0.8	15	19	n.d.
17	6-OMe	5'-$CONH_2$	94	41557	442	n.d.
18	6-OMe	5'-COMe	2.1	255	121	80
19	6-OMe	5'-CH_2COOH	1216	37796	31	n.d.
20	6-OMe	5'-CH_2COOMe	6.9	199	29	n.d.
21	6-OMe	5'-CH_2OH	9.1	614	68	93
22	6-OMe	5'-CH_2OMe	0.2	31	155	83
23	6-OMe	4'-CH_2OH	22	1760	80	92
24	6-OMe	4'-CH_2OMe	2.2	435	198	97
25	6-OMe	5'-CH(OH)Me	0.5	99	198	78
26	6-OMe	5'-CH(OMe)Me	0.2	10	50	n.d.
27	6-OMe	5'-Ph	4.8	151	32	n.d.
28	6-OMe	-	0.6	67	112	57
29	6-OMe-3-Me	-	3.1	843	272	45
30	-	-	0.5	64	128	6
fadrozole	-	-	1.0	10	10	8

[a] Mean value of four experiments, standard deviation usually less than 25 %, n.d. = not determined. [b] Hamster fibroblasts expressing human CYP11B2; substrate deoxycorticosterone, 100 nM. [c] Hamster fibroblasts expressing human CYP11B1; substrate deoxycorticosterone, 100 nM. [d] IC_{50} CYP11B1/IC_{50} CYP11B2. [e] Mean value of two experiments, standard deviation less than 5 %; n.d. = not determined. [f] Recombinantly expressed enzyme from baculovirus-infected insect microsomes (Supersomes); inhibitor concentration, 2.0 µM; furafylline, 55 % inhibition. [g] These compounds were described previously.[22,23] [h] n.a. = no acivity (7 % inhibition at an inhibitor concentration of 500 nM).

Beside introduction of small residues in 4'- and 5'-position, an extension of the heterocyclic moiety by a condensed phenyl ring afforded the extraordinary potent isoquinoline compounds **28**–**30** with IC_{50} values in the range of 0.5–3.1 nM. Even the sterically demanding 5'-phenyl residue of compound **27** was still tolerated (IC_{50} = 4.8 nM). In general, changing the carbocyclic core (naphthalene, 3-methyl- or dihydro-derivative) while simultaneously keeping the substitution pattern of the heterocycle had only little effect on the CYP11B2 inhibition as shown by the series **11**–**13** (IC_{50} = 1.2–4.2 nM) and **28**–**30** (IC_{50} = 0.5–3.1 nM). With regard to the inhibitory activity at the highly homologous CYP11B1, most of the tested compounds were less active than at CYP11B2. However, a noticeable inhibition with IC_{50} values in the range of 10–100 nM was observed in some cases. In particular, the 5'-methoxyalkylpyridine derivatives **22** (IC_{50} = 31 nM) and **26** (IC_{50} = 10 nM) as well as the methyl ester **16** (IC_{50} = 15 nM) turned out to be potent CYP11B1 inhibitors. Although introduction of substituents in the heterocyclic moiety mostly resulted in a moderate decrease in selectivity compared to the unsubstituted derivatives, the selectivity factors were still high for most of the tested compounds (factor 100–200). In case of 6-methoxy-3-methylnaphthalene **2**, the introduction of substituents in the heterocyclic moiety led to an enhanced selectivity. A methoxy substituent in 5'-position as accomplished in compound **12** increased the selectivity factor from 150 to 230 and the isoquinoline derivative **29** proved to be one of the most selective CYP11B2 inhibitors of the series with a selectivity factor of 272, thus being 27-fold more selective than fadrozole (selectivity factor = 10).

Inhibition of Hepatic and Steroidogenic CYP Enzymes (Tables 1 and 2). In order to further examine the influence of heteroaryl substitution on selectivity, the compounds were tested for inhibition of the hepatic CYP1A2 enzyme. CYP1A2 was strongly inhibited by all previous CYP11B2 inhibitors of the naphthalene and dihydronaphthalene type with unsubstituted heme-coordinating heterocycle, e.g., **1**–**4** exhibited more than 90 % inhibition at an inhibitor concentration of 2 μM (Table 1). With regard to the potent CYP1A2 inhibitor **1**, derivatization of the heterocycle gave rise to compounds with a slightly reduced inhibitory potency, e.g., compounds **14**, **18**, **22**, and **25** displaying approximately 80 % inhibition. A pronounced decrease of CYP1A2 inhibition was observed in case of compounds **9**, **13**, and **29**–**30** (6 –57 %). However, the dihydronaphthalenes **6**, **13**, and **30** turned out to be chemically unstable and decomposition in DMSO solution was observed after storage at 2 °C (~80 % purity after three days) yielding considerable amounts of the aromatized analogues and traces of unidentified degradation products. Therefore, they were not taken into account for further biological evaluations despite their outstanding CYP1A2 selectivity. The CYP1A2 inhibition of some compounds was not determined at all due to either a low CYP11B2 potency (**15**, **17**, and **19**) or low CYP11B1 selectivity (**16**, **20**, **26**, and **27**).

For a set of four structurally diverse compounds (**9**, **11**, **18**, and **28**), an extended selectivity profile including inhibition of the steroidogenic enzymes CYP17 and CYP19 as well as inhibition of some crucial hepatic CYP enzymes (CYP2B6, CYP2C9, CYP2C19, CYP2D6, CYP3A4) was determined (Table 2). The inhibition of CYP17 was determined with the 50,000 *g* sediment of the *E. coli* homogenate recombinantly expressing human CYP17, progesterone (25 μM) as substrate, and the inhibitors

at a concentration of 2 μM.[37] The tested compounds turned out to be moderately potent inhibitors of CYP17. The inhibition values ranked around 40 % corresponding with IC_{50} values of approximately 2000 nM or higher. The inhibition of CYP19 at an inhibitor concentration of 500 nM was determined *in vitro* by use of human placental microsomes and [1β-^{3}H]androstenedione as substrate as described by Thompson and Siiteri[38] using our modification.[39] In this assay, no inhibition of CYP19 was observed for compounds **11**, **18**, and **28**. Only the amino substituted compound **9** displayed a moderate inhibition of 47 %. The IC_{50} values of the compounds for the inhibition of the hepatic CYP enzymes CYP1A2, CYP2B6, CYP2C9, CYP2C19, CYP2D6, and CYP3A4 were determined using recombinantly expressed enzymes from baculovirus-infected insect microsomes (Supersomes). The values of the CYP1A2 inhibition matched well the previously determined percental inhibition (Table 1). Methoxy compound **11** with 91 % inhibition at 500 nM turned out to be a potent CYP1A2 inhibitor (IC_{50} = 83 nM) whereas the inhibitory potency decreased to 488 nM in case of the ketone derivative **18**. A pronounced selectivity regarding the CYP1A2 inhibition was observed in case of compounds **9** and **28** with IC_{50} values of approximately 1.5 μM. In most cases, the other investigated CYP enzymes were unaffected, e.g., IC_{50} values of **9** were greater than 10 μM versus CYP2B6, CYP2C9, CYP2C19, CYP2D6, and CYP3A4.

Table 2. Inhibition of selected steroidogenic and hepatic CYP enzymes *in vitro*

	% inhibition[a]		IC_{50} value[b] (nM)					
compd	CYP17[c]	CYP19[d]	CYP1A2[e,f]	CYP2B6[e,g]	CYP2C9[e,h]	CYP2C19[e,i]	CYP2D6[e,j]	CYP3A4[e,k]
9	42	47	1420	> 50000	48970	45800	11100	21070
11	41	14	83	> 25000	1888	> 25000	> 25000	1913
18	36	< 5	488	> 50000	> 200000	> 200000	> 200000	9070
28	39	7	1619	16540	1270	3540	33110	3540

[a] Mean value of four experiments, standard deviation less than 10 %. [b] Mean value of two experiments, standard deviation less than 5 %. [c] *E. coli* expressing human CYP17; substrate progesterone, 25 μM; inhibitor concentration 2.0 μM; ketoconazole, IC_{50} = 2780 nM. [d] Human placental CYP19; substrate androstenedione, 500 nM, inhibitor concentration 500 nM; fadrozole, IC_{50} = 30 nM. [e] Recombinantly expressed enzymes from baculovirus-infected insect microsomes (Supersomes). [f] Furafylline, IC_{50} = 2419 nM. [g] Tranylcypromine, IC_{50} = 6240 nM. [h] Sulfaphenazole, IC_{50} = 318 nM. [i] Tranylcypromine, IC_{50} = 5950 nM. [j] Quinidine, IC_{50} = 14 nM. [k] Ketoconazole, IC_{50} = 57 nM.

Pharmacokinetic Profile of Compounds 1, 9, and 28 (Table 3). The pharmacokinetic profile of compounds **9** and **28** was determined after peroral application to male Wistar rats and compared to the unsubstituted parent compound **1**. After administration of a 5 mg/kg dose in a cassette (N = 5), plasma samples were collected over 24 h and plasma concentrations were determined by HPLC-MS/MS. Fadrozole which was used as a reference compound displayed the highest plasma levels ($AUC_{0-\infty}$ = 3575 ng·h/mL), followed by **1** (1544 ng·h/mL) and **28** (762 ng·h/mL). At all sampling points, the amounts of **9** detected were found below the limit of quantification (1.5 ng per mL plasma). This experimental result may be either due to a fast metabolism of the aromatic amine or due to a lacking ability of this compound to permeate the cell membrane under physiological conditions. The half-lives were between 2.2–5.4 h in which the elimination of fadrozole occurs faster than the elimination of the naphthalenes **1** and **28**. Compound **28** is slowly absorbed as indicated by the t_{max} of 6 h whereas **1** is

absorbed as fast as fadrozole (t_{max} = 1 h). Furthermore, no obvious sign of toxicity was noted in any animal over the duration of the experiment (24 h).

Table 3. Pharmacokinetic profile of compounds **1**, **9**, and **28**

compd[a]	$t_{1/2\ z}$ (h)[b]	t_{max} (h)[c]	C_{max} (ng/mL)[d]	$AUC_{0-\infty}$ (ng·h/mL)[e]
1	5.4	1.0	222	1544
9	n.d.[f]	n.d.[f]	< 1.5[g]	n.d.[f]
28	3.2	6.0	81	762
fadrozole	2.2	1.0	454	3575

[a] All compounds were applied perorally at a dose of 5 mg per kg body weight in four different cassette dosing experiments using male Wistar rats. [b] Terminal half-life. [c] Time of maximal concentration. [d] Maximal concentration. [e] Area under the curve. [f] n.d. = not detectable. [g] Below the limit of quantification.

Discussion and Conclusion

The results obtained in the present study revealed that a variety of substituents in 4'- and 5'-position is tolerated with regard to the CYP11B2 potency. Most of the tested compounds were more potent than the unsubstituted parent compounds and IC_{50} values less than 1 nM were observed in 7 cases (e.g., **22** and **26**, IC_{50} = 0.2 nM). Some of the compounds were also potent CYP11B1 inhibitors (e.g., **26**, IC_{50} = 10 nM). Interestingly, a precise relationship between the inhibition of CYP11B2 and CYP11B1 was observed: An increased or decreased inhibitory activity at the one enzyme was accompanied by an increased or decreased inhibitory activity at the other enzyme. For instance, based on the unsubstituted parent compound **1**, introduction of the methoxyalkyl substituent in compound **26** resulted in an enhanced inhibition of both CYP11B2 (IC_{50} = 0.2 nM) and CYP11B1 (IC_{50} = 10 nM), whereas introduction of the hydroxy group in compound **10** resulted in a decreased inhibitory potency at both CYP11B isoforms in a comparable order of magnitude (CYP11B2, IC_{50} = 94 nM; CYP11B1, IC_{50} = 8925 nM). This trend becomes particularly evident when plotting the CYP11B2 versus the CYP11B1 pIC_{50} values of the compounds presented in Table 1 revealing a reasonable linear correlation (r^2 = 0.86, n = 29). The finding that it is to some extent possible to change the inhibitory potency by the heteroaryl derivatization without significantly changing the selectivity versus either CYP11B2 or CYP11B1 is an indication that the inhibitor binding proceeds via similar protein-inhibitor interactions of the heterocyclic moiety with both CYP11B isoforms. Contrariwise, it has been shown earlier by us that variation of the carbocyclic skeleton instead of the heterocycle can significantly influence the selectivity. Therefore, no correlation is observed for a plot of the CYP11B2 and CYP11B1 pIC_{50} values of the naphthalenes[22] and dihydronaphthalenes[23] described previously by us that are functionalized with an unsubstituted 3-pyridine as heme complexing heterocycle (r^2 = 0.30, n = 20). Consistent with these findings, it can be assumed that both enzymes, CYP11B2 and CYP11B1, are structurally more diverse in the naphthalene binding site than in the heterocyclic binding site. Interesting structure-activity relationships could also be observed with respect to electronic properties. Compounds bearing protic substituents in 5'-position rather poorly inhibited CYP11B2 whereas bioisosteric exchange by aprotic residues gave rise to highly potent aldosterone

synthase inhibitors, e.g., the inhibitory potency increased by a factor of 40 from carboxamide **17** (IC_{50} = 94 nM) to the ethanone **18** (IC_{50} = 2.1 nM). A comparable increase of potency was observed when the protic hydroxy group was replaced by the aprotic methoxy group, e.g., the IC_{50} value decreased by a factor of 20 in case of compound **11** compared to the phenol **10** or by a factor of 40 in case of compound **22** compared to the primary alcohol **21**. Similarly, the methyl esters **16** and **20** were more active than the corresponding carboxylic acids **15** and **19**. However, a lack of membrane permeability must be taken into consideration as an alternative explanation. Figure 1 shows the molecular electrostatic potentials (MEP) mapped on the electron density surface of compounds **17**, **10**, and **21** and their bioisosteric analogues **18**, **11**, and **22**. Both the shape and the geometry of the compounds as well as the electrostatic potential distribution in the naphthalene moiety are very similar. In addition, all compounds contain a region in which the nitrogen of the pyridine ring presents a negative potential. However, areas with a distinct positive potential in the pyridine moiety are present in compounds **17**, **10**, and **21** showing low inhibitory potency. In case of the highly potent bioisosters, these areas display less positive potential values with a more uniformly distributed electron charge. Hence, the difference in the electrostatic potential distribution is a reasonable explanation for the varying binding behavior within this set of compounds.

Figure 1[a]

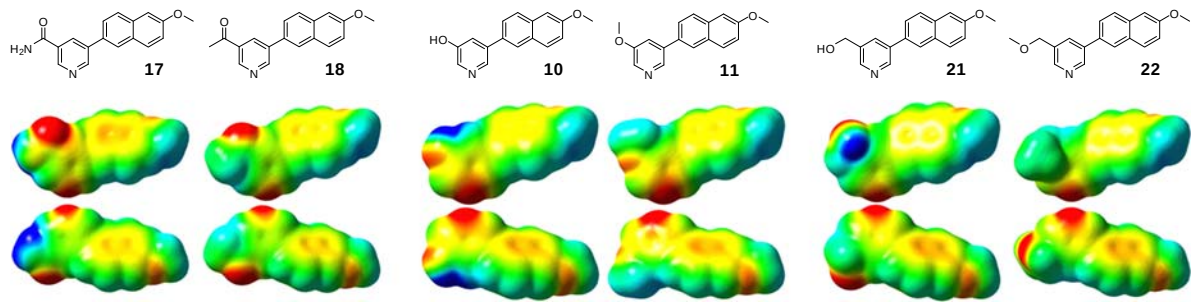

[a] MEP of compounds **17**, **18**, **10**, **11**, **21**, and **22** (front and back view). The electrostatic potential surfaces were plotted with GaussView 3.0 in a range of –18.83 kcal/mol (red) to +21.96 kcal/mol (blue).

The heteroaryl derivatization had also a noticeable influence on the CYP1A2 potency of the compounds. Most of the substituted derivatives were still inhibiting CYP1A2 for more than 90 % at a concentration of 2 µM. With respect to the compounds with a 6-methoxynaphthalene core, a slight decrease to approximately 80 % inhibition was observed in some cases. This effect was due to the introduction of substituents in 5'-position of the heterocycle. While no decrease of CYP1A2 inhibition was observed in case of the rather small substituents in compounds **10**, **11**, and **21** (hydroxy, methoxy, and hydroxymethyl), a slight increase of the sterical bulk in compounds **14**, **18**, **22**, and **25** (ethoxy, acetyl, methoxymethyl, and hydroxyethyl) resulted in a decrease in CYP1A2 inhibition to 78–85 %. On the other hand, some derivatives proved to be significantly less active with approximately 50 % inhibition of CYP1A2, including the 4'-amino-substituted compound **9** and the isoquinoline **28** with IC_{50} values of 1420 nM and 1619 nM, respectively. The effect of changing 3-pyridine by

4-isoquinoline as heme-complexing heterocycle is particularly noteworthy. The three isoquinoline derivatives **28**, **29**, and **30** are considerably less active at CYP1A2 (6–57 % inhibition) than their unsubstituted analogues **1**, **2**, and **5** (73–98 % inhibition). An explanation might be found in the geometry of these molecules. The isoquinoline constrains the rotation around the carbon–carbon bond between the heterocycle and the naphthalene, especially in presence of the additional *ortho*-methyl groups in **29** and **30**. Thus, a coplanar conformation becomes energetically disfavored compared to the pyridine analogues and the sterically demanding heterocycle rotates out of the naphthalene plane. This loss of planarity is a reasonable explanation for the reduced inhibitory potency since both CYP1A2 substrates and inhibitors are usually small-volume molecules with a planar shape (e.g., caffeine[40] and furafylline[41]). An even more drastic effect on the CYP1A2 potency was observed in case of the dihydronaphthalene type compounds. While the unsubstituted parent compound **5** exhibited 74 % inhibition, introduction of the methoxy substituent in compound **13** led to a reduction to 18 % and the isoquinoline derivative **30** displayed only 6 % inhibition. The partly saturated core structure becomes flexible and disturbs the planarity. Factors other than steric might play an additional role for the decreased CYP1A2 inhibition, e.g., disturbed π-π-stacking contacts with aromatic amino acids in the CYP1A2 binding pocket due to the reduced number of aromatic carbons. Aromaticity has been identified to correlate positively with CYP1A2 inhibition in recent QSAR studies.[42] As dihydronaphthalenes **13** and **30** were found to be unstable in DMSO solution, the low potencies might be due to substance degradation. However, the decomposition (~20 % after three days) afforded mainly the aromatized naphthalene analogues, i.e., **12** and **29** both displaying higher CYP1A2 inhibition than **13** and **30**.

In conclusion, we have shown that modifying the lead compounds **I** and **II** by introduction of substituents in the heterocyclic moiety has a clear effect on the activity and selectivity profile. Some substituents induced a significant increase in inhibitory potency versus CYP11B2. Compounds **22** and **26** with subnanomolar IC_{50} values are the most potent aldosterone synthase inhibitors so far. The undesirable high CYP1A2 inhibition that is present in the previously investigated derivatives could be overcome by certain residues, giving rise to compounds with an advantageous overall selectivity profile. It was also demonstrated that the naphthalene type aldosterone synthase inhibitors **1** and **28** were able to cross the gastrointestinal tract and reached the general circulation. Presently, the elucidated concepts are used to systematically modify other lead structures whereof some are under investigation for their ability to reduce aldosterone levels *in vivo*.

Experimental Section

Chemical and Analytical Methods. Melting points were measured on a Mettler FP1 melting point apparatus and are uncorrected. ^{1}H NMR and ^{13}C spectra were recorded on a Bruker DRX-500 instrument. Chemical shifts are given in parts per million (ppm), and tetramethylsilane (TMS) was used as internal standard for spectra obtained in DMSO-d_6 and $CDCl_3$. All coupling constants (J) are given in hertz. Mass spectra (LC/MS) were measured on a TSQ Quantum (Thermo Electron Corporation) instrument with a RP18 100-3 column (Macherey Nagel) and with water/acetonitrile

mixtures as eluents. Elemental analyses were carried out at the Department of Chemistry, University of Saarbrücken. Reagents were used as obtained from commercial suppliers without further purification. Solvents were distilled before use. Dry solvents were obtained by distillation from appropriate drying reagents and stored over molecular sieves. Flash chromatography was performed on silica gel 40 (35/40–63/70 μM) with hexane/ethyl acetate mixtures as eluents, and the reaction progress was determined by thin-layer chromatography analyses on Alugram SIL G/UV254 (Macherey Nagel). Visualization was accomplished with UV light and $KMnO_4$ solution. All microwave irradiation experiments were carried out in a CEM-Discover monomode microwave apparatus.

The following compounds were prepared according to previously described procedures: 6-Methoxy-3-methyl-3,4-dihydronaphthalen-1(2*H*)-one (**2e**),[32] (2*E*)-4-hydroxy-4-(3-methoxyphenyl)-3-methyl-2-butenoic acid (**2g**),[32] 5-bromopyridin-3-ol (**10a**).[29]

Synthesis of the Target Compounds

Procedure A.[27] Pyridine boronic acid (0.75 mmol, 1 equivalent), aryl bromide or -triflate (0.9–1.3 equivalents), and tetrakis(triphenylphosphane)palladium(0) (43 mg, 37.5 μmol, 5 mol %) were suspended in 1.5 mL DMF in a 10 mL septum-capped tube containing a stirring magnet. To this was added a solution of $NaHCO_3$ (189 mg, 2.25 mmol, 3 equivalents) in 1.5 mL water and the vial was sealed with a Teflon cap. The mixture was irradiated with microwaves for 15 min at a temperature of 150 °C with an initial irradiation power of 100 W. After the reaction, the vial was cooled to 40 °C, the crude mixture was partitioned between ethyl acetate and water and the aqueous layer was extracted three times with ethyl acetate. The combined organic layers were dried over $MgSO_4$ and the solvents were removed in vacuo. The coupling products were obtained after flash chromatography on silica gel (petroleum ether/ethyl acetate mixtures) and/or crystallization. If an oil was obtained, it was transferred into the hydrochloride salt by 1N HCl solution in diethyl ether.

Procedure B.[34] In a microwave tube alkenyl bromide **7** (1 equivalent), pyridine boronic acid (1.3 equivalent), tetrabutylammonium bromide (1 equivalent), sodium carbonate (3.5 equivalents) and palladium acetate (1.5 mol %) were suspended in water/acetone 3.5/3 to give a 0.15 M solution of bromide **7** under an atmosphere of nitrogen. The septum sealed vessel was irradiated under stirring and simultaneous cooling for 15 min at 150 °C with an initial irradiation power of 150 W. The reaction mixture was cooled to room temperature, diluted with a saturated ammonium chloride solution and extracted several times with diethyl ether. The combined extracts were washed with brine, dried over $MgSO_4$, concentrated and purified by flash chromatography on silica gel. The resulting oil was transferred into the hydrochloride salt by a 5-6 N HCl solution in 2-propanol and crystallized from ethanol.

Procedure C. To a suspension of NaH (1.15 equivalents, 60 % dispersion in oil) in 5 mL dry THF at was added dropwise a solution of alcohol (1 equivalent) in 5 mL THF at room temperature under an atmosphere of nitrogen. After hydrogen evolution ceased, a solution of methyliodide (3.3 equivalents) in 5 mL THF was added dropwise, and the resulting mixture was stirred for 5 h at room temperature.

The mixture was then treated with saturated aqueous NH_4Cl solution and extracted three times with ethyl acetate. The combined organic layers were washed with water and brine, dried over $MgSO_4$ and the solvent was evaporated in vacuo. The crude product was flash chromatographed on silica gel (petroleum ether/ethyl acetate mixtures) to afford the pure methylether. If an oil was obtained, it was transferred into the hydrochloride salt by 1N HCl solution in diethyl ether.

Procedure D. To a 0.05 M solution of carbonyl compound in dry methanol was added sodium borohydride (2 equivalents). The reaction mixture was stirred for 1 h, diluted with diehtylether and treated with saturated aqueous $NaHCO_3$ solution. The mixture was then extracted three times with ethyl acetate, washed twice with saturated aqueous $NaHCO_3$ solution and once with brine and dried over $MgSO_4$. The filtrate was concentrated in vacuo, and the residue was filtered through a short pad of silica gel or flash chromatographed on silica gel (petroleum ether/ethyl acetate mixtures) to afford the corresponding alcohols.

3-(6-Methoxy-3-methylnaphthalen-2-yl)pyridine (2) was obtained according to procedure A starting from **2a** (377 mg, 1.50 mmol) and 3-pyridineboronic acid (240 mg, 1.95 mmol) after flash chromatography on silica gel (petroleum ether/ethyl acetate, 4/1, R_f = 0.16) as a white solid (304 mg, 1.22 mmol, 81 %), mp 106–107 °C. MS *m/z* 250.06 (MH^+). Anal. ($C_{17}H_{15}NO$) C, H, N.

3-(6-Methoxy-3-methyl-3,4-dihydronaphthalen-2-yl)pyridine (5) was obtained according to procedure B starting from **2b** (127 mg, 0.50 mmol) and 3-pyridineboronic acid (80 mg, 0.65 mmol) after flash chromatography on silica gel (petroleum ether/ethyl acetate, 4/1, R_f = 0.20), precipitation as HCl salt and crystallization from ethanol as a white solid (50 mg, 0.17 mmol, 35 %), mp (HCl salt) 186–187 °C. MS *m/z* 252.02 (MH^+). Anal. ($C_{17}H_{17}NO \cdot HCl \cdot 0.2H_2O$) C, H, N.

6-(Pyridin-3-yl)-7,8-dihydronaphthalene-2-carbonitrile (6) was prepared according to procedure A starting from 3-pyridineboronic acid (107 mg, 0.87 mmol) and **6a** (189 mg, 0.62 mmol). After flash chromatography on silica gel (petroleum ether/ethyl acetate, 2/1, R_f = 0.10) pure **6** was obtained as a white, crystalline solid (100 mg, 0.43 mmol, 69 %). Treatment with hydrochloride acid (0.1 N in Et_2O) yielded the hydrochloride salt of **6** (110 mg, 0.41 mmol, 66 %) as a white solid, mp (HCl salt) 264–268 °C. MS *m/z* 223.23 (MH^+). Anal. ($C_{16}H_{12}N_2 \cdot HCl \cdot 0.4H_2O$) C, H, N.

3-(6-Methoxynaphthalen-2-yl)-4-methylpyridine (7) was prepared according to procedure A starting from 6-methoxy-2-naphthaleneboronic acid (131 mg, 0.65 mmol) and 3-bromo-4-methylpyridine (86 mg, 0.50 mmol). After flash chromatography on silica gel (petroleum ether/ethyl acetate, 7/3, R_f = 0.10) pure **7** was obtained as a white solid (65 mg, 0.26 mmol, 52 %), mp (HCl salt) 172–174 °C. MS *m/z* 250.30 (MH^+). Anal. ($C_{17}H_{15}NO \cdot HCl \cdot 0.1H_2O$) C, H, N.

6-(4-Methylpyridin-3-yl)-2-naphthonitrile (8). Triflate **8a** (151 mg, 0.50 mmol), 4-methyl-3-pyridineboronic acid (89 mg, 0.65 mmol), K_2CO_3 (138 mg, 1.0 mmol) and $Pd(dppf)Cl_2$ (37 mg, 0.05 mmol) were suspended in 4.0 mL of a 4:4:1 mixture of toluene/acetone/water. This mixture was heated to 125 °C by microwave irradiation for 15 minutes (initial irradiation power 150 W). After cooling to room temperature, 15 mL of distilled water were added and the reaction mixture was extracted four times with 10 mL of Et_2O. After washing the combined organic fractions with water

(twice) and brine, drying over $MgSO_4$ and evaporation of the solvent crude product **8** was obtained as a yellow solid (127 mg). Further purification by flash chromatography on silica gel (petroleum ether/ethyl acetate, 2/5, R_f = 0.20) and subsequent crystallization of the free base as hydrochloride salt gave 52 mg (0.19 mmol, 37 %) of pure **8** (HCl salt) as an yellowish solid, mp (HCl salt) decomposition above 210 °C. MS *m/z* 245.30 (MH^+). Anal. ($C_{17}H_{12}N_2 \cdot HCl \cdot 0.5H_2O$) C, H, N.

3-(6-Methoxynaphthalen-2-yl)pyridin-4-amine (9) was prepared according to procedure A starting from 6-methoxy-2-naphthaleneboronic acid (131 mg, 0.65 mmol) and 3-bromopyridin-4-amine (86 mg, 0.50 mmol). After crystallization from acetone pure **9** was obtained as a white solid (39 mg, 0.16 mmol, 31 %), mp 155–156 °C. MS *m/z* 251.28 (MH^+). Anal. ($C_{16}H_{14}N_2O$) C, H, N.

5-(6-Methoxynaphthalen-2-yl)pyridin-3-ol (10) was prepared according to procedure A starting from 6-methoxy-2-naphthaleneboronic acid (131 mg, 0.65 mmol) and **10a** (87 mg, 0.50 mmol). After crystallization from acetone/diethyl ether pure **10** was obtained as an off-white solid (86 mg, 0.34 mmol, 68 %), mp 172–175 °C. MS *m/z* 252.02 (MH^+). Anal. ($C_{16}H_{13}NO_2 \cdot 0.7H_2O$) C, H, N: calcd, 5.31, found, 5.79.

3-Methoxy-5-(6-methoxynaphthalen-2-yl)pyridine (11) was prepared according to procedure A starting from 6-methoxy-2-naphthaleneboronic acid (131 mg, 0.65 mmol) and 3-bromo-5-methoxypyridine (94 mg, 0.50 mmol). After flash chromatography on silica gel (petroleum ether/ethyl acetate, 7/3, R_f = 0.10) pure **11** was obtained as a white solid (80 mg, 0.30 mmol, 60 %), mp (HCl salt) 211–214 °C. ^{1}H-NMR (500 MHz, CD_3OD): δ = 3.96 (s, 3H), 4.15 (s, 3H), 7.23 (dd, ^3J = 9.1 Hz, ^4J = 2.5 Hz, 1H), 7.32 (d, ^4J = 2.2 Hz, 1H), 7.85 (dd, ^3J = 8.5 Hz, ^4J = 1.9 Hz, 1H), 7.92 (d, ^3J = 8.8 Hz, 1H), 7.97 (d, ^3J = 8.5 Hz, 1H), 8.29 (d, ^4J = 1.5 Hz, 1H), 8.52 (s, 1H), 8.54 (s, 1H), 8.86 (s, 1H). ^{13}C-NMR (125 MHz, CD_3OD): δ = 57.9, 58.3, 108.5, 120.9, 121.9, 128.1, 128.5, 130.2, 131.4, 132.5, 134.5, 136.7, 138.9, 139.1, 142.6, 158.4, 160.4. MS *m/z* 266.26 (MH^+). Anal. ($C_{17}H_{15}NO_2 \cdot HCl \cdot 0.3H_2O$) C, H, N.

3-Methoxy-5-(6-methoxy-3-methylnaphthalen-2-yl)pyridine (12) was obtained according to procedure A starting from **2a** (377 mg, 1.50 mmol) and 5-methoxy-3-pyridineboronic acid (298 mg, 1.95 mmol) after flash chromatography on silica gel (petroleum ether/ethyl acetate, 3/1, R_f = 0.16) as a white solid (328 mg, 1.17 mmol, 78 %), mp 106–107 °C. ^{1}H-NMR (500 MHz, $CDCl_3$): δ = 2.40 (s, 3H), 3.91 (s, 3H), 3.94 (s, 3H), 7.12 (m, 2H), 7.23 (dd, ^4J = 2.8 Hz, ^4J = 1.9 Hz, 1H), 7.62 (s, 1H), 7.64 (s, 1H), 7.71 (d, ^3J = 8.8 Hz, 1H), 8.28 (d, ^4J = 1.9 Hz, 1H), 8.33 (d, ^4J = 2.8 Hz, 1H). ^{13}C-NMR (125 MHz, $CDCl_3$): δ = 21.0, 55.3, 55.6, 104.9, 118.6, 121.5, 127.4, 127.5, 128.6, 129.2, 134.1, 134.4, 134.5, 135.8, 138.0, 142.6, 155.2, 158.1. MS *m/z* 280.08 (MH^+). Anal. ($C_{18}H_{17}NO_2$) C, H, N.

3-Methoxy-5-(6-methoxy-3-methyl-3,4-dihydronaphthalen-2-yl)pyridine (13) was obtained according to procedure B starting from **2b** (253 mg, 1.00 mmol) and 5-methoxy-3-pyridineboronic acid (199 mg, 1.30 mmol) after flash chromatography on silica gel (petroleum ether/ethyl acetate, 4/1, R_f = 0.14), precipitation as HCl salt and crystallization from ethanol as a yellow solid (84 mg, 0.26 mmol, 26 %), mp (HCl salt) 181–182 °C. ^{1}H-NMR (500 MHz, CD_3OD): δ = 0.94 (d, ^3J = 7.0 Hz,

3H), 2.71 (dd, ^2J = 15.3 Hz, ^3J = 1.2 Hz, 1H), 3.02 (m, 1H), 3.13 (dd, ^2J = 15.5 Hz, ^3J = 6.4 Hz, 1H), 3.74 (s, 3H), 4.01 (s, 3H), 6.72 (m, 2H), 7.15 (d, ^3J = 8.2 Hz, 1H), 7.19 (s, 1H), 8.22 (m, 1H), 8.34 (d, ^4J = 2.4 Hz, 1H), 8.59 (d, ^4J = 1.5 Hz, 1H). ^{13}C-NMR (125 MHz, CD_3OD): δ = 17.8, 30.6, 36.7, 55.8, 57.9, 112.9, 115.6, 116.6, 127.0, 127.2, 127.8, 129.8, 130.3, 132.3, 137.1, 137.2, 150.9, 160.1. MS *m/z* 281.96 (MH^+). Anal. ($C_{18}H_{19}NO_2 \cdot HCl \cdot 0.2H_2O$) C, H, N.

3-Ethoxy-5-(6-methoxynaphthalen-2-yl)pyridine (14) was prepared according to procedure A starting from 6-methoxy-2-naphthaleneboronic acid (131 mg, 0.65 mmol) and **14a** (101 mg, 0.50 mmol). After crystallization from ethyl acetate/petroleum ether pure **14** was obtained as a white solid (33 mg, 0.17 mmol, 23 %), mp decomposition above 130 °C. MS *m/z* 280.05 (MH^+). Anal. ($C_{18}H_{17}NO_2 \cdot 0.2H_2O$) C, H, N.

5-(6-Methoxynaphthalen-2-yl)pyridine-3-carboxylic acid (15) was prepared according to procedure A starting from 6-methoxy-2-naphthaleneboronic acid (131 mg, 0.65 mmol) and 5-bromonicotinic acid (101 mg, 0.50 mmol). After crystallization from methanol/water pure **15** was obtained as an off-white solid (74 mg, 0.26 mmol, 53 %), mp decomposition above 300 °C. MS *m/z* 279.98 (MH^+). Anal. ($C_{17}H_{13}NO_3 \cdot HCl \cdot 0.3H_2O$) C, H, N.

Methyl 5-(6-methoxynaphthalen-2-yl)pyridine-3-carboxylate (16). Carboxylic acid **15** (45 mg, 0.16 mmol) was dissolved in 20 mL dry methanol and 0.05 mL concentrated H_2SO_4 (98%) was added. The whole mixture was refluxed for 10 h and thereafter the excess methanol was distilled off. The residue was taken up in 50 mL ethyl acetate and the organic layer was washed several times with 5 % aqueous Na_2CO_3 solution, water and brine. After drying over $MgSO_4$, the solvent was evaporated in vacuo. After flash chromatography on silica gel (petroleum ether/ethyl acetate, 7/3, R_f = 0.34) pure **16** was obtained as an off-white solid (28 mg, 0.10 mmol, 60 %), mp 150–151 °C. MS *m/z* 293.97 (MH^+). Anal. ($C_{18}H_{14}NO_3$) C, H, N.

5-(6-Methoxynaphthalen-2-yl)pyridine-3-carboxamide (17) was prepared according to procedure A starting from 6-methoxy-2-naphthaleneboronic acid (131 mg, 0.65 mmol) and 5-bromonicotinamide (92 mg, 0.50 mmol). After crystallization from acetone/diethyl ether pure **17** was obtained as a white solid (55 mg, 0.20 mmol, 40 %), mp 245–247 °C. MS *m/z* 279.07 (MH^+). Anal. ($C_{17}H_{14}N_2O_2$) C, H, N.

1-[5-(6-Methoxynaphthalen-2-yl)pyridin-3-yl]ethanone (18) was prepared according to procedure A starting from 6-methoxy-2-naphthaleneboronic acid (131 mg, 0.65 mmol) and 3-acetyl-5-bromopyridine (100 mg, 0.50 mmol). After crystallization from acetone/diethyl ether pure **18** was obtained as a white solid (75 mg, 0.27 mmol, 54 %), mp 159–160 °C. MS *m/z* 278.09 (MH^+). Anal. ($C_{18}H_{15}NO_2 \cdot 0.1H_2O$) C, H, N.

[5-(6-Methoxynaphthalen-2-yl)pyridin-3-yl]acetic acid (19) was prepared according to procedure A starting from 6-methoxy-2-naphthaleneboronic acid (131 mg, 0.65 mmol) and 5-bromo-3-pyridineacetic acid (108 mg, 0.50 mmol). After crystallization from methanol/water pure **19** was obtained as a white solid (70 mg, 0.24 mmol, 48 %), mp decomposition above 210 °C. MS *m/z* 293.97 (MH^+). Anal. ($C_{18}H_{15}NO_3 \cdot 0.5H_2O$) C, H, N.

Methyl [5-(6-methoxynaphthalen-2-yl)pyridin-3-yl]acetate (20) was prepared as described for **16** starting from **19** (145 mg, 0.49 mmol). After flash chromatography on silica gel (petroleum ether/ethyl acetate, 1/1, R_f = 0.18) pure **20** was obtained as a white solid (81 mg, 0.26 mmol, 53 %), mp 145–146 °C. MS *m/z* 308.04 (MH^+). Anal. ($C_{19}H_{17}NO_3$) C: calcd, 74.25, found, 74.72, H, N.

[5-(6-Methoxynaphthalen-2-yl)pyridin-3-yl]methanol (21) was prepared according to procedure A starting from 6-methoxy-2-naphthaleneboronic acid (131 mg, 0.65 mmol) and **21a** (94 mg, 0.50 mmol). After crystallization from acetone/diethyl ether pure **21** was obtained as a white solid (86 mg, 0.32 mmol, 65 %), mp 193–194 °C. MS *m/z* 266.05 (MH^+). Anal. ($C_{17}H_{15}NO_2 \cdot 0.1H_2O$) C, H, N.

3-(Methoxymethyl)-5-(6-methoxynaphthalen-2-yl)pyridine (22) was prepared according to procedure C starting from **21** (150 mg, 0.57 mmol) using methyl iodide (82 µL, 1.32 mmol). After flash chromatography on silica gel (petroleum ether/ethyl acetate, 1/1, R_f = 0.22) pure **22** was obtained as an off-white solid (80 mg, 0.29 mmol, 50 %), mp 121–122 °C. MS *m/z* 279.91 (MH^+). Anal. ($C_{18}H_{17}NO_2$) C, H, N.

[4-(6-Methoxynaphthalen-2-yl)pyridin-3-yl]methanol (23) was prepared according to procedure A starting from 6-methoxy-2-naphthaleneboronic acid (131 mg, 0.65 mmol) and **23a** (94 mg, 0.50 mmol). After crystallization from acetone/diethyl ether pure **23** was obtained as a white solid (90 mg, 0.34 mmol, 68 %), mp decomposition above 240 °C. MS *m/z* 266.05 (MH^+). Anal. ($C_{17}H_{15}NO_2 \cdot 0.2H_2O$) C, H, N.

4-(Methoxymethyl)-3-(6-methoxynaphthalen-2-yl)pyridine (24) was prepared according to procedure C starting from **23** (150 mg, 0.57 mmol) using methyl iodide (82 µL, 1.32 mmol). After flash chromatography on silica gel (petroleum ether/ethyl acetate, 1/1, R_f = 0.23) pure **24** was obtained as an off-white solid (74 mg, 0.26 mmol, 46 %), mp (HCl salt) 174–177 °C. MS *m/z* 279.91 (MH^+). Anal. ($C_{18}H_{17}NO_2 \cdot 0.2H_2O$) C, H, N.

1-[5-(6-Methoxynaphthalen-2-yl)-pyridin-3-yl]ethanol (25) was prepared according to procedure D starting from **18** (50 mg, 0.18 mmol) using $NaBH_4$ (8.0 mg, 0.21 mmol). After flash chromatography on silica gel (petroleum ether/ethyl acetate, 1/1, R_f = 0.24) pure **25** was obtained as a white solid (28 mg, 0.10 mmol, 56 %), mp 154–155 °C. MS *m/z* 280.05 (MH^+). Anal. ($C_{18}H_{17}NO_2$) C, H, N.

3-(1-Methoxyethyl)-5-(6-methoxynaphthalen-2-yl)pyridine (26) was prepared according to procedure C starting from **25** (70 mg, 0.25 mmol) using methyl iodide (41 µL, 0.66 mmol). After flash chromatography on silica gel (petroleum ether/ethyl acetate, 1/1, R_f = 0.23) pure **26** was obtained as an yellowish solid (26 mg, 0.08 mmol, 35 %), mp 124–125 °C. MS *m/z* 294.11 (MH^+). Anal. ($C_{19}H_{19}NO_2$) C, H, N.

3-(6-Methoxynaphthalen-2-yl)-5-phenylpyridine (27) was prepared according to procedure A starting from 6-methoxy-2-naphthaleneboronic acid (394 mg, 1.95 mmol) and 3-bromo-5-phenylpyridine (351 mg, 1.50 mmol). After flash chromatography on silica gel (petroleum ether/ethyl acetate, 2/1, R_f = 0.23) pure **27** was obtained as a white, crystalline solid (455 mg, 1.46 mmol, 97 %), mp 216–217 °C. MS *m/z* 312.09 (MH^+). Anal. ($C_{22}H_{17}NO \cdot 0.4H_2O$) C, H, N.

4-(6-Methoxynaphthalen-2-yl)isoquinoline (28) was prepared according to procedure A starting from 6-methoxy-2-naphthaleneboronic acid (131 mg, 0.65 mmol) and 4-bromoisoquinoline (104 mg, 0.50 mmol). After flash chromatography on silica gel (petroleum ether/ethyl acetate, 7/3, R_f = 0.21) pure **28** was obtained as a white solid (44 mg, 0.16 mmol, 31 %), mp 185–186 °C. MS *m/z* 286.07 (MH^+). Anal. ($C_{20}H_{15}NO \cdot 0.1H_2O$) C, H, N.

4-(6-Methoxy-3-methylnaphthalen-2-yl)isoquinoline (29) was obtained according to procedure A starting from **2a** (377 mg, 1.50 mmol) and 4-isoquinolineboronic acid (337 mg, 1.95 mmol) after flash chromatography on silica gel (dichloromethane/methanol 99/1, R_f = 0.26) as yellow oil which solidified with diethyl ether as a pale yellow solid (178 mg, 0.59 mmol, 40 %), mp 156–157 °C. MS *m/z* 300.10 (MH^+). Anal. ($C_{21}H_{11}NO$) C, H, N.

4-(6-Methoxy-3-methyl-3,4-dihydronaphthalen-2-yl)isoquinoline (30) was obtained according to procedure B starting from **2b** (253 mg, 1.00 mmol) and 4-isoquinolineboronic acid (225 mg, 1.30 mmol) after two flash chromatographical separations on silica gel (petroleum ether/ethyl acetate, 5/1, R_f = 0.20 and dichloromethane/methanol 99/1, R_f = 0.27) and precipitation as HCl salt as a yellow solid (112 mg, 0.33 mmol, 17 %), mp 149–150 °C. MS *m/z* 302.18 (MH^+). Anal. ($C_{21}H_{19}NO \cdot HCl \cdot 0.2H_2O$) C, H, N.

Biological Methods. 1. Enzyme Preparations. CYP17 and CYP19 preparations were obtained by described methods: the 50,000 *g* sediment of *E. coli* expressing human CYP17[37] and microsomes from human placenta for CYP19.[39] **2. Enzyme Assays.** The following enzyme assays were performed as previously described: CY17[37] and CYP19.[39] **3. Activity and Selectivity Assay Using V79 Cells.** V79 MZh 11B1 and V79 MZh 11B2 cells[36] were incubated with [4-^{14}C]-11-deoxycorticosterone as substrate and inhibitor in at least three different concentrations. The enzyme reactions were stopped by addition of ethyl acetate. After vigorous shaking and a centrifugation step (10,000 *g*, 2 min), the steroids were extracted into the organic phase, which was then separated. The conversion of the substrate was analyzed by HPTLC and a phosphoimaging system as described.[10,22] **4. Inhibition of Human Hepatic CYP Enzymes.** The recombinantly expressed enzymes from baculovirus-infected insect microsomes (Supersomes) were used and the manufacturer's instructions (www.gentest.com) were followed. **5. *In Vivo* Pharmacokinetics.** Animal trials were conducted in accordance with institutional and international ethical guidelines for the use of laboratory animals. Male Wistar rats weighing 317–322 g (Janvier, France) were housed in a temperature-controlled room (20–22 °C) and maintained in a 12 h light/12 h dark cycle. Food and water were available *ad libitum*. The animals were anaesthetised with a ketamine (135mg/kg)/xylazine (10mg/kg) mixture, and cannulated with silicone tubing via the right jugular vein. Prior to the first blood sampling, animals were connected to a counterbalanced system and tubing, to perform blood sampling in the freely moving rat. Separate stock solutions (5 mg/mL) were prepared for the tested compounds in Labrasol/Water (1:1; v/v), leading to a clear solution. Immediately before application, the cassette dosing mixture was prepared by adding equal volumes of the 5 stock solutions to end up with a final concentration of 1 mg/mL for each compound. The mixture was applied perorally to 3 rats with an injection volume of 5 mL/kg

(Time 0). 400 µL of blood were taken via jugularis catheter 1 hour before application and then 1 and 2 hours after application. Immediately, equal volume (400 µL) of 0.9 % NaCl (37 °C) was re-injected intravenously to keep the blood volume stable. 4, 6, 8, 10 and 24 hours after application 250 µL of blood were sampled without balancing the blood volume. Blood samples were centrifuged at 3000 *g* for 10 minutes at 4 °C. Plasma was harvested and kept at –20 °C until analysis. The mean of absolute plasma concentrations (±SEM) was calculated for the 3 rats and the regression was performed on group mean values. The pharmacokinetic analysis was performed using a noncompartment model (PK Solutions 2.0, Summit Research Services). HPLC-MS/MS analysis and quantification of the samples was carried out on a Surveyor-HPLC-system coupled with a TSQ Quantum (ThermoFinnigan) triple quadrupole mass spectrometer equipped with an electrospray interface (ESI).

Computational Methods. MEP. For each docked compound geometry optimization was performed at the B3LYP/6-31G* density functional levels by means of the Gaussian03 software and the molecular electrostatic potential (MEP) maps were plotted using GaussView3, the 3-D molecular graphics package of Gaussian.[43] These electrostatic potential surfaces were generated by mapping 6-31G* electrostatic potentials onto surfaces of molecular electron density (isovalue = 0.002 electron/Å).[44]

Acknowledgement. We thank Ms. Gertrud Schmitt and Ms. Jeannine Jung for their help in performing the *in vitro* tests. S. L. is grateful to Saarland University for a scholarship (Landesgraduierten-Förderung). Thanks are due to Prof. J. J. Rob Hermans, University of Maastricht, The Netherlands, for supplying the V79 CYP11B1 cells, and Prof. Rita Bernhardt, Saarland University, for supplying the V79 CYP11B2 cells.

Supporting Information Available: Individual plasma levels of each compound and animal, graphs and equations of the linear regression of pIC_{50} values, NMR-spectroscopic data of compounds **2**, **5**–**10**, **14**–**30**, full experimental details and spectroscopic characterization of the reaction intermediates **2a**–**2d**, **2f**, **6a**, **6b**, **8a**, **14a**, **21a**, **23a**, elemental analysis results of compounds **2**, **5**–**30**. This information is available free of charge via the Internet at http://pubs.acs.org.

References

(1) (a) Takeda Y. Vascular synthesis of aldosterone: role in hypertension. *Mol. Cell. Endocrinol.* **2004**, *217*, 75–79. (b) Davies, E.; MacKenzie, S. M. Extra-adrenal production of corticosteroids. *Clin. Exp. Pharmacol. Physiol.* **2003**, *30*, 437–445.

(2) Kawamoto, T.; Mitsuuchi, Y.; Toda, K.; Yokoyama, Y.; Miyahara, K.; Miura, S.; Ohnishi, T.; Ichikawa, Y.; Nakao, K.; Imura, H.; Ulick, S.; Shizuta, Y. Role of steroid 11β-hydroxylase and steroid 18-hydroxylase in the biosynthesis of glucocorticoids and mineralocorticoids in humans. *Proc. Natl. Acad. Sci. U.S.A.* **1992**, *89*, 1458–1462.

(3) (a) Brilla, C. G. Renin-angiotensin-aldosterone system and myocardial fibrosis. *Cardiovasc. Res.* **2000**, *47*, 1–3. (b) Lijnen, P.; Petrov, V. Induction of cardiac fibrosis by aldosterone. *J. Mol. Cell. Cardiol.* **2000**, *32*, 865–879.

(4) Pitt, B.; Zannad, F.; Remme, W. J.; Cody, R.; Castaigne, A.; Perez, A.; Palensky, J.; Wittes, J. The effect of spironolactone on morbidity and mortality in patients with severe heart failure. *N. Engl. J. Med.* **1999**, *341*, 709–717.

(5) Pitt, B.; Remme, W.; Zannad, F.; Neaton, J.; Martinez, F.; Roniker, B.; Bittman, R.; Hurley, S.; Kleiman, J.; Gatlin, M. Eplerenone, a selective aldosterone blocker, in patients with left ventricular dysfunction after myocardial infarction. *N. Eng. J. Med.* **2003**, *348*, 1309–1321.

(6) Khan, N. U. A.; Movahed, A. The role of aldosterone and aldosterone-receptor antagonists in heart failure. *Rev. Cardiovasc. Med.* **2004**, *5*, 71–81.

(7) Bell, M. G.; Gernert, D. L.; Grese, T. A.; Belvo, M. D.; Borromeo, P. S.; Kelley, S. A.; Kennedy, J. H.; Kolis, S. P.; Lander, P. A.; Richey, R.; Sharp, V. S.; Stephenson, G. A.; Williams, J. D.; Yu, H.; Zimmerman, K. M.; Steinberg, M. I.; Jadhav, P. K. (S)-N-{3-[1-Cyclopropyl-1-(2,4-difluoro-phenyl)-ethyl]-1H-indol-7-yl}-methanesulfonamide: A potent, nonsteroidal, functional antagonist of the mineralocorticoid receptor. *J. Med. Chem.* **2007**, *50*, 6443–6445.

(8) (a) Delcayre, C.; Swynghedauw, B. Molecular mechanisms of myocardial remodeling. The role of aldosterone. *J. Mol. Cell. Cardiol.* **2002**, *34*, 1577–1584. (b) de Resende, M. M.; Kauser, K.; Mill, J. G. Regulation of cardiac and renal mineralocorticoid receptor expression by captopril following myocardial infarction in rats. *Life Sci.* **2006**, *78*, 3066–3073.

(9) (a) Wehling, M. Specific, nongenomic actions of steroid hormones. *Annu. Rev. Physiol.* **1997**, *59*, 365–393. (b) Lösel, R.; Wehling, M. Nongenomic actions of steroid hormones. *Nature Rev. Mol. Cell. Biol.* **2003**, *4*, 46–55. (c) Chai, W.; Garrelds, I. M.; Arulmani, U.; Schoemaker, R. G.; Lamers, J. M. J.; Danser, A. H. J.; Genomic and nongenomic effects of aldosterone in the rat heart: Why is spironolactone cardioprotective? *Br. J. Pharmacol.* **2005**, *145*, 664–671. (d) Chai, W.; Garrelds, I. M.; de Vries, R.; Batenburg, W. W.; van Kats, J. P.; Danser, A. H. J. Nongenomic effects of aldosterone in the human heart: Interaction with angiotensin II. *Hypertension* **2005**, *46*, 701–706.

(10) Ehmer, P. B.; Bureik, M.; Bernhardt, R.; Müller, U.; Hartmann, R. W. Development of a test system for inhibitors of human aldosterone synthase (CYP11B2): Screening in fission yeast and evaluation of selectivity in V79 cells. *J. Steroid Biochem. Mol. Biol.* **2002**, *81*, 173–179.

(11) Hartmann, R. W.; Müller, U.; Ehmer, P. B. Discovery of selective CYP11B2 (aldosterone synthase) inhibitors for the therapy of congestive heart failure and myocardial fibrosis. *Eur. J. Med. Chem.* **2003**, *38*, 363–366.

(12) (a) Yamakita, N.; Chiou, S.; Gomez-Sanchez, C. E. Inhibition of aldosterone biosynthesis by 18-ethynyl-deoxycorticosterone. *Endocrinology* **1991**, *129*, 2361–2366. (b) Hartmann, R. W. Selective inhibition of steroidogenic P450 enzymes: Current status and future perspectives. *Eur. J. Pharm. Sci.* **1994**, *2*, 15–16.

(13) (a) Viger, A.; Coustal, S.; Perard, S.; Piffeteau, A.; Marquet, A. 18-Substituted progesterone derivatives as inhibitors of aldosterone biosynthesis. *J. Steroid Biochem.* **1989**, *33*, 119–124. (b) Delorme, C.; Piffeteau, A.; Viger, A.; Marquet, A. Inhibition of bovine cytochrome P-$450_{11\beta}$ by 18-unsaturated progesterone derivatives. *Eur. J. Biochem.* **1995**, *232*, 247–256. (c) Delome, C.; Piffeteau, A.; Sobrio, F.; Marquet, A. Mechanism-based inactivation of bovine cytochrome P-$450_{11\beta}$ by 18-unsaturated progesterone derivatives. *Eur. J. Biochem.* **1997**, *248*, 252–260.

(14) Davioud, E.; Piffeteau, A.; Delorme, C.; Coustal, S.; Marquet, A. 18-Vinyldeoxycorticosterone: a potent inhibitor of the bovine cytochrome P-$450_{11\beta}$. *Bioorg. Med. Chem.* **1998**, *6*, 1781–1788.

(15) Taymans, S. E.; Pack, S.; Pak, E.; Torpy, D. J.; Zhuang, Z.; Stratakis, C. A. Human CYP11B2 (aldosterone synthase) maps to chromosome 8q24.3. *J. Clin. Endocrinol. Metab.* **1998**, *83*, 1033–1036.

(16) (a) Häusler, A.; Monnet, G.; Borer, C.; Bhatnagar, A. S. Evidence that corticosterone is not an obligatory intermediate in aldosterone biosynthesis in the rat adrenal. *J. Steroid Biochem.* **1989**, *34*, 567–570. (b) Demers, L. M.; Melby, J. C.; Wilson, T. E.; Lipton, A.; Harvey, H. A.; Santen, R. J. The effects of CGS 16949A, an aromatase inhibitor on adrenal mineralocorticoid biosynthesis. *J. Clin. Endocrinol. Metab.* **1990**, *70*, 1162–1166.

(17) Fiebeler, A.; Nussberger, J.; Shagdarsuren, E.; Rong, S.; Hilfenhaus, G.; Al-Saadi, N.; Dechend, R.; Wellner, M.; Meiners, S.; Maser-Gluth, C.; Jeng, A. Y.; Webb, R. L.; Luft, F. C.; Muller, D. N. Aldosterone synthase inhibitor ameliorates angiotensin II-induced organ damage. *Circulation* **2005**, *111*, 3087–3094.

(18) (a) Ksander, G.; Hu, Q.-Y. Fused imidazole derivatives for the treatment of disorders mediated by aldosterone synthase and/or 11-beta-hydroxylase and/or aromatase. PCT Int. Appl. WO2008027284, 2008. (b) Papillon J.; Ksander, G. M; Hu, Q.-Y. Preparation of tetrahydroimidazo[1,5-a]pyrazine derivatives as aldosterone synthase and/or 11β-hydroxylase inhibitors. PCT Int. Appl. WO2007139992, 2007. (c) Adams, C.; Papillon, J.; Ksander, G. M. Preparation of imidazole derivatives as aldosterone synthase inhibitors. PCT Int. Appl. WO2007117982, 2007. (d) Ksander, G. M.; Meredith, E.; Monovich, L. G.; Papillon, J.; Firooznia, F.; Hu, Q.-Y. Preparation of condensed imidazole derivatives for the inhibition of aldosterone synthase and aromatase. PCT Int. Appl. WO2007024945, 2007. (e) Firooznia, F. Preparation of imidazo[1,5a]pyridine derivatives for treatment of aldosterone mediated diseases. PCT Int. Appl. WO2004046145, 2004. (f) McKenna, J. Preparation of imidazopyrazines and imidazodiazepines as agents for the treatment of aldosterone mediated conditions. PCT Int. Appl. WO2004014914, 2004.

(19) (a) Herold, P.; Mah, R.; Tschinke, V.; Stojanovic, A.; Marti, C.; Jelakovic, S.; Stutz, S. Preparation of imidazo compounds as aldosterone synthase inhibitors. PCT Int. Appl. WO2007116099, 2007. (b) Herold, P.; Mah, R.; Tschinke, V.; Stojanovic, A.; Marti, C.; Jelakovic, S.; Bennacer, B.; Stutz, S. Preparation of spiro-imidazo derivatives as aldosterone synthase inhibitors. PCT Int. Appl. WO2007116098, 2007. (c) Herold, P.; Mah, R.; Tschinke, V.; Stojanovic, A.; Marti, C.; Stutz, S. Preparation of imidazo compounds as aldosterone synthase inhibitors. PCT Int. Appl. WO2007116097, 2007. (d) Herold, P.; Mah, R.; Tschinke, V.; Quirmbach, M.; Marti, C.; Stojanovic, A.; Stutz, S. Preparation of fused imidazoles as aldosterone synthase inhibitors. PCT Int. Appl. WO2007065942, 2007. (e) Herold, P.; Mah, R.; Tschinke, V.; Stojanovic, A.; Marti, C.; Jotterand, N.; Schumacher, C.; Quirmbach, M. Preparation of heterocyclic

spiro-compounds as aldosterone synthase inhibitors. PCT Int. Appl. WO2006128853, 2006. (f) Herold, P.; Mah, R.; Tschinke, V.; Stojanovic, A.; Marti, C.; Jotterand, N.; Schumacher, C.; Quirmbach, M. Preparation of heterocyclic spiro-compounds as aldosterone synthase inhibitors. PCT Int. Appl. WO2006128852, 2006. (g) Herold, P.; Mah, R.; Tschinke, V.; Stojanovic, A.; Marti, C.; Jotterand, N.; Schumacher, C.; Quirmbach, M. Preparation of fused imidazoles as aldosterone synthase inhibitors. PCT Int. Appl. WO2006128851, 2006. (h) Herold, P.; Mah, R.; Tschinke, V.; Schumacher, C.; Marti, C.; Quirmbach, M. Preparation of fused heterocycles as aldosterone synthase inhibitors. PCT Int. Appl. WO2006005726, 2006. (i) Herold, P.; Mah, R.; Tschinke, V.; Schumacher, C.; Quirmbach, M. Preparation of imidazopyridines and related analogs as aldosterone synthase inhibitors. PCT Int. Appl. WO2005118557, 2005. (j) Herold, P.; Mah, R.; Tschinke, V.; Schumacher, C.; Quirmbach, M. Preparation of tetrahydro-imidazo[1,5-a]pyridin derivatives as aldosterone synthase inhibitors. PCT Int. Appl. WO2005118581, 2005. (k) Herold, P.; Mah, R.; Tschinke, V.; Schumacher, C.; Behnke, D.; Quirmbach, M. Preparation of nitrogen-containing heterobicyclic compounds as aldosterone synthase inhibitors. PCT Int. Appl. WO2005118541, 2005.

(20) Ulmschneider, S.; Müller-Vieira, U.; Mitrenga, M.; Hartmann, R. W.; Oberwinkler-Marchais, S.; Klein, C. D.; Bureik, M.; Bernhardt, R.; Antes, I.; Lengauer, T. Synthesis and evaluation of imidazolylmethylenetetrahydronaphthalenes and imidazolylmethyleneindanes: Potent inhibitors of aldosterone synthase. *J. Med. Chem.* **2005**, *48*, 1796–1805.

(21) Ulmschneider, S.; Müller-Vieira, U.; Klein, C. D.; Antes, I.; Lengauer, T.; Hartmann, R. W. Synthesis and evaluation of (pyridylmethylene)tetrahydronaphthalenes/-indanes and structurally modified derivatives: Potent and selective inhibitors of aldosterone synthase. *J. Med. Chem.* **2005**, *48*, 1563–1575.

(22) Voets, M.; Antes, I.; Scherer, C.; Müller-Vieira, U.; Biemel, K.; Barassin, C.; Oberwinkler-Marchais, S.; Hartmann, R. W. Heteroaryl substituted naphthalenes and structurally modified derivatives: Selective inhibitors of CYP11B2 for the treatment of congestive heart failure and myocardial fibrosis. *J. Med. Chem.* **2005**, *48*, 6632–6642.

(23) Voets, M.; Antes, I.; Scherer, C.; Müller-Vieira, U.; Biemel, K.; Oberwinkler-Marchais, S.; Hartmann, R. W. Synthesis and evaluation of heteroaryl-substituted dihydronaphthalenes and indenes: Potent and selective inhibitors of aldosterone synthase (CYP11B2) for the treatment of congestive heart failure and myocardial fibrosis. *J. Med. Chem.* **2006**, *49*, 2222–2231.

(24) Ulmschneider, S.; Negri, M.; Voets, M.; Hartmann, R. W. Development and evaluation of a pharmacophore model for inhibitors of aldosterone synthase (CYP11B2). *Bioorg. Med. Chem. Lett.* **2006**, *16*, 25–30.

(25) (a) Eaton, D. L.; Gallagher, E. P.; Bammler, T. K.; Kunze, K. L. Role of cytochrome P4501A2 in chemical carcinogenesis: Implications for human variability in expression and enzyme activity. *Pharmacogenetics* **1995**, *5*, 259–274. (b) Guengerich, F.; Parikh, A.; Turesky, R. J.; Josephy, P. D. Interindividual differences in the metabolism of environmental toxicants: Cytochrome P450 1A2 as a prototype. *Mutat. Res.* **1999**, *428*, 115–124.

(26) Miyaura, N.; Suzuki, A. Palladium-catalyzed cross-coupling reactions of organoboron compounds. *Chem. Rev.* **1995**, *95*, 2457–2483.

(27) Appukkuttan, P.; Orts, A. B.; Chandran, R. P.; Goeman, J. L.; van der Eycken, J.; Dehaen, W.; van der Eycken, E. Generation of a small library of highly electron-rich 2-(hetero)aryl-substituted phenethylamines by the Suzuki-Miyaura reaction: A short synthesis of an apogalanthamine analogue. *Eur. J. Org. Chem.* **2004**, 3277–3285.

(28) Bengtson, A.; Hallberg, A.; Larhed, M. Fast synthesis of aryl triflates with controlled microwave heating. *Org. Lett.* **2002**, *4*, 1231–1233.

(29) Kertesz, D. J.; Martin, M.; Palmer, W. S. Process for preparing pyridazinone compounds. PCT Int. Appl. WO2005100323, 2005.

(30) Lézé, M.-P.; Le Borgne, M.; Pinson, P.; Palusczak, A.; Duflos, M.; Le Baut, G.; Hartmann, R. W. Synthesis and biological evaluation of 5-[(aryl)(1H-imidazol-1-yl)methyl]-1H-indoles: Potent and selective aromatase inhibitors. *Bioorg. Med. Chem. Lett.* **2006**, *16*, 1134–1137.

(31) Carreño, M. C.; García-Cerrada, S.; Urbano, A. From central to helical chirality: Synthesis of P and M enantiomers of [5]helicenequinones and bisquinones from (SS)-2-(p-tolylsulfinyl)-1,4-benzoquinone. *Chem. Eur. J.* **2003**, *9*, 4118–4131.

(32) Heyer, D.; Fang, J.; Navas III, F.; Katamreddy, S. R.; Peckham, J. P.; Turnbull, P. S.; Miller, A. B.; Akwabi-Ameyaw, A. Chemical compounds. PCT Int. Appl. WO2006002185, 2006.

(33) Fitzgerald, D. H.; Muirhead, K. M.; Botting, N. P. A comparative study on the inhibition of human and bacterial kynureninase by novel bicyclic kynurenine analogues. *Bioorg. Med. Chem.* **2001**, *9*, 983–989.

(34) (a) Leadbeater, N. E.; Marco, M. Ligand-free palladium catalysis of the suzuki reaction in water using microwave heating. *Org. Lett.* **2002**, *4*, 2973–2976. (b) Liu, L.; Zhang, Y.; Xin, B. Synthesis of biaryls and polyaryls by ligand-free suzuki reaction in aqueous phase. *J. Org. Chem.* **2006**, *71*, 3994–3997.

(35) Li, D.; Zhao, B.; Sim, S.; Li, T.; Liu, A., Liu, L. F.; LaVoie, E. J. 8,9-Methylenedioxybenzo[i]-phenanthridines: Topoisomerase I-targeting activity and cytotoxicity. *Bioorg. Med. Chem.* **2003**, *11*, 3795–3805.

(36) (a) Denner, K.; Bernhardt, R. Inhibition studies of steroid conversions mediated by human CYP11B1 and CYP11B2 expressed in cell cultures. In *Oxygen Homeostasis and Its Dynamics*, 1st ed.; Ishimura, Y., Shimada, H., Suematsu, M., Eds.; Springer-Verlag: Tokyo, Berlin, Heidelberg, New York, 1998; pp 231–236. (b) Denner, K.; Doehmer, J.; Bernhardt, R. Cloning of CYP11B1 and CYP11B2 from normal human adrenal and their functional expression in COS-7 and V79 chinese hamster cells. *Endocr. Res.* **1995**, *21*, 443–448. (c) Böttner, B.; Denner, K.; Bernhardt, R. Conferring aldosterone synthesis to human CYP11B1 by replacing key amino acid residues with CYP11B2-specific ones. *Eur. J. Biochem.* **1998**, *252*, 458–466.

(37) (a) Ehmer, P. B.; Jose, J.; Hartmann, R. W. Development of a simple and rapid assay for the evaluation of inhibitors of human 17α-hydroxylase-$C_{17,20}$-lyase (P450c17) by coexpression of P450c17 with NADPH-cytochrome-P450-reductase in *Escherichia coli*. *J. Steroid Biochem. Mol. Biol.* **2000**, *75*, 57–63; (b) Hutschenreuter, T. U.; Ehmer, P. B.; Hartmann, R. W. Synthesis of hydroxy derivatives of highly potent nonsteroidal CYP17 inhibitors as potential metabolites and evaluation of their activity by a non cellular assay using recombinant enzyme. *J. Enzyme Inhib. Med. Chem.* **2004**, *19*, 17–32.

(38) Thompson, E. A.; Siiteri, P. K. Utilization of oxygen and reduced nicotinamide adenine dinucleotide phosphate by human placental microsomes during aromatization of androstenedione. *J. Biol. Chem.* **1974**, *249*, 5364–5372.

(39) Hartmann, R. W.; Batzl, C. Aromatase inhibitors. Synthesis and evaluation of mammary tumor inhibiting activity of 3-alkylated 3-(4-aminophenyl)piperidine-2,6-diones. *J. Med. Chem.* **1986**, *29*, 1362–1369.

(40) Butler, M. A.; Iwasaki, M.; Guengerich, F. P.; Kadlubar, F. F. Human cytochrome P-450$_{PA}$ (P-450IA2), the phenacetin O-deethylase, is primarily responsible for the hepatic 3-demethylation of caffeine and N-oxidation of carcinogenic arylamines. *Proc. Natl. Acad. Sci. U.S.A.* **1989**, *86*, 7696–7700.

(41) Sesardic, D.; Boobis, A. R.; Murray, B. P.; Murray, S.; Segura, J.; de la Torre, R.; Davies, D. S. Furafylline is a potent and selective inhibitor of cytochrome P450IA2 in man. *Br. J. Clin. Pharmacol.* **1990**, *29*, 651–663.

(42) (a) Chohan, K. K.; Paine, S. W.; Mistry, J.; Barton, P.; Davis, A. M. A rapid computational filter for cytochrome P450 1A2 inhibition potential of compound libraries. *J. Med. Chem.* **2005**, *48*, 5154–5161. (b) Korhonen, L. E.; Rahnasto, M.; Mähönen, N. J.; Wittekindt, C.; Poso, A.; Juvonen, R. O.; Raunio, H. Predictive three-dimensional quantitative structure-activity relationship of cytochrome P450 1A2 inhibitors. *J. Med. Chem.* **2005**, *48*, 3808–3815.

(43) GaussView, Version 3.0, Dennington I.; Roy; Keith, T.; Millam, J.; Eppinnett, K.; Hovell, W. L.; Gilliland, R.; Semichem, Inc., Shawnee Mission, KS, **2003**.

(44) Petti, M. A.; Shepodd, T. J.; Barrans, R. E..; Dougherty, D. A. "Hydrophobic" binding of water-soluble guests by high-symmetry, chiral hosts. An electron-rich receptor site with a general affinity for quaternary ammonium compounds and electron-deficient π systems. *J. Am. Chem. Soc.* **1988**, *110*, 6825–6840.

3.2 Novel Aldosterone Synthase Inhibitors with Extended Carbocyclic Skeleton by a Combined Ligand-Based and Structure-Based Drug Design Approach

Simon Lucas, Ralf Heim, Matthias Negri, Iris Antes, Christina Ries, Katarzyna E. Schewe, Alessandra Bisi, Silvia Gobbi and Rolf W. Hartmann

This manuscript has been published as an article in the

Journal of Medicinal Chemistry **2008**, *51*, 6138–6149.

Paper II

Abstract: Pharmacophore modeling of a series of aldosterone synthase (CYP11B2) inhibitors triggered the design of compounds **11** and **12** by extending a previously established naphthalene molecular scaffold (e.g., present in molecules **1** and **2**) via introduction of a phenyl or benzyl residue in 3-position. These additional aromatic moieties have been hypothesized to fit into the newly identified hydrophobic pharmacophore feature HY3. Subsequent docking studies in our refined CYP11B2 protein model have been performed prior to synthesis to estimate the inhibitory properties of the proposed molecules. While phenyl-substituted compound **11** (IC_{50} > 500 nM) did not dock under the given pharmacophore constraint (i.e., the Fe(heme)-N(ligand) interaction), benzyl-substituted compound **12** (IC_{50} = 154 nM) was found to exploit a previously unexplored sub-pocket of the inhibitor binding site. By structural optimization based on the pharmacophore hypothesis, 25 novel compounds were synthesized, amongst them highly potent CYP11B2 inhibitors (e.g., **17**, IC_{50} = 2.7 nM) with pronounced selectivity toward the most important steroidogenic and hepatic CYP enzymes.

Introduction

Aldosterone synthase (CYP11B2), a mitochondrial cytochrome P450 enzyme that is localized mainly in the adrenal cortex, is the key enzyme of mineralocorticoid biosynthesis. It catalyzes the terminal three oxidation steps in the biogenesis of aldosterone in humans.[1] This hormone is the most important circulating mineralocorticoid and plays a crucial role in the electrolyte and fluid homeostasis mainly by binding to epithelial mineralocorticoid receptors (MR) promoting sodium reabsorption and potassium secretion. Since the sodium movement is followed by water via osmosis, aldosterone is a key regulator of blood volume and blood pressure. Abnormally increased plasma levels of aldosterone have been diagnosed in different cardiovascular diseases such as elevated blood pressure, congestive heart failure, and myocardial fibrosis.[2] Inhibitors of the angiotensin-converting enzyme (ACE) which are in use for the treatment of hypertension and congestive heart failure can initially induce a down-regulation of circulating aldosterone. However, increased levels of aldosterone are frequently observed after several months of therapy.[3] This phenomenon termed 'aldosterone escape' is a limiting factor of ACE inhibitors and shows that novel therapeutic concepts combating the effects of elevated aldosterone levels are needed. Two recent clinical studies (RALES and EPHESUS) demonstrated that treatment with mineralocorticoid receptor antagonists in addition to the standard therapy resulted in a decrease of mortality in patients with chronic congestive heart failure and in patients after myocardial infarction, respectively.[4,5] The use of spironolactone, however, is accompanied by severe progestational and antiandrogenic side effects due to its affinity to other steroid receptors. Moreover, the elevated plasma aldosterone concentrations are left unaffected on a pathological level which raises several issues. First, the elevated aldosterone plasma levels do not induce a homologous down-regulation but an up-regulation of the aldosterone receptor.[6] This fact complicates a long-term therapy as MR antagonists are likely to become ineffective. Furthermore, the high concentrations promote nongenomic actions of aldosterone which are in general not blocked by receptor antagonists.[7] Pathological aldosterone concentrations have been identified to induce a negative inotropic effect in human trabeculae and to potentiate the vasoconstrictor effect of angiotensin II in coronary arteries in rapid, nongenomic manner.[8] Thus, aldosterone is intrinsically capable to further deteriorate heart function by acting nongenomically.

A novel therapeutic strategy with potential to overcome the drawbacks of MR antagonists is the blockade of aldosterone formation, preferably by inhibiting CYP11B2, the key enzyme of its biosynthesis. Aldosterone synthase has been proposed as a potential pharmacological target by our group as early as 1994,[9] followed soon thereafter by the hypothesis that inhibitors of CYP11B2 could serve as drugs for the treatment of hyperaldosteronism, congestive heart failure and myocardial fibrosis.[10,11] Consequent structural optimization of a hit discovered by a compound library screening led to a series of nonsteroidal aldosterone synthase inhibitors with high selectivity toward other cytochrome P450 enzymes.[12–15]

In the present study, we describe the design and synthesis of a series of 3-benzyl-substituted pyridylnaphthalenes and structurally related compounds (Chart 1) by a combined ligand-based and structure-based drug design approach as well as the determination of their biological activity regarding human CYP11B2 for potency. Selectivity is a prerequisite for a CYP11B2 inhibitor, especially with regard to other cytochrome P450 enzymes as they are likely to interact with other CYP enzymes in a similar way (e.g., by complexation of the heme iron). Taking into consideration that the key enzyme of glucocorticoid biosynthesis, 11β-hydroxylase (CYP11B1), and CYP11B2 have a sequence homology of approximately 93 %,[16] the selectivity issue becomes especially critical for the design of CYP11B2 inhibitors. On that account, all compounds were tested for their inhibitory potency versus CYP11B1 to determine their selectivity. A set of compounds was additionally tested for inhibitory activity versus the steroidogenic enzymes CYP17 (17α-hydroxylase-C17,20-lyase) and CYP19 (aromatase) as well as selected hepatic drug-metabolizing CYP enzymes (CYP1A2, CYP2B6, CYP2C9, CYP2C19, CYP2D6, and CYP3A4).

Chart 1. Title Compounds

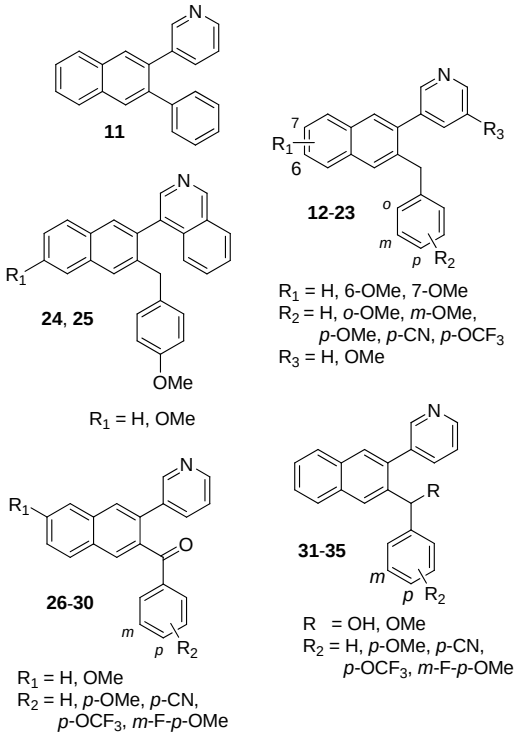

Results

Inhibitor Design Concept

In our search for new lead compounds as CYP11B2 inhibitors structurally differing from the previously discovered pyridylnaphthalenes such as **1** and **2**,[14] we identified imidazolylmethylene-substituted flavones (e.g., **3**–**10**) to be aldosterone synthase inhibitors with moderate to high inhibitory potency by compound library screening (Table 1). These compounds that originally have been described as aromatase inhibitors[17] display CYP11B2 inhibition in a range of 73–94 % at a con-

centration of 500 nM with methoxy-functionalized **6** being most active (IC_{50} = 11 nM), albeit without showing selectivity versus the highly homologous CYP11B1 (see supplementary material for selectivity data).

Table 1. Inhibition of Human Adrenal CYP11B2 *In Vitro* (Compounds **1**–**10**)

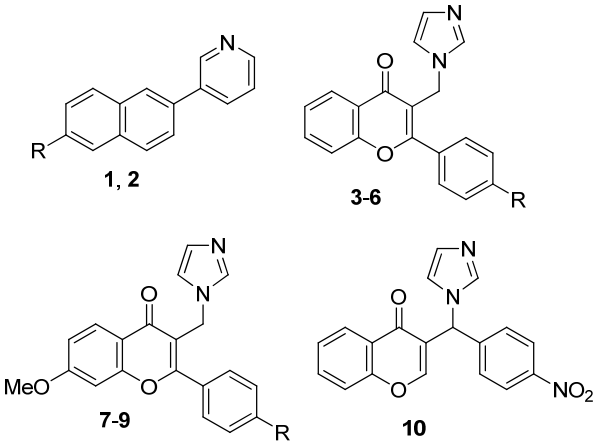

		% inhibition[a] CYP11B2[b]
compd	R	[IC_{50} (nM)[c]]
1	H	92 [28]
2	OMe	91 [6.2]
3	H	88 [28]
4	NO_2	81 [95]
5	Br	90 [25]
6	OMe	94 [11]
7	H	86 [124]
8	Br	80 [n.d.]
9	NO_2	73 [n.d.]
10		77 [187]

[a] Mean value of at least two experiments, standard deviation usually less than 10 %; inhibitor concentration, 500 nM. [b] Hamster fibroblasts expressing human CYP11B2; substrate deoxycorticosterone, 100 nM. [c] Mean value of at least four experiments, standard deviation usually less than 25 %, n.d. = not determined; fadrozole, IC_{50} = 1 nM.

Recently, a pharmacophore model for aldosterone synthase inhibitors was built by superimposition of a series of heteroaryl-substituted methyleneindanes[12,13] and naphthalenes[14,15] synthesized in our laboratory and subsequently validated by pyridine-substituted acenaphthenes as hybrid structures that fit into the four identified pharmacophoric points (i.e., a heterocyclic nitrogen and three ring centroids).[18] The most potent compounds of the latter substance classes together with the most potent flavone type inhibitors were used as training set for the generation of an extended pharmacophore model by applying the GALAHAD[19] pharmacophore generation module of SYBYL molecular modeling software. In the top ranked pharmacophore model, best in three of the most indicative ranking criteria of this software (Pareto ranking,[20] Specificity, and Mol-query), the earlier pharma-

cophoric points[18] were confirmed, namely the hydrophobic features HY0, HY1, HY2a, HY2b as well as the acceptor atom features AA1, AA2a, and AA2b (Figure 1).

Figure 1[a]

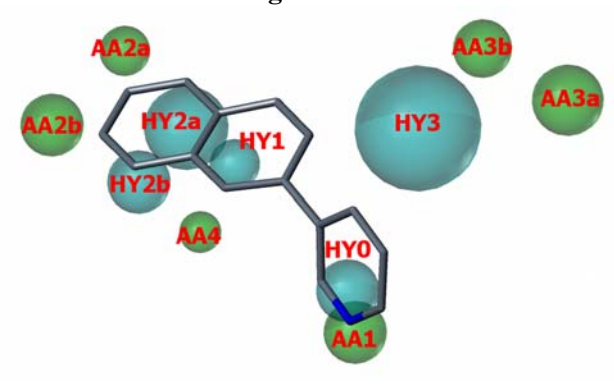

[a] Compound **1** mapped to the pharmacophore model. The newly identified hydrophobic feature HY3 as well as the acceptor atom features AA3a and AA3b are not exploited by inhibitors with a naphthalene molecular scaffold. Pharmacophoric features are color-coded: Cyan for hydrophobic regions (HY0–HY3) and green for acceptor atom features (AA1–4).

A novel and voluminous hydrophobic area HY3 was identified next to HY1, along with the acceptor atom features AA3a and AA3b (see supplementary material for exact pharmacophore geometric properties) as well as an additional acceptor atom feature AA4. Rationalizing the given information, the two sample compounds **11** and **12** (Chart 2) were designed by modifying our previously reported naphthalene derivatives **1** and **2** to exploit the newly discovered pharmacophoric feature HY3. As suggested by the model and visualized in Figure 1, introduction of a hydrophobic substituent in 3-position of the naphthalene skeleton should be favorable to exploit the voluminous hydrophobic feature HY3 of the pharmacophore. The phenyl residue directly bound to the naphthalene core in compound **11** creates a conformationally constrained structure in which both rotational degrees of freedom of the two aryl–aryl bonds are limited since they are located *ortho* to each other. The benzyl motive in compound **12** leads to an increased flexibility of the spatial property distribution by rotation around the two benzylic carbon–carbon bonds. Furthermore, the aromatic ring moves apart from the naphthalene core by one methylene unit.

Chart 2. Proposed Lead Structures **11** and **12**

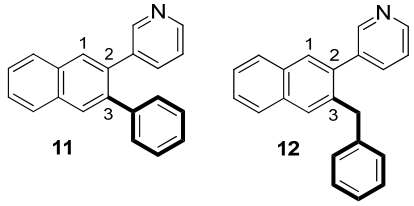

In order to elucidate the role of conformational flexibility and the exact position of the aryl moiety for optimal inhibitor binding, docking studies were performed (Figure 2). For this purpose, we used the CYP11B2 protein model that has been built[12] and subsequently validated[13–15] by our group as well as the same docking calculations that have been performed in these studies.

Figure 2[a]

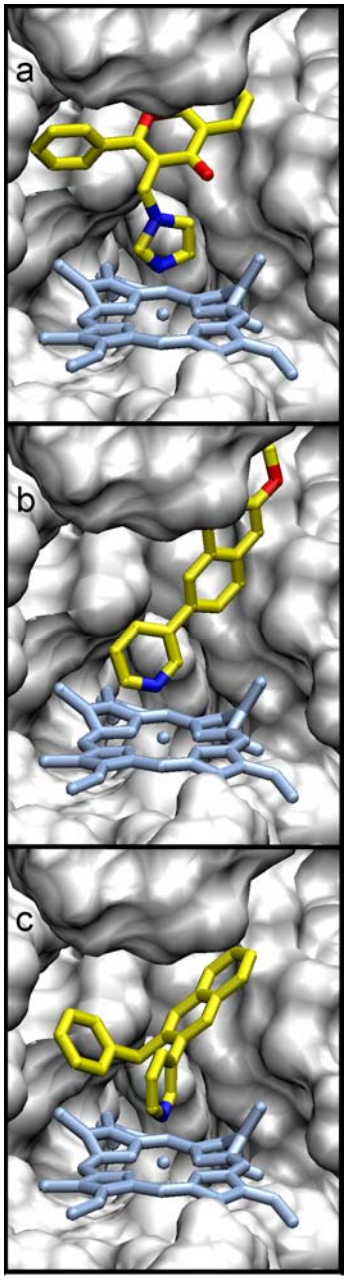

[a] Structure of the CYP11B2–inhibitor complexes of **3** (a), **2** (b) and **12** (c). Surface of the binding pocket (grey) surrounding the inhibitor and the heme co-factor (light blue). The inhibitors are presented in yellow; nitrogen atoms are colored in blue and oxygen atoms are in red. Unlike **2**, the inhibitors **3** and **12** exploit an additional sub-pocket of the inhibitor binding site.

Previous investigations have identified the binding affinity to the target enzyme to be highly dependent on the geometry of the coordinative bond between the heme iron and the heterocyclic nitrogen. An angle of the Fe–N straight line with the porphyrin plane close to 90° (i.e., the heterocyclic nitrogen lone pair arranges perpendicular to the heme group) provides an optimal orbital overlap corresponding to a high inhibitory potency.[14,15] The analysis of the docking mode of compound **3** led to the identification of a new sub-pocket which interacts with the aryl moiety (Figure 2a). This sub-pocket was not considered as potential binding site during our previous design efforts due to the fact that the formerly investigated compounds such as **2** did not occupy this binding site (Figure 2b). The above considerations led to the design of compounds **11** and **12**. Both compounds combine the pyridylnaphthalene skeleton of compound **1** with an additional aryl motive which should be able to interact with the newly identified sub-pocket. However, compound **11** proved to be too rigid to fit into the binding site and could thus not be docked successfully into the binding pocket under the given pharmacophore constraint, that is the Fe(heme)-N(ligand) interaction. A directed heme-Fe–N interaction was defined perpendicular to the heme-plane. This pharmacophore constraint was applied to ensure the right binding mode of the inhibitors with the heme-cofactor. The constraint requires the existence of an inhibitor-nitrogen-atom on the surface of an interaction cone with a 20 degree radius, which has its origin at the Fe-atom and points perpendicular to the heme-plane (with a length of 2.2 Å). Obviously, the conformationally restricted phenyl moiety of compound **11** undergoes repulsive interaction with amino acids of the binding pocket or with the heme-cofactor under the above mentioned constraint (i.e., when the pyridine moiety forms a coordinative bond to the heme iron), thus preventing that the molecule successfully docks into the CYP11B2 protein model. Contrariwise, the 3-benzyl substituted analog **12** is more flexible due to an additional methylene spacer between the two ring systems and thus fitted adequately into the binding site (Figure 2c). From these docking results we concluded that the methylene group of the potential inhibitor should provide the flexibility necessary to adapt to the binding site geometry.

Chemistry

The phenyl-substituted pyridylnaphthalene **11** was obtained as shown in Scheme 1 by two subsequent Suzuki coupling[21] steps, whereof the first proceeded between 3-bromopyridine and 3-methoxy-2-naphthaleneboronic acid **11d**. The boronic acid **11d** was accessible by *ortho*-lithiation of 2-methoxynaphthalene and in situ addition of trimethylborate as described previously.[22] After demethylation of **11c** by refluxing in concentrated hydrobromic acid, the intermediate naphthol was transferred into the triflate **11a** by a microwave-enhanced method described by Bengtson et al.[23] A second Suzuki coupling using controlled microwave heating afforded compound **11**.[24]

The benzyl-substituted derivatives **12**–**16**, **19**, and **21**–**25** were synthesized by the route shown in Scheme 2. Starting from a 3-hydroxy-2-naphtoic acid, few functional group inversions led to the carbaldehydes **12e**–**14e**. These transformations were performed by a 4-step sequence starting with an esterification[25] and subsequent introduction of a protection group to the naphthalene hydroxy group of

12h and **13h** (i.e., methyl in **12g** or benzyl in **13g** and **14g**).[26] Lithium borohydride reduction[27] followed by TEMPO oxidation[28] (of primary alcohol **12f**) or Parik-Doehring oxidation[29] (of **13f** and **14f**) afforded the corresponding carbaldehydes **12e**–**14e**. Grignard reaction with various substituted phenylmagnesium halogenides afforded the phenyl-naphthylalcohols **12d**–**16d**, and **19d**. Hydrogenolytic removal of the hydroxy group was accomplished by treatment with $NaBH_4$ and $AlCl_3$ in refluxing THF.[30] After deprotection using BBr_3 (for de-methylation of **12c**) or ammonium formate under Pd-catalysis[31] (for de-benzylation of **13c**–**16c**, and **19c**) and subsequent triflate formation,[23] the heterocycle was introduced by microwave-enhanced Suzuki coupling[24] giving rise to the benzyl-substituted pyridylnaphthalenes **12**–**16**, **19**, and **21**–**25**.

Scheme 1[a]

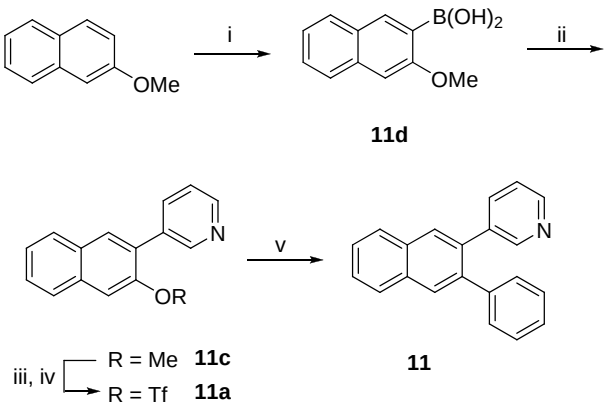

[a] Reagents and conditions: i) *n*BuLi, $B(OMe)_3$, THF, –78 °C, then HCl/water; ii) 3-bromopyridine, $Pd(PPh_3)_4$, toluene/ethanol, aq. Na_2CO_3, reflux; iii) conc. HBr, reflux; iv) Tf_2NPh, K_2CO_2, THF, µw, 120 °C; v) phenylboronic acid, $Pd(PPh_3)_4$, aq. $NaHCO_3$, DMF, µw, 150 °C.

Scheme 2[a]

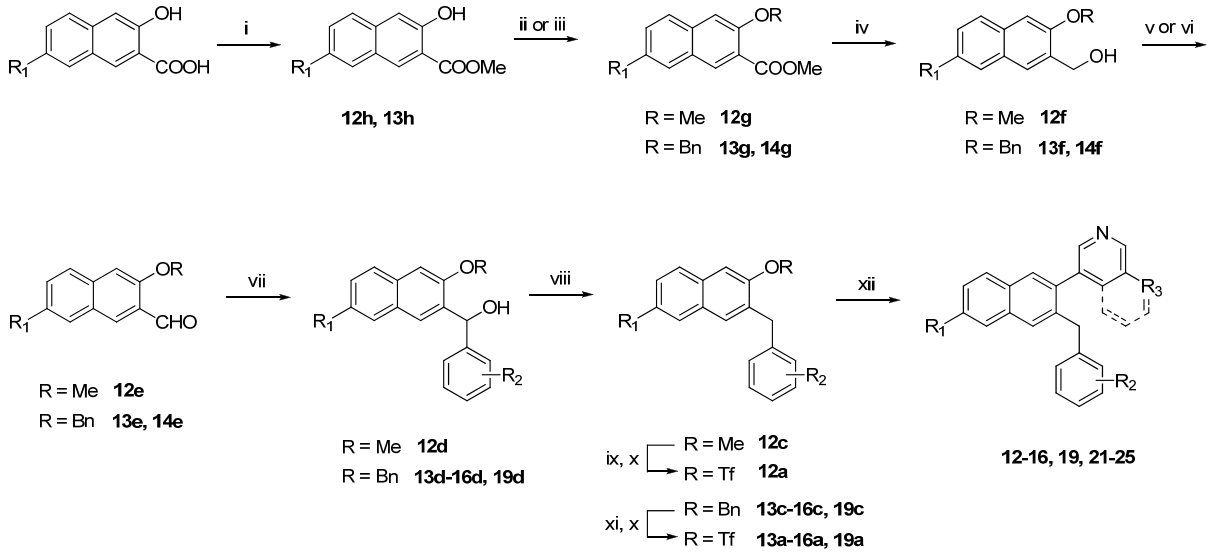

[a] Reagents and conditions: i) methanol, H_2SO_4, reflux; ii) MeI, K_2CO_3, 18-crown-6, acetone, reflux (for R = Me); iii) BnBr, K_2CO_3, 18-crown-6, acetone, reflux (for R = Bn); iv) $LiBH_4$, THF/toluene, reflux; v) NCS, TEMPO, nBu_4NCl, aq. $Na_2CO_3/NaHCO_3$, CH_2Cl_2; rt (for R = Me); vi) SO_3·py, NEt_3, DMSO, rt (for R = Bn); vii) ArMgX, THF, 0 °C, then aq. NH_4Cl; viii) $NaBH_4$, $AlCl_3$, THF, reflux; ix) BBr_3, CH_2Cl_2, –20 °C; x) Tf_2NPh, K_2CO_2, THF, µw, 120 °C; xi) ammonium formate, Pd/C, THF/methanol, reflux; xii) heteroarylboronic acid, $Pd(PPh_3)_4$, aq. $NaHCO_3$, DMF, µw, 150 °C.

Alternatively, the benzyl-substituted pyridylnaphthalenes **17**, **18**, and **20** were obtained by the route shown in Scheme 3. Applying the presented transformations afforded the benzoyl-substituted derivatives **26**–**30** and the corresponding hydroxymethylene analogues **31**–**34** as reaction intermediates. The sequence toward the 3-benzoyl-substituted 2-naphthols **26b**–**30b** was reported previously by Li et al. and starts with an *ortho*-lithiation of 2-methoxy- or 2,7-dimethoxynaphthalene, followed by in situ addition of a Weinreb amide. Regioselective demethylation of the obtained methanones **26c**–**30c** at the naphthalene-position *ortho* to the benzoyl residue was accomplished by treatment with BCl_3/nBu_4NI at –78 °C.[32] After triflate formation, a 3-pyridyl residue was introduced by Suzuki coupling to afford compounds **26**–**30**. The corresponding alcohols **20a** and **31**–**34** were obtained by sodium borohydride reduction. The methyl ether **35** was synthesized by treating **31** with methyl iodide and NaH in THF. The benzyl-substituted pyridylnaphthalenes **17**, **18**, and **20** were obtained by in situ iodotrimethylsilane mediated reduction.[33,34] However, reduction by this method did not succeed in the case of **32**, neither by other commonly used hydrogenolysis protocols.[30,35]

Scheme 3[a]

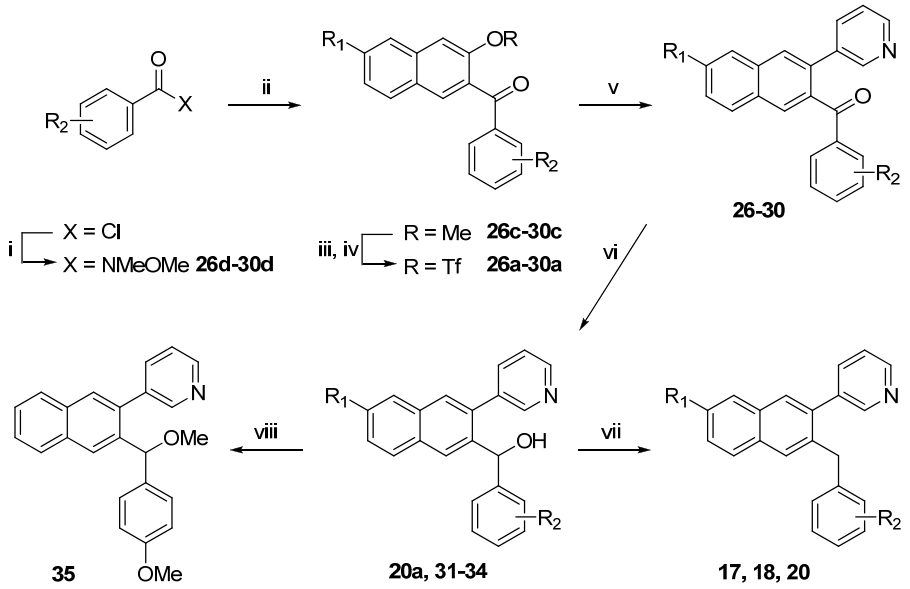

[a] Reagents and conditions: i) *N*,*O*-dimethylhydroxylamine hydrochloride, NEt_3, CH_2Cl_2, rt; ii) *n*BuLi, 2-methoxynaphthalene (for R_1 = H) or 2,7-dimethoxynaphthalene (for R_1 = OMe), TMEDA, THF, –78 °C, then HCl/water; iii) BCl_3, nBu_4NI, CH_2Cl_2, –78 °C to rt; iv) Tf_2O, pyridine, CH_2Cl_2, 0 °C; v) pyridineboronic acid, $Pd(PPh_3)_4$, aq. Na_2CO_3, toluene/ethanol, reflux; vi) $NaBH_4$, methanol, 0 °C; vii) Me_3SiCl, NaI, CH_3CN, 55 °C; viii) MeI, NaH, THF, rt.

Biological Results

Inhibition of Human Adrenal Corticoid Producing CYP11B2 and CYP11B1 *In Vitro* (Table 2). The inhibitory activities of the compounds were determined in V79 MZh cells expressing either human CYP11B2 or CYP11B1.[10,36] The V79 MZh cells were incubated with [^{14}C]-deoxycorticosterone as substrate and the inhibitor in different concentrations. The product formation was monitored by HPTLC using a phosphoimager. Fadrozole, an aromatase (CYP19) inhibitor with proven ability to

reduce corticoid formation *in vitro*[37] and *in vivo*[38] was used as a reference (CYP11B2, IC_{50} = 1 nM; CYP11B1, IC_{50} = 10 nM).

Table 2. Inhibition of Human Adrenal CYP11B2 and CYP11B1 *In Vitro* (Compounds **11**–**35**)

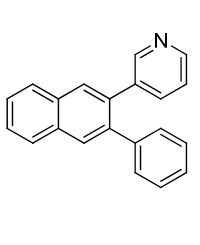

11

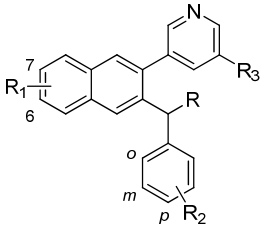

12-23, 31-35

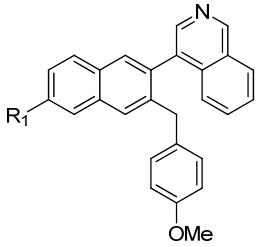

24, 25

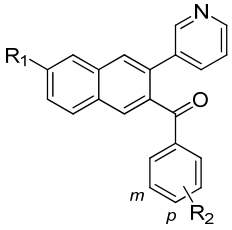

26-30

					% inhibition[a]	IC_{50} value[b] (nM)		
					V79 11B2[c]	V79 11B2[c]	V79 11B1[d]	selectivity
compd	R_1	R_2	R_3	R	hCYP11B2	hCYP11B2	hCYP11B1	factor[e]
11					8	n.d.	n.d.	n.d.
12	H	H	H	H	76	154	953	6
13	6-OMe	H	H	H	85	53	640	12
14	H	*o*-OMe	H	H	24	n.d.	n.d.	n.d.
15	H	*m*-OMe	H	H	62	n.d.	n.d.	n.d.
16	H	*p*-OMe	H	H	89	7.8	2804	359
17	H	*p*-CN	H	H	93	2.7	1956	724
18	H	*p*-OCF_3	H	H	95	3.9	3559	913
19	6-OMe	*p*-OMe	H	H	95	11	4329	394
20	7-OMe	*p*-OMe	H	H	35	n.d.	n.d.	n.d.
21	H	*p*-OMe	OMe	H	93	7.7	1811	235
22	6-OMe	*p*-OMe	OMe	H	96	7.6	2452	322
23	6-OMe	H	OMe	H	90	24	2936	122
24	H				98	3.0	785	262
25	OMe				94	5.0	735	147
26	H	*p*-OMe	H		79	119	24003	202
27	H	*m*-F-*p*-OMe	H		78	65	19816	305
28	H	*p*-CN	H		88	30	9639	321
29	H	*p*-OCF_3	H		91	28	11307	404
30	OMe	*p*-OMe	H		25	n.d.	n.d.	n.d.
31	H	*p*-OMe	H	OH	57	n.d.	n.d.	n.d.
32	H	*m*-F-*p*-OMe	H	OH	51	n.d.	n.d.	n.d.
33	H	*p*-CN	H	OH	59	n.d.	n.d.	n.d.
34	H	*p*-OCF_3	H	OH	63	n.d.	n.d.	n.d.
35	H	*p*-OMe	H	OMe	23	n.d.	n.d.	n.d.
fadrozole					-	1	10	10

[a] Mean value of at least two experiments, standard deviation usually less than 10 %; inhibitor concentration, 500 nM. [b] Mean value of at least four experiments, standard deviation usually less than 25 %, n.d. = not determined. [c] Hamster fibroblasts expressing human CYP11B2; substrate deoxycorticosterone, 100 nM. [d] Hamster fibroblasts expressing human CYP11B1; substrate deoxycorticosterone, 100 nM. [e] IC_{50} CYP11B1/IC_{50} CYP11B2, n.d. = not determined.

Compound **11** with a phenyl residue directly bound to the naphthalene core shows no significant activity at the target enzyme with only 8 % inhibition at an inhibitor concentration of 500 nM (Table 2). Insertion of a methylene linker into the biaryl bond results in an increased inhibitory potency at CYP11B2 in compound **12** (IC_{50} = 154 nM). Introduction of a methoxy residue in *ortho*- or *meta*-position of the benzylic moiety as accomplished in compounds **14** and **15** results in a significantly decreased inhibitory potency whereas the same substituent in *para*-position gives rise to the highly potent CYP11B2 inhibitor **16** (IC_{50} = 7.8 nM) with pronounced selectivity versus CYP11B1 (IC_{50} = 2804). The cyano and trifluoromethoxy-substituted analogues **17** and **18** are highly potent as well and about 700-fold and 900-fold more selective for CYP11B2. Derivatization of the naphthalene core by a methoxy group is readily tolerated in 6-position as accomplished in compounds **13**, **19**, **22**, **23**, and **25**. The inhibitory profile of the 6-methoxy derivatives regarding the two CYP11B isoforms is thereby comparable to the corresponding hydrogen analogues with a slightly increased selectivity factor in most cases. On the other hand, introduction of methoxy in 7-position results in a decrease of the inhibition to less than 40 % at an inhibitor concentration of 500 nM (**20** and **30**). Modification of the pyridine moiety which has recently been shown to increase the activity and selectivity of naphthalene type CYP11B2 inhibitors[39] affords compounds **21**–**25** with IC_{50} values in the range of 3–24 nM. Replacing the methylene linker by a carbonyl group as accomplished in compounds **26**–**29** results in a slightly reduced inhibitory potency (IC_{50} = 16–118 nM), albeit the high CYP11B1 selectivity is retained (factor 200–500). Introducing hydroxymethylene (**31**–**34**) or methoxymethylene (**35**) as linker between the aryls leads to a significant loss of inhibitory activity to approximately 60 % at an inhibitor concentration of 500 nM in the case of compounds **31**–**34** and to an almost complete loss in the case of compound **35**.

Inhibition of Steroidogenic and Hepatic CYP Enzymes (Tables 3 and 4). A set of 12 compounds was investigated for inhibition of the steroidogenic enzymes CYP17 and CYP19 (Table 3). The inhibition of CYP17 was investigated using the 50,000 *g* sediment of the *E. coli* homogenate recombinantly expressing human CYP17 and progesterone (25 μM) as substrate.[40] The inhibition values were measured at an inhibitor concentration of 2 μM. In general, the compounds show no or only little inhibition of less than 25 %. As an exception, compound **22** exhibits 51 % inhibition which is in the range of the reference ketoconazole (IC_{50} = 2780 nM). The inhibition of CYP19 at an inhibitor concentration of 500 nM was determined *in vitro* with human placental microsomes and [1β-^{3}H]androstenedione as substrate as described by Thompson and Siiteri[41] using our modification.[42] Most of the compounds display only a moderate aromatase inhibition of less than 40 % whereof four compounds do not inhibit CYP19 at all (**21**, **24**, **25**, and **28**). The *para*-cyano-substituted derivative **17** shows a pronounced activity (60 %) and introduction of methoxy in 6-position of the naphthalene core as accomplished in compounds **19**, **22**, and **23** results likewise in a remarkably increased inhibition. Most notably, compound **19** is a highly potent CYP19 inhibitor exhibiting an IC_{50} value of 38 nM, thus being almost as active as the reference fadrozole (IC_{50} = 30 nM).

Table 3. Inhibition of Human CYP17 and CYP19 *In Vitro*

	% inhibition[a]			% inhibition[a]	
compd	CYP17[b]	CYP19[c]	compd	CYP17[b]	CYP19[c]
16	< 5	39	**23**	26	73
17	25	60	**24**	< 5	< 5
18	10	45	**25**	21	6
19	< 5	92[d]	**26**	5	19
21	28	6	**28**	7	< 5
22	51	49	**29**	8	17

[a] Mean value of three experiments, standard deviation usually less than 10 %. [b] *E. coli* expressing human CYP17; substrate progesterone, 25 μM; inhibitor concentration, 2.0 μM; ketoconazole, IC_{50} = 2.78 μM. [c] Human placental CYP19; substrate androstenedione, 500 nM; inhibitor concentration, 500 nM; fadrozole, IC_{50} = 30 nM. [d] IC_{50} = 38 nM.

A selectivity profile relating to inhibition of crucial hepatic CYP enzymes (CYP1A2, CYP2B6, CYP2C9, CYP2C19, CYP2D6, and CYP3A4) was determined for compounds **16**, **17**, **19**, and **28** by use of recombinantly expressed enzymes from baculovirus-infected insect microsomes. Table 4 shows the inhibition at a concentration of 10 μM and 1 μM. It becomes apparent that some enzymes are affected only to a minor degree by all compounds including CYB2B6 and CYP2D6. On the other hand, CYP2C9 is strongly inhibited in most cases. The benzoyl derivative **28** with less than 40 % inhibition at 1 μM concentration at all CYP enzymes is the most selective compound within this series. The worst selectivity profile is observed in the case of **19** inhibiting CYP2C9, CYP2C19, and CYP3A4 with pronounced potency.

Table 4. Inhibition of Selected Hepatic CYP Enzymes *In Vitro*

	% inhibition[a]											
	CYP1A2[b,c]		CYP2B6[b,d]		CYP2C9[b,e]		CYP2C19[b,f]		CYP2D6[b,g]		CYP3A4[b,h]	
compd	10 μM	1 μM	10 μM	1 μM	10 μM	1 μM	10 μM	1 μM	10 μM	1 μM	10 μM	1 μM
16	77	23	48	< 5	92	51	32	< 5	6	< 5	79	30
17	83	41	69	24	96	78	87	62	62	23	17	9
19	59	13	61	8	98[i]	96[i]	96	74	7	< 5	89	60
28	47	22	43	14	74	35	43	< 5	51	23	62	23

[a] Mean value of two experiments, standard deviation usually less than 10 %. [b] Recombinantly expressed enzymes from baculovirus-infected insect microsomes (Supersomes). [c] Furafylline, IC_{50} = 2.42 μM. [d] Tranylcypromine, IC_{50} = 6.24 μM. [e] Sulfaphenazole, IC_{50} = 318 nM. [f] Tranylcypromine, IC_{50} = 5.95 μM. [g] Quinidine, IC_{50} = 14 nM. [h] Ketoconazole, IC_{50} = 57 nM. [i] IC_{50} = 64 nM.

Discussion and Conclusion

The inhibitor design concept of the present study triggered the synthesis of compounds **11** and **12** as potential new lead structures by extending a previously established naphthalene molecular scaffold via introduction of a phenyl or benzyl residue in 3-position. Subsequently, docking studies in our CYP11B2 protein model were performed in order to check for spatial consistency with the pharmacophore hypothesis. It was found that while phenyl-substituted **11** did not dock under the given pharmacophore constraint (Fe(heme)-N(ligand) interaction), benzyl-substituted **12** adequately fits into

the binding site by exploiting a previously unexplored sub-pocket. These findings were confirmed by experimental results showing that 3-phenyl-substituted pyridylnaphthalene **11** exhibits no significant CYP11B2 inhibition *in vitro*. In accordance with the docking results, benzyl analog **12** is a moderately potent aldosterone synthase inhibitor (IC_{50} = 154 nM). The selectivity versus CYP11B1, however, is rather poor with an only 6-fold increased IC_{50} value compared to CYP11B2. The following lead optimization was accomplished by considering the SAR results obtained previously from the structures of the known inhibitors which have been used for the generation of the pharmacophore model (e.g., **1**–**10**). Methoxy substitution in compound **6** afforded the most active compound of the flavone series (IC_{50} = 11 nM) and was therefore chosen as a model substituent to figure out the optimal substituent position in the benzyl moiety of **12**. In case of the pyridylnaphthalenes, methoxy in 6-position as accomplished in **2** proved to be favorable in terms of both inhibitory potency and selectivity.[14]

Within the present set of compounds, interesting structure-activity and structure-selectivity relationships can be observed, particularly with regard to the benzyl and the naphthalene moieties. The benzylic part of the investigated molecules represents a pivotal region for structural optimization and is to a great extent dependent on the position of substituents in terms of both inhibitory activity and selectivity toward the highly homologous CYP11B1. Placing methoxy in *ortho*- or *meta*-position of the benzyl residue significantly reduces the inhibitory potency. Most notably, the inhibition decreases to 24 % at an inhibitor concentration of 500 nM in case of *ortho*-methoxy-derivatized compound **14**. Contrariwise, methoxy in *para*-position as accomplished in compound **16** increases the CYP11B2 activity by a factor of 20 compared to the hydrogen analog **12** and the selectivity toward CYP11B1 clearly improves (selectivity factor = 359). The experimental observations can be explained by the docking results of compounds **16** and **19**, both bearing a *para*-methoxy group (Figure 3). The introduction of this substituent into the benzyl moiety as accomplished in **16** leads to interactions of the compound with the residues of Pro452, Val339, and Thr279, thus stabilizing the complex formed by coordination of the heme iron by the heterocyclic nitrogen considerably (Figure 3a). In compound **19**, a second methoxy group was introduced at the 6-position of the naphthalene scaffold (Figure 3b). This leads to no additional stabilization of the complex, but to a slightly increased selectivity versus CYP11B1. The same trend was observed previously for the binding properties of a series of substituted pyridylnaphthalenes.[14,15] The *para*-cyano and *para*-trifluoromethoxy derivatives **17** and **18** are likewise highly potent and display IC_{50} values of 2.7 nM and 3.9 nM, respectively, which corroborates the importance of *para*-substitution for activity. Keeping in mind the high homology of the two CYP11B isoforms, the selectivity factors relating to CYP11B1 inhibition of the latter compounds are particularly noteworthy. Compound **17** displays an approximately 700-fold and compound **18** a 900-fold stronger inhibition of CYP11B2 versus CYP11B1.

Figure 3.

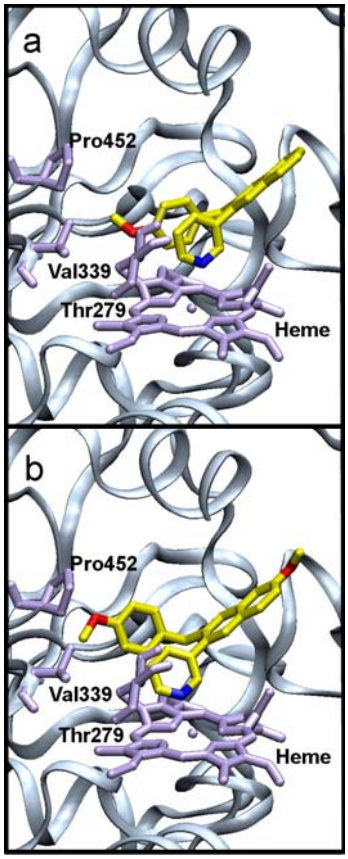

Figure 3. Structure of the CYP11B2 binding pocket with the docked inhibitors **16** (a) and **19** (b). Details of the active site, showing inhibitor, heme co-factor and the interacting residues of Pro452, Val339, and Thr279.

In the naphthalene molecular scaffold, introduction of a methoxy substituent in 7-position results in a decreased inhibitory potency (**20**, **30**) whereas the same substituent is readily tolerated in 6-position and even slightly increases the CYP11B1 selectivity in most cases. Figure 4 shows the 6-methoxy substituted derivative **19** mapped to the pharmacophore model. It is obvious that this compound nearly perfectly exploits both the well known (HY0, HY1, HY2a, AA1, AA2a) and the newly identified (HY3, AA3b) interaction areas which is reflected by the high inhibitory potency of this compound and underlines the predictive power of our pharmacophore hypothesis.

The *para*-methoxy group in the benzyl moiety of **19** which has been found to be responsible for both high inhibitory activity at CYP11B2 and selectivity versus CYP11B1 fits to the acceptor atom feature AA3b. Hence, targeting this interaction area is a promising strategy in the future design of potent and selective aldosterone synthase inhibitors. With respect to the selectivity profile relating to inhibition of several other CYP enzymes, it becomes apparent that 6-methoxylation endows the benzylnaphthalenes with an increased inhibitory potency at CYP19 as in the case of compounds **19**, **22**, and **23**, for example 6-methoxy derivative **19** is a highly potent CYP19 inhibitor displaying an activity similar to fadrozole. In addition, the latter compound strongly inhibits several hepatic CYP enzymes (i.e., CYP2C9, CYP2C19, and CYP3A4).

Figure 4.

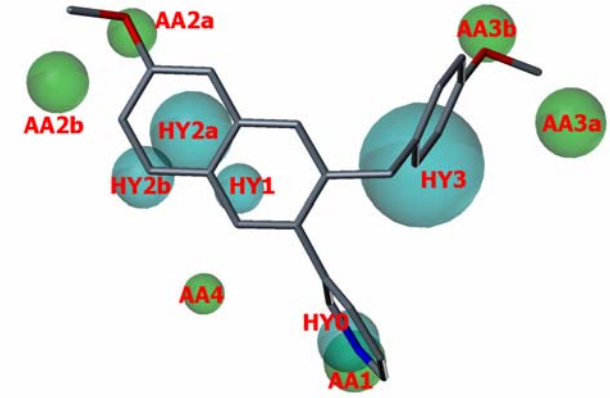

Compound **19** shows an enhanced fit to the pharmacophore hypothesis compared to **1** by additionally exploiting the features HY3 and AA3b. Pharmacophoric features are color-coded: Cyan for hydrophobic regions (HY0–HY3) and green for acceptor atom features (AA1–4).

Varying the substitution pattern of the pyridine site induces no distinct changes of the CYP11B2 potency in case of **21** and **22**. Again, 6-methoxylation in compound **22** increases the selectivity versus CYP11B1 compared to **21**. A slightly decreased selectivity versus CYP11B1 is observable in case of the isoquinoline derivatives **24** and **25** due to a moderate increase in CYP11B1 potency (IC_{50} < 1000 nM) which corresponds to previously observed results within the pyridylnaphthalene series.[39] Contrary to the finding that 6-methoxylation effects a slightly improved selectivity (as shown in previous studies[14,15] and observed in case of compounds **13**, **19**, and **22** compared to **12**, **16**, and **21**), the 6-methoxynaphthalene compound **25** is less selective than the hydrogen analog **24**. Derivatization of the methylene linker in compounds **26**–**35** leads to a decrease in inhibitory potency. The carbonyl analogues **26**, **28**, and **29** are slightly less active than their methylene analogues. On the other hand, CYP11B1 inhibition is reduced to the same degree and the high selectivity is maintained. Again, *para*-trifluoromethoxy has the strongest effect on the inhibitory discrimination between the two CYP11B isoforms and derivative **29** is approximately 400-fold less active at CYP11B1 compared to CYP11B2. In case of the *para*-cyanobenzoyl compound **28**, a decreased inhibition of the sex-hormone producing CYP17, CYP19 as well as the hepatic CYP1A2, CYP2B6, CYP2C9, CYP2C19, and CYP2D6 enzymes is found compared to the benzyl analog **17**, thus providing an advantageous overall CYP selectivity profile for this compound. Other variations of the methylene moiety as accomplished in the hydroxy- and methoxymethylene derivatives **30**–**35** lead to a pronounced decrease of inhibitory activity compared to the unsubstituted analogues. These compounds display 51–63 % inhibition at an inhibitor concentration of 500 nM in case of hydroxy substitution (**30**–**34**) and only 23 % in case of methoxy substitution (**35**). Obviously, the decrease in potency with increasing substituent size (hydrogen < carbonyl < hydroxy < methoxy) reflects the increase of steric repulsion between the aryl–aryl spacer and the enzyme parts (i.e., Leu343 and heme co-factor) separating the naphthalene binding site from the sub-pocket interacting with the benzyl residue.

In summary, it has been shown that our CYP11B2 pharmacophore model has predictive power to identify prospective lead structures. Based on the results of the pharmacophore model, a new class of pyridylnaphthalene derivatives with extended carbocyclic skeleton was synthesized. Derivatives with *para*-functionalized benzyl moiety in 3-position of the naphthalene molecular scaffold thoroughly satisfied the spatial constraints imposed by the pharmacophore model and turned out to be highly potent aldosterone synthase inhibitors. The most active compound, *para*-cyanobenzyl derivative **17**, displayed nanomolar potency at the target enzyme (IC_{50} = 2.7 nM). In addition, docking studies using our CYP11B2 protein model proved to be a useful tool to estimate the inhibitory properties of proposed new molecules and to explain structure-activity relationships. The binding behavior of compounds **11** and **12** was adequately predicted by the docking results. Furthermore, it was shown that the high inhibitory potency of the *para*-substituted derivative **16** is the outcome of stabilizing interactions with the residues of Pro452, Val339, and Thr279. The selectivity versus CYP11B1 (up to a factor of 900) which is especially remarkable with respect to the high homology of the two CYP11B isoforms was found to be a consequence of *para*-substitution and hence of exploiting the AA3b pharmacophoric feature as well. Currently, further studies are underway to evaluate selected compounds for their *in vivo* properties.

Experimental Section

Chemical and Analytical Methods. Melting points were measured on a Mettler FP1 melting point apparatus and are uncorrected. ^{1}H NMR and ^{13}C spectra were recorded on a Bruker DRX-500 instrument. Chemical shifts are given in parts per million (ppm), and tetramethylsilane (TMS) was used as internal standard for spectra obtained in DMSO-d_6 and $CDCl_3$. All coupling constants (J) are given in Hertz. Mass spectra (LC/MS) were measured on a TSQ Quantum (Thermo Electron Corporation) instrument with a RP18 100-3 column (Macherey Nagel) and with water/acetonitrile mixtures as eluents. Elemental analyses were carried out at the Department of Chemistry, University of Saarbrücken. Reagents were used as obtained from commercial suppliers without further purification. Solvents were distilled before use. Dry solvents were obtained by distillation from appropriate drying reagents and stored over molecular sieves. Flash chromatography was performed on silica gel 40 (35/40–63/70 μM) with petroleum ether/ethyl acetate mixtures as eluents, and the reaction progress was determined by thin-layer chromatography analyses on Alugram SIL G/UV254 (Macherey Nagel). Visualization was accomplished with UV light and $KMnO_4$ solution. All microwave irradiation experiments were carried out in a CEM-Discover monomode microwave apparatus.

The following compounds were prepared according to previously described procedures: 3-(3-methoxynaphthalen-2-yl)pyridine (**11c**),[14] (3-methoxynaphtalene-2-yl)boronic acid (**11d**),[22] methyl 3-methoxynaphthalene-2-carboxylate (**12g**),[26] methyl 3-hydroxynaphthalene-2-carboxylate (**12h**),[25] (3-hydroxynaphthalen-2-yl)(4-methoxyphenyl)methanone (**26b**),[32] (3-methoxynaphthalen-2-yl)(4-methoxyphenyl)methanone (**26c**),[32] *N*,4-Dimethoxy-*N*-methylbenzamide (**26d**),[32] 4-[(3-hydroxy-

naphthalen-2-yl)carbonyl]benzonitrile (**28b**),[32] 4-[(3-mehoxynaphthalen-2-yl)carbonyl]benzonitrile (**28c**),[32] 4-Cyano-*N*-methoxy-*N*-methylbenzamide (**28d**).[32]

Synthesis of the Target Compounds

Procedure A.[24] Boronic acid (0.75 mmol, 1 equivalent), aryl bromide or -triflate (0.9–1.3 equivalents), and tetrakis(triphenylphosphane)palladium(0) (43 mg, 37.5 μmol, 5 mol %) were suspended in 1.5 mL DMF in a 10 mL septum-capped tube containing a stirring magnet. To this was added a solution of $NaHCO_3$ (189 mg, 2.25 mmol, 3 equivalents) in 1.5 mL water and the vial was sealed with an Teflon cap. The mixture was irradiated with microwaves for 15 min at a temperature of 150 °C with an initial irradiation power of 100 W. After the reaction, the vial was cooled to 40 °C, the crude mixture was partitioned between ethyl acetate and water and the aqueous layer was extracted three times with ethyl acetate. The combined organic layers were dried over $MgSO_4$ and the solvents were removed in vacuo. The coupling products were obtained after flash chromatography on silica gel (petroleum ether/ethyl acetate mixtures) and/or crystallization. If an oil was obtained, it was dissolved in diethyl ether/methanol and tranferred into the hydrochloride salt by 1N HCl solution in isopropanol/diethyl ether, followed by filtration and optional crystallization from acetone. Analytical data refer to the free base unless otherwise noted.

Procedure B. Boronic acid (1 equivalent), aryl bromide or -triflate (1.3–1.5 equivalents), and tetrakis(triphenylphosphane)palladium(0) (5 mol %) were suspended in toluene/ethanol 4/1 to give a 0.07–0.1 M solution of boronic acid under an atosphere of nitrogen. To this was added a 1 N aqueous solution of Na_2CO_3 (6 equivalents). The mixture was then refluxed for 12–18 h, cooled to room temperature, diluted with water and extracted several times with ethyl acetate. The combined extracts were dried over $MgSO_4$, concentrated and purified by flash chromatography on silica gel (petroleum ether/ethyl acetate mixtures) and/or crystallization. If an oil was obtained, it was dissolved in diethyl ether/methanol and tranferred into the hydrochloride salt by 1N HCl solution in isopropanol/diethyl ether, followed by filtration and optional crystallization from acetone. Analytical data refer to the free base unless otherwise noted.

Procedure C.[33,34] To a 0.6 M solution of NaI (6 equivalents) in acetonitrile was added chlorotrimethylsilane (6 equivalents) at room temperature, and the mixture was stirred for 30 min before cooling to 0 °C with an ice-water bath. Then, a 1 M solution of the phenylnaphthylalcohol (1 equivalent) in acetonitrile was added dropwise. After complete addition the mixture was heated at 55 °C for 3 h. After recooling to room temperature, the reaction was quenched by addition of saturated aqueous $NaHCO_3$ solution. The layers were separated, and the aqueous layer extracted twice with ethyl acetate The combined organic layers were washed with a solution of $Na_2S_2O_3$, water and brine. The extracts were dried over $MgSO_4$, concentrated and purified by flash chromatography on silica gel (petroleum ether/ethyl acetate mixtures). If an oil was obtained, it was dissolved in diethyl ether/methanol and tranferred into the hydrochloride salt by 1N HCl solution in isopropanol/diethyl ether, followed by filtration and optional crystallization from acetone. Analytical data refer to the free base unless otherwise noted.

Procedure D. To a 0.05 M solution of benzoylnaphthalene in dry methanol was added sodium borohydride (2 equivalents) at such a rate as to maintain the internal reaction temperature below 5 °C. The reaction mixture was stirred for 1 h, diluted with diehtylether and treated with saturated aqueous $NaHCO_3$ solution. The mixture was then extracted three times with ethyl acetate, washed twice with saturated aqueous $NaHCO_3$ solution and once with brine and dried over $MgSO_4$. The filtrate was concentrated in vacuo, and the residue was flash chromatographed on silica gel (petroleum ether/ethyl acetate mixtures) to afford the corresponding alcohols.

3-(3-Phenylnaphthalen-2-yl)pyridine (11) was obtained according to procedure A from **11a** (657 mg, 1.86 mmol) and phenylboronic acid (854 mg, 4.00 mmol) after flash chromatography on silica gel (petroleum ether/ethyl acetate, 7/3, R_f = 0.22) as a colorless oil (195 mg, 0.69 mmol, 37 %), precipitation of the hydrochloride salt afforded a highly hygroscopic solid, mp (HCl salt) 106–109 °C. MS *m/z* 282.70 (MH^+). Anal. ($C_{21}H_{15}N \cdot HCl \cdot 1.5H_2O$) C, H, N.

3-(3-Benzylnaphthalen-2-yl)pyridine (12) was obtained according to procedure A from **12a** (433 mg, 1.18 mmol) and 3-pyridineboronic acid (105 mg, 0.85 mmol) after flash chromatography on silica gel (petroleum ether/ethyl acetate, 4/1, R_f = 0.19) as a colorless oil (186 mg, 0.63 mmol, 74 %), mp (HCl salt) 197–198 °C. MS *m/z* 296.14 (MH^+). Anal. ($C_{22}H_{17}N \cdot HCl \cdot 0.6H_2O$) C, H, N.

3-(3-Benzyl-6-methoxynaphthalen-2-yl)pyridine (13) was obtained according to procedure A from **13a** (462 mg, 1.17 mmol) and 3-pyridineboronic acid (100 mg, 0.81 mmol) after flash chromatography on silica gel (petroleum ether/ethyl acetate, 4/1, R_f = 0.18) as a colorless oil (196 mg, 0.60 mmol, 74 %), mp (HCl salt) 170–172 °C. MS *m/z* 326.09 (MH^+). Anal. ($C_{23}H_{19}NO \cdot HCl \cdot 0.6H_2O$) C, H, N.

3-[3-(2-Methoxybenzyl)naphthalen-2-yl]pyridine (14) was obtained according to procedure A from **14a** (462 mg, 1.17 mmol) and 3-pyridineboronic acid (100 mg, 0.81 mmol) after flash chromatography on silica gel (petroleum ether/ethyl acetate, 7/3, R_f = 0.26) as colorless oil (161 mg, 0.50 mmol, 61 %), mp (HCl salt) 214–216 °C. MS *m/z* 326.02 (MH^+). Anal. ($C_{23}H_{19}NO \cdot HCl \cdot 0.6H_2O$) C, H, N.

3-[3-(3-Methoxybenzyl)naphthalen-2-yl]pyridine (15) was obtained according to procedure A from **15a** (433 mg, 1.09 mmol) and 3-pyridineboronic acid (92 mg, 0.75 mmol) after flash chromatography on silica gel (petroleum ether/ethyl acetate, 4/1, R_f = 0.13) as a colorless oil (162 mg, 0.50 mmol, 66 %), mp (HCl salt) 161–162 °C. MS *m/z* 326.02 (MH^+). Anal. ($C_{23}H_{19}NO \cdot HCl \cdot 0.6H_2O$) C, H, N.

3-[3-(4-Methoxybenzyl)naphthalen-2-yl]pyridine (16) was obtained according to procedure A from **16a** (476 mg, 1.20 mmol) and 3-pyridineboronic acid (92 mg, 0.75 mmol) after flash chromatography on silica gel (petroleum ether/ethyl acetate, 4/1, R_f = 0.14) as a colorless oil (199 mg, 0.56 mmol, 75 %), mp (HCl salt) 180–182 °C. ^{1}H-NMR (500 MHz, $CDCl_3$): δ = 3.75 (s, 3H), 4.00 (s, 2H), 6.72 (d, ^3J = 8.8 Hz, 2H), 6.82 (d, ^3J = 8.8 Hz, 2H), 7.26 (ddd, ^3J = 7.9 Hz, ^3J = 4.7 Hz, ^5J = 0.9 Hz, 1H), 7.45–7.52 (m, 3H), 7.68 (s, 1H), 7.70 (s, 1H), 7.79–7.83 (m, 2H), 8.55 (dd, ^4J = 2.2 Hz, ^5J = 0.9 Hz, 1H), 8.59 (dd, ^3J = 4.7 Hz, ^4J = 1.9 Hz, 1H). ^{13}C-NMR (125 MHz, $CDCl_3$): δ = 39.0, 55.2,

113.7, 122.7, 126.0, 126.4, 127.3, 127.6, 128.9, 129.4, 129.7, 132.0, 132.4, 133.1, 136.6, 137.06, 137.13, 148.2, 149.9, 157.9. MS *m/z* 326.16 (MH^+). Anal. ($C_{23}H_{19}NO \cdot HCl \cdot 0.6H_2O$) C, H, N.

4-(3-Pyridin-3-yl-naphthalen-2-ylmethyl)benzonitrile (17) was obtained according to procedure C from **33** (841 mg, 2.50 mmol), sodium iodide (2.25 g, 15.0 mmol) and chlorotrimethylsilane (1.63 g, 15.0 mmol) after flash chromatography on silica gel (petroleum ether/ethyl acetate, 7/3, R_f = 0.15) as a colorless oil (486 mg, 1.52 mmol, 61 %), mp (HCl salt) 130–131 °C. MS *m/z* 321.33 (MH^+). Anal. ($C_{23}H_{16}N_2 \cdot HCl \cdot 0.8H_2O$) C, H, N.

3-[3-(4-Trifluoromethoxybenzyl)naphthalen-2-yl]pyridine (18) was obtained according to procedure C from **34** (395 mg, 1.00 mmol), sodium iodide (899 mg, 6.0 mmol) and chlorotrimethylsilane (652 mg, 6.0 mmol) after flash chromatography on silica gel (petroleum ether/ethyl acetate, 4/1, R_f = 0.28) as a colorless oil (292 mg, 0.77 mmol, 77 %), precipitation of the hydrochloride salt afforded a highly hygroscopic solid, mp (HCl salt) 139–142 °C. MS *m/z* 379.90 (MH^+). Anal. ($C_{24}H_{17}F_3NO \cdot HCl \cdot 0.2H_2O$) C, H, N.

3-[6-Methoxy-3-(4-methoxybenzyl)naphthalen-2-yl]pyridine (19) was obtained according to procedure A from **19a** (512 mg, 1.20 mmol) and 3-pyridineboronic acid (113 mg, 0.92 mmol) after flash chromatography on silica gel (petroleum ether/ethyl acetate, 7/3, R_f = 0.18) as a colorless oil (189 mg, 0.55 mmol, 60 %), mp (HCl salt) 114–115 °C. ^{1}H-NMR (500 MHz, $CDCl_3$): δ = 3.75 (s, 3H), 3.91 (s, 3H), 3.98 (s, 2H), 6.73 (d, ^3J = 8.5 Hz, 2H), 6.84 (d, ^3J = 8.5 Hz, 2H), 7.09 (d, ^4J = 2.5 Hz, 1H), 7.13 (dd, ^3J = 9.0 Hz, ^4J = 2.5 Hz, 1H), 7.25 (dd, ^3J = 8.0 Hz, ^3J = 4.8 Hz, 1H), 7.51 (m, 1H), 7.57 (s, 1H), 7.60 (s, 1H), 7.71 (d, ^3J = 8.9 Hz, 1H), 8.54 (d, ^4J = 1.9 Hz, 1H), 8.56 (dd, ^3J = 4.8 Hz, ^4J = 1.5 Hz, 1H). ^{13}C-NMR (125 MHz, $CDCl_3$): δ = 38.9, 55.2, 55.3, 105.2, 113.7, 119.0, 122.8, 127.5, 127.8, 129.1, 129.2, 129.8, 132.6, 134.4, 134.8, 136.8, 137.3, 137.6, 148.1, 150.1, 157.9, 158.1. MS *m/z* 356.25 (MH^+). Anal. ($C_{24}H_{21}NO_2 \cdot HCl \cdot 0.8H_2O$) C, H, N.

3-[7-Methoxy-3-(4-methoxybenzyl)naphthalen-2-yl]pyridine (20) was obtained according to procedure C from **20a** (400 mg, 1.08 mmol), sodium iodide (1.65 g, 11.0 mmol) and chlorotrimethylsilane (1.20 g, 11.0 mmol) after flash chromatography on silica gel (petroleum ether/ethyl acetate, 7/3, R_f = 0.11) as a colorless oil (148 mg, 0.42 mmol, 39 %), mp (HCl salt) 101–103 °C. MS *m/z* 356.04 (MH^+). Anal. ($C_{24}H_{21}NO_2 \cdot HCl \cdot 0.1H_2O$) C, H, N.

3-Methoxy-5-[3-(4-methoxybenzyl)naphthalen-2-yl]pyridine (21) was obtained according to procedure A from **16a** (396 mg, 1.00 mmol) and 5-methoxy-3-pyridineboronic acid acid (130 mg, 0.85 mmol) after flash chromatography on silica gel (petroleum ether/ethyl acetate, 7/3, R_f = 0.21) as a colorless oil (149 mg, 0.42 mmol, 49 %), mp (HCl salt) 106–108 °C. MS *m/z* 356.09 (MH^+). Anal. ($C_{24}H_{21}NO_2 \cdot HCl \cdot 0.5H_2O$) C, H, N.

3-Methoxy-5-[6-methoxy-3-(4-methoxybenzyl)naphthalen-2-yl]pyridine (22) was obtained according to procedure A from **19a** (426 mg, 1.00 mmol) and 5-methoxy-3-pyridineboronic acid acid (130 mg, 0.85 mmol) after flash chromatography on silica gel (petroleum ether/ethyl acetate, 7/3, R_f = 0.18) as colorless plates (244 mg, 0.63 mmol, 75 %), mp 129–130 °C. MS *m/z* 385.91 (MH^+). Anal. ($C_{25}H_{23}NO_3$) C, H, N.

3-(3-Benzyl-6-methoxynaphthalen-2-yl)5-methoxypyridine (23) was obtained according to procedure A from **13a** (396 mg, 1.00 mmol) and 5-methoxy-3-pyridineboronic acid acid (130 mg, 0.85 mmol) after flash chromatography on silica gel (petroleum ether/ethyl acetate, 7/3, R_f = 0.21) as a colorless oil (221 mg, 0.62 mmol, 73 %), mp (HCl salt) 119–121 °C. MS *m/z* 356.09 (MH^+). Anal. ($C_{24}H_{21}NO_2 \cdot HCl \cdot 0.2H_2O$) C, H, N.

4-[3-(4-Methoxybenzyl)naphthalen-2-yl]isoquinoline (24) was obtained according to procedure A from **16a** (396 mg, 1.00 mmol) and 4-isoquinolineboronic acid (130 mg, 0.75 mmol) after flash chromatography on silica gel (petroleum ether/ethyl acetate, 7/3, R_f = 0.20) as a colorless oil (178 mg, 0.47 mmol, 63 %), mp (HCl salt) 202–203 °C. MS *m/z* 376.12 (MH^+). Anal. ($C_{27}H_{21}NO \cdot HCl \cdot 0.5H_2O$) C, H, N.

4-[6-Methoxy-3-(4-methoxybenzyl)naphthalen-2-yl]isoquinoline (25) was obtained according to procedure A from **19a** (456 mg, 1.07 mmol) and 4-isoquinolineboronic acid (130 mg, 0.75 mmol) after flash chromatography on silica gel (petroleum ether/ethyl acetate, 7/3, R_f = 0.18) and crystallization from acetone/diethyl ether as colorless plates (178 mg, 0.44 mmol, 59 %), mp 158–159 °C. MS *m/z* 406.00 (MH^+). Anal. ($C_{28}H_{23}NO_2$) C, H, N.

(4-Methoxyphenyl)(3-pyridin-3-yl-naphthalen-2-yl)methanone (26) was obtained according to procedure B from **26a** (4.02 g, 9.80 mmol) and 3-pyridineboronic acid (1.02 g, 8.33 mmol) after flash chromatography on silica gel (petroleum ether/ethyl acetate, 1/1, R_f = 0.22) as an off-white solid (2.66 g, 7.84 mmol, 94 %), mp 69–72 °C. MS *m/z* 340.07 (MH^+). Anal. ($C_{23}H_{17}NO_2 \cdot 0.2H_2O$) C, H, N.

(3-Fluoro-4-methoxyphenyl)(3-pyridin-3-yl-naphthalen-2-yl)methanone (27) was obtained according to procedure B from **27a** (4.19 g, 9.78 mmol) and 3-pyridineboronic acid (1.02 g, 8.33 mmol) after flash chromatography on silica gel (petroleum ether/ethyl acetate, 1/1, R_f = 0.16) as an off-white solid (2.52 g, 7.05 mmol, 85 %), mp 96–97 °C. MS *m/z* 358.00 (MH^+). Anal. ($C_{23}H_{16}FNO_2 \cdot 0.1H_2O$) C, H, N.

4-(3-Pyridin-3-yl-naphthalene-2-carbonyl)benzonitrile (28) was obtained according to procedure B from **28a** (3.0 g, 7.40 mmol) and 3-pyridineboronic acid (1.0 g, 8.20 mmol) after flash chromatography on silica gel (petroleum ether/ethyl acetate, 7/3, R_f = 0.15) as yellowish needles (1.67 g, 5.0 mmol, 68 %), mp 135–136 °C. MS *m/z* 335.05 (MH^+). Anal. ($C_{23}H_{14}N_2O \cdot 0.1H_2O$) C, H, N.

(3-Pyridin-3-yl-naphthalen-2-yl)(4-trifluoromethoxyphenyl)methanone (29) was obtained according to procedure B from **29a** (4.57 g, 9.84 mmol) and 3-pyridineboronic acid (1.02 g, 8.33 mmol) after flash chromatography on silica gel (petroleum ether/ethyl acetate, 7/3, R_f = 0.20) as a colorless oil (3.20 g, 8.14 mmol, 98 %), precipitation of the hydrochloride salt afforded a highly hygroscopic solid, mp (HCl salt) 116–118 °C. MS *m/z* 393.89 (MH^+). Anal. ($C_{23}H_{14}F_3NO_2 \cdot HCl$) C, H, N.

(4-Methoxyphenyl)(6-methoxy-3-pyridin-3-yl-naphthalen-2-yl)methanone (30) was obtained according to procedure B from **30a** (1.54 g, 3.50 mmol) and 3-pyridineboronic acid (374 mg, 3.0 mmol) after flash chromatography on silica gel (petroleum ether/ethyl acetate, 1/1, R_f = 0.08) and

crystallization from methanol as a white solid (723 mg, 1.96 mmol, 65 %), mp 140–141 °C. MS *m/z* 370.10 (MH^+). Anal. ($C_{24}H_{19}NO_3 \cdot 0.2H_2O$) C, H, N.

(4-Methoxyphenyl)(3-pyridin-3-yl-naphthalen-2-yl)methanol (31) was obtained according to pocedure D from **26** (1.02 g, 3.0 mmol) and sodium borohydride (226 mg, 6.0 mmol) after flash chromatography on silica gel (petroleum ether/ethyl acetate, 1/1, R_f = 0.18) as a colorless solid (597 mg, 1.75 mmol, 58 %), mp 77–78 °C. MS *m/z* 342.10 (MH^+). Anal. ($C_{23}H_{19}NO_2 \cdot 0.3H_2O$) C, H, N.

(3-Fluoro-4-methoxyphenyl)(3-pyridin-3-yl-naphthalen-2-yl)methanol (32) was obtained according to procedure D from **27** (2.11 g, 5.91 mmol) and sodium borohydride (246 mg, 6.50 mmol) after flash chromatography on silica gel (petroleum ether/ethyl acetate, 1/1, R_f = 0.19) as a yellowish solid (543 mg, 1.51 mmol, 26 %), mp 75–76 °C. MS *m/z* 359.96 (MH^+). Anal. ($C_{23}H_{18}FNO_2 \cdot 0.5H_2O$) C, H, N.

4-[Hydroxy-(3-pyridin-3-yl-naphthalen-2-yl)methyl]benzonitrile (33) was obtained according to procedure D from **28** (1.46 g, 4.37 mmol) and sodium borohydride (182 mg, 4.80 mmol) after flash chromatography on silica gel (petroleum ether/ethyl acetate, 1/1, R_f = 0.16) as a colorless solid (1.22 g, 3.63 mmol, 83 %), mp 101–103 °C. MS *m/z* 336.93 (MH^+). Anal. ($C_{23}H_{16}N_2O \cdot 0.5H_2O$) C, H, N.

(3-Pyridin-3-yl-naphthalen-2-yl)(4-trifluoromethoxyphenyl)methanol (34) was obtained according to Procedure D from **29** (2.80 g, 7.12 mmol) and sodium borohydride (295 mg, 7.80 mmol) after flash chromatography on silica gel (petroleum ether/ethyl acetate, 1/1, R_f = 0.32) as a colorless solid (1.86 g, 4.70 mmol, 66 %), mp 65–66 °C. MS *m/z* 396.20 (MH^+). Anal. ($C_{23}H_{16}F_3NO_2 \cdot 0.2H_2O$) C, H, N.

3-{3-[Methoxy-(4-methoxyphenyl)methyl]naphthalen-2-yl}pyridine (35). To a suspension of NaH (40 mg, 1.0 mmol, 60% dispersion in oil) in 5 mL dry THF at was added dropwise a solution of **31** (300 mg, 0.88 mmol) in 5 mL THF at room temperature under an atmosphere of nitrogen. After hydrogen evolution ceased, a solution of methyliodide (59 µL, 0.95 mmol) in 5 mL THF was added dropwise, and the resulting mixture was stirred for 5 h at room temperature. After 2 h an additional 59 µl methyliodide was added. The mixture was then treated with saturated aqueous NH_4Cl solution and extracted three times with ethyl acetate. The combined organic layers were washed with water and brine, dried over $MgSO_4$ and the solvent was evaporated in vacuo. **35** was obtained after flash chromatography on silica gel (petroleum ether/ethyl acetate, 1/1, R_f = 0.39) as colorless oil (226 mg, 0.64 mmol, 72 %), mp (HCl salt) 113–114 °C. MS *m/z* 356.11 (MH^+). Anal. ($C_{24}H_{21}NO_2 \cdot HCl \cdot 0.7H_2O$) C, H, N.

Biological Methods. 1. Enzyme Preparations. CYP17 and CYP19 preparations were obtained by described methods: the 50,000 *g* sediment of *E. coli* expressing human CYP17[40] and microsomes from human placenta for CYP19.[42] **2. Enzyme Assays.** The following enzyme assays were performed as previously described: CY17[40] and CYP19.[42] **3. Activity and Selectivity Assay Using V79 Cells.** V79 MZh 11B1 and V79 MZh 11B2 cells[36] were incubated with [4-^{14}C]-11-deoxycorticosterone as substrate and inhibitor in at least three different concentrations. The enzyme reactions were stopped by

addition of ethyl acetate. After vigorous shaking and a centrifugation step (10,000 *g*, 2 min), the steroids were extracted into the organic phase, which was then separated. The conversion of the substrate was analyzed by HPTLC and a phosphoimaging system as described.[10,36] **4. Inhibition of Human Hepatic CYP Enzymes.** The recombinantly expressed enzymes from baculovirus-infected insect microsomes (Supersomes) were used and the manufacturer's instructions (www.gentest.com) were followed.

Computational Methods. 1. Pharmacophore Modeling. The most potent compounds of the heteroaryl substituted methyleneindane and naphthalene derivatives and the most potent flavones were selected as training set (see supplementary material for composition of the training set) for the generation of an extended pharmacophore model. GALAHAD,[19] the pharmacophore generation module of SYBYL 7.3.2 (Sybyl, Tripos Inc., St. Louis, Missouri, USA), was used to generate pharmacophore hypotheses of the series of inhibitors form hypermolecules incorporating the structural information of the dataset and alignments from sets of ligand molecules. In the genetic algorithm, default values were used. In the present case, 100 models were generated and the best 20 pharmacophore-hypotheses were saved. GALAHAD takes into account energetics, steric similarity, and pharmacophoric overlap, while accommodating conformational flexibility, ambiguous stereochemistry, alternative ring configurations, multiple partial match constraints, and alternative feature mappings among molecules. All the other molecules of the library were then aligned using each of the 20 pharmacophores as a template, and the best pharmacophore was selected. The top ranked model was the best in three of the most indicative ranking criteria of the used software (Pareto ranking,[20] Specificity, and Mol-query). An additional donor site feature not shown in the figures) was manually added to simulate the complexation of the heme iron by the sp^2-hybridized nitrogen (AA1) in order to fix the orientation of the lone pair of the sp^2-hybridized nitrogen. This refined pharmacophore model was selected as molecular query for the alignment of our database library. The core of the pharmacophoric scheme is formed by five hydrophobic features (HY0, HY1, HY2a, HY2b) and the acceptor atom (AA) spheres represent the H-bond acceptors. In some cases, the acceptor feature AA2a overlapped a donor feature (data not shown), indicating the presence of an OH function. The final pharmacophore model consists of 12 pharmacophoric features: 4 essential ones (HY0, AA1, HY1), necessary for basal inhibitory potency, and 8 partial matches (HY2, HY2b, AA2a, AA2b, HY3, AA3a, AA3b, and AA4). **2. Protein Modeling and Docking.** Using the resolved human cytochrome CYP2C9 structure (PDB code: 1OG5)[43] as template, a homology model was build and refined for CYP11B2. This work has been described in more detail by our group in four recent papers.[12–15] In this study selected compounds were docked into the refined homology model using FlexX-Pharm.[44] A pharmacophore constraint was applied to ensure the right binding mode of the inhibitors with the heme-cofactor. For this purpose the standard Fe–N interaction parameters of FlexX[45,46] were modified and a directed heme-Fe–N interaction was defined perpendicular to the heme-plane. The constraint requires the existence of an inhibitor-nitrogen-atom on the surface of an interaction cone with a 20 degree radius, which has its origin at the Fe-atom and points perpendicular

to the heme-plane (with a length of 2.2 Å). Only docking solutions were accepted, which fulfill this constraint. For all other ligand-protein interactions the standard FlexX interaction parameters and geometries were used. The protein-ligand interactions were analyzed using the FlexX software.

Acknowledgement. We thank Gertrud Schmitt and Jeannine Jung for their help in performing the *in vitro* tests. The investigation of the hepatic CYP profile by Dr. Ursula Müller-Vieira, Pharmacelsus CRO, Saarbrücken, is highly appreciated. S. L. is grateful to Saarland University for a scholarship (Landesgraduierten-Förderung). Thanks are due to Prof. J. J. Rob Hermans, University of Maastricht, The Netherlands, for supplying the V79 CYP11B1 cells, and Prof. Rita Bernhardt, Saarland University, for supplying the V79 CYP11B2 cells.

Supporting Information Available: Additional inhibitory data of compounds **1**–**10** (CYP11B1 inhibition and selectivity factors), NMR spectroscopic data of the target compounds **11**–**15**, **17**, **18**, **20**–**35**, full experimental details and spectroscopic characterization of the reaction intermediates **11a**–**16a**, **19a**, **20a**, **26a**–**30a**, **11b**–**16b**, **19b**, **26b**–**30b**, **11c**–**16c**, **19c**, **11d**–**16d**, **19d**, **26d**–**30d**, **12e**–**14e**, **12f**–**14f**, **12g**–**14g**, **12h**, **13h**, elemental analysis results and purity data (LC/MS) of compounds **11**–**35**, pharmacophore modeling training set and pharmacophore geometric properties. This information is available free of charge via the Internet at http://pubs.acs.org.

References

(1) Kawamoto, T.; Mitsuuchi, Y.; Toda, K.; Yokoyama, Y.; Miyahara, K.; Miura, S.; Ohnishi, T.; Ichikawa, Y.; Nakao, K.; Imura, H.; Ulick, S.; Shizuta, Y. Role of steroid 11β-hydroxylase and steroid 18-hydroxylase in the biosynthesis of glucocorticoids and mineralocorticoids in humans. *Proc. Natl. Acad. Sci. U.S.A.* **1992**, *89*, 1458–1462.

(2) (a) Brilla, C. G. Renin-angiotensin-aldosterone system and myocardial fibrosis. *Cardiovasc. Res.* **2000**, *47*, 1–3. (b) Lijnen, P.; Petrov, V. Induction of cardiac fibrosis by aldosterone. *J. Mol. Cell. Cardiol.* **2000**, *32*, 865–879.

(3) (a) Struthers, A. D. Aldosterone escape during angiotensin-converting enzyme inhibitor therapy in chronic heart failure. *J. Card. Fail.* **1996**, *2*, 47–54. (b) Sato, A.; Saruta, T. Aldosterone escape during angiotensin-converting enzyme inhibitor therapy in essential hypertensive patients with left ventricular hypertrophy. *J. Int. Med. Res.* **2001**, *29*, 13–21.

(4) Pitt, B.; Zannad, F.; Remme, W. J.; Cody, R.; Castaigne, A.; Perez, A.; Palensky, J.; Wittes, J. The effect of spironolactone on morbidity and mortality in patients with severe heart failure. *N. Engl. J. Med.* **1999**, *341*, 709–717.

(5) Pitt, B.; Remme, W.; Zannad, F.; Neaton, J.; Martinez, F.; Roniker, B.; Bittman, R.; Hurley, S.; Kleiman, J.; Gatlin, M. Eplerenone, a selective aldosterone blocker, in patients with left ventricular dysfunction after myocardial infarction. *N. Eng. J. Med.* **2003**, *348*, 1309–1321.

(6) Delcayre, C.; Swynghedauw, B. Molecular mechanisms of myocardial remodeling. The role of aldosterone. *J. Mol. Cell. Cardiol.* **2002**, *34*, 1577–1584.

(7) (a) Wehling, M. Specific, nongenomic actions of steroid hormones. *Annu. Rev. Physiol.* **1997**, *59*, 365–393. (b) Lösel, R.; Wehling, M. Nongenomic actions of steroid hormones. *Nature Rev. Mol. Cell. Biol.* **2003**, *4*, 46–55.

(8) Chai, W.; Garrelds, I. M.; de Vries, R.; Batenburg, W. W.; van Kats, J. P.; Danser, A. H. J. Nongenomic effects of aldosterone in the human heart: Interaction with angiotensin II. *Hypertension* **2005**, *46*, 701–706.

(9) Hartmann, R. W. Selective inhibition of steroidogenic P450 enzymes: Current status and future perspectives. *Eur. J. Pharm. Sci.* **1994**, *2*, 15–16.

(10) Ehmer, P. B.; Bureik, M.; Bernhardt, R.; Müller, U.; Hartmann, R. W. Development of a test system for inhibitors of human aldosterone synthase (CYP11B2): Screening in fission yeast and evaluation of selectivity in V79 cells. *J. Steroid Biochem. Mol. Biol.* **2002**, *81*, 173–179.

(11) Hartmann, R. W.; Müller, U.; Ehmer, P. B. Discovery of selective CYP11B2 (aldosterone synthase) inhibitors for the therapy of congestive heart failure and myocardial fibrosis. *Eur. J. Med. Chem.* **2003**, *38*, 363–366.

(12) Ulmschneider, S.; Müller-Vieira, U.; Mitrenga, M.; Hartmann, R. W.; Oberwinkler-Marchais, S.; Klein, C. D.; Bureik, M.; Bernhardt, R.; Antes, I.; Lengauer, T. Synthesis and evaluation of imidazolylmethylenetetrahydronaphthalenes and imidazolylmethyleneindanes: Potent inhibitors of aldosterone synthase. *J. Med. Chem.* **2005**, *48*, 1796–1805.

(13) Ulmschneider, S.; Müller-Vieira, U.; Klein, C. D.; Antes, I.; Lengauer, T.; Hartmann, R. W. Synthesis and evaluation of (pyridylmethylene)tetrahydronaphthalenes/-indanes and structurally modified derivatives: Potent and selective inhibitors of aldosterone synthase. *J. Med. Chem.* **2005**, *48*, 1563–1575.

(14) Voets, M.; Antes, I.; Scherer, C.; Müller-Vieira, U.; Biemel, K.; Barassin, C.; Oberwinkler-Marchais, S.; Hartmann, R. W. Heteroaryl substituted naphthalenes and structurally modified derivatives: Selective inhibitors of CYP11B2 for the treatment of congestive heart failure and myocardial fibrosis. *J. Med. Chem.* **2005**, *48*, 6632–6642.

(15) Voets, M.; Antes, I.; Scherer, C.; Müller-Vieira, U.; Biemel, K.; Oberwinkler-Marchais, S.; Hartmann, R. W. Synthesis and evaluation of heteroaryl-substituted dihydronaphthalenes and indenes: Potent and selective inhibitors of aldosterone synthase (CYP11B2) for the treatment of congestive heart failure and myocardial fibrosis. *J. Med. Chem.* **2006**, *49*, 2222–2231.

(16) Taymans, S. E.; Pack, S.; Pak, E.; Torpy, D. J.; Zhuang, Z.; Stratakis, C. A. Human CYP11B2 (aldosterone synthase) maps to chromosome 8q24.3. *J. Clin. Endocrinol. Metab.* **1998**, *83*, 1033–1036.

(17) (a) Cavalli, A.; Bisi, A.; Bertucci, C.; Rosini, C.; Paluszcak, A.; Gobbi, S.; Giorgio, E.; Rampa, A.; Belluti, F.; Piazzi, L.; Valenti, P.; Hartmann, R. W.; Recanatini M. Enantioselective nonsteroidal aromatase inhibitors identified through a multidisciplinary medicinal chemistry approach. *J. Med. Chem.* **2005**, *48*, 7282–7289. (b) Gobbi, S.; Cavalli, A.; Rampa, A.; Belluti, F.; Piazzi, L.; Paluszcak, A.; Hartmann, R. W.; Recanatini, M.; Bisi, A. Lead optimization providing a series of flavone derivatives as potent nonsteroidal inhibitors of the cytochrome P450 aromatase enzyme. *J. Med. Chem.* **2006**, *49*, 4777–4780.

(18) Ulmschneider, S.; Negri, M.; Voets, M.; Hartmann, R. W. Development and evaluation of a pharmacophore model for inhibitors of aldosterone synthase (CYP11B2). *Bioorg. Med. Chem. Lett.* **2006**, *16*, 25–30.

(19) (a) Richmond, N. J.; Abrams, C. A.; Wolohan, P. R.; Abrahamian, E.; Willett, P.; Clark, R. D. GALAHAD: 1. Pharmacophore identification by hypermolecular alignment of ligands in 3D. *J. Comput. Aided Mol. Des.* **2006**, *20*, 567–587. (b) Shepphird, J. K.; Clark, R. D. A marriage made in torsional space: Using GALAHAD models to drive pharmacophore multiplet searches. *J. Comput. Aided Mol. Des.* **2006**, *20*, 763–771. (c) http://www.tripos.com.

(20) Gillet, V. J.; Willett, P.; Fleming, P. J.; Green, D. V. S. Designing focused libraries using MoSELECT. *J. Mol. Graph. Model.* **2003**, *20*, 491–498.

(21) Miyaura, N.; Suzuki, A. Palladium-catalyzed cross-coupling reactions of organoboron compounds. *Chem. Rev.* **1995**, *95*, 2457–2483.

(22) Chowdhury, S.; Georghiou, P. E. Synthesis and properties of a new member of the calixnaphthalene family: A C2-symmetrical endo-calix[4]naphthalene. *J. Org. Chem.* **2002**, *67*, 6808–6811.

(23) Bengtson, A.; Hallberg, A.; Larhed, M. Fast synthesis of aryl triflates with controlled microwave heating. *Org. Lett.* **2002**, *4*, 1231–1233.

(24) Appukkuttan, P.; Orts, A. B.; Chandran, R., P.; Goeman, J. L.; van der Eycken, J.; Dehaen, W.; van der Eycken, E. Generation of a small library of highly electron-rich 2-(hetero)aryl-substituted phenethylamines by the Suzuki-Miyaura reaction: A short synthesis of an apogalanthamine analogue. *Eur. J. Org. Chem.* **2004**, 3277–3285.

(25) Miller, L. E.; Hanneman, W. W.; St. John, W. L.; Smeby, R. R. The reactivity of the methyl group in 2-methyl-3-nitronaphthalene. *J. Am. Chem. Soc.* **1954**, *76*, 296–297.

(26) Wu, K.-C.; Lin, Y.-S.; Yeh, Y.-S.; Chen, C.-Y.; Ahmed, M. O.; Chou, P.-T.; Hon, Y.-S. Design and synthesis of intramolecular hydrogen bonding systems. Their application in metal cation sensing based on excited-state proton transfer reaction. *Tetrahedron* **2004**, *60*, 11861–11868.

(27) Brown, H. C.; Narasimhan, S.; Choi, Y. M.; Selective reductions. 30. Effect of cation and solvent on the reactivity of saline borohydrides for reduction of carboxylic esters. Improved procedures for the conversion of esters to alcohols by metal borohydrides. *J. Org. Chem.* **1982**, *47*, 4702–4708.

(28) Einhorn, J.; Einhorn, C.; Ratajczak, F.; Pierre, J.-L. Efficient and highly selective oxidation of primary alcohols to aldehydes by N-chlorosuccinimide mediated by oxoammonium salts. *J. Org. Chem.* **1996**, *61*, 7452–7454.

(29) Parikh, J. R.; Doering, W. v. E. Sulfur trioxide in the oxidation of alcohols by dimethyl sulfoxide. *J. Am. Chem. Soc.* **1967**, *89*, 5505–5507.

(30) Ono, A.; Suzuki, N.; Kamimura, J. Hydrogenolysis of diaryl and aryl alkyl ketones and carbinols by sodium borohydride and anhydrous aluminum(III) chloride. *Synthesis* **1987**, 736–738.

(31) Bieg, T.; Szeja, W. Removal of O-benzyl protective groups by catalytic transfer hydrogenation. *Synthesis* **1985**, 76–77.

(32) Li, X.; Hewgley, J. B.; Mulrooney, C. A.; Yang, J.; Kozlowski, M. C. Enantioselective oxidative biaryl coupling reactions catalyzed by 1,5-diazadecalin metal complexes: Efficient formation of chiral functionalized BINOL derivatives. *J. Org. Chem.* **2003**, *68*, 5500–5511.

(33) Stoner, E. J.; Cothron, D. A.; Balmer, M. K.; Roden, B. A. Benzylation via tandem Grignard reaction-iodotrimethylsilane (TMSI) mediated reduction. *Tetrahedron* **1995**, *51*, 11043–11062.

(34) Cain, G. A.; Holler, E. R. Extended scope of in situ iodotrimethylsilane mediated selective reduction of benzylic alcohols. *Chem. Commun.* **2001**, 1168–1169.

(35) (a) Nakamura, H.; Wu, C.; Inouye, S.; Murai, A. Design, synthesis, and evaluation of the transition-state inhibitors of coelenterazine bioluminescence: Probing the chiral environment of active site. *J. Am. Chem. Soc.* **2001**, *123*, 1523–1524. (b) Gribble, G. W.; Leese, R. M.; Evans, B. E. Reactions of sodium borohydride in acidic media; IV. Reduction of diarylmethanols and triarylmethanols in trifluoroacetic acid. *Synthesis* **1977**, 172–176.

(36) (a) Denner, K.; Bernhardt, R. Inhibition studies of steroid conversions mediated by human CYP11B1 and CYP11B2 expressed in cell cultures. In *Oxygen Homeostasis and Its Dynamics*, 1st ed.; Ishimura, Y., Shimada, H., Suematsu, M., Eds.; Springer-Verlag: Tokyo, Berlin, Heidelberg, New York, 1998; pp 231–236. (b) Denner, K.; Doehmer, J.; Bernhardt, R. Cloning of CYP11B1 and CYP11B2 from normal human adrenal and their functional expression in COS-7 and V79 chinese hamster cells. *Endocr. Res.* **1995**, *21*, 443–448. (c) Böttner, B.; Denner, K.; Bernhardt, R. Conferring aldosterone synthesis to human CYP11B1 by replacing key amino acid residues with CYP11B2-specific ones. *Eur. J. Biochem.* **1998**, *252*, 458–466.

(37) Lamberts, S. W.; Bruining, H. A.; Marzouk, H.; Zuiderwijk, J.; Uitterlinden, P.; Blijd, J. J.; Hackeng, W. H.; de Jong, F. H. The new aromatase inhibitor CGS-16949A suppresses aldosterone and cortisol production by human adrenal cells *in vitro*. *J. Clin. Endocrinol. Metab.* **1989**, *69*, 896–901.

(38) Demers, L. M.; Melby, J. C.; Wilson, T. E.; Lipton, A.; Harvey, H. A.; Santen, R. J. The effects of CGS 16949A, an aromatase inhibitor on adrenal mineralocorticoid biosynthesis. *J. Clin. Endocrinol. Metab.* **1990**, *70*, 1162–1166.

(39) Heim, R.; Lucas, S.; Grombein, C. M.; Ries, C.; Schewe, K. E.; Negri, M.; Müller-Vieira, U.; Birk, B.; Hartmann, R. W. Overcoming undesirable CYP1A2 inhibition of pyridylnaphthalene type aldosterone synthase inhibitors: Influence of heteroaryl derivatization on potency and selectivity. *J. Med. Chem.* **2008**, *51*, 5064–5074.

(40) (a) Ehmer, P. B.; Jose, J.; Hartmann, R. W. Development of a simple and rapid assay for the evaluation of inhibitors of human 17α-hydroxylase-$C_{17,20}$-lyase (P450c17) by coexpression of P450c17 with NADPH-cytochrome-P450-reductase in *Escherichia coli. J. Steroid Biochem. Mol. Biol.* **2000**, *75*, 57–63; (b) Hutschenreuter, T. U.; Ehmer, P. B.; Hartmann, R. W. Synthesis of hydroxy derivatives of highly potent nonsteroidal CYP17 inhibitors as potential metabolites and evaluation of their activity by a non cellular assay using recombinant enzyme. *J. Enzyme Inhib. Med. Chem.* **2004**, *19*, 17–32.

(41) Thompson, E. A.; Siiteri, P. K. Utilization of oxygen and reduced nicotinamide adenine dinucleotide phosphate by human placental microsomes during aromatization of androstenedione. *J. Biol. Chem.* **1974**, *249*, 5364–5372.

(42) Hartmann, R. W.; Batzl, C. Aromatase inhibitors. Synthesis and evaluation of mammary tumor inhibiting activity of 3-alkylated 3-(4-aminophenyl)piperidine-2,6-diones. *J. Med. Chem.* **1986**, *29*, 1362–1369.

(43) Williams, P. A.; Cosme, J.; Ward, A.; Angove, H. C.; Matak Vinkovic, D.; Jhoti, H. Crystal structure of human cytochrome P4502C9 with bound warfarin. *Nature* **2003**, *424*, 464–468.

(44) Hindle, S. A.; Rarey, M.; Buning, C.; Lengauer, T. Flexible docking under pharmacophore type constraints. *J. Comput. Aided Mol. Des.* **2002**, *16*, 129–149.

(45) Rarey, M.; Kramer, B.; Lengauer, T.; Klebe G. A fast flexible docking method using an incremental construction algorithm. *J. Mol. Biol.* **1996**, *261*, 470–489.

(46) Rarey, M.; Kramer, B.; Lengauer, T. Multiple automatic base selection: Protein-ligand docking based on incremental construction without manual intervention. *J. Comput. Aided Mol. Des.* **1997**, *11*, 369–384.

3.3 *In Vivo* Active Aldosterone Synthase Inhibitors with Improved Selectivity: Lead Optimization Providing a Series of Pyridine Substituted 3,4-Dihydro-1*H*-quinolin-2-one Derivatives

Simon Lucas, Ralf Heim, Christina Ries, Katarzyna E. Schewe, Barbara Birk and Rolf W. Hartmann

This manuscript has been published as an article in the

Journal of Medicinal Chemistry **2008**, *51*, 8077-8087

Paper III

Abstract: Pyridine substituted naphthalenes (e.g., **I–III**) constitute a class of potent inhibitors of aldosterone synthase (CYP11B2). To overcome the unwanted inhibition of the hepatic enzyme CYP1A2, we aimed at reducing the number of aromatic carbons of these molecules because aromaticity has previously been identified to correlate positively with CYP1A2 inhibition. As hypothesized, inhibitors with a tetrahydronaphthalene type molecular scaffold (**1**–**11**) exhibit a decreased CYP1A2 inhibition. However, tetralone **9** turned out to be cytotoxic to the human cell line U-937 at higher concentrations. Consequent structural optimization culminated in the discovery of heteroaryl substituted 3,4-dihydro-1*H*-quinolin-2-ones (**12**–**26**), with **12**, a bioisostere of **9**, being none toxic up to 200 μM. The investigated molecules are highly selective toward both CYP1A2 and a wide range of other cytochrome P450 enzymes and show a good pharmacokinetic profile *in vivo* (e.g., **12** with a peroral bioavailability of 71%). Furthermore, isoquinoline derivative **21** proved to significantly reduce plasma aldosterone levels of ACTH stimulated rats.

Introduction

The progressive nature of congestive heart failure (CHF) is a consequence of a neurohormonal imbalance that involves a chronic activation of the renin-angiotensin-aldosterone system (RAAS) in response to reduced cardiac output and reduced renal perfusion. Aldosterone and angiotensin II (Ang II) are excessively released, leading to increased blood volume and blood pressure as a consequence of epithelial sodium retention as well as Ang II mediated vasoconstriction and finally to a further reduction of cardiac output.[1] The RAAS is pathophysiologically stimulated in a vicious cycle of neurohormonal activation that counteracts the normal negative feedback loop regulation. The most important circulating mineralocorticoid, aldosterone, acts by binding to specific mineralocorticoid receptors (MR) located in the cytosol of target epithelial cells. Thereby, renal sodium reabsorption and potassium secretion are promoted in the distal tubule and the collecting duct of the nephron. Elevated blood volume and thus blood pressure results from water that follows the sodium movement via osmosis. In addition to these indirect effects on heart function, aldosterone exerts direct effects on the heart by activating nonepithelial MRs in cardiomyocytes, fibroblasts and endothelial cells. Synthesis and deposition of fibrillar collagens in the fibroblasts result in myocardial fibrosis.[2] Relatively inelastic collagen fibers stiffen the heart muscle which deteriorates the myocardial function and consequently enhances the neurohormonal imbalance by further stimulation of the RAAS. In addition to the effects of circulating aldosterone deriving from adrenal secretion, Satoh et al. reported that aldosterone produced locally in the heart triggers myocardial fibrosis, too.[3] Recent clinical studies with the MR antagonists spironolactone and eplerenone gave evidence for the pivotal role of aldosterone in the progression of cardiovascular diseases. Blocking the aldosterone action by functional antagonism of its receptor reduced the mortality and significantly reduced the symptoms of heart failure.[4] Furthermore, follow-up studies revealed that cardiac fibrosis can not only be prevented but also reversed by use of spironolactone.[5]

However, several issues are unsolved by this therapeutic strategy. Spironolactone binds rather unselectively to the aldosterone receptor and also has some affinity to other steroid receptors, provoking adverse side effects.[4] Although eplerenone is more selective, clinically relevant hyperkalemia remains a principal therapeutic risk.[6] Another crucial point is the high concentration of circulating aldosterone which is not lowered by MR antagonistic therapy and raises several issues. First, the elevated aldosterone plasma levels do not induce a homologous down-regulation but an up-regulation of the aldosterone receptor which complicates a long-term therapy since MR antagonists are likely to become ineffective.[7] Furthermore, the nongenomic actions of aldosterone are in general not blocked by receptor antagonists and can occur despite MR antagonistic treatment.[8] A novel therapeutic strategy for the treatment of hyperaldosteronism, congestive heart failure and myocardial fibrosis with potential to overcome the drawbacks of MR antagonists was recently suggested by us:[9,10] Blockade of aldosterone production by inhibiting the key enzyme of its biosynthesis, aldosterone synthase (CYP11B2), a mitochondrial cytochrome P450 enzyme that is localized mainly in the adrenal cortex and catalyzes the terminal three oxidation steps in the biogenesis of aldosterone in humans.[11]

Consequent structural optimization of a hit discovered by compound library screening led to a series of nonsteroidal aldosterone synthase inhibitors with high selectivity versus other cytochrome P450 enzymes.[12,13] Pyridine-substituted naphthalenes[14,15] such as **I**–**III** (Chart 1) and dihydronaphthalenes,[16] the most potent and selective compounds that emerged from our drug discovery program, however, revealed two major pharmacological drawbacks: A strong inhibition of the hepatic drug metabolizing enzyme CYP1A2 and no inhibitory effect on the aldosterone production *in vivo* by using a rat model.

Chart 1. Pyridylnaphthalene Type CYP11B2 Inhibitors **I**–**III** and Design Strategy for 3,4-Dihydro-1*H*-quinolin-2-one Derivatives (e.g., **12** and **14**)

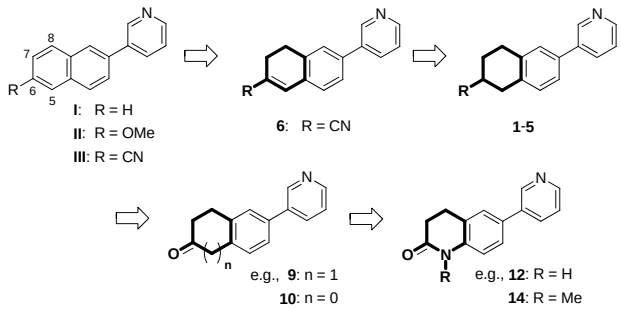

In the present study, we describe the design and the synthesis of pyridine-substituted 3,4-dihydro-1*H*-quinolin-2-ones and structurally related compounds as highly potent and selective CYP11B2 inhibitors (Chart 2). The design concept toward these molecules is based on a systematic reduction of aromaticity by saturation of the hydrocarbons C_5 to C_8 of the naphthalene moiety and subsequent chemical modification of the fully saturated ring (Chart 1). The inhibitory activity of the title compounds was determined in V79 MZh cells expressing human CYP11B2. The selectivity was investigated with respect to the highly homologous 11β-hydroxylase (CYP11B1) as well as other crucial steroid- or drug-metabolizing cytochrome P450 enzymes (CYP17, CYP19, CYP1A2, CYP2B6, CYP2C9, CYP2C19, CYP2D6, and CYP3A4). The *in vivo* pharmacokinetic profile of some promising compounds was determined in male Wistar rats in both cassette and single dosing experiments. Furthermore, plasma protein binding and cytotoxicity studies were performed. The isoquinoline derivative **21** was investigated for aldosterone lowering effects in vivo using ACTH stimulated rats.

Chart 2. Title Compounds

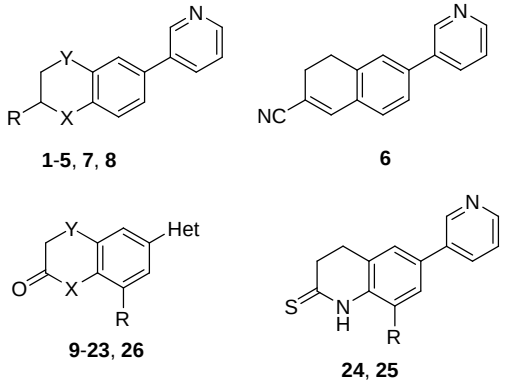

Results

Chemistry

The key step for the synthesis of the title compounds was a Suzuki coupling to introduce the heterocycle, mostly 3-pyridine. In case of the unsubstituted tetrahydronaphthalene **1** the cross-coupling was accomplished by a microwave enhanced method[17] using 3-pyridineboronic acid and triflate **1a** which was prepared from the corresponding tetrahydronaphthol (Scheme 1).[18] Compounds **7**, **8**, and **26** were synthesized via Suzuki coupling from commercially available arylbromides and 3-pyridineboronic acid under microwave heating.

Scheme 1[a]

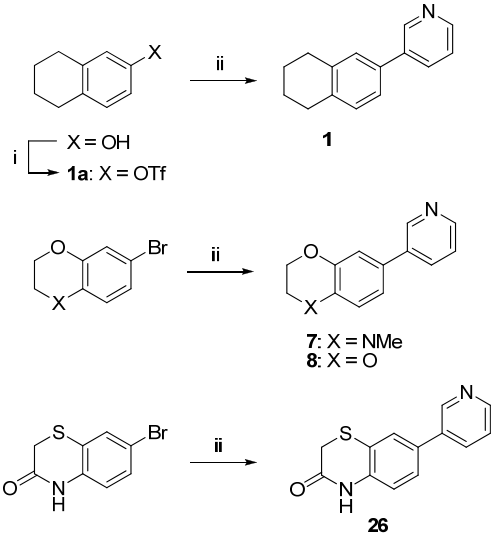

[a] Reagents and conditions: i) Tf_2NPh, K_2CO_2, THF, μw, 120 °C; ii) pyridineboronic acid, $Pd(PPh_3)_4$, aq. $NaHCO_3$, DMF, μw, 150 °C.

The synthesis of compounds **2**–**6** and **9**–**11** (Scheme 2) started from either 6-bromo-2-tetralone (n = 1) or 5-bromo-1-indanone (n = 0) as key building blocks. Suzuki coupling afforded the heterocycle-substituted analogues **9**–**11**. Dihydronaphthalene derivative **6** was prepared by treatment

of tetralone **9** with KHMDS, *in situ* quenching the enolate with Tf_2NPh[19] and Pd-catalyzed cyanation[20] of the intermediate enoltriflate. The hydroxy-substituted tetrahydronaphthalene **2** was obtained by sodium borohydride reduction of the carbonyl group[21] to afford **2a** and subsequent Suzuki coupling. *O*-Alkylation of **2** afforded the corresponding methoxy- (**3**) and ethoxy-substituted (**4**) derivatives. The 6-cyano-derivatized analog **5** was prepared in three consecutive steps starting with a one-pot cyanohydrin/elimination step.[22] The intermediate α,β-unsaturated nitrile **5b** was treated with $NaBH_4$ in refluxing ethanol to reduce the double bond.[23] Final Suzuki coupling of **5a** with 3-pyridineboronic acid afforded the tetrahydronaphthalene **5**.

Scheme 2[a]

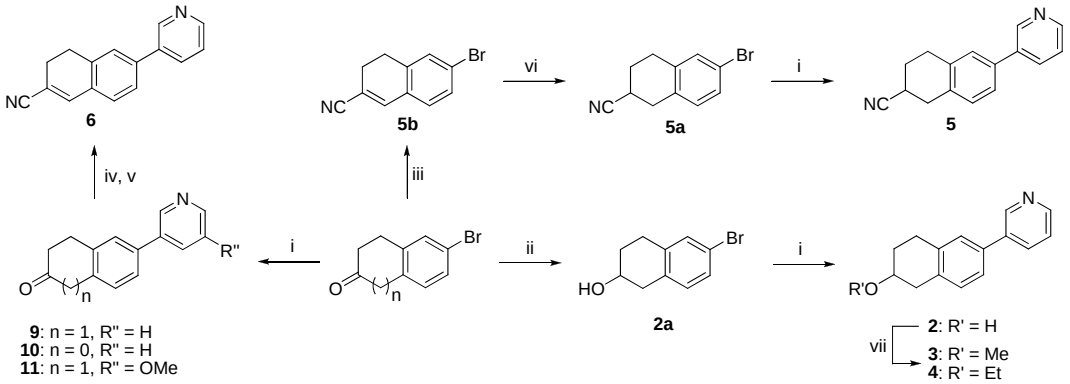

[a] Reagents and conditions: i) heteroarylboronic acid, $Pd(PPh_3)_4$, aq. $NaHCO_3$, DMF, μw, 150 °C; ii) $NaBH_4$, methanol, 0 °C; iii) Me_3SiCN, ZnI_2, toluene, rt, then $POCl_3$, pyridine, reflux; iv) Tf_2NPh, KHMDS, THF/toluene, –78 °C; v) $Zn(CN)_2$, $Pd(PPh_3)_4$, DMF, 100 °C; vi) $NaBH_4$, ethanol, reflux; vii) alkyl halogenide, NaH, THF, 50 °C.

The synthetic route for the compounds with a dihydro-1*H*-quinolin-2-one or structurally related scaffold was accomplished as outlined in Scheme 3. The initial bromination procedures yielding either **12a** or **13a** have been described previously.[24,25] Subsequent *N*-alkylation was accomplished by treating the quinolinones with alkyl halogenide and potassium *tert*-butylate in DMF to afford the intermediates **14a**–**16a**.[26] A nitro substituent was selectively introduced in 8-position of **10a** by sulphonitric acid to yield **18a**.[27] The obtained bromoarenes were transformed into the heterocycle-substituted analogues **12**–**16** and **18**–**23** by Suzuki coupling. Treating **12** with *N*-chlorosuccinimide in DMF at 65 °C afforded the 8-chloro derivative **17** as the only regioisomer. Conversion of the dihydroquinolinones **12** and **17** into the thio analogues **24** and **25** was carried out using Lawessons reagent in refluxing toluene.

Scheme 3[a]

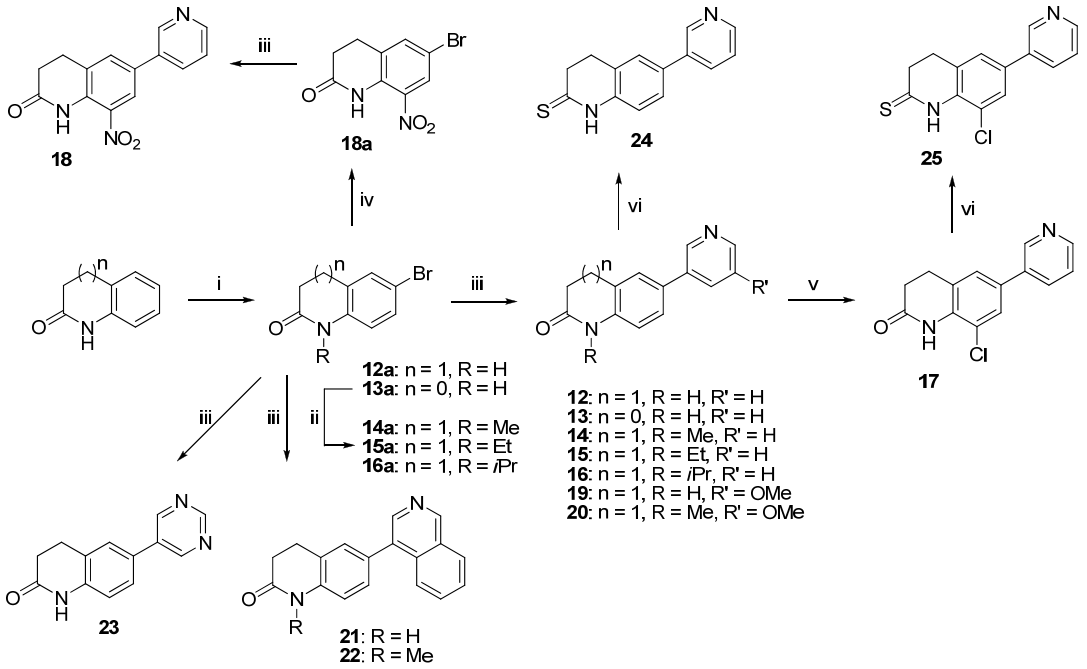

[a] Reagents and conditions: i) NBS, DMF, 0 °C (n = 1) or: Br_2, KBr, water, reflux (n = 0); ii) alkyl halogenide, KO*t*Bu, DMF, rt; iii) heteroarylboronic acid, $Pd(PPh_3)_4$, aq. $NaHCO_3$, DMF, μw, 150 °C or: $Pd(PPh_3)_4$, aq. Na_2CO_3, toluene/ethanol, reflux; iv) HNO_3/H_2SO_4, rt; v) NCS, DMF, 65 °C; vi) Lawesson's reagent, toluene, reflux.

Biology

Inhibition of Human Adrenal Corticoid Producing CYP11B2 and CYP11B1 *In Vitro* (Table 1). The inhibitory activities of the compounds were determined in V79 MZh cells expressing either human CYP11B2 or CYP11B1.[10,28] The V79 MZh cells were incubated with [^{14}C]-deoxycorticosterone as substrate and the inhibitor in different concentrations. The product formation was monitored by HPTLC using a phosphoimager. Fadrozole, an aromatase (CYP19) inhibitor with ability to reduce corticoid formation *in vitro*[29] and *in vivo*[30] was used as a reference (CYP11B2, IC_{50} = 1 nM; CYP11B1, IC_{50} = 10 nM).

Most of the compounds presented in Table 1 show a strong inhibition of the target enzyme. Within the tetrahydro- and dihydronaphthalene series (compounds **1**–**6**), a substituent in 6-position of the carbocyclic skeleton induces an increased inhibitory potency in case of methoxy- (compound **3**) and cyano-substituents (compounds **5**, **6**) as well as a dramatic increase in selectivity toward CYP11B1, most notably in methoxy derivative **3** (selectivity factor = 347). Contrariwise, introduction of hetero-atoms into the saturated ring leads to a decrease of CYP11B2 inhibition (e.g., **7** and **8**). The carbonyl derivatives **9**–**11** are also highly potent (IC_{50} = 1.8–7.8 nM) and selective aldosterone synthase inhibitors. Tetralone **9** is the most selective compound of the present series displaying a CYP11B1 IC_{50} value 496-fold higher than the CYP11B2 IC_{50} value. The derivatives with dihydro-1*H*-quinolin-2-one molecular scaffold (**12**–**26**) exhibit a pronounced inhibitory potency at the target enzyme

(IC_{50} = 0.1–64 nM) and are selective with respect to CYP11B1 inhibition (selectivity factor = 44–440). A significant decrease in inhibitory potency can be observed for derivatization of the lactam nitrogen by an isopropyl residue (compound **16**) whereas methyl (compound **14**) and ethyl (compound **15**) are tolerated in this position. The activity also decreases for 3-pyridine being replaced by 5-pyrimidine (compound **23**) as heterocyclic moiety. Introduction of a nitro substituent in 8-position results in the rather moderate CYP11B2 inhibitor **18** (IC_{50} = 64 nM) with lower CYP11B1 selectivity. Contrariwise, a chloro substituent in the same position (compound **17**) increases the inhibitory potency by a factor of 7 compared to the hydrogen analog **12**. The most potent inhibitors are obtained when the 3-pyridine moiety is modified by 5-methoxylation or replaced by 4-isoquinoline resulting in subnanomolar IC_{50} values for compounds **20**–**22** (IC_{50} = 0.1–0.2 nM). Isoquinoline derivative **22** displays an IC_{50} value as low as 0.1 nM and is the most potent aldosterone synthase inhibitor known so far and also shows a pronounced inhibitory potency at CYP11B1 (IC_{50} = 6.9 nM). The same trend was observed previously for the binding properties of a series of heteroaryl-substituted naphthalenes.[31] Thionation of the lactam carbonyl results in a slightly reduced CYP11B1 selectivity as seen in compounds **24** and **25** compared to the oxygen analogues **12** and **17**. Moreover, incorporation of a sulfur atom into the lactam moiety in compound **26** induces a dramatic loss of CYP11B1 selectivity (selectivity factor = 44).

Table 1. Inhibition of Human Adrenal CYP11B2 and CYP11B1 *In Vitro*

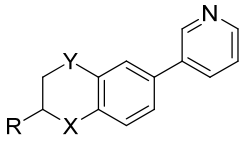

1-5, 7, 8

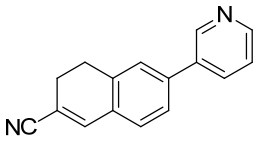

6

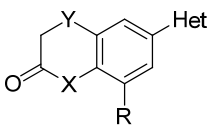

9-23, 26

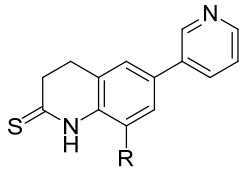

24, 25

					% inhibition[a]	IC_{50} value[b] (nM)		
					V79 11B2[c]	V79 11B2[c]	V79 11B1[d]	selectivity
compd	R	X	Y	Het	hCYP11B2	hCYP11B2	hCYP11B1	factor[e]
1	H	CH_2	CH_2		82	29	1977	68
2	OH	CH_2	CH_2		86	44	4921	112
3	OMe	CH_2	CH_2		97	3.3	1145	347
4	OEt	CH_2	CH_2		92	30	4371	146
5	CN	CH_2	CH_2		94	5.1	745	146
6					97	1.6	290	181
7	H	NMe	O		71	101	5970	59
8	H	O	O		70	154	13378	87
9	H	CH_2	CH_2	3-pyridine	97	7.8	3964	496
10	H	-	CH_2	3-pyridine	90	4.4	819	186
11	H	CH_2	CH_2	5-methoxy-3-pyridine	94	1.8	191	106
12	H	NH	CH_2	3-pyridine	88	28	6746	241
13	H	NH	-	3-pyridine	85	14	5952	425
14	H	NMe	CH_2	3-pyridine	92	2.6	742	289
15	H	NEt	CH_2	3-pyridine	93	22	5177	235
16	H	N*i*Pr	CH_2	3-pyridine	39	n.d.	n.d.	n.d.
17	Cl	NH	CH_2	3-pyridine	97	3.8	1671	440
18	NO_2	NH	CH_2	3-pyridine	78	64	5402	84
19	H	NH	CH_2	5-methoxy-3-pyridine	91	2.7	339	126
20	H	NMe	CH_2	5-methoxy-3-pyridine	94	0.2	87	435
21	H	NH	CH_2	4-isoquinoline	94	0.2	33	187
22	H	NMe	CH_2	4-isoquinoline	99	0.1	6.9	69
23	H	NH	CH_2	5-pyrimidine	57	n.d.	n.d.	n.d.
24	H				97	3.1	580	187
25	Cl				97	4.2	769	183
26	H	NH	S	3-pyridine	92	12	525	44
fadrozole						1	10	10

[a] Mean value of at least four experiments, standard deviation less than 10 %; inhibitor concentration, 500 nM. [b] Mean value of at least four experiments, standard deviation usually less than 25 %, n.d. = not determined. [c] Hamster fibroblasts expressing human CYP11B2; substrate deoxycorticosterone, 100 nM. [d] Hamster fibroblasts expressing human CYP11B1; substrate deoxycorticosterone, 100 nM. [e] IC_{50} CYP11B1/IC_{50} CYP11B2, n.d. = not determined.

Inhibition of Steroidogenic and Hepatic CYP Enzymes (Tables 2 and 3). The inhibition of CYP17 was investigated using the 50,000 *g* sediment of the *E. coli* homogenate recombinantly expressing human CYP17 and progesterone (25 μM) as substrate.[32] The percental inhibition values were measured at an inhibitor concentration of 2.5 μM. Most of the investigated compounds display rather low inhibitory action on CYP17 (Table 2). However, a distinct inhibition in the range of

31–74 % at a concentration of 2.5 μM is observed in case of the tetrahydro- and dihydronaphthalenes **2**–**6** which is comparable to the naphthalene parent compounds **I**–**III** (40–73 %). All other derivatives, including the keto analogues **9**–**11** and the investigated dihydro-1*H*-quinolin-2-ones, are considerably less active at CYP17 (< 22 %). Exceptions from this are lactam **12** (41 % inhibition) and the thiolactam analog **24** (72 %). The inhibition of CYP19 at a concentration of 500 nM was determined *in vitro* with human placental microsomes and [1β-^{3}H]androstenedione as substrate as described by Thompson and Siiteri[33] using our modification.[34] In most cases, the inhibitory action on CYP19 is low (< 30 %) at the chosen concentration (Table 2). Exceptions are observed in case of the keto derivatives **10** and **11** as well as the lactam derivatives **13**–**15** displaying aromatase inhibition in the range of 53–63 %.

Table 2. Inhibition of Human CYP17, CYP19, and CYP1A2 *In Vitro*

	% inhibition[a] [IC_{50} value[b] (μM)]		
compd	CYP17[c]	CYP19[d]	CYP1A2[e]
I	40	[5.727]	99 [n.d.]
II	72	[0.586]	98 [n.d.]
III	73	[> 36]	97 [n.d.]
2	49	23	74 [0.598]
3	44	22	80 [0.443]
4	31	10	73[0.619]
5	38	< 5	72 [0.658]
6	74	< 5	90 [0.181]
9	20	31	60 [1.55]
10	< 5	53	57 [1.55]
11	21	58	57 [1.56]
12	41	21	50 [1.95]
13	< 5	62	25 [6.58]
14	8	54	53 [1.79]
15	< 5	63	36 [3.48]
17	7	17	14 [30.6]
19	12	< 5	25 [5.24]
20	< 5	5	20 [16.5]
21	22	< 5	< 5 [> 150]
24	72	< 5	77 [0.637]

[a] Mean value of three experiments, standard deviation less than 10 %. [b] Mean value of two experiments, standard deviation less than 5 %. [c] *E. coli* expressing human CYP17; substrate progesterone, 25 μM; inhibitor concentration, 2.5 μM; ketoconazole, IC_{50} = 2.78 μM. [d] Human placental CYP19; substrate androstenedione, 500 nM; inhibitor concentration, 500 nM; fadrozole, IC_{50} = 30 nM. [e] Recombinantly expressed enzymes from baculovirus-infected insect microsomes (Supersomes); inhibitor concentration, 2.0 μM; furafylline, IC_{50} = 2.42 μM.

A selectivity profile relating to inhibition of crucial hepatic CYP enzymes (CYP1A2, CYP2B6, CYP2C9, CYP2C19, CYP2D6, and CYP3A4) was determined by use of recombinantly expressed enzymes from baculovirus-infected insect microsomes. As previous studies have shown that aldosterone synthase inhibitors of the naphthalene type are potent inhibitors of CYP1A2 but otherwise rather selective versus important hepatic CYP enzymes,[14,15] most of the newly prepared compounds were first and foremost tested for their inhibitory action on CYP1A2 (Table 2). The parent compounds **I**–**III** are highly potent inhibitors of CYP1A2 (> 95 % inhibition at concentration of 2 μM). Based on these naphthalene type compounds, the inhibitory potency slightly decreases in case of the dihydronaphthalene derivative **6** (90 %) and the tetrahydronaphthalene derivatives **2**–**5** (72–80 %). The keto analogues **9**–**11** exhibit 57–60 % inhibition corresponding with IC_{50} values of 1.55–1.56 μM. A further decrease of CYP1A2 inhibition to less than 50 % is observed for the investigated lactam bioisosters **12**–**15**, **17**, and **19**–**21**. This is especially true for chloro-substituted **17** as well as compounds **20** and **21** with modified heterocycle displaying IC_{50} values greater than 15 μM, but also for indanone **13** and methoxypyridine derivative **19** with IC_{50} values greater than 5 μM. However, compound **24**, the thio analog of **12**, displays a pronounced inhibitory potency (IC_{50} = 0.637 μM). Some compounds were also scrutinized for inhibition of other crucial hepatic CYP enzymes (Table 3). The data presented in Table 3 reveal that the investigated CYP enzymes are rather unaffected by the compounds with tetrahydronaphthalene (**3**), tetralone (**9**–**11**) as well as dihydro-1*H*-quinolin-2-one (**12**, **14**, and **21**) type molecular scaffold and with few exceptions (i.e., **9**, **11** at CYP3A4 and **21** at CYP2C9), the IC_{50} values measured are significantly greater than 10 μM.

Table 3. Inhibition of Selected Hepatic CYP Enzymes *In Vitro*

	IC_{50} value[a] (μM)				
compd	CYP2B6[b,c]	CYP2C9[b,d]	CYP2C19[b,e]	CYP2D6[b,f]	CYP3A4[b,g]
3	47.4	16.3	> 200	> 200	12.2
9	> 50	28.3	41.5	171	6.21
10	> 50	123	147	> 200	> 200
11	> 50	12.9	45.4	> 200	3.75
12	> 50	58.9	> 200	171	127
14	> 50	125	122	> 200	> 200
21	> 100	2.86	9.15	> 50	> 50

[b] Mean value of two experiments, standard deviation less than 5 %. [b] Recombinantly expressed enzymes from baculovirus-infected insect microsomes (Supersomes). [c] Tranylcypromine, IC_{50} = 6.24 μM. [d] Sulfaphenazole, IC_{50} = 318 nM. [e] Tranylcypromine, IC_{50} = 5.95 μM. [f] Quinidine, IC_{50} = 14 nM. [g] Ketoconazole, IC_{50} = 57 nM.

Plasma Protein Binding (Table 4). The plasma protein binding of compounds **9**, **10**, and **12** was determined by ultrafiltration. Test solutions of an aliquot of concentrated test compound and rat or human plasma were incubated at 37 °C for 1 hour and then centrifuged at 8000 *g* for 20 min. Ultrafiltrates were analyzed for drug concentrations by LC-MS/MS. The plasma protein binding of the investigated CYP11B2 inhibitors was found to be low. The bound form of keto compounds **9** and **10**

ranks between 22–25 % in both human and rat plasma. In case of the bioisosteric dihydro-1*H*-quinolin-2-one **12**, the amount of freely available compound is lower (approximately 60 % bound).

Table 4. Plasma Protein Binding of Compounds **9**, **10**, and **12**

compd	PPB[a] (% bound)	
	rat	human
9	25	24
10	24	22
12	60	61

[a] Determined by analysis of the ultrafiltrates via LC-MS/MS; the degree of binding to the plasma proteins (PPB) is calculated by the following equation: % PPB = (1–[ligand$_{ultrafiltrate}$] /[ligand$_{total}$])·100.

***In Vivo* Pharmacokinetics (Table 5).** The pharmacokinetic profile of selected compounds was determined after peroral application to male Wistar rats. Plasma samples were collected over 24 h and plasma concentrations were determined by HPLC-MS/MS. Compounds **9**–**12** and **14** were investigated in cassette dosing experiments (peroral dose = 5 mg/kg) and compared to fadrozole. All five compounds show comparable absorption rates (t_{max} = 4–6 h) and terminal half-lifes ($t_{1/2\,z}$ = 2.3–3.9 h). The slowest elimination is observed in case of tetralone **11** ($t_{1/2\,z}$ = 3.9 h) and dihydro-1*H*-quinolin-2-one **12** ($t_{1/2\,z}$ = 3.8 h). Within this series, compound **10** shows the highest maximal concentration (C_{max}) in plasma (300 ng/mL) followed in the same range by compound **12** (261 ng/mL). Using the area under the curve ($AUC_{0-\infty}$) as a ranking criterion, the bioavailability after peroral cassette dosing increases in the order **11** (212 ng·h/mL) < **14** (659 ng·h/mL) < **9** (727 ng·h/mL) < **12** (1753 ng·h/mL) < **10** (3178 ng·h/mL). Compounds **12** and **21** were investigated in single dosing experiments (peroral dose = 25 mg/kg). The amounts of the test compounds found in the plasma after peroral application are rather high in case of **21** ($AUC_{0-\infty}$ = 1658 ng·h/mL) and high in case of **12** ($AUC_{0-\infty}$ = 4762 ng·h/mL). Comparing the AUC of peroral with intravenous (dose = 1 mg/kg) application of dihydro-1*H*-quinolin-2-one **12** reveals an absolute bioavailability of 71 %.

Table 5. Pharmacokinetic Profile of Compounds **9**–**12**, **14**, and **21**

compd	dose (mg/kg)[a]	$t_{1/2\,z}$ (h)[b]	t_{max} (h)[c]	C_{max} (ng/mL)[d]	$AUC_{0-\infty}$ (ng·h/mL)[e]
9[f]	5	3.5	4.0	104	727
10[f]	5	2.4	4.0	300	3178
11[f]	5	3.9	4.0	35	212
12[f,g]	5	3.8	4.0	261	1753
12	25	1.2	1.0	1537	4762
12	1[h]	1.7	-	-	270
14[f]	5	2.3	6.0	86	659
21	25	2.9	2.0	134	1658
fadrozole[f,g]	5	3.2	1.0	471	3207

[a] Compounds were applied perorally to male Wistar rats. [b] Terminal half-life. [c] Time of maximal concentration. [d] Maximal concentration. [e] Area under the curve. [f] These compounds were investigated in a cassette dosing approach. [g] Mean value of two experiments. [h] Intravenous application.

Among the molecules with a cyclic ketone molecular scaffold, indanone **10** shows the highest availability in the plasma in the cassette dosing experiment with an $AUC_{0-\infty}$ in the range of the marketed drug fadrozole ($AUC_{0-\infty}$ = 3207 ng·h/mL). The tetralone derivatives **9** and **11** exhibit significantly lower $AUC_{0-\infty}$ values (factor 4–15) albeit being eliminated in a decelerated rate ($t_{1/2\ z}$ = 3.5–3.9 h). Similarly, *N*-alkylation of **12** as accomplished in **14** decreases the $AUC_{0-\infty}$ value by a factor of approximately 3. Obviously, introduction of additional methyl or methylene units lowers the bioavailability which might be due to the metabolic vulnerability of these residues and providing potential sites for oxidative transformations. In the single dosing experiments, isoquinoline derivative **21** (with additional benzene moiety compared to **12**) displays an $AUC_{0-\infty}$ somewhat lower than that of unsubstituted **12** (factor 3) as well as a lower maximal concentration in the plasma (factor 11). Contrariwise, the terminal half-life of **21** is greater. This becomes particularly apparent from Figure 1 where the mean profile of plasma levels (ng/mL) in rat versus time after oral application (25 mg/kg) of compounds **12** (Figure 1a) and **21** (Figure 1b) are shown. The concentrations of **21** are rather constant and rank between 90–130 ng/mL in a timeframe of 0.5–8 hours after application, albeit the plasma levels are considerably lower than the plasma levels of **12**.

Figure 1[a]

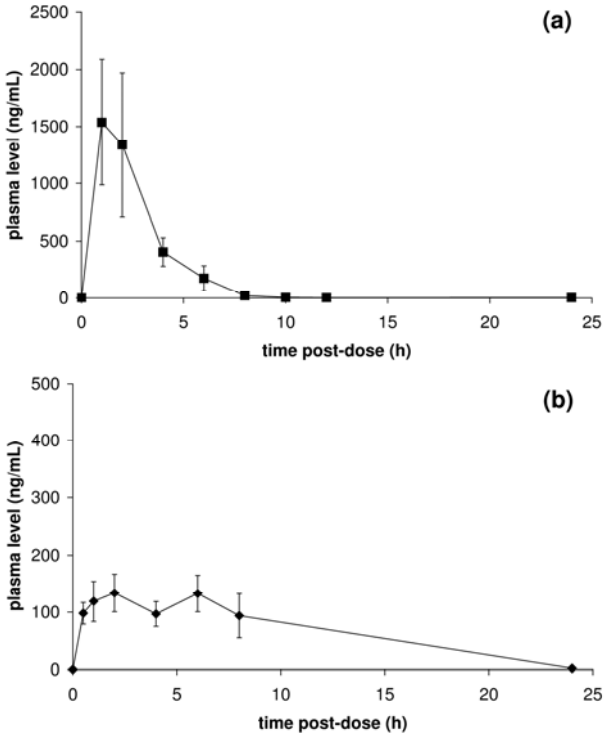

[a] Mean profile (±) SEM of plasma levels (ng/ml) in rat versus time after oral application (25 mg/kg) of compounds **12** (a) and **21** (b) determined in single dosing experiments.

Discussion and Conclusion

Selectivity is a prerequisite of any drug candidate to avoid adverse side effects. In the development process of aldosterone synthase inhibitors, it is a crucial point to investigate the selectivity profile toward other cytochrome P450 enzymes at an early stage. It is known that the concept of heme-iron complexation (e.g., by nitrogen-containing heterocycles) is an appropriate strategy to discover highly potent and selective inhibitors. Due to this binding mechanism, however, a putative CYP11B2 inhibitor is potentially capable of interacting with other CYP enzymes by similarly binding to the heme co-factor with its metal binding moiety. Taking into consideration that the key enzyme of glucocorticoid biosynthesis, 11β-hydroxylase (CYP11B1), and CYP11B2 have a sequence homology of approximately 93%,[35] the selectivity issue is especially critical for the design of CYP11B2 inhibitors. Recently, we have demonstrated that 3-pyridine substituted naphthalenes such as **I**–**III** provide an ideal molecular scaffold for high inhibitory potency at the target enzyme CYP11B2 as well as high selectivity toward several other CYP enzymes (e.g., CYP11B1, CYP17, CYP19).[14] However, these compounds strongly inhibit the hepatic enzyme CYP1A2 (e.g., compounds **I**–**III** in Table 2) that makes up about 10% of the overall cytochrome P450 content in the liver and metabolizes aromatic and heterocyclic amines as well as polycyclic aromatic hydrocarbons. In recent QSAR studies, CYP1A2 inhibition has been identified to correlate positively with aromaticity and lipophilicity.[36] Furthermore, both CYP1A2 substrates and inhibitors are usually small-volume molecules with a planar shape (e.g., caffeine[37] and furafylline[38]). Rationalizing these findings, our design strategy aimed at reducing the aromaticity and disturbing the planarity of the molecules while keeping the pharmacophoric points[39] of the naphthalene molecular scaffold (see Chart 1).

These considerations led to the development of pyridine substituted dihydro- and tetrahydronaphthalenes **1**–**6**. The compounds are potent aldosterone synthase inhibitors with pronounced selectivity toward CYP11B1. As hypothesized, a decrease of CYP1A2 inhibition can be observed along with decreased aromaticity (i.e., number of aromatic carbons) and planarity within this series. While the fully aromatized naphthalenes **I**–**III** exhibit 97–99% inhibition at a concentration of 2 μM, dihydronaphthalene **6** is slightly less potent (90%) and the tetrahydro derivatives **1**–**5** are significantly less potent (72–80%) inhibitors of CYP1A2. However, IC_{50} values are still below 1 μM and thus the molecules are rather strongly inhibiting CYP1A2. Further increase in CYP1A2 selectivity is achieved by introduction of a keto group into the saturated ring as accomplished in compounds **9**–**11**. The inhibitory potencies toward CYP1A2 clearly decrease to IC_{50} values of approximately 1.5 μM. Presumably, the decrease in CYP1A2 inhibition is due to a reduced lipophilicity of the cyclic ketone scaffold compared to the tetrahydronaphthalene scaffold. Lipophilicity has been hypothesized to be one of the most important variables determining CYP1A2 inhibition.[36] Furthermore, the highly potent aldosterone synthase inhibitors **9** (IC_{50} = 7.8 nM) and **10** (IC_{50} = 4.4 nM) show reasonable plasma levels after peroral application to male Wistar rats (Table 5). However, due to the risk of the dialkyl ketone moiety to trigger unwanted cytotoxic effects, tetralone **9** was tested against the human cell line U-937 prior to further optimization. The experiment revealed that this compound significantly

reduces the fractional survival of the U-937 cells at concentrations greater than 100 μM (Figure 2). Although the cytotoxic effect is seen only at rather high concentrations, which might not play a critical role under physiological conditions, a structural modification of the cyclic ketone moiety was performed with the aim to prevent this potential pharmacological drawback at an early stage by choosing a none toxic scaffold for further structural modifications. Subsequent bioisosteric exchange by a lactam moiety gave rise to the dihydro-1*H*-quinolin-2-one derivatives **12**–**26**. Contrary to tetralone **9**, dihydro-1*H*-quinolin-2-one **12** exhibits no distinct cytotoxic effect on U-937 cells up to the highest concentration tested (Figure 2). In addition, compound **12** is an even slightly less potent inhibitor of CYP1A2 (IC_{50} = 1.95 μM) than the analogous tetralone (IC_{50} = 1.55 μM) which is again in correspondence with the reduced lipophilicity compared to the bioisosteric **9**. Contrariwise, lipophilicity does not influence the CYP1A2 potency within the series of dihydro-1*H*-quinolin-2-ones (**12**–**21**) as does the substitution pattern of the molecules, especially in the heterocyclic moiety (e.g., **20** and **21**). It is also striking that even minor structural variations such as introduction of a chloro substituent into the dihydro-1*H*-quinolin-2-one core as accomplished in **17** can induce an almost complete loss of CYP1A2 activity.

Figure 2[a]

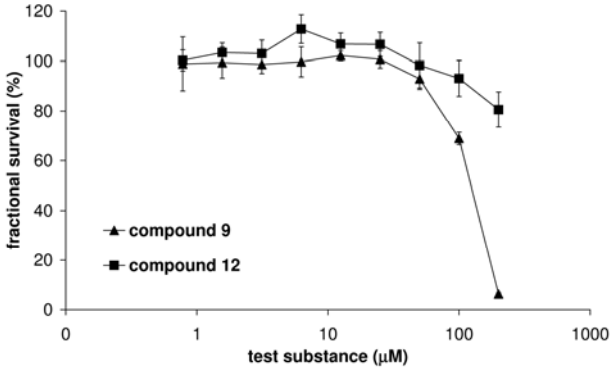

[a] Mean profile (±) SEM of fractional survival (%) of human U-937 cells in presence of compound **9** or **12**.

Pharmacokinetic investigations performed with compound **12** reveal a peroral absolute bioavailability of 71%. Compounds **14** and **21** are also capable of crossing the gastrointestinal tract and reach the general circulation after peroral application. However, their total range of absorption is below that of **12**. The plasma protein binding of inhibitor **12** was found to be low in both rat and human plasma (approximately 60%), indicating that a sizeable free fraction of circulating compound is present in the plasma. Within the series of dihydro-1*H*-quinolin-2-one type inhibitors **12**–**26**, most compounds are highly active at the target enzyme. This particularly applies to the derivatives with a functionalized pyridine heterocycle, for example methoxy derivative **20** (IC_{50} = 0.2 nM) and isoquinoline derivatives **21** (IC_{50} = 0.2 nM) and **22** (IC_{50} = 0.1 nM). By introduction of a chloro substituent in the 8-position or methoxy in the 5-position of the pyridine heterocycle, the selectivity increases to a factor of greater than 400 (**17**, **20**). Hence, these compounds are approximately 40-fold

more selective than fadrozole (selectivity factor = 10). With respect to the high homology of the two CYP11B isoforms, this experimental result is particularly noteworthy.

In order to measure aldosterone-lowering effects in rats, we investigated the most potent and selective inhibitors of the present series for their ability to block aldosterone biosynthesis in V79 MZh cells expressing *rat* CYP11B2 prior to *in vivo* experiments. The results revealed that only compound **21** (and to a minor degree also the *N*-methyl analog **22**) shows a moderate inhibitory action toward rat CYP11B2 *in vitro* which corroborates our expectations concerning potential problems due to species cross-over, presumably as a consequence of a rather low sequence identity of the human and the rat CYP11B2 enzyme (approximately 69%).[40] The most potent compound in the rat assay, isoquinoline derivative **21**, is also a highly potent inhibitor of human CYP11B2 *in vitro* (IC_{50} = 0.2 nM) and exhibits a pronounced selectivity toward other CYP enzymes. Examination of availability in plasma following peroral administration of this compound to rats revealed a good half-life (2.9 h) and reasonable plasma levels ($AUC_{0-\infty}$ = 1658 ng·h/mL following a 25 mg/kg dose). For the *in vivo* study, we used the animal model of Häusler et al. where the animals receive a subcutaneous injection of ACTH (1 mg/kg) 16 hours before test item application to stimulate the gluco- and mineralocorticoid biosynthesis and the aldosterone levels are determined using RIA.[40,41] The plasma aldosterone levels of the individual animals of this study are shown in Figure 3. It becomes apparent that ACTH treatment induces a significant increase of the aldosterone levels. Within the vehicle-treated group (animals 7–10, Figure 3b), the concentrations found in the plasma are rather constant over the duration of the experiment (6 h). To six animals (compound **21** group) isoquinoline derivative **21** was intravenously applied in a 20 mg/kg dose after 16 hours upon ACTH treatment (animals 1–6, Figure 3a). A significant aldosterone-lowering effect can already be observed after 15 min. Within a timeframe of 0.5–3 hours, the aldosterone concentrations are maximally reduced to 36–63% of the prior ACTH level for the individual animals of the compound **21** group.

Figure 3[a]

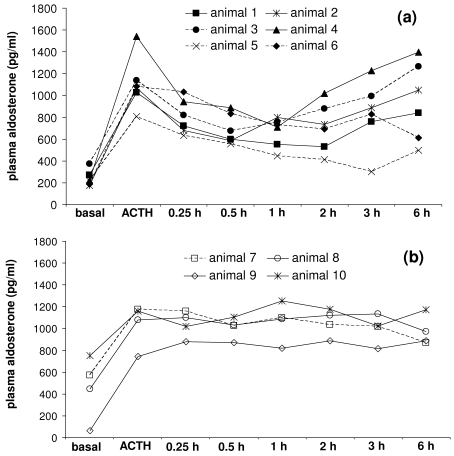

[a] Lowering of aldosterone plasma levels *in vivo* of (a) the compound **21** treated group (animals 1–6) and (b) the vehicle treated group (animals 7–10). Shown are the aldosterone plasma levels of the individual animals pre-dose before s.c. application of 1 mg/kg ACTH, and before i.v. application of 20 mg/kg **21** (animals 1–6) or vehicle (animals 7–10), followed by sampling 0.25, 0.5, 1, 2, 3, and 6 hours post-dose.

In summary, nonsteroidal aldosterone synthase inhibitors with a dihydro-1*H*-quinolin-2-one molecular scaffold are superior to the previously investigated pyridylnaphthalenes such as **I**–**III**. Most compounds exhibit a potent inhibitory activity at the target enzyme and isoquinoline derivative **22** is the most potent CYP11B2 inhibitor described so far (IC_{50} = 0.1 nM). The selectivity versus other steroidogenic as well as hepatic cytochrome P450 enzymes is generally high. Most notably, the strong inhibition of the hepatic CYP1A2 enzyme (> 95% at a concentration of 2 μM) present in the naphthalene type inhibitors is significantly lower in case of the dihydro-1*H*-quinolin-2-ones with IC_{50} values up to > 150 μM (**21**). The investigated molecules reach the circulation after peroral administration to rats (e.g., **12** with a peroral bioavailability of 71%). Moreover, it has been found, that isoquinoline derivative **21** significantly reduces the plasma aldosterone levels of ACTH stimulated rats. Our current research focuses on further *in vivo* investigations of compound **21** and structurally related compounds in disease oriented models to determine their capability to prevent or reverse myocardial fibrosis and reduce CHF induced mortality.

Experimental Section

Chemical and Analytical Methods. Melting points were measured on a Mettler FP1 melting point apparatus and are uncorrected. ^{1}H NMR and ^{13}C spectra were recorded on a Bruker DRX-500 instrument. Chemical shifts are given in parts per million (ppm), and tetramethylsilane (TMS) was used as internal standard for spectra obtained in DMSO-d_6 and $CDCl_3$. All coupling constants (J) are given in hertz. Mass spectra (LC/MS) were measured on a TSQ Quantum (Thermo Electron Corporation) instrument with a RP18 100-3 column (Macherey Nagel) and with water/acetonitrile mixtures as eluents. GC/MS spectra were measured on a GCD Series G1800A (Hewlett Packard) instrument with an Optima-5-MS (0.25 µM, 30 m) column (Macherey Nagel). Elemental analyses were carried out at the Department of Chemistry, University of Saarbrücken. Reagents were used as obtained from commercial suppliers without further purification. Solvents were distilled before use. Dry solvents were obtained by distillation from appropriate drying reagents and stored over molecular sieves. Flash chromatography was performed on silica gel 40 (35/40–63/70 µM) with petroleum ether/ethyl acetate mixtures as eluents, and the reaction progress was determined by thin-layer chromatography analyses on Alugram SIL G/UV254 (Macherey Nagel). Visualization was accomplished with UV light and $KMnO_4$ solution. All microwave irradiation experiments were carried out in a CEM-Discover monomode microwave apparatus.

The following compounds were prepared according to previously described procedures: 6-bromo-1,2,3,4-tetrahydronaphthalen-2-ol (**2a**),[21] 6-bromo-3,4-dihydroquinolin-2(1*H*)-one (**12a**),[24] 5-bromo-1,3-dihydro-2*H*-indol-2-one (**13a**),[25] 6-bromo-8-nitro-3,4-dihydroquinolin-2(1*H*)-one (**18a**).[27]

Synthesis of the Target Compounds

Procedure A.[17] Boronic acid (0.75 mmol, 1 equivalent), aryl bromide or -triflate (0.9–1.3 equivalents), and tetrakis(triphenylphosphane)palladium(0) (43 mg, 37.5 µmol, 5 mol %) were suspended in 1.5 mL DMF in a 10 mL septum-capped tube containing a stirring magnet. To this was added a solution of $NaHCO_3$ (189 mg, 2.25 mmol, 3 equivalents) in 1.5 mL water and the vial was sealed with an Teflon cap. The mixture was irradiated with microwaves for 15 min at a temperature of 150 °C with an initial irradiation power of 100 W. After the reaction, the vial was cooled to 40 °C, the crude mixture was partitioned between ethyl acetate and water and the aqueous layer was extracted three times with ethyl acetate. The combined organic layers were dried over $MgSO_4$ and the solvents were removed in vacuo. The coupling products were obtained after flash chromatography on silica gel (petroleum ether/ethyl acetate mixtures) and/or crystallization.

Procedure B. Boronic acid (1 equivalent), aryl bromide or (1.3–1.5 equivalents), and tetrakis(triphenylphosphane)palladium(0) (5 mol %) were suspended in toluene/ethanol 4/1 to give a 0.07–0.1 M solution of boronic acid under an atosphere of nitrogen. To this was added a 1 N aqueous solution of Na_2CO_3 (6 equivalents). The mixture was then refluxed for 12–18 h, cooled to room temperature, diluted with water and extracted several times with ethyl acetate. The combined extracts were dried over $MgSO_4$, concentrated and purified by flash chromatography on silica gel (petroleum ether/ethyl acetate mixtures) and/or crystallization.

3-(5,6,7,8-tetrahydronaphthalen-2-yl)pyridine (1) was obtained according to procedure A from **1a** (280 mg, 1.0 mmol), 3-pyridineboronic acid (160 mg, 1.3 mmol) and $NaHCO_3$ (252 mg, 3.0 mmol) after flash chromatography on silica gel (petroleum ether/ethyl acetate, 2/1, R_f = 0.20) as a pale yellow oil (142 mg, 0.68 mmol, 68 %), mp (HCl salt) 200–202 °C. LC/MS *m/z* 210.27 (MH^+). Anal. ($C_{15}H_{15}N$·HCl) C, H, N.

6-Pyridin-3-yl-1,2,3,4-tetrahydronaphthalen-2-ol (2) was obtained according to procedure A from **2a** (114 mg, 0.50 mmol) and 3-pyridineboronic acid (80 mg, 0.65 mmol) after flash chromatography on silica gel (ethyl acetate, R_f = 0.27) as a colorless solid (96 mg, 0.43 mmol, 86 %), mp 118–120 °C. LC/MS *m/z* 226.23 (MH^+). Anal. ($C_{15}H_{15}NO$·0.1H_2O) C, H, N.

3-(6-Methoxy-5,6,7,8-tetrahydronaphthalen-2-yl)pyridine (3). To a suspension of NaH (73 mg, 1.84 mmol, 60 % dispersion in oil) in 10 mL dry THF was added dropwise a solution of **2** (345 mg, 1.53 mmol) in 5 mL THF at room temperature. The mixture was heated to 50 °C until evolution of hydrogen ceased and then cooled to room temperature again. Thereupon, a solution of methyl iodide (326 mg, 2.30 mmol) in 5 mL THF was added via canula and stirring was continued at 50 °C for 3 h. The mixture was treated with saturated NH_4Cl solution and extracted three times with ethyl acetate. The combined organic extracts were washed with water and brine, dried over $MgSO_4$ and evaporated to dryness. The crude product was purified by flash chromatography on silica gel (petroleum ether/ethyl acetate, 7/3, R_f = 0.09) to afford **3** as a colorless oil (289 mg, 1.21 mmol, 79 %), mp (HCl salt) 188–190 °C. LC/MS *m/z* 240.29 (MH^+). Anal. ($C_{16}H_{17}NO$·HCl·0.6H_2O) C, H, N.

3-(6-Ethoxy-5,6,7,8-tetrahydronaphthalen-2-yl)pyridine (4) was obtained as described for **3** starting from **2** (270 mg, 1.20 mmol), NaH (58 mg, 1.44 mmol, 60 % dispersion in oil) and ethyl bromide (196 mg, 1.80 mmol) after flash chromatography on silica gel (petroleum ether/ethyl acetate, 1/1, R_f = 0.31) as a colorless oil (198 mg, 0.78 mmol, 65 %), mp (HCl salt) 186–188 °C. LC/MS *m/z* 254.29 (MH^+). Anal. ($C_{17}H_{19}NO$·HCl·0.5H_2O) C, H, N.

6-Pyridin-3-yl-1,2,3,4-tetrahydronaphthalene-2-carbonitrile (5) was obtained according to procedure A from **5a** (130 mg, 0.55 mmol) and 3-pyridineboronic acid (88 mg, 0.72 mmol) after flash chromatography on silica gel (petroleum ether/ethyl acetate, 1/1, R_f = 0.17) as a colorless solid (91 mg, 0.39 mmol, 71 %), mp 110–111 °C. ^{1}H-NMR (500 MHz, $CDCl_3$): δ = 2.12 (m, 1H), 2.23 (m, 1H), 2.92 (m, 1H), 3.02–3.13 (m, 3H), 3.18 (dd, ^2J = 16.4 Hz, ^3J = 5.7 Hz, 1H), 7.19 (d, ^3J = 7.9 Hz, 1H), 7.31 (s, 1H), 7.33–7.37 (m, 2H), 7.83 (m, 1H), 8.57 (dd, ^3J = 5.0 Hz, ^4J = 1.6 Hz, 1H), 8.80 (d, ^4J = 1.6 Hz, 1H). ^{13}C-NMR (125 MHz, $CDCl_3$): δ = 25.5, 26.1, 27.1, 32.1, 121.8, 123.5, 125.1, 127.8, 129.8, 132.3, 134.2, 135.5, 136.2, 136.4, 148.2, 148.5. LC/MS *m/z* 235.26 (MH^+). Anal. ($C_{16}H_{14}N_2$·0.1H_2O) C, H, N.

6-Pyridin-3-yl-3,4-dihydronaphthalene-2-carbonitrile (6). To a solution of **6a** (562 mg, 1.58 mmol) in 10 mL degassed DMF were added zinc cyanide (117 mg, 1.00 mmol) and tetrakis-(triphenylphosphane)palladium(0) (173 mg, 0.15 mmol) and the mixture was heated at 100 °C for 2 h. After cooling to room temperature, the mixture was diluted with 200 mL of water and extracted three times with ethyl acetate. The combined organic extracts were washed with water and brine, dried over

$MgSO_4$ and evaporated to dryness. The crude product was crystallized from petroleum ether/ethyl acetate to afford **6** as colorless needles (286 mg, 1.23 mol, 78 %), mp 142–143 °C. LC/MS *m/z* 233.23 (MH^+). Anal. ($C_{16}H_{12}N_2$) C, H, N.

4-Methyl-7-pyridin-3-yl-3,4-dihydro-2*H*-1,4-benzoxazine (7) was obtained according to procedure A from 7-bromo-4-methyl-3,4-dihydro-2*H*-1,4-benzoxazine (228 mg, 1.00 mmol) and 3-pyridineboronic acid (160 mg, 1.30 mmol) after flash chromatography on silica gel (petroleum ether/ethyl acetate, 1/1, R_f = 0.26) as an off-white solid (102 mg, 0.45 mmol, 45 %), mp 70–72 °C. LC/MS *m/z* 227.21 (MH^+). Anal. ($C_{14}H_{14}N_2O$) C, H, N.

3-(2,3-Dihydro-1,4-benzodioxin-6-yl)pyridine (8) was obtained according to procedure A from 6-bromo-2,3-dihydro-1,4-benzodioxine (215 mg, 1.00 mmol) and 3-pyridineboronic acid (160 mg, 1.30 mmol) after flash chromatography on silica gel (petroleum ether/ethyl acetate, 7/3, R_f = 0.14) as a colorless solid (184 mg, 0.86 mmol, 86 %), mp 59–61 °C. LC/MS *m/z* 214.19 (MH^+). Anal. ($C_{16}H_{12}N_2$) C, H, N.

6-Pyridin-3-yl-3,4-dihydronaphthalen-2(1*H*)-one (9) was obtained according to procedure A from 6-bromo-2-tetralone (113 mg, 0.50 mmol) and 3-pyridineboronic acid (80 mg, 0.65 mmol) after flash chromatography on silica gel (petroleum ether/ethyl acetate, 1/1, R_f = 0.15) as a colorless oil (97 mg, 0.43 mmol, 86 %), mp (HCl salt) 180–182 °C. LC/MS *m/z* 224.20 (MH^+). Anal. ($C_{15}H_{13}NO{\cdot}HCl{\cdot}0.4H_2O$) C, H, N.

5-Pyridin-3-yl-2,3-dihydro-1*H*-inden-1-one (10) was obtained according to procedure A from 5-bromo-1-indanone (211 mg, 1.00 mmol) and 3-pyridineboronic acid (160 mg, 1.30 mmol) after flash chromatography on silica gel (petroleum ether/ethyl acetate, 1/1, R_f = 0.14) as a colorless solid (146 mg, 0.69 mmol, 69 %), mp 122–123 °C. LC/MS *m/z* 210.69 (MH^+). Anal. ($C_{14}H_{11}NO{\cdot}0.1H_2O$) C, H, N.

6-(5-Methoxypyridin-3-yl)-3,4-dihydronaphthalen-2(1*H*)-one (11) was obtained according to procedure A from 6-bromo-2-tetralone (225 mg, 1.00 mmol) and 5-methoxy-3-pyridineboronic acid (199 mg, 1.30 mmol) after flash chromatography on silica gel (petroleum ether/ethyl acetate, 1/1, R_f = 0.15) as an off-white solid (133 mg, 0.53 mmol, 53 %), mp 109–110 °C. LC/MS *m/z* 254.01 (MH^+). Anal. ($C_{16}H_{15}NO_2$) C, H, N.

6-Pyridin-3-yl-3,4-dihydroquinolin-2(1*H*)-one (12) was obtained according to procedure B from **12a** (2.71 g, 12.0 mmol) and 3-pyridineboronic acid (1.23 g, 10.0 mmol) after crystallization from acetone/diethyl ether as colorless needles (2.15 g, 9.59 mmol, 96 %), mp 181–183 °C. ^{1}H-NMR (500 MHz, DMSO-d_6): δ = 2.49 (t, ^3J = 7.3 Hz, 2H), 2.95 (t, ^3J = 7.3 Hz, 2H), 6.95 (d, ^3J = 8.2 Hz, 1H), 7.43 (ddd, ^3J = 7.9 Hz, ^3J = 4.7 Hz, ^5J = 0.6 Hz, 1H), 7.51 (dd, ^3J = 8.2 Hz, ^4J = 2.2 Hz, 1H), 7.56 (d, ^4J = 2.1 Hz, 1H), 8.00 (ddd, ^3J = 7.9 Hz, ^4J = 2.2 Hz, ^4J = 1.6 Hz, 1H), 8.50 (dd, ^3J = 4.7 Hz, ^4J = 1.5 Hz, 1H), 8.84 (d, ^4J = 2.2 Hz, 1H), 10.19 (s, 1H). ^{13}C-NMR (125 MHz, DMSO-d_6): δ = 24.8, 30.3, 115.6, 123.8, 124.3, 125.6, 126.2, 130.6, 133.4, 135.2, 138.4, 147.2, 147.8, 170.2. LC/MS *m/z* 225.25 (MH^+). Anal. ($C_{14}H_{12}N_2O{\cdot}0.1H_2O$) C, H, N.

5-Pyridin-3-yl-1,3-dihydro-2*H*-indol-2-one (13) was obtained according to procedure A from **13a** (159 mg, 0.75 mmol) and 3-pyridineboronic acid (123 mg, 1.00 mmol) after crystallization from acetone/diethyl ether as colorless needles (129 mg, 0.61 mmol, 81 %), mp 218–220 °C. LC/MS *m/z* 211.01 (MH^+). Anal. ($C_{13}H_{10}N_2O \cdot 0.3H_2O$) C, H, N.

1-Methyl-6-pyridin-3-yl-3,4-dihydroquinolin-2(1*H*)-one (14) was obtained according to procedure A from **14a** (110 mg, 0.46 mmol) and 3-pyridineboronic acid (74 mg, 0.60 mmol) after flash chromatography on silica gel (petroleum ether/ethyl acetate, 2/3, R_f = 0.07) as colorless needles (83 mg, 0.35 mmol, 76 %), mp 100–101 °C. LC/MS *m/z* 239.80. Anal. ($C_{15}H_{14}N_2O \cdot 0.1H_2O$) C, H, N.

1-Ethyl-6-pyridin-3-yl-3,4-dihydroquinolin-2(1*H*)-one (15) was obtained according to procedure A from **15a** (229 mg, 0.90 mmol) and 3-pyridineboronic acid (92 mg, 0.75 mmol) after flash chromatography on silica gel (petroleum ether/ethyl acetate, 1/1, R_f = 0.09) and crystallization from acetone/diethyl ether as colorless plates (125 mg, 0.50 mmol, 55 %), mp 91–92 °C. LC/MS *m/z* 253.00 (MH^+). Anal. ($C_{16}H_{16}N_2O \cdot 0.1H_2O$) C, H, N.

1-(1-Methylethyl)-6-pyridin-3-yl-3,4-dihydroquinolin-2(1*H*)-one (16) was obtained according to procedure A from **16a** (174 mg, 0.65 mmol) and 3-pyridineboronic acid (74 mg, 0.60 mmol) after flash chromatography on silica gel (petroleum ether/ethyl acetate, 1/1, R_f = 0.14) as a colorless solid (47 mg, 0.18 mmol, 29 %), mp 100–101 °C. LC/MS *m/z* 267.10 (MH^+). Anal. ($C_{17}H_{18}N_2O$) C, H, N.

8-Chloro-6-pyridin-3-yl-3,4-dihydroquinolin-2(1*H*)-one (17). To a solution of **12** (560 mg, 2.50 mmol) in 5 mL DMF was added *N*-chlorosuccinimide (368 mg, 2.75 mmol) in 5 mL DMF over a period 2 h at 65 °C. After additional 3 h at 65 °C, the mixture was poured into ice water and extracted three times with ethyl acetate. The combined organic layers were washed with water and brine, dried over $MgSO_4$ and the solvent was evaporated in vacuo. **17** was obtained after flash chromatography on silica gel (petroleum ether/ethyl acetate, 3/7, R_f = 0.15) and crystallization from acetone/diethyl ether as colorless needles (225 mg, 0.87 mmol, 35 %), mp 177–178 °C. GC/MS *m/z* 258.95 (M^+). Anal. ($C_{14}H_{11}ClN_2O \cdot 0.1H_2O$) C, H, N.

8-Nitro-6-pyridin-3-yl-3,4-dihydroquinolin-2(1*H*)-one (18) was obtained according to procedure B from **18a** (1.0 g, 3.70 mmol) and 3-pyridineboronic acid (546 mg, 4.44 mmol) after flash chromatography on silica gel (ethyl acetate, R_f = 0.15) as yellow needles (311 mg, 1.16 mmol, 31 %), mp 187–189 °C. LC/MS *m/z* 269.94 (MH^+). Anal. ($C_{14}H_{11}N_3O_3$) C, H, N.

6-(5-Methoxypyridin-3-yl)-3,4-dihydroquinolin-2(1*H*)-one (19) was obtained according to procedure A from **12a** (170 mg, 0.75 mmol) and 5-methoxy-3-pyridineboronic acid (150 mg, 0.98 mmol) after crystallization from acetone/diethyl ether as colorless needles (77 mg, 0.30 mmol, 40 %), mp 213–215 °C. LC/MS *m/z* 255.02 (MH^+). Anal. ($C_{15}H_{14}N_2O_2$) C, H, N.

6-(5-methoxypyridin-3-yl)-1-methyl-3,4-dihydroquinolin-2(1*H*)-one (20) was obtained according to procedure A from **14a** (200 mg, 0.83 mmol) and 5-methoxy-3-pyridineboronic acid (115 g, 0.75 mmol) after crystallization from acetone/diethyl ether as colorless needles (132 mg, 0.49 mmol, 66 %), mp 158–159 °C. LC/MS *m/z* 268.95 (MH^+). Anal. ($C_{16}H_{16}N_2O_2 \cdot 0.1H_2O$) C, H, N.

6-Isoquinolin-4-yl-3,4-dihydroquinolin-2(1*H*)-one (21) was obtained according to procedure B from **12a** (1.55 g, 6.85 mmol) and 4-isoquinolineboronic acid (950 mg, 5.50 mmol) after crystallization from acetone/diethyl ether as colorless needles (800 mg, 2.92 mmol, 53 %), mp 221–222 °C. LC/MS *m/z* 275.04 (MH^+). Anal. ($C_{18}H_{14}N_2O \cdot 0.1H_2O$) C, H, N.

6-Isoquinolin-4-yl-1-methyl-3,4-dihydroquinolin-2(1*H*)-one (22) was obtained according to procedure A from **14a** (264 mg, 1.10 mmol) and 4-isoquinolineboronic acid (172 mg, 1.00 mmol) after crystallization from acetone/diethyl ether as colorless needles (163 mg, 0.57 mmol, 57 %), mp 175–176 °C. LC/MS *m/z* 289.91 (MH^+). Anal. ($C_{19}H_{16}N_2O$) C, H, N.

6-Pyrimidin-5-yl-3,4-dihydroquinolin-2(1*H*)-one (23) was obtained according to procedure A from **12a** (226 mg, 1.00 mmol) and 5-pyrimidineboronic acid (103 mg, 0.83 mmol) after crystallization from ethanol as colorless needles (75 mg, 0.33 mmol, 40 %), mp 232–233 °C. LC/MS *m/z* 225.74 (MH^+). Anal. ($C_{13}H_{11}N_3O \cdot 0.2H_2O$) C, H, N.

6-Pyridin-3-yl-3,4-dihydroquinoline-2(1*H*)-thione (24). A suspension of **12** (395 mg, 1.76 mmol) and Lawesson's reagent (356 mg, 0.88 mmol) in dry toluene was refluxed for 30 min under an atmosphere of nitrogen. After cooling to room temperature, the solvent was removed in vacuo and the residue was purified by flash chromatography on silica gel (petroleum ether/ethyl acetate, 3/7, R_f = 0.31) to afford **24** as yellow plates (63 mg, 0.26 mmol, 15 %), mp 265–267 °C. LC/MS *m/z* 241.05 (MH^+). Anal. ($C_{14}H_{12}N_2S$) C, H, N.

8-Chloro-6-pyridin-3-yl-3,4-dihydroquinoline-2(1*H*)-thione (25) was obtained as described for **24** starting from **17** (900 mg, 3.48 mmol) and Lawesson's reagent (985 mg, 2.44 mmol) after flash chromatography on silica gel (ethyl acetate, R_f = 0.26) and crystallization from acetone/diethyl ether as yellow needles (212 mg, 0.77 mmol, 22 %), mp 174–175 °C. GC/MS *m/z* 273.95 ($M^{35}Cl^+$), 275.95 ($M^{37}Cl^+$). Anal. ($C_{14}H_{11}ClN_2S$) C, H, N.

7-Pyridin-3-yl-2*H*-1,4-benzothiazin-3(4*H*)-one (26) was obtained according to general procedure B from 7-bromo-2*H*-1,4-benzothiazin-3(4*H*)-one (1.15 g, 4.71 mmol) and 3-pyridineboronic acid (695 mg, 5.56 mmol) after flash chromatography on silica gel (petroleum ether/ethyl acetate, 1/1, R_f = 0.20) and crystallization from ethanol as colorless needles (486 mg, 2.01 mmol, 43 %), mp 238–240 °C. LC/MS *m/z* 242.99 (MH^+). Anal. ($C_{13}H_{10}N_2OS \cdot 0.2H_2O$) C, H, N.

Biological Methods. 1. Enzyme Preparations. CYP17 and CYP19 preparations were obtained by described methods: the 50,000 *g* sediment of *E. coli* expressing human CYP17[32] and microsomes from human placenta for CYP19.[34] **2. Enzyme Assays.** The following enzyme assays were performed as previously described: CY17[32] and CYP19.[34] **3. Activity and Selectivity Assay Using V79 Cells.** V79 MZh 11B1 and V79 MZh 11B2 cells[10,28] were incubated with [4-^{14}C]-11-deoxycorticosterone as substrate and inhibitor in at least three different concentrations. The enzyme reactions were stopped by addition of ethyl acetate. After vigorous shaking and a centrifugation step (10,000 *g*, 2 min), the steroids were extracted into the organic phase, which was then separated. The conversion of the substrate was analyzed by HPTLC and a phosphoimaging system as described. **4. Inhibition of**

Human Hepatic CYP Enzymes. The recombinantly expressed enzymes from baculovirus-infected insect microsomes (Supersomes) were used and the manufacturer's instructions (www.gentest.com) were followed. **5. *In Vivo* Pharmacokinetics.** Animal trials were conducted in accordance with institutional and international ethical guidelines for the use of laboratory animals. Cassette dosing: Male Wistar rats weighing 297–322 g (Janvier, France) were housed in a temperature-controlled room (20–24 °C) and maintained in a 12 h light/12 h dark cycle. Food and water were available ad libitum. The animals were anaesthetised with a ketamine (135 mg/kg)/xylazine (10 mg/kg) mixture, and cannulated with silicone tubing via the right jugular vein. Prior to the first blood sampling, animals were connected to a counterbalanced system and tubing, to perform blood sampling in the freely moving rat. Separate stock solutions (5 mg/mL) were prepared for the tested compounds in labrasol/water (1:1; v/v), leading to a clear solution. Immediately before application, the cassette dosing mixture was prepared by adding equal volumes of the stock solutions to end up with a final concentration of 1 mg/mL for each compound. The mixture was applied perorally to 3 rats with an injection volume of 5 mL/kg (Time 0). Blood samples (250 µl) were collected 1 hour before application and 1, 2, 4, 6, 8, and 24 hours thereafter. They were centrifuged at 650 *g* for 10 minutes at 4 °C and then the plasma was harvested and kept at –20 °C until LC/MS analysis. To 50 µL of rat plasma sample and calibration standard 100 µL acetonitrile containing the internal standard was added. Samples and standards were vigorously shaken and centrifuged for 10 minutes at 6000 *g* and 20 °C. For the test items, an additional dilution was performed by mixing 50 µL of the particle free supernatant with 50 µL water. An aliquot was transferred to 200 µL sampler vials and subsequently subjected to LC-MS/MS. HPLC-MS/MS analysis and quantification of the samples was carried out on a Surveyor-HPLC-system coupled with a TSQ Quantum (ThermoFinnigan) triple quadrupole mass spectrometer equipped with an electrospray interface (ESI). The mean of absolute plasma concentrations (±SEM) was calculated for the 3 rats and the regression was performed on group mean values. The pharmacokinetic analysis was performed using a noncompartment model (PK Solutions 2.0, Summit Research Services). Single dosing: The single dose experiments were performed as described for the cassette dosing procedure with male Wistar rats weighing 234–276 g (Janvier, France). Separate stock solutions (5 mg/mL) were prepared for compound **12** in PEG400/water/ethanol (50:40:10; v/v/v) and for compound **21** in labrasol/water (1:1; v/v), leading to clear solutions. Compound **12** was applied at 25 mg/kg perorally and 1 mg/kg intravenously and compound **21** at 25 mg/kg perorally to 4 rats each. Additional blood samples were taken 10 and 12 hours after application in case of peroral application and 0.08, 0.25, 0.50, and 0.75 hours in case of intravenous application of compound **12**, respectively. **6. Plasma Protein Binding.** A 10 mM test compound solution and ketoprofen solution is prepared in acetonitrile. The test compound solution is diluted with solvent to the 50 fold concentration (150 µM, working solution) used in the assay (3 µM). In a 1.5 mL eppendorff vial, 3 µL working solution are given to 147 µL serum (rat or human) and mixed. For recovery the same dilutions are done in ultrafiltrated serum. The solutions are incubated for 1 hour at 37 °C. The whole samples (6 test solutions, 6 recovery samples) are centrifuged at 8000 *g*

for 20 min using Centrifree micropartition devices (Millipore). 75 µL of ultra filtrate (UF) sample is removed for sample preparation. To 75 µL of sample or 150 µL calibration standard, 75 µL or 150 µL acetonitrile containing the internal standard (ketoprofen, 1 µM) is added to precipitate plasma proteins. Samples are then vigorously shaken (10 sec.) and centrifuged for 10 minutes at 6000 *g* and 20 °C. An aliquot (70 µL) of the particle-free supernatant is subsequently subjected to LC-MS/MS. The degree of binding to the plasma proteins (PPB) is calculated by the following equation: % Protein binding = $(1–[\text{ligand}_{\text{ultrafiltrat}}]/[\text{ligand}_{\text{total}}])\cdot 100$. **7. Cytotoxicity.** Cell viability upon drug exposure was determined using a fluorimetric alamar blue conversion assay using a 96-well plate format. Briefly, U-937 cells (human monocytic leukemia) were seeded in growth medium into 96-well plates at a final density of 5x10E4 cells/ml and exposed to the respective compounds for the indicated time intervals (6 replicates per concentration). At the end of the exposure time, alamar blue (Biosource International, Camarillo, CA) was added at 10% (v/v) and incubated for 4 hours. Fluorescence intensity was quantitated using a Wallac Victor fluorescence plate reader (Perkin Elmer, Wellesley, MA) at 530 nm excitation and 590 nm emission. Relative viability of cells was determined in relation to the untreated control. Control wells containing compound only were included to detect potential interference of the compound with the indicator system. Also, media only controls were included to account for background fluorescence. Viability of cells prior to cytotoxicity experiments was determine by Trypan Blue staining. Cells were diluted 1:3 in 0.4% (w/v) Trypan Blue (Sigma), and counted in a hemacytomer.

Acknowledgement. The assistance in performing the *in vitro* tests by Gertrud Schmitt and Jeannine Jung is highly appreciated. We would also like to acknowledge the undergraduate research participants Judith Horzel, Helena Rübel, and Thomas Jakoby whose work contributed to the presented results. S. L. is grateful to Saarland University for a scholarship (Landesgraduierten-Förderung). Thanks are due to Prof. J. J. Rob Hermans, University of Maastricht, The Netherlands, for supplying the V79 CYP11B1 cells, and Prof. Rita Bernhardt, Saarland University, for supplying the V79 CYP11B2 cells. The determination of the cyctotoxicity by Dr. Reiner Class, Pharmacelsus CRO, Saarbrücken, as well as the investigation of the hepatic CYP profile by Dr. Ursula Müller-Vieira, Pharmacelsus CRO, is gratefully acknowledged.

Supporting Information Available: Aldosterone concentrations in the individual animals at all sampling points, NMR spectroscopic data of the target compounds **1**–**4**, **6**–**11**, **13**–**26**, full experimental details and spectroscopic characterization of the reaction intermediates **1a**, **5a**, **5b**, **6a**, **14a**–**16a**, elemental analysis results of compounds **1**–**26**. This information is available free of charge via the Internet at http://pubs.acs.org.

References

(1) Weber, K. T. Aldosterone in congestive heart failure. *N. Engl. J. Med.* **2001**, *345*, 1689–1697.

(2) (a) Brilla, C. G. Renin-angiotensin-aldosterone system and myocardial fibrosis. *Cardiovasc. Res.* **2000**, *47*, 1–3. (b) Lijnen, P.; Petrov, V. Induction of cardiac fibrosis by aldosterone. *J. Mol. Cell. Cardiol.* **2000**, *32*, 865–879.

(3) Satoh, M.; Nakamura, M.; Saitoh, H.; Satoh, H.; Akatsu, T.; Iwasaka, J.; Masuda, T.; Hiramori, K. Aldosterone synthase (CYP11B2) expression and myocardial fibrosis in the failing human heart. *Clin. Sci.* **2002**, *102*, 381–386.

(4) (a) Pitt, B.; Zannad, F.; Remme, W. J.; Cody, R.; Castaigne, A.; Perez, A.; Palensky, J.; Wittes, J. The effect of spironolactone on morbidity and mortality in patients with severe heart failure. *N. Engl. J. Med.* **1999**, *341*, 709–717. (b) Pitt, B.; Remme, W.; Zannad, F.; Neaton, J.; Martinez, F.; Roniker, B.; Bittman, R.; Hurley, S.; Kleiman, J.; Gatlin, M. Eplerenone, a selective aldosterone blocker, in patients with left ventricular dysfunction after myocardial infarction. *N. Eng. J. Med.* **2003**, *348*, 1309–1321.

(5) Izawa, H.; Murohara, T.; Nagata, K.; Isobe, S.; Asano, H.; Amano, T.; Ichihara, S.; Kato, T.; Ohshima, S.; Murase, Y.; Iino, S.; Obata, K.; Noda, A.; Okumura, K.; Yokota, M. Mineralocorticoid receptor antagonism ameliorates left ventricular diastolic dysfunction and myocardial fibrosis in mildly symptomatic patients with idiopathic dilated cardiomyopathy: a pilot study. *Circulation* **2005**, *112*, 2940–2945.

(6) Juurlink, D. N.; Mamdani, M. M.; Lee, D. S.; Kopp, A.; Austin, P. C.; Laupacis, A.; Redelmeier, D. A. Rates of hyperkalemia after publication of the Randomized Aldactone Evaluation Study. *N. Engl. J. Med.* **2004**, *351*, 543–551.

(7) Delcayre, C.; Swynghedauw, B. Molecular mechanisms of myocardial remodeling. The role of aldosterone. *J. Mol. Cell. Cardiol.* **2002**, *34*, 1577–1584.

(8) (a) Wehling, M. Specific, nongenomic actions of steroid hormones. *Annu. Rev. Physiol.* **1997**, *59*, 365–393. (b) Lösel, R.; Wehling, M. Nongenomic actions of steroid hormones. *Nature Rev. Mol. Cell. Biol.* **2003**, *4*, 46–55.

(9) Hartmann, R. W. Selective inhibition of steroidogenic P450 enzymes: Current status and future perspectives. *Eur. J. Pharm. Sci.* **1994**, *2*, 15–16.

(10) Ehmer, P. B.; Bureik, M.; Bernhardt, R.; Müller, U.; Hartmann, R. W. Development of a test system for inhibitors of human aldosterone synthase (CYP11B2): Screening in fission yeast and evaluation of selectivity in V79 cells. *J. Steroid Biochem. Mol. Biol.* **2002**, *81*, 173–179.

(11) Kawamoto, T.; Mitsuuchi, Y.; Toda, K.; Yokoyama, Y.; Miyahara, K.; Miura, S.; Ohnishi, T.; Ichikawa, Y.; Nakao, K.; Imura, H.; Ulick, S.; Shizuta, Y. Role of steroid 11β-hydroxylase and steroid 18-hydroxylase in the biosynthesis of glucocorticoids and mineralocorticoids in humans. *Proc. Natl. Acad. Sci. U.S.A.* **1992**, *89*, 1458–1462.

(12) Ulmschneider, S.; Müller-Vieira, U.; Mitrenga, M.; Hartmann, R. W.; Oberwinkler-Marchais, S.; Klein, C. D.; Bureik, M.; Bernhardt, R.; Antes, I.; Lengauer, T. Synthesis and evaluation of imidazolylmethylenetetrahydronaphthalenes and imidazolylmethyleneindanes: Potent inhibitors of aldosterone synthase. *J. Med. Chem.* **2005**, *48*, 1796–1805.

(13) Ulmschneider, S.; Müller-Vieira, U.; Klein, C. D.; Antes, I.; Lengauer, T.; Hartmann, R. W. Synthesis and evaluation of (pyridylmethylene)tetrahydronaphthalenes/-indanes and structurally modified derivatives: Potent and selective inhibitors of aldosterone synthase. *J. Med. Chem.* **2005**, *48*, 1563–1575.

(14) Voets, M.; Antes, I.; Scherer, C.; Müller-Vieira, U.; Biemel, K.; Barassin, C.; Oberwinkler-Marchais, S.; Hartmann, R. W. Heteroaryl substituted naphthalenes and structurally modified derivatives: Selective inhibitors of CYP11B2 for the treatment of congestive heart failure and myocardial fibrosis. *J. Med. Chem.* **2005**, *48*, 6632–6642.

(15) Lucas, S.; Heim, R.; Negri, M.; Antes, I.; Ries, C.; Schewe, K. E.; Bisi, A.; Gobbi, S.; Hartmann, R. W. Novel aldosterone synthase inhibitors with extended carbocyclic skeleton by a combined ligand-based and structure-based drug design approach. *J. Med. Chem.* **2008**, in press.

(16) Voets, M.; Antes, I.; Scherer, C.; Müller-Vieira, U.; Biemel, K.; Oberwinkler-Marchais, S.; Hartmann, R. W. Synthesis and evaluation of heteroaryl-substituted dihydronaphthalenes and indenes: Potent and selective inhibitors of aldosterone synthase (CYP11B2) for the treatment of congestive heart failure and myocardial fibrosis. *J. Med. Chem.* **2006**, *49*, 2222–2231.

(17) Appukkuttan, P.; Orts, A. B.; Chandran, R., P.; Goeman, J. L.; van der Eycken, J.; Dehaen, W.; van der Eycken, E. Generation of a small library of highly electron-rich 2-(hetero)aryl-substituted phenethylamines by the Suzuki-Miyaura reaction: A short synthesis of an apogalanthamine analogue. *Eur. J. Org. Chem.* **2004**, 3277–3285.

(18) Bengtson, A.; Hallberg, A.; Larhed, M. Fast synthesis of aryl triflates with controlled microwave heating. *Org. Lett.* **2002**, *4*, 1231–1233.

(19) Carrenño, M. C.; García-Cerrada, S.; Urbano, A. From central to helical chirality: Synthesis of P and M enantiomers of [5]helicenequinones and bisquinones from (SS)-2-(p-tolylsulfinyl)-1,4-benzoquinone. *Chem. Eur. J.* **2003**, *9*, 4118–4131.

(20) Selnick, H. G.; Smith, G. R.; Tebben, A. J. An improved procedure for the cyanation of aryl triflates: A convenient synthesis of 6-cyano-1,2,3,4-tetrahydroisoquinoline. *Synth. Commun.* **1995**, *25*, 3255–3261.

(21) Tschaen, D. M.; Abramson, L.; Cai, D.; Desmond, R.; Dolling, U.-H.; Frey, L.; Karady, S.; Shi, Y.-J.; Verhoeven, T. R. Asymmetric Synthesis of MK-0499. *J. Org. Chem.* **1995**, *60*, 4324–4330.

(22) Mewshaw, R. E.; Edsall, R. J., Jr.; Yang, C.; Manas, E. S.; Xu, Z. B.; Henderson, R. A.; Keith, J. C., Jr.; Harris, H. A. ERβ ligands. 3. Exploiting two binding orientations of the 2-phenylnaphthalene scaffold to achieve ERβ selectivity. *J. Med. Chem.* **2005**, *48*, 3953–3979.

(23) DeBernardis, J. F.; Kerkman, D. J.; Winn, M.; Bush, E. N.; Arendsen, D. L.; McClellan, W. J.; Kyncl, J. J.; Basha, F. Z. Conformationally defined adrenergic agents. 1. Design and synthesis of novel α_2 selective adrenergic agents: Electrostatic repulsion based conformational prototypes. *J. Med. Chem.* **1985**, *28*, 1319–1404.

(24) Occhiato, E. G.; Ferrali, A.; Menchi, G.; Guarna, A.; Danza, G.; Comerci, A.; Mancina, R.; Serio, M.; Garotta, G.; Cavalli, A.; De Vivo, M.; Recanatini, M. Synthesis, biological activity, and three-dimensional quantitative structure-activity relationship model for a series of benzo[*c*]quinolizin-3-ones, nonsteroidal inhibitors of human steroid 5α-reductase 1. *J. Med. Chem.* **2004**, *47*, 3546–3560.

(25) Fröhner, W.; Monse, B.; Braxmeier, T. M.; Casiraghi, L.; Sahagún, H.; Seneci, P. Regiospecific synthesis of mono-N-substituted indolopyrrolocarbazoles. *Org. Lett.* **2005**, *7*, 4573–4576.

(26) Bach, T.; Grosch, B.; Strassner, T.; Herdtweck, E. Enantioselective [6π]-photocyclization reaction of an acrylanilide mediated by a chiral host. Interplay between enantioselective ring closure and enantioselective protonation. *J. Org. Chem.* **2003**, *68*, 1107–1116.

(27) Adams, N. D.; Darcy, M. G.; Dhanak, D.; Duffy, K. J.; Fitch, D. M.; Knight, S. D.; Newlander, K. A.; Shaw, A. N. Compounds, compositions and methods. PCT Int. Appl. WO2006113432, 2006.

(28) (a) Denner, K.; Bernhardt, R. Inhibition studies of steroid conversions mediated by human CYP11B1 and CYP11B2 expressed in cell cultures. In *Oxygen Homeostasis and Its Dynamics*, 1st ed.; Ishimura, Y., Shimada, H., Suematsu, M., Eds.; Springer-Verlag: Tokyo, Berlin, Heidelberg, New York, 1998; pp 231–236. (b) Denner, K.; Doehmer, J.; Bernhardt, R. Cloning of CYP11B1 and CYP11B2 from normal human adrenal and their functional expression in COS-7 and V79 chinese hamster cells. *Endocr. Res.* **1995**, *21*, 443–448. (c) Böttner, B.; Denner, K.; Bernhardt, R. Conferring aldosterone synthesis to human CYP11B1 by replacing key amino acid residues with CYP11B2-specific ones. *Eur. J. Biochem.* **1998**, *252*, 458–466.

(29) Lamberts, S. W.; Bruining, H. A.; Marzouk, H.; Zuiderwijk, J.; Uitterlinden, P.; Blijd, J. J.; Hackeng, W. H.; de Jong, F. H. The new aromatase inhibitor CGS-16949A suppresses aldosterone and cortisol production by human adrenal cells *in vitro*. *J. Clin. Endocrinol. Metab.* **1989**, *69*, 896–901.

(30) Demers, L. M.; Melby, J. C.; Wilson, T. E.; Lipton, A.; Harvey, H. A.; Santen, R. J. The effects of CGS 16949A, an aromatase inhibitor on adrenal mineralocorticoid biosynthesis. *J. Clin. Endocrinol. Metab.* **1990**, *70*, 1162–1166.

(31) Heim, R.; Lucas, S.; Grombein, C. M.; Ries, C.; Schewe, K. E.; Negri, M.; Müller-Vieira, U.; Birk, B.; Hartmann, R. W. Overcoming undesirable CYP1A2 inhibition of pyridylnaphthalene type aldosterone synthase inhibitors: Influence of heteroaryl derivatization on potency and selectivity. *J. Med. Chem.* **2008**, *51*, 5064–5074.

(32) (a) Ehmer, P. B.; Jose, J.; Hartmann, R. W. Development of a simple and rapid assay for the evaluation of inhibitors of human 17α-hydroxylase-$C_{17,20}$-lyase (P450c17) by coexpression of P450c17 with NADPH-cytochrome-P450-reductase in *Escherichia coli*. *J. Steroid Biochem. Mol. Biol.* **2000**, *75*, 57–63; (b) Hutschenreuter, T. U.; Ehmer, P. B.; Hartmann, R. W. Synthesis of hydroxy derivatives of highly potent nonsteroidal CYP17 inhibitors as potential metabolites and evaluation of their activity by a non cellular assay using recombinant enzyme. *J. Enzyme Inhib. Med. Chem.* **2004**, *19*, 17–32.

(33) Thompson, E. A.; Siiteri, P. K. Utilization of oxygen and reduced nicotinamide adenine dinucleotide phosphate by human placental microsomes during aromatization of androstenedione. *J. Biol. Chem.* **1974**, *249*, 5364–5372.

(34) Hartmann, R. W.; Batzl, C. Aromatase inhibitors. Synthesis and evaluation of mammary tumor inhibiting activity of 3-alkylated 3-(4-aminophenyl)piperidine-2,6-diones. *J. Med. Chem.* **1986**, *29*, 1362–1369.

(35) Taymans, S. E.; Pack, S.; Pak, E.; Torpy, D. J.; Zhuang, Z.; Stratakis, C. A. Human CYP11B2 (aldosterone synthase) maps to chromosome 8q24.3. *J. Clin. Endocrinol. Metab.* **1998**, *83*, 1033–1036.

(36) (a) Chohan, K. K.; Paine, S. W.; Mistry, J.; Barton, P.; Davis, A. M. A rapid computational filter for cytochrome P450 1A2 inhibition potential of compound libraries. *J. Med. Chem.* **2005**, *48*, 5154–5161. (b) Korhonen, L. E.; Rahnasto, M.; Mähönen, N. J.; Wittekindt, C.; Poso, A.; Juvonen, R. O.; Raunio, H. Predictive three-dimensional quantitative structure-activity relationship of cytochrome P450 1A2 inhibitors. *J. Med. Chem.* **2005**, *48*, 3808–3815.

(37) Butler, M. A.; Iwasaki, M.; Guengerich, F. P.; Kadlubar, F. F. Human cytochrome P-450$_{PA}$ (P-450IA2), the phenacetin O-deethylase, is primarily responsible for the hepatic 3-demethylation of caffeine and N-oxidation of carcinogenic arylamines. *Proc. Natl. Acad. Sci. U.S.A.* **1989**, *86*, 7696–7700.

(38) Sesardic, D.; Boobis, A. R.; Murray, B. P.; Murray, S.; Segura, J.; de la Torre, R.; Davies, D. S. Furafylline is a potent and selective inhibitor of cytochrome P450IA2 in man. *Br. J. Clin. Pharmacol.* **1990**, *29*, 651–663.

(39) Ulmschneider, S.; Negri, M.; Voets, M.; Hartmann, R. W. Development and evaluation of a pharmacophore model for inhibitors of aldosterone synthase (CYP11B2). *Bioorg. Med. Chem. Lett.* **2006**, *16*, 25–30.

(40) Ries, C.; Lucas, S.; Heim, R.; Hartmann, R. W. Selective aldosterone synthase inhibitors reduce aldosterone formation *in vitro* and *in vivo*. *J. Steroid Biochem. Mol. Biol.* **2009**, *116*, 121-126.

(41) Häusler, A.; Monnet, G.; Borer, C.; Bhatnagar, A. S. Evidence that corticosterone is not an obligatory intermediate in aldosterone biosynthesis in the rat adrenal. *J. Steroid Biochem.* **1989**, *34*, 567–570.

3.4 Fine-Tuning the Selectivity of Aldosterone Synthase Inhibitors: SAR Insights from Studies of Heteroaryl Substituted 1,2,5,6-Tetrahydropyrrolo[3,2,1-ij]quinolin-4-one Derivatives

Simon Lucas, Ralf Heim, Christina Ries and Rolf W. Hartmann

This manuscript will be submitted for publication as an article to the

Journal of Medicinal Chemistry **2010**

Paper IV

Abstract: Pyridine substituted 3,4-dihydro-1*H*-quinolin-2-ones (e.g., **I** and **II**) constitute a class of highly potent and selective inhibitors of aldosterone synthase (CYP11B2), a promising target for the treatment of hyperaldosteronism, congestive heart failure and myocardial fibrosis. Amongst the latter, ethyl-substituted **II** is particularly striking due to a pronounced CYP1A2 selectivity. Rigidification of **II** by incorporation of the ethyl group into a 5- or 6-membered ring affords compounds with a pyrroloquinolinone or pyridoquinolinone molecular scaffold (e.g., **1** and **2**). It was found that these molecules are even more potent and selective CYP11B2 inhibitors than their corresponding open-chain analogues. Moreover, pyrroloquinolinone **1** exhibits no inhibition of the six most important hepatic CYP enzymes (IC_{50} > 10 μM) as well as a bioavailability ($AUC_{0-\infty}$ = 3464 ng·h/mL) in the range of the marketed drug fadrozole ($AUC_{0-\infty}$ = 3207 ng·h/mL). The SAR studies disclose structural features for either strong or weak inhibition of the highly homologous 11β-hydroxylase (CYP11B1). These results are not only important for fine-tuning the selectivity but also for the development of selective CYP11B1 inhibitors that are of interest for the treatment of Cushing's syndrome and metabolic syndrome.

Introduction

Congestive heart failure (CHF) is a condition of insufficient cardiac output and reduced systemic blood flow which provokes a chronic activation of the renin-angiotensin-aldosterone system (RAAS). As a consequence, the excessive release of angiotensin II (Ang II) and aldosterone leads to an increased blood pressure and finally to a further deterioration of heart function, mainly mediated via epithelial sodium retention by mineralocorticoid receptor (MR) activation as well as Ang II mediated vasoconstriction.[1] Moreover, aldosterone is known to exert direct effects on the heart. Activation of nonepithelial MRs stimulates the progressive synthesis and deposition of fibrillar collagens in fibroblasts and results in myocardial fibrosis.[2] Until today, various drug classes targeting the RAAS have been developed in order to interrupt the vicious circle of chronic neurohormonal activation, acting either by inhibition of the key regulator enzymes or by blocking the actions of the effector hormones by functional antagonism, affording a successful treatment of heart failure and hypertension. Inhibitors of the angiotensin converting enzyme (ACE) proved to trigger a down-regulation of circulating aldosterone, but increased levels of aldosterone may be seen after several months of therapy, presumably due to potassium stimulated secretion.[3] The persistence of aldosterone secretion despite treatment with ACE inhibitors and the evidence of the deleterious effects of aldosterone on cardiovascular function led to the assumption that blocking the mineralocorticoid receptor might provide additional benefit. This hypothesis has been corroborated in two recent clinical trials by using the MR antagonists spironolactone and eplerenone in addition to standard therapy of patients with chronic congestive heart failure and in patients after myocardial infarction, respectively.[4] Aldosterone antagonistic therapy, however, raises several issues. Spironolactone can induce severe side effects due to its low selectivity toward other steroid hormone receptors. Although eplerenone is more selective, clinically relevant hyperkalemia remains a principal therapeutic risk.[5] Moreover, the elevated plasma aldosterone concentrations are left unaffected on a pathological level, promoting the up-regulation of MR expression[6] and nongenomic aldosterone effects[7] on the insufficient heart.

Hence, we hypothesized a novel approach for the treatment of hyperaldosteronism, congestive heart failure and myocardial fibrosis by combating the elevated plasma aldosterone levels via blockade of aldosterone synthase (CYP11B2), the key enzyme of mineralocorticoid biosynthesis.[8,9] This mitochondrial cytochrome P450 enzyme is localized mainly in the zona glomerulosa of the adrenal gland and catalyzes the terminal three oxidation steps in the biogenesis of aldosterone in humans via initial hydroxylation of 11-deoxycorticosterone at 11β-position to yield corticosterone, followed by two subsequent hydroxylations at C_{18} and water release to yield aldosterone (Chart 1).[10] In addition to the potential therapeutic utility in cardiovascular diseases, radiolabelled inhibitors of that enzyme might be a useful tool for molecular imaging of CYP11B expression in adrenocortical tissue and thus for the diagnosis of adrenal tumors.[11] Due to selectively binding to CYP11B2, these compounds are also interesting for the imaging of Conn adenomas which are characterized by high expression of CYP11B2.[12]

Chart 1. CYP11B2 Catalyzed Biosynthesis of Aldosterone

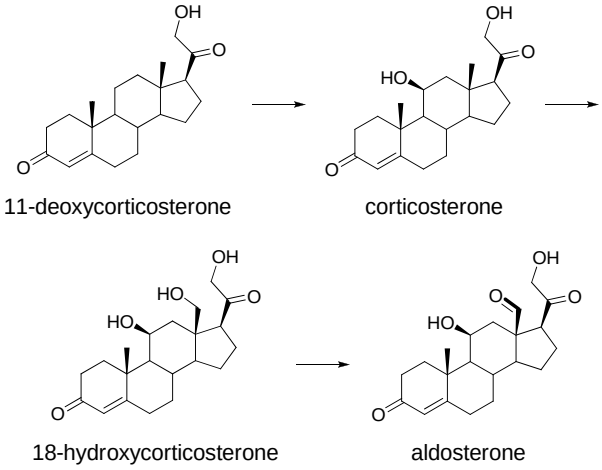

An obstacle in the development of a putative CYP11B2 inhibitor is to accomplish selectivity versus other cytochrome P450 (CYP) enzymes since complexation of the heme iron which is a widespread interaction motive is likely to occur in other CYP enzymes as well. The selectivity issue becomes especially critical with respect to 11β-hydroxylase (CYP11B1), the key enzyme of glucocorticoid biosynthesis whose amino acid sequence exhibits a homology of 93 % compared to CYP11B2.[13] A drug discovery program launched in our laboratory led to a series of nonsteroidal aldosterone synthase inhibitors with high selectivity versus other cytochrome P450 enzymes by consequent structural optimization of a hit discovered by compound library screening.[14,15] Pyridine-substituted naphthalenes[16,17] and dihydronaphthalenes,[18] the most potent and selective compounds that emerged from the development process, however, revealed two major pharmacological drawbacks: A strong inhibition of the hepatic drug metabolizing enzyme CYP1A2 and no inhibitory effect on the aldosterone production *in vivo* by using a rat model.

Chart 2. Title Compounds

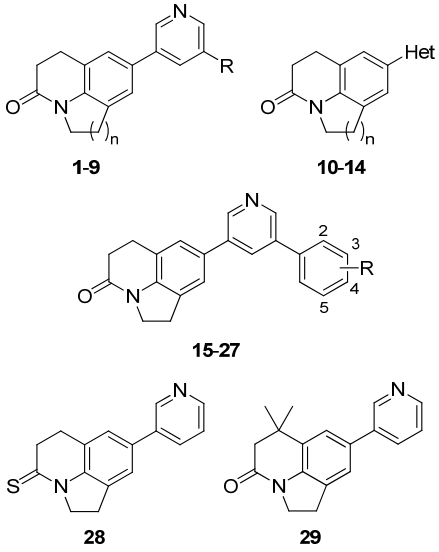

In the present study, we describe the development of 1,2,5,6-tetrahydropyrrolo[3,2,1-*ij*]quinolin-4-ones and structurally related compounds (Chart 2) as highly potent aldosterone synthase inhibitors with improved selectivity against other crucial CYP enzymes, such as CYP11B1, the steroidogenic enzymes CYP17 (17α-hydroxylase-C17,20-lyase) and CYP19 (aromatase) as well as the six most important drug-metabolizing cytochrome P450 enzymes (CYP1A2, CYP2B6, CYP2C9, CYP2C19, CYP2D6 and CYP3A4). The *in vivo* pharmacokinetic profile of some promising compounds was determined in male Wistar rats.

Results

Inhibitor Design Concept

Preliminary studies aiming at the design of nonsteroidal aldosterone synthase inhibitors performed in our laboratory have demonstrated that 3-pyridine substituted naphthalenes provide an ideal molecular scaffold for a strong inhibition of the target enzyme CYP11B2 as well as high selectivity versus several other CYP enzymes (e.g., CYP11B1, CYP17, CYP19).[16,18] These molecules, however, revealed two major pharmacological drawbacks: A strong inhibition of the hepatic drug metabolizing enzyme CYP1A2 and no inhibitory effect on the aldosterone production *in vivo* by using a rat model. In a recent study, we demonstrated that changing the naphthalene by a 3,4-dihydro-1*H*-quinolin-2-one skeleton affords highly potent CYP11B2 inhibitors such as **I** and **II** (Chart 3) with pronounced selectivity versus other CYP enzymes including CYP1A2, as well as aldosterone-lowering properties in vivo.[19] Amongst the latter compounds, ethyl-substituted derivative **II** displayed a remarkably little inhibition of CYP1A2. Therefore, this molecule was chosen as starting point for further structural optimization. Incorporation of the ethyl group into a 5- or 6-membered ring affords the pyrroloquinolinone **1** and the pyridoquinolinone **2**, respectively. In the present study, the chemical modification is mainly directed to the heterocyclic moiety since both potency and selectivity have been identified in previous investigations to be highly dependent on heterocyclic derivatization.[20]

Chart 3. Development of Compounds **1** and **2**

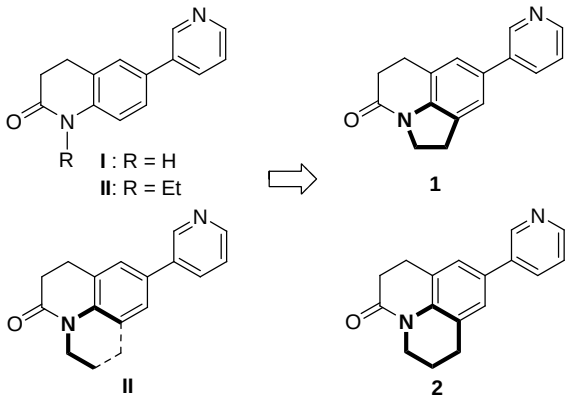

Chemistry

The key synthetic transformation toward the target compounds was a Suzuki coupling to connect the pyrrolo- or pyridoquinolinone scaffold to various *N*-heterocyclic systems, in most cases a derivative of 3-pyridine (Scheme 1). The advanced intermediates **1a**, **2a** as well as **29a** were prepared in three consecutive steps starting from commercially available indoline or 1,2,3,4-tetrahydroquinoline as initial building block. The sequence of amide formation and subsequent Friedel-Crafts cyclization to afford **1b** and **2b** has been described previously and was also used for the synthesis of the *gem*-dimethyl analog **29a**.[21] Regioselective bromination was accomplished by treating the fused heterocycles with *N*-bromosuccinimide in DMF at 0 °C. The pyrrolo- or pyridoquinolinones **1**–**4**, **10**–**13**, and **29** were obtained by Suzuki coupling of the arylbromides **1a**, **2a** or **29a** with an *N*-heterocyclic boronic acid.[22] Copper catalyzed *N*-arylation of **1a** with imidazole gave rise to the 1-imidazolyl derivative **14**.[23] Alternatively, the bromo-substituted pyrroloquinolinone **1a** was transformed into the corresponding pinacol boronate **3a** by treating with bis(pinacolato)diboron under palladium catalysis[24] and was subsequently used for cross-coupling with a derivatized 3-bromopyridine to afford compounds **5**–**9**, and **15**–**27**. If not commercially available, the 3-bromopyridines used in this step were prepared as outlined in Scheme 2 either from 3-bromo-5-methoxypyridine by demethylation and subsequent alkylation (**5a**, **6a**) or from 3,5-dibromopyridine by Suzuki coupling with a substituted arylboronic acid (**16a**–**27a**). The hydroxypyridine **7** was synthesized by treating the corresponding methoxy derivative **3** with concentrated hydrobromic acid under reflux. Thionation of pyrroloquinolinone **1** with Lawessons reagent in dry toluene afforded the thioanalog **28**.

Scheme 1[a]

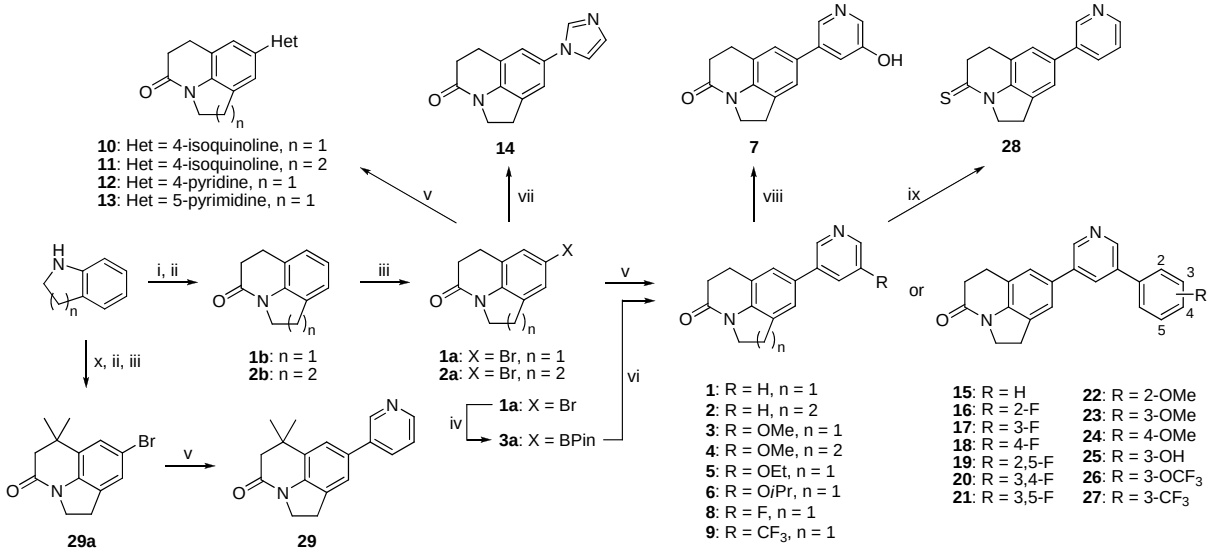

[a] Reagents and conditions: i) 3-chloropropanoyl chloride, acetone reflux; ii) $AlCl_3$, NaCl, 150 °C; iii) NBS, DMF, 0 °C; iv) bis(pinacolato)diboron, $Pd(dppf)Cl_2$, KOAc, DMSO, 80 °C; v) heteroarylboronic acid, $Pd(PPh_3)_4$, aq. $NaHCO_3$, DMF, μw, 150 °C or: heteroarylboronic acid, $Pd(PPh_3)_4$, aq. Na_2CO_3, toluene/ethanol, reflux; vi) heteroarylbromide, $Pd(PPh_3)_4$, aq. Na_2CO_3, toluene/ethanol, reflux; vii) Cu_2SO_4, K_2CO_3, 180 °C; viii) conc HBr, reflux; ix) Lawessons reagent, toluene, reflux, x) 3,3-dimethylacryloylchloride, acetone reflux. (Het = heteroaryl, BPin = pinacol boronate)

Scheme 2[a]

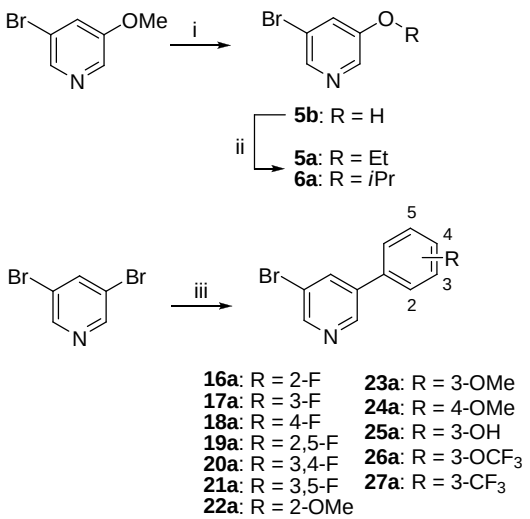

[a] Reagents and conditions: i) conc HBr, reflux; ii) alkylhalogenide, K_2CO_3, DMF, rt; iii) arylboronic acid, $Pd(PPh_3)_4$, aq. Na_2CO_3, toluene/ethanol, reflux.

Biological Results

Inhibition of Human Adrenal Corticoid Producing CYP11B2 and CYP11B1 *In Vitro* (Table 1). The inhibitory activities of the compounds were determined in V79 MZh cells expressing either human CYP11B2 or CYP11B1.[9,25] The V79 MZh cells were incubated with [^{14}C]-deoxycorticosterone as substrate and the inhibitor in different concentrations. The product formation was monitored by HPTLC using a phosphoimager. Fadrozole, an aromatase (CYP19) inhibitor with proven ability to reduce corticoid formation *in vitro*[26] and *in vivo*[27] was used as a reference (CYP11B2, IC_{50} = 1 nM; CYP11B1, IC_{50} = 10 nM).

Most of the investigated molecules are highly potent aldosterone synthase inhibitors displaying IC_{50} values in the low nanomolar range (< 5 nM). An extraordinary high activity is observed in case of the isoquinoline derivatives **10** and **11** with sub-nanomolar IC_{50} values (0.2 nM). Replacing 3-pyridine by other nitrogen containing heterocycles induces a decrease in inhibitory potency. The 5-pyrimidine (**13**) and 1-imidazole (**14**) derivatives are less active (IC_{50} = 56–89 nM) than the 3-pyridine analog **1** (IC_{50} = 1.1 nM) and the corresponding 4-pyridine compound **12** lacks any inhibitory activity on CYP11B2 (< 10 % inhibition at a concentration of 500 nM). The same trend was observed previously for the binding properties of a series of substituted pyridylnaphthalenes.[16] A slight decrease in CYP11B2 potency (IC_{50} = 16–33 nM) is also observed in case of some aryl-substituents in 5-position of the pyridine heterocycle (**21**, **26**, and **27**). A *gem*-dimethyl group in the quinolinone moiety as accomplished in compound **29** is not tolerated in terms of CYP11B2 potency. The inhibition of the highly homologous CYP11B1 is significantly lower than the CYP11B2 inhibition for all investigated molecules resulting in selectivity factors in the range of 15–957 (fadrozole, selectivity factor = 10).

Table 1. Inhibition of Human Adrenal CYP11B2 and CYP11B1 *In Vitro*

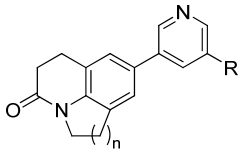

1-9

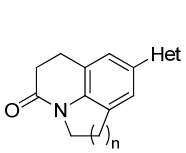

10-14

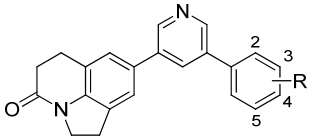

15-27

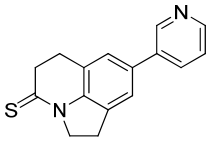

28

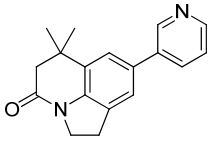

29

				% inhibition[a]	IC_{50} value[b] (nM)		
				V79 11B2[c]	V79 11B2[c]	V79 11B1[d]	selectivity
compd	n	R	Het	hCYP11B2	hCYP11B2	hCYP11B1	factor[e]
1	1	H		90	1.1	715	650
2	2	H		95	2.4	2296	957
3	1	OMe		98	0.6	247	412
4	2	OMe		95	0.9	545	606
5	1	OEt		92	1.0	158	158
6	1	O*i*Pr		96	2.2	103	47
7	1	OH		94	4.3	2045	476
8	1	F		97	4.4	1288	293
9	1	CF_3		96	5.9	141	24
10	1		4-isoquinoline	98	0.2	13	65
11	2		4-isoquinoline	95	0.2	34	170
12	1		4-pyridine	7	n.d.	n.d.	n.d.
13	1		5-pyrimidine	81	56	28546	510
14	1		1-imidazole	87	89	2077	23
15		H		97	1.3	58	45
16		2-F		92	0.7	43	61
17		3-F		97	1.4	490	350
18		4-F		96	0.9	40	44
19		2,5-F		80	3.6	183	51
20		3,4-F		89	2.3	496	215
21		3,5-F		81	18	1748	97
22		2-OMe		86	2.4	128	53
23		3-OMe		86	4.6	1374	299
24		4-OMe		95	1.4	21	15
25		3-OH		92	1.2	44	37
26		3-OCF_3		92	16	2058	129
27		3-CF_3		80	33	4646	141
28				96	1.2	333	278
29				48	n.d.	n.d.	n.d.
fadrozole					1	10	10

[a] Mean value of at least four experiments, standard deviation less than 10 %; inhibitor concentration, 500 nM. [b] Mean value of at least four experiments, standard deviation usually less than 25 %, n.d. = not determined. [c] Hamster fibroblasts expressing human CYP11B2; substrate deoxycorticosterone, 100 nM. [d] Hamster fibroblasts expressing human CYP11B1; substrate deoxycorticosterone, 100 nM. [e] IC_{50} CYP11B1/IC_{50} CYP11B2, n.d. = not determined.

Inhibition of Steroidogenic and Hepatic CYP Enzymes (Tables 2 and 3). A subset of 12 compounds was investigated for inhibition of the steroidogenic enzymes CYP17 and CYP19 (Table 2). The inhibition of CYP17 was investigated using the 50,000 *g* sediment of the *E. coli* homogenate recombinantly expressing human CYP17 and progesterone (25 μM) as substrate.[28] The inhibition values were measured at an inhibitor concentration of 2 μM. The inhibition of CYP19 at an inhibitor concentration of 500 nM was determined *in vitro* with human placental microsomes and [1β-^{3}H] androstenedione as substrate as described by Thompson and Siiteri[29] using our modification.[30] Pyridoquinolinone **2** is a moderately potent aromatase inhibitor (69 % inhibition). All other investigated molecules are highly selective toward both CYP17 and CYP19, usually displaying less than 10 % inhibition.

Table 2. Inhibition of Human CYP17 and CYP19 *In Vitro*

	% inhibition[a]			% inhibition[a]	
compd	CYP17[b]	CYP19[c]	compd	CYP17[b]	CYP19[c]
1	6	18	**11**	5	< 5
2	6	69	**13**	5	5
3	< 5	5	**17**	7	6
4	< 5	5	**20**	< 5	< 5
8	< 5	< 5	**23**	< 5	< 5
10	6	< 5	**28**	11	5

[a] Mean value of three experiments, standard deviation less than 10 %. [b] *E. coli* expressing human CYP17; substrate progesterone, 25 μM; inhibitor concentration, 2.0 μM; ketoconazole, IC_{50} = 2.78 μM. [c] Human placental CYP19; substrate androstenedione, 500 nM; inhibitor concentration, 500 nM; fadrozole, IC_{50} = 30 nM.

A selectivity profile relating to inhibition of crucial hepatic CYP enzymes (CYP1A2, CYP2B6, CYP2C9, CYP2C19, CYP2D6, and CYP3A4) was determined for compounds **1**–**4**, **11**, and **17** by use of recombinantly expressed enzymes from baculovirus-infected insect microsomes. The unsubstituted pyrroloquinolinone **1** exhibits a pronounced selectivity toward all investigated CYP enzymes. CYP2B6, CYP2C19, CYP2D6, and CYP3A4 are not inhibited at all (< 5 % inhibition at a concentration of 10 μM). The inhibition of CYP1A2 and CYP2C9 is in the range of 41–43 % corresponding with IC_{50} values of approximately 10 μM or higher. Compounds **2**–**4**, and **11** display an increased CYP1A2 inhibition (24–47 % at a concentration of 1 μM) compared to **1** whereas the CYP1A2 potency of **17** is in the range of the unsubstituted analog **1**. Furthermore, isoquinoline derivative **11** is a rather potent inhibitor of both CYP2C9 and CYP2C19 (IC_{50} < 1 μM). Compound **17** displays a distinct inhibition of CYP2C9 (79 % at a concentration of 10 μM) but is otherwise rather selective toward the other CYP enzymes investigated (IC_{50} > 10 μM). However, it becomes apparent from the results presented in Table 3 that none of the substituted derivatives **2**–**4**, **11** and **17** matches the selectivity of the unsubstituted parent compound **1**.

Table 3. Inhibition of Selected Hepatic CYP Enzymes *In Vitro*

	% inhibition[a]											
	CYP1A2[b,c]		CYP2B6[b,d]		CYP2C9[b,e]		CYP2C19[b,f]		CYP2D6[b,g]		CYP3A4[b,h]	
compd	10 µM	1 µM	10 µM	1 µM	10 µM	1 µM	10 µM	1 µM	10 µM	1 µM	10 µM	1 µM
1	43	8	< 5	< 5	41	6	< 5	< 5	< 5	< 5	< 5	< 5
2	83	41	36	27	40	19	44	8	n.d.	n.d.	21	6
3	72	37	8	< 5	42	23	30	7	13	9	19	14
4	87	47	n.d.	n.d.	63	34	61	11	n.d.	n.d.	24	12
11	63	24	n.d.	n.d.	97	73	96	67	n.d.	n.d.	< 5	< 5
17	38	9	13	< 5	79	39	21	n.d.	9	< 5	43	37

[a] Mean value of two experiments, standard deviation less than 5 %. [b] Recombinantly expressed enzymes from baculovirus-infected insect microsomes (Supersomes). [c] Furafylline, IC_{50} = 2.42 µM. [d] Tranylcypromine, IC_{50} = 6.24 µM. [e] Sulfaphenazole, IC_{50} = 318 nM. [f] Tranylcypromine, IC_{50} = 5.95 µM. [g] Quinidine, IC_{50} = 14 nM. [h] Ketoconazole, IC_{50} = 57 nM.

***In Vivo* Pharmacokinetics (Table 4).** The pharmacokinetic profile of selected compounds was determined after peroral application to male Wistar rats. Plasma samples were collected over 24 h and the concentrations were determined by HPLC-MS/MS. Compounds **1**, **3**, and **4** were investigated in a cassette dosing approach (peroral dose = 5 mg/kg) and compared to fadrozole. All three compounds show comparable terminal half-lifes ($t_{1/2\ z}$ = 2.0–2.9 h) which are in the range of the reference fadrozole ($t_{1/2\ z}$ = 3.2 h). Contrariwise, the absorbance of compounds **1** and **3** (t_{max} = 4 h) is slower as the absorbance of fadrozole (t_{max} = 1 h). Within this series, fadrozole shows the highest maximal concentration (C_{max}) in plasma (471 ng/mL) followed by compound **1** (317 ng/mL). The maximal amount of the other test items (**3** and **4**) found in the plasma after peroral application is significantly lower (< 50 ng/mL). Using the area under the curve ($AUC_{0-\infty}$) as a ranking criterion, pyrroloquinolinone **1** exhibits the highest bioavailability (3464 ng·h/mL), thus slightly exceeding the bioavailability of the reference compound (3207 ng·h/mL). Methoxylation of the heterocycle as accomplished in **3** results in a significant decrease of the $AUC_{0-\infty}$ (557 ng·h/mL). A further decrease is observed for the corresponding pyridoquinolinone **4** (51 ng·h/mL). The influence of varying the molecular scaffold of compound **1** becomes particularly apparent from Figure 1 where the mean profile of plasma levels (ng/mL) in rat versus time after oral application (5 mg/kg) in a cassette of compounds **1**, **3** and **4** are shown. In the course of the *in vivo* experiment, no obvious sign of toxicity was noted in any animal over the duration of the experiment (24 h).

Table 4. Pharmacokinetic Profile of Compounds **1**, **3**, and **4**

compd	$t_{1/2\ z}$ (h)[b]	t_{max} (h)[c]	C_{max} (ng/mL)[d]	$AUC_{0-\infty}$ (ng·h/mL)[e]
1	2.4	4.0	317	3464
3	2.9	4.0	60	557
4	2.0	2.0	4.9	51
fadrozole[f]	3.2	1.0	471	3207

[a] All compounds were applied perorally (5 mg/kg) to male Wistar rats in a cassette dosing approach. [b] Terminal half-life. [c] Time of maximal concentration. [d] Maximal concentration. [e] Area under the curve. [f] Mean value of two experiments.

Figure 1[a]

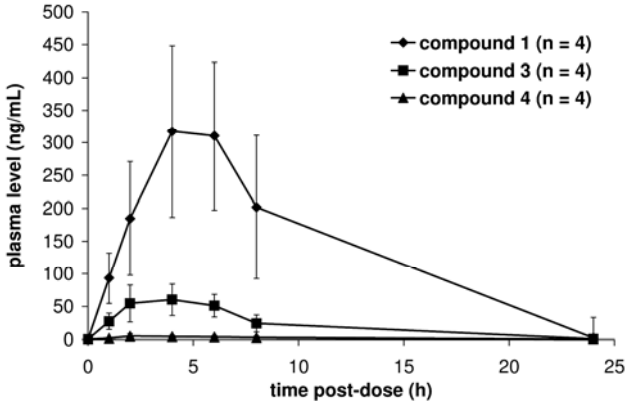

[a] Mean profile (±) SEM of plasma levels (ng/ml) in rat versus time after oral application (5 mg/kg) of compounds **1**, **3**, and **4** determined in a cassette dosing experiment.

Discussion and Conclusion

Within the present set of compounds, interesting structure-activity relationships (SAR) can be observed, especially with respect to the inhibition of 11β-hydroxylase (CYP11B1) and thus selectivity. On the one hand, selectivity is influenced by the ring-size of the carbocycle condensed to the quinolinone moiety. Within the series of pyrido-condensed compounds (**2**, **4**, and **11**), the CYP11B1 inhibition is significantly decreased compared to the corresponding pyrroloquinolinone analogues (**1**, **3**, and **10**), whereas the CYP11B2 inhibition is in a comparable range. This leads to an enhanced selectivity for the pyridoquinolinone derivatives. Pyridoquinolinone **2** is the most selective compound of the present series (selectivity factor = 957). Hence, the selectivity increases nearly by a factor of 100 compared to fadrozole (selectivity factor = 10). This experimental result is particularly noteworthy with respect to the high homology of the two CYP11B isoforms. However, it was demonstrated by pharmacokinetic studies of **3** and **4** that ring expansion to the 6-membered carbocycle is accompanied by an approximately 10-fold decrease in bioavailability as indicated by an $AUC_{0-\infty}$ of 557 ng·h/mL (**3**) and 51 ng·h/mL (**4**), respectively. On the other hand, the substitution pattern of the pyridine moiety was found to significantly influence the CYP11B1 selectivity. Obviously, the size of substituents in 5-position of the heterocycle plays a crucial role in CYP11B1 inhibition. This becomes particularly evident in the series of pyrroloquinolinone compounds with alkoxy derivatized heterocycle. The inhibitory potency at CYP11B1 increases with the substituent size in the order **1** (R = H, IC_{50} = 715 nM) < **3** (R = OMe, IC_{50} = 247 nM) < **5** (R = OEt, IC_{50} = 158 nM) < **6** (R = O*i*Pr, IC_{50} = 103 nM). Contrariwise, the inhibition of CYP11B2 is in a comparable range for these compounds (IC_{50} = 0.6–2.2 nM), that is the selectivity factor decreases in the same order from 650 (**1**) to 47 (**6**). A pronounced increase in CYP11B1 inhibition is observed in case of the introduction of additional aryl moieties. Replacing 3-pyridine by 4-isoquinoline results in a dramatic increase in CYP11B1 potency for both the pyrrolo-condensed (**10**, increase by a factor of 55) and pyrido-condensed

(**11**, factor 68) derivative whereas the CYP11B2 inhibition increases to a minor degree (factor 6–12). The same trend can be observed for several compounds with additional aryl substituent in 5-position of the pyridine moiety (e.g., **15**, **16**, **18**, **22**, **24**, and **25**). The latter compounds display a CYP11B2 inhibition in a range of 0.7–2.4 nM which is readily comparable to the unsubstituted parent compound **1** (IC_{50} = 1.1 nM). Contrariwise, the CYP11B1 inhibition increases up to 36-fold compared to **1** (IC_{50} = 715 nM) to IC_{50} values of 21–128 nM corresponding to a rather low selectivity (factor 15–61). Obviously, the introduction of additional aromatic rings and to a minor degree also sterically demanding aliphatic residues (e.g., isopropoxy) in the pyridine moiety leads to additional interactions of the inhibitors with CYP11B1, thus stabilizing the formed CYP11B1-inhibitor complexes considerably. This observation correlates with homology modeling results suggesting that the putative binding sites of both CYP11B isoforms contain many hydrophobic amino acids (e.g., Ala313, Phe321, Pro322, Val378, Phe381, Leu382, Tyr485, and Ile488).[31] In principal, these residues can interact with the additional aryl moiety by hydrophobic or π-π stacking contacts. Docking studies of imidazolylmethyleneindanes into our CYP11B2 model revealed that the inhibitor is predominantly bound through hydrophobic interactions with residues of the I-helix and Phe106, except for the nitrogen-metal coordination with the heme iron.[14] Since the position of the heme has been hypothesized to be shifted by approximately 20° in the two CYP11B enzymes,[32] it is likely that the 'network' of hydrophobic groups in the binding pocket accommodates the inhibitors in a different way in CYP11B1, thus affording additional stabilization of the phenyl moiety.

Moreover, it is striking that *meta* substituents in the aryl moiety can trigger CYP11B1 selectivity again. With exception of the 3-hydroxy derivative **25**, all compounds bearing a substituent in 3-position of the benzene moiety (i.e., **17**, **20**, **21**, **23**, **26**, and **27**) exhibit a decreased CYP11B1 potency with IC_{50} values in a range of 490–4646 nM and thus selectivity factors up to 350 (**17**). This obvious off/on-switch of CYP11B1 potency is of particular interest. From unsubstituted parent compound **1** (IC_{50} = 715 nM), derivatization with phenyl in 5-position of the pyridine moiety leads to a significant increase of inhibitory potency in compound **15** (IC_{50} = 58 nM) whereas the *meta*-fluorophenyl analog **17** exhibits a low inhibitory potency again (IC_{50} = 490 nM). Coevally, these three compounds display virtually the same aldosterone synthase inhibition (IC_{50} = 1.1–1.4 nM), which means that a variety of sterically demanding substituents in the pyridine moiety is readily tolerated in the CYP11B2 binding pocket, however, lead to no further stabilization of the complexes formed by coordination of the heme iron by the heterocyclic nitrogen. Contrariwise, 3-pyridine substituted pyrroloquinolinone derivatives such as **1** are per se rather poor CYP11B1 inhibitors and require an additional benzene moiety, and thus a further stabilization of the formed complexes mainly through hydrophobic or π-π stacking interactions, for basal inhibitory potency. Amongst these compounds are highly potent CYP11B1 inhibitors, for example isoquinoline derivative **10** (IC_{50} = 13 nM) and *para*-methoxyphenyl derivative **24** (IC_{50} = 21 nM). Obviously the *meta*-substituted analogues do not adequately fit into the CYP11B1 binding pocket or loose contact to the heme iron while minimizing unfavorable contacts with the enzyme. Only 3-hydroxy derivative **25** displays a pronounced CYP11B1 inhibition (IC_{50} = 44 nM).

This is an indication for stabilizing interactions by the hydroxy group acting as hydrogen bond donor which might compensate an eventual weakening of the Fe–N interaction.

The above biological results that derivatization of the 3-pyridine moiety of pyrroloquinolinone type compounds is a tool for fine-tuning the CYP11B1 selectivity are in contrast to previous findings in the series of inhibitors with a naphthalene molecular scaffold. In the latter case, substituents in the heterocyclic moiety led to a change of inhibition of both the CYP11B isoforms in a comparable order of magnitude, resulting in a reasonable linear correlation of the corresponding pIC_{50} values ($r^2 = 0.86$) and thus a rather constant selectivity factor.[20] We interpreted this finding as a consequence of similar protein-inhibitor interactions of the heterocyclic moiety with both CYP11B isoforms due to structural similarities in the heterocyclic binding site. As a matter of fact, the selectivity is significantly influenced by the substitution pattern of the heterocycle within the present set of compounds which is an indication for a binding mode of the pyrroloquinolinone derivatives different from that of the naphthalene analogues.

In summary, the present study provides extensive SAR results relating to CYP11B2 and CYP11B1 inhibition. The influence of certain structural modifications on the 11β-hydroxylase (CYP11B1) activity is particularly noteworthy. On the one hand, CYP11B1 inhibition is an important selectivity criterion for aldosterone synthase inhibitors. On the other hand, selective CYP11B1 inhibitors could be used for the treatment of Cushing's syndrome and metabolic syndrome. Although several potent CYP11B1 inhibitors have been described previously, in-depth SAR studies were usually focused on the concurrent CYP11B2 activity. Herein, we clearly identified structural features important for high inhibitory CYP11B1 potency, namely sterically demanding lipophilic residues or aromatic residues in the heterocyclic moiety or condensed to the heterocycle, giving rise to a series of highly potent 11β-hydroxylase inhibitors (e.g., *para*-methoxyphenyl derivative **24**, IC_{50} = 21 nM). Slight variation of these compounds, for example introduction of *meta*-substituents into the phenyl moiety, led to a significant loss of CYP11B1 inhibition again, providing selective CYP11B2 inhibitors. In the majority of cases, the investigated molecules are potent aldosterone synthase inhibitors selective toward the steroidogenic enzymes CYP11B1, CYP17, and CYP19 displaying no significant inhibition (except for **2**). The unsubstituted parent compound **1** shows also no significant inhibition of the six most important hepatic CYP enzymes (IC_{50} > 10 μM). In addition, this highly potent and selective aldosterone synthase inhibitor reaches high plasma concentrations ($AUC_{0-\infty}$ = 3464 ng·h/mL) after peroral application to rats and even slightly exceeds the bioavailability of the marketed drug fadrozole ($AUC_{0-\infty}$ = 3207 ng·h/mL). Currently, further studies with inhibitor **1** are underway to evaluate aldosterone-lowering effects *in vivo*.

Experimental section

Chemical and Analytical Methods. Melting points were measured on a Mettler FP1 melting point apparatus and are uncorrected. ^{1}H NMR and ^{13}C spectra were recorded on a Bruker DRX-500 instrument. Chemical shifts are given in parts per million (ppm), and tetramethylsilane (TMS) was used as internal standard for spectra obtained in DMSO-d_6 and $CDCl_3$. All coupling constants (J) are given in hertz. Mass spectra (LC/MS) were measured on a TSQ Quantum (Thermo Electron Corporation) instrument with a RP18 100-3 column (Macherey Nagel) and with water/acetonitrile mixtures as eluents. GC/MS spectra were measured on a GCD Series G1800A (Hewlett Packard) instrument with an Optima-5-MS (0.25 µM, 30 m) column (Macherey Nagel). Elemental analyses were carried out at the Department of Chemistry, University of Saarbrücken. Reagents were used as obtained from commercial suppliers without further purification. Solvents were distilled before use. Dry solvents were obtained by distillation from appropriate drying reagents and stored over molecular sieves. Flash chromatography was performed on silica gel 40 (35/40–63/70 µM) with petroleum ether/ethyl acetate mixtures as eluents, and the reaction progress was determined by thin-layer chromatography analyses on Alugram SIL G/UV254 (Macherey Nagel). Visualization was accomplished with UV light and $KMnO_4$ solution. All microwave irradiation experiments were carried out in a CEM-Discover monomode microwave apparatus.

The following compounds were prepared according to previously described procedures: 1,2,5,6-tetrahydro-4*H*-pyrrolo[3,2,1-*ij*]quinolin-4-one (**1b**),[21] 2,3,6,7-tetrahydro-1*H*,5*H*-pyrido[3,2,1-*ij*]quinolin-5-one (**2b**),[21] 5-bromopyridin-3-ol (**5b**),[20] 3-bromo-5-ethoxypyridine (**5a**).[20]

Synthesis of the Target Compounds

Procedure A.[22] Boronic acid (0.75 mmol, 1 equivalent), aryl bromide or -triflate (0.9–1.3 equivalents), and tetrakis(triphenylphosphane)palladium(0) (43 mg, 37.5 µmol, 5 mol %) were suspended in 1.5 mL DMF in a 10 mL septum-capped tube containing a stirring magnet. To this was added a solution of $NaHCO_3$ (189 mg, 2.25 mmol, 3 equivalents) in 1.5 mL water and the vial was sealed with an Teflon cap. The mixture was irradiated with microwaves for 15 min at a temperature of 150 °C with an initial irradiation power of 100 W. After the reaction, the vial was cooled to 40 °C, the crude mixture was partitioned between ethyl acetate and water and the aqueous layer was extracted three times with ethyl acetate. The combined organic layers were dried over $MgSO_4$ and the solvents were removed in vacuo. The coupling products were obtained after flash chromatography on silica gel (petroleum ether/ethyl acetate mixtures) and/or crystallization. If an oil was obtained, it was tranferred into the hydrochloride salt by 1N HCl solution in diethyl ether.

Procedure B. Boronic acid (1 equivalent), aryl bromide or (1.3–1.5 equivalents), and tetrakis(triphenylphosphane)palladium(0) (5 mol %) were suspended in toluene/ethanol 4/1 to give a 0.07–0.1 M solution of boronic acid under an atosphere of nitrogen. To this was added a 1 N aqueous solution of Na_2CO_3 (6 equivalents). The mixture was then refluxed for 12–18 h, cooled to room temperature, diluted with water and extracted several times with ethyl acetate. The combined extracts were dried over $MgSO_4$, concentrated and purified by flash chromatography on silica gel (petroleum

ether/ethyl acetate mixtures) and/or crystallization. If an oil was obtained, it was tranferred into the hydrochloride salt by 1 N HCl solution in diethyl ether.

8-Pyridin-3-yl-1,2,5,6-tetrahydro-4*H*-pyrrolo[3,2,1-*ij*]quinolin-4-one (1) was obtained according to procedure B from **1a** (5.19 g, 20.6 mmol) and 3-pyridineboronic acid (2.30 g, 18.7 mmol) after flash chromatography on silica gel (ethyl acetate, R_f = 0.08) and crystallization from acetone/diethylether as colorless plates (83 mg, 0.33 mmol, 49 %), mp 153–154 °C. ^{1}H-NMR (500 MHz, $CDCl_3$): δ = 2.72 (t, ^3J = 7.8 Hz, 2H), 3.03 (t, ^3J = 7.8 Hz, 2H), 3.25 (t, ^3J = 8.5 Hz, 2H), 4.13 (t, ^3J = 8.5 Hz, 2H), 7.20 (s, 1H), 7.28 (s, 1H), 7.32 (ddd, ^3J = 7.8 Hz, ^3J = 4.8 Hz, ^5J = 0.5 Hz, 1H), 7.79 (ddd, ^3J = 7.8 Hz, ^4J = 2.2 Hz, ^4J = 1.6 Hz, 1H), 8.54 (dd, ^3J = 4.7 Hz, ^4J = 1.4 Hz, 1H), 8.59 (d, ^4J = 2.0 Hz, 1H). ^{13}C-NMR (125 MHz, $CDCl_3$): δ = 24.5, 27.7, 31.6, 45.5, 120.7, 122.4, 123.5, 124.7, 129.9, 133.5, 134.0, 136.7, 141.6, 148.1, 167.6. MS *m/z* 251.22 (MH^+). Anal. ($C_{16}H_{14}N_2O$) C, H, N.

9-Pyridin-3-yl-1,2,6,7-tetrahydro-5*H*-pyrido[3,2,1-*ij*]quinolin-3-one (2) was obtained according to procedure A from **2a** (266 mg, 1.0 mmol) and 3-pyridineboronic acid (92 mg, 0.75 mmol) after flash chromatography on silica gel (petroleum ether/ethyl acetate, 2/3, R_f = 0.12) and crystallization from acetone/diethylether as colorless needles (116 mg, 0.44 mmol, 59 %), mp 122–123 °C. MS *m/z* 265.07 (MH^+). Anal. ($C_{17}H_{16}N_2O_2$) C, H, N.

8-(5-Methoxypyridin-3-yl)-1,2,5,6-tetrahydro-4*H*-pyrrolo[3,2,1-*ij*]quinolin-4-one (3) was obtained according to procedure A from **1a** (252 mg, 1.0 mmol) and 5-methoxy-3-pyridineboronic acid (115 mg, 0.75 mmol) after flash chromatography on silica gel (ethyl acetate, R_f = 0.09) as colorless needles (74 mg, 0.26 mmol, 35 %), mp 171–172 °C. MS *m/z* 281.02 (MH^+). Anal. ($C_{17}H_{16}N_2O_2$) C, H, N

9-(5-Methoxypyridin-3-yl)-1,2,6,7-tetrahydro-5*H*-pyrido[3,2,1-*ij*]quinolin-3-one (4) was obtained according to procedure A from **2a** (266 mg, 1.0 mmol) and 5-methoxy-3-pyridineboronic acid (115 mg, 0.75 mmol) after flash chromatography on silica gel (petroleum ether/ethyl acetate, 2/3, R_f = 0.08) and crystallization from acetone/diethylether as colorless needles (63 mg, 0.21 mmol, 28 %), mp 148–150 °C. MS *m/z* 295.02 (MH^+). Anal. ($C_{18}H_{18}N_2O_2 \cdot 0.2H_2O$) C, H, N.

8-(5-Ethoxypyridin-3-yl)-1,2,5,6-tetrahydro-4*H*-pyrrolo[3,2,1-*ij*]quinolin-4-one (5) was obtained according to procedure B from **3a** (300 mg, 1.0 mmol) and **5a** (242 mg, 1.2 mmol) after flash chromatography on silica gel (petroleum ether/ethyl acetate, 1/9, R_f = 0.10) and crystallization from acetone/diethylether as colorless needles (132 mg, 0.45 mmol, 45 %), mp 171–172 °C. MS *m/z* 295.16 (MH^+). Anal. ($C_{18}H_{18}N_2O_2$) C, H, N.

8-(5-Isopropoxypyridin-3-yl)-1,2,5,6-tetrahydro-4*H*-pyrrolo[3,2,1-*ij*]quinolin-4-one (6) was obtained according to procedure B from **3a** (359 mg, 1.20 mmol) and **6a** (281 mg, 1.30 mmol) after flash chromatography on silica gel (petroleum ether/ethyl acetate, 3/7, R_f = 0.07) as colorless plates (196 mg, 0.63 mmol, 53 %), mp 154–155 °C. MS *m/z* 309.15 (MH^+). Anal. ($C_{19}H_{20}N_2O_2 \cdot 0.2H_2O$) C, H, N.

8-(5-Hydroxypyridin-3-yl)-1,2,5,6-tetrahydro-4*H*-pyrrolo[3,2,1-*ij*]quinolin-4-one (7). A solution of **3** (95 mg, 0.34 mmol) in 35 ml concentrated hydrobromic acid was heated under reflux for 18 h. After cooling to room temperature, the reaction mixture was neutralized with saturated $NaHCO_3$ solution and extracted with ethyl acetate (3 x 200 ml). The crude product which was obtained after evaporation of the solvent was purified by flash chromatography on silica gel (ethyl acetate, $R_f = 0.06$) and washing with ethanol, yielding the hydroxy compound **7** as colorless solid (75 mg, 0.28 mmol, 83 %). The solid was dissolved in diethyl THF/methanol and tranferred into the hydrochloride salt by 1N HCl solution in isopropanol/diethyl ether, followed by filtration and crystallization from acetone, mp (HCl salt) >300 °C. MS *m/z* 267.94 (MH^+). Anal. ($C_{16}H_{14}N_2O_2$) C, H, N.

8-(5-Fluoropyridin-3-yl)-1,2,5,6-tetrahydro-4*H*-pyrrolo[3,2,1-*ij*]quinolin-4-one (8) was obtained according to procedure B from **3a** (359 mg, 1.2 mmol) and 3-bromo-5-fluoropyridine (211 mg, 1.2 mmol) after flash chromatography on silica gel (petroleum ether/ethyl acetate, 1/1, $R_f = 0.09$) and crystallization from acetone/diethylether as colorless needles (202 mg, 0.75 mmol, 63 %), mp 157–158 °C. MS *m/z* 269.83 (MH^+). Anal. ($C_{16}H_{13}FN_2O \cdot 0.3H_2O$) C, H, N.

8-[5-(Trifluoromethyl)pyridin-3-yl]-1,2,5,6-tetrahydro-4*H*-pyrrolo[3,2,1-*ij*]quinolin-4-one (9) was obtained according to procedure B from **3a** (329 mg, 1.1 mmol) and 3-bromo-5-(trifluoromethyl)pyridine (249 mg, 1.1 mmol) after flash chromatography on silica gel (petroleum ether/ethyl acetate, 1/1, $R_f = 0.14$) and crystallization from acetone/diethylether as colorless needles (248 mg, 0.78 mmol, 71 %), mp 211–212 °C. MS *m/z* 318.95 (MH^+). Anal. ($C_{17}H_{13}F_3N_2O$) C, H, N.

8-Isoquinolin-4-yl-1,2,5,6-tetrahydro-4*H*-pyrrolo[3,2,1-*ij*]quinolin-4-one (10) was obtained according to procedure A from **1a** (252 mg, 1.0 mmol) and 4-isoquinolineboronic acid (227 mg, 0.9 mmol) after flash chromatography on silica gel (petroleum ether/ethyl acetate, 2/3, $R_f = 0.13$) as colorless needles (93 mg, 0.31 mmol, 34 %), mp 184–185 °C. MS *m/z* 301.15 (MH^+). Anal. ($C_{20}H_{16}N_2O \cdot 0.2H_2O$) C, H, N.

9-Isoquinolin-4-yl-1,2,6,7-tetrahydro-5*H*-pyrido[3,2,1-*ij*]quinolin-3-one (11) was obtained according to procedure A from **2a** (266 mg, 1.0 mmol) and 4-isoquinolineboronic acid (227 mg, 0.9 mmol) after flash chromatography on silica gel (petroleum ether/ethyl acetate, 2/3, $R_f = 0.10$) and crystallization from acetone/diethylether as colorless needles (173 mg, 0.55 mmol, 61 %), mp 158–159 °C. MS *m/z* 315.24 (MH^+). Anal. ($C_{21}H_{18}N_2O$) C, H, N.

8-Pyridin-4-yl-1,2,5,6-tetrahydro-4*H*-pyrrolo[3,2,1-*ij*]quinolin-4-one (12) was obtained according to procedure B from **1a** (627 mg, 3.50 mmol) and 4-pyridineboronic acid (369 mg, 3.0 mmol) after crystallization from ethanol as yellow crystals (225 mg, 0.90 mmol, 30 %), mp 173–174 °C. MS *m/z* 251.01 (MH^+). Anal. ($C_{16}H_{14}N_2O$) C, H, N.

8-Pyrimidin-5-yl-1,2,5,6-tetrahydro-4*H*-pyrrolo[3,2,1-*ij*]quinolin-4-one (13) was obtained according to procedure B from **1a** (627 mg, 3.50 mmol) and 5-pyrimidineboronic acid (372 mg, 3.0 mmol) after crystallization from acetone as a yellow crystals (324 mg, 1.29 mmol, 43 %), mp 185–186 °C. MS *m/z* 251.85 (MH^+). Anal. ($C_{15}H_{13}N_3O \cdot 0.3H_2O$) C, H, N.

8-Imidazol-1-yl-1,2,5,6-tetrahydro-4*H*-pyrrolo[3,2,1-*ij*]quinolin-4-one (14). Imidazole (628 mg, 9.23 mmol), **1a** (2.12 g, 8.39 mmol), potassium carbonate (1.28 g, 9.23 mmol) and copper(II)sulfate (160 mg, 1.0 mmol) were mixed and heated at 180 °C for 10 h under an atmosphrere of dry nitrogen. After being cooled to room temperature, the reaction mixture was poured into 150 ml water and extracted with ethyl acetate (3 x 100 ml). After drying with $MgSO_4$ and evaporating of the solvent, the crude product was purified by two subsequent crystallizations from acetone to yield a colorless solid (674 mg, 2.82 mg, 34 %), mp 123–124 °C. MS *m/z* 240.02 (MH^+). Anal. ($C_{14}H_{13}N_3O \cdot 0.2H_2O$) C, H, N.

8-(5-Phenylpyridin-3-yl)-1,2,5,6-tetrahydro-4*H*-pyrrolo[3,2,1-*ij*]quinolin-4-one (15) was obtained according to procedure B from **3a** (325 mg, 1.07 mmol) and 3-bromo-5-phenylpyridine (301 mg, 1.28 mmol) after flash chromatography on silica gel (petroleum ether/ethyl acetate, 2/3, R_f = 0.09) as colorless plates (150 mg, 0.46 mmol, 43 %), mp 188–189 °C. MS *m/z* 326.79 (MH^+). Anal. ($C_{22}H_{18}N_2O \cdot 0.4H_2O$) C, H, N.

8-[5-(2-Fluorophenyl)pyridin-3-yl]-1,2,5,6-tetrahydro-4*H*-pyrrolo[3,2,1-*ij*]quinolin-4-one (16) was obtained according to procedure B from **3a** (389 mg, 1.30 mmol) and **16a** (311 mg, 1.12 mmol) after flash chromatography on silica gel (petroleum ether/ethyl acetate, 2/3, R_f = 0.09) as colorless solid (239 mg, 0.69 mmol, 56 %), mp 245–247 °C. MS *m/z* 345.19 (MH^+). Anal. ($C_{22}H_{17}FN_2O \cdot 0.3H_2O$) C, H, N.

8-[5-(3-Fluorophenyl)-pyridin-3-yl]-1,2,5,6-tetrahydro-4*H*-pyrrolo[3,2,1-*ij*]quinolin-4-one (17) was obtained according to procedure B from **3a** (360 mg, 1.20 mmol) and **17a** (378 mg, 1.50 mmol) after flash chromatography on silica gel (petroleum ether/ethyl acetate, 2/3, R_f = 0.08) as colorless needles (97 mg, 0.28 mmol, 23 %), mp 181–182 °C. MS *m/z* 345.26 (MH^+). Anal. ($C_{22}H_{17}FN_2O$) C, H, N.

8-[5-(4-Fluorophenyl)-pyridin-3-yl]-1,2,5,6-tetrahydro-4*H*-pyrrolo[3,2,1-*ij*]quinolin-4-one (18) was obtained according to procedure B from **3a** (463 mg, 1.55 mmol) and **18a** (440 mg, 1.75 mmol) after flash chromatography on silica gel (petroleum ether/ethyl acetate, 2/3, R_f = 0.05) as colorless needles (189 mg, 0.55 mmol, 35 %), mp 233–234 °C. MS *m/z* 345.05 (MH^+). Anal. ($C_{22}H_{17}FN_2O \cdot 0.6H_2O$) C, H, N.

8-[5-(2,5-Difluorophenyl)pyridin-3-yl]-1,2,5,6-tetrahydro-4*H*-pyrrolo[3,2,1-*ij*]quinolin-4-one (19) was obtained according to procedure B from **3a** (430 mg, 1.44 mmol) and **19a** (338 mg, 1.25 mmol) after flash chromatography on silica gel (petroleum ether/ethyl acetate, 3/7, R_f = 0.08) as colorless solid (371 mg, 1.02 mmol, 82 %), mp 189–190 °C. MS *m/z* 362.97 (MH^+). Anal. ($C_{22}H_{16}F_2N_2O \cdot 0.2H_2O$) C, H, N.

8-[5-(3,4-Difluorophenyl)pyridin-3-yl]-1,2,5,6-tetrahydro-4*H*-pyrrolo[3,2,1-*ij*]quinolin-4-one (20) was obtained according to procedure B from **3a** (449 mg, 1.50 mmol) and **20a** (367 mg, 1.36 mmol) after flash chromatography on silica gel (petroleum ether/ethyl acetate, 1/4, R_f = 0.07) as colorless needles (110 mg, 0.30 mmol, 22 %), mp 204–205 °C. MS *m/z* 363.11 (MH^+). Anal. ($C_{22}H_{16}F_2N_2O \cdot 0.3H_2O$) C, H, N.

8-[5-(3,5-Difluorophenyl)pyridin-3-yl]-1,2,5,6-tetrahydro-4*H*-pyrrolo[3,2,1-*ij*]quinolin-4-one (21) was obtained according to procedure B from **3a** (404 mg, 1.35 mmol) and **21a** (315 mg, 1.17 mmol) after flash chromatography on silica gel (petroleum ether/ethyl acetate, 3/7, R_f = 0.10) as colorless solid (104 mg, 0.29 mmol, 25 %), mp 228–229 °C. MS *m/z* 363.81 (MH^+). Anal. ($C_{22}H_{16}F_2N_2O \cdot 0.6H_2O$) C, H, N.

8-[5-(2-Methoxyphenyl)pyridin-3-yl]-1,2,5,6-tetrahydro-4*H*-pyrrolo[3,2,1-*ij*]quinolin-4-one (22) was obtained according to procedure B from **3a** (512 mg, 1.71 mmol) and **22a** (430 mg, 1.63 mmol) after flash chromatography on silica gel (petroleum ether/ethyl acetate, 1/4, R_f = 0.10) as colorless needles (106 mg, 0.29 mmol, 18 %), mp 186–187 °C. MS *m/z* 356.95 (MH^+). Anal. ($C_{23}H_{20}N_2O_2$) C, H, N.

8-[5-(3-Methoxyphenyl)pyridin-3-yl]-1,2,5,6-tetrahydro-4*H*-pyrrolo[3,2,1-*ij*]quinolin-4-one (23) was obtained according to procedure B from **3a** (329 mg, 1.10 mmol) and **23a** (270 mg, 1.02 mmol) after flash chromatography on silica gel (ethyl acetate, R_f = 0.09) as colorless solid (62 mg, 0.17 mmol, 17 %), mp 207–208 °C. MS *m/z* 357.09 (MH^+). Anal. ($C_{23}H_{20}N_2O_2 \cdot 0.2H_2O$) C, H, N.

8-[5-(4-Methoxyphenyl)pyridin-3-yl]-1,2,5,6-tetrahydro-4*H*-pyrrolo[3,2,1-*ij*]quinolin-4-one (24) was obtained according to procedure B from **3a** (389 mg, 1.30 mmol) and **24a** (315 mg, 1.19 mmol) after flash chromatography on silica gel (ethyl acetate, R_f = 0.08) as colorless needles (182 mg, 0.51 mmol, 43 %), mp 220–221 °C. MS *m/z* 357.09 (MH^+). Anal. ($C_{23}H_{20}N_2O_2 \cdot 0.5H_2O$) C, H, N.

8-[5-(3-hydroxyphenyl)pyridin-3-yl]-1,2,5,6-tetrahydro-4*H*-pyrrolo[3,2,1-*ij*]quinolin-4-one (25) was obtained according to procedure B from **3a** (430 mg, 1.44 mmol) and **25a** (313 mg, 1.25 mmol) after crystallization from ethanol as colorless needles (93 mg, 0.27 mmol, 22 %), mp 286–288 °C. MS *m/z* 343.03 (MH^+). Anal. ($C_{22}H_{18}N_2O_2 \cdot 0.7H_2O$) C, H, N.

8-{5-[3-(Trifluoromethoxy)phenyl]pyridin-3-yl}-1,2,5,6-tetrahydro-4*H*-pyrrolo[3,2,1-*ij*]quinolin-4-one (26) was obtained according to procedure B from **3a** (382 mg, 1.28 mmol) and **26a** (370 mg, 1.16 mmol) after flash chromatography on silica gel (petroleum ether/ethyl acetate, 1/4, R_f = 0.11) as colorless solid (332 mg, 0.81 mmol, 70 %), mp 160–161 °C. MS *m/z* 410.90 (MH^+). Anal. ($C_{23}H_{17}F_3N_2O_2$) C, H, N.

8-{5-[3-(Trifluoromethyl)phenyl]pyridin-3-yl}-1,2,5,6-tetrahydro-4*H*-pyrrolo[3,2,1-*ij*]quinolin-4-one (27) was obtained according to procedure B from **3a** (344 mg, 1.15 mmol) and **27a** (330 mg, 1.09 mmol) after flash chromatography on silica gel (petroleum ether/ethyl acetate, 2/3, R_f = 0.05) as colorless solid (276 mg, 0.70 mmol, 64 %), mp 154–153 °C. MS *m/z* 395.01 (MH^+). Anal. ($C_{23}H_{14}F_3N_2O$) C, H, N.

8-Pyridin-3-yl-1,2,5,6-tetrahydro-4*H*-pyrrolo[3,2,1-*ij*]quinoline-4-thione (28). A suspension of **1** (900 mg, 3.60 mmol) and Lawesson's reagent (1.45 g, 3.60 mmol) in 50 ml dry toluene and 5 ml dry THF was refluxed for 30 min under an atmosphere of nitrogen. After cooling to room temperature, the solvent was removed in vacuo and the residue was purified by flash chromatography on silica gel

(petroleum ether/ethyl acetate, 1/1, R_f = 0.25) to afford **28** as yellow solid (155 mg, 0.58 mmol, 16 %). The solid was dissolved in diethyl ether/methanol and tranferred into the hydrochloride salt by 1N HCl solution in isopropanol/diethyl ether, followed by filtration and crystallization from acetone, mp (HCl salt) 281–283 °C. MS *m/z* 267.10 (MH^+). Anal. ($C_{16}H_{14}N_2S \cdot HCl \cdot 0.2H_2O$) C, H, N.

6,6-Dimethyl-8-pyridin-3-yl-1,2,5,6-tetrahydro-4*H*-pyrrolo[3,2,1-*ij*]quinolin-4-one (29) was obtained according to procedure B from **29a** (280 mg, 1.0 mmol) and 3-pyridineboronic acid (92 mg, 0.75 mmol) after flash chromatography on silica gel (petroleum ether/ethyl acetate, 1/9, R_f = 0.09) and crystallization from acetone as colorless needles (48 mg, 0.17 mmol, 23 %), mp 178–180 °C. MS *m/z* 279.14 (MH^+). Anal. ($C_{18}H_{18}N_2O \cdot 0.2H_2O$) C, H, N.

Biological Methods. 1. Enzyme Preparations. CYP17 and CYP19 preparations were obtained by described methods: the 50,000 *g* sediment of *E. coli* expressing human CYP17[28] and microsomes from human placenta for CYP19.[30] **2. Enzyme Assays.** The following enzyme assays were performed as previously described: CY17[28] and CYP19.[30] **3. Activity and Selectivity Assay Using V79 Cells.** V79 MZh 11B1 and V79 MZh 11B2 cells[9,25] were incubated with [4-^{14}C]-11-deoxycorticosterone as substrate and inhibitor in at least three different concentrations. The enzyme reactions were stopped by addition of ethyl acetate. After vigorous shaking and a centrifugation step (10,000 *g*, 2 min), the steroids were extracted into the organic phase, which was then separated. The conversion of the substrate was analyzed by HPTLC and a phosphoimaging system as described.[9,25] **4. Inhibition of Human Hepatic CYP Enzymes.** The recombinantly expressed enzymes from baculovirus-infected insect microsomes (Supersomes) were used and the manufacturer's instructions (www.gentest.com) were followed. **5. *In Vivo* Pharmacokinetics.** Animal trials were conducted in accordance with institutional and international ethical guidelines for the use of laboratory animals. Male Wistar rats weighing 260–280 g (Janvier, France) were housed in a temperature-controlled room (20–24 °C) and maintained in a 12 h light/12 h dark cycle. Food and water were available ad libitum. The animals were anaesthetised with a ketamine (90 mg/kg)/xylazine (10 mg/kg) mixture, and cannulated with silicone tubing via the right jugular vein. Prior to the first blood sampling, animals were connected to a counterbalanced system and tubing, to perform blood sampling in the freely moving rat. Separate stock solutions (5 mg/mL) were prepared for the tested compounds in labrasol/water (1:1; v/v), leading to a clear solution. Immediately before application, the cassette dosing mixture was prepared by adding equal volumes of the stock solutions to end up with a final concentration of 1 mg/mL for each compound. The mixture was applied perorally to 4 rats with an injection volume of 5 mL/kg (Time 0). Blood samples (250 µl) were collected 1 hour before application and 1, 2, 4, 6, 8, and 24 hours thereafter. They were centrifuged at 650 *g* for 10 minutes at 4 °C and then the plasma was harvested and kept at –20 °C until LC/MS analysis. To 50 µL of rat plasma sample and calibration standard 100 µL acetonitrile containing the internal standard was added. Samples and standards were vigorously shaken and centrifuged for 10 minutes at 6000 *g* and 20 °C. For the test items, an additional dilution was performed by mixing 50 µL of the particle free supernatant with 50 µL water. An aliquot was transferred to 200 µL sampler vials and subsequently subjected to LC-MS/MS. HPLC-

MS/MS analysis and quantification of the samples was carried out on a Surveyor-HPLC-system coupled with a TSQ Quantum (ThermoFinnigan) triple quadrupole mass spectrometer equipped with an electrospray interface (ESI). The mean of absolute plasma concentrations (±SEM) was calculated for the 4 rats and the regression was performed on group mean values. The pharmacokinetic analysis was performed using a noncompartment model (PK Solutions 2.0, Summit Research Services).

Acknowledgement. We thank Gertrud Schmitt and Jeannine Jung for their help in performing the *in vitro* tests. We would also like to acknowledge the undergraduate research participants Judith Horzel and Helena Rübel whose work contributed to the presented results. The investigation of the hepatic CYP profile by Dr. Ursula Müller-Vieira and the pharmacokinetic studies by Dr. Barbara Birk, Pharmacelsus CRO, Saarbrücken, are highly appreciated. S. L. is grateful to Saarland University for a scholarship (Landesgraduierten-Förderung). Thanks are due to Prof. J. J. Rob Hermans, University of Maastricht, The Netherlands, for supplying the V79 CYP11B1 cells, and Prof. Rita Bernhardt, Saarland University, for supplying the V79 CYP11B2 cells.

Supporting Information Available: NMR spectroscopic data of the target compounds **2**–**29**, full experimental details and spectroscopic characterization of the reaction intermediates **1a**–**3a**, **6a**, **16a**–**27a**, **29a**, **29b**, elemental analysis results and purity data (LC-MS) of compounds **1**–**29**. This information is available free of charge via the Internet at http://pubs.acs.org.

References

(1) Weber, K. T. Aldosterone in congestive heart failure. *N. Engl. J. Med.* **2001**, *345*, 1689–1697.

(2) (a) Brilla, C. G. Renin-angiotensin-aldosterone system and myocardial fibrosis. *Cardiovasc. Res.* **2000**, *47*, 1–3. (b) Lijnen, P.; Petrov, V. Induction of cardiac fibrosis by aldosterone. *J. Mol. Cell. Cardiol.* **2000**, *32*, 865–879.

(3) (a) Struthers, A. D. Aldosterone escape during angiotensin-converting enzyme inhibitor therapy in chronic heart failure. *J. Card. Fail.* **1996**, *2*, 47–54. (b) Sato, A.; Saruta, T. Aldosterone escape during angiotensin-converting enzyme inhibitor therapy in essential hypertensive patients with left ventricular hypertrophy. *J. Int. Med. Res.* **2001**, *29*, 13–21.

(4) (a) Pitt, B.; Zannad, F.; Remme, W. J.; Cody, R.; Castaigne, A.; Perez, A.; Palensky, J.; Wittes, J. The effect of spironolactone on morbidity and mortality in patients with severe heart failure. *N. Engl. J. Med.* **1999**, *341*, 709–717. (b) Pitt, B.; Remme, W.; Zannad, F.; Neaton, J.; Martinez, F.; Roniker, B.; Bittman, R.; Hurley, S.; Kleiman, J.; Gatlin, M. Eplerenone, a selective aldosterone blocker, in patients with left ventricular dysfunction after myocardial infarction. *N. Eng. J. Med.* **2003**, *348*, 1309–1321.

(5) Juurlink, D. N.; Mamdani, M. M.; Lee, D. S.; Kopp, A.; Austin, P. C.; Laupacis, A.; Redelmeier, D. A. Rates of hyperkalemia after publication of the Randomized Aldactone Evaluation Study. *N. Engl. J. Med.* **2004**, *351*, 543–551.

(6) Delcayre, C.; Swynghedauw, B. Molecular mechanisms of myocardial remodeling. The role of aldosterone. *J. Mol. Cell. Cardiol.* **2002**, *34*, 1577–1584.

(7) (a) Wehling, M. Specific, nongenomic actions of steroid hormones. *Annu. Rev. Physiol.* **1997**, *59*, 365–393. (b) Lösel, R.; Wehling, M. Nongenomic actions of steroid hormones. *Nature Rev. Mol. Cell. Biol.* **2003**, *4*, 46–55.

(8) Hartmann, R. W. Selective inhibition of steroidogenic P450 enzymes: Current status and future perspectives. *Eur. J. Pharm. Sci.* **1994**, *2*, 15–16.

(9) Ehmer, P. B.; Bureik, M.; Bernhardt, R.; Müller, U.; Hartmann, R. W. Development of a test system for inhibitors of human aldosterone synthase (CYP11B2): Screening in fission yeast and evaluation of selectivity in V79 cells. *J. Steroid Biochem. Mol. Biol.* **2002**, *81*, 173–179.

(10) Kawamoto, T.; Mitsuuchi, Y.; Toda, K.; Yokoyama, Y.; Miyahara, K.; Miura, S.; Ohnishi, T.; Ichikawa, Y.; Nakao, K.; Imura, H.; Ulick, S.; Shizuta, Y. Role of steroid 11β-hydroxylase and steroid 18-hydroxylase in the biosynthesis of glucocorticoids and mineralocorticoids in humans. *Proc. Natl. Acad. Sci. U.S.A.* **1992**, *89*, 1458–1462.

(11) (a) Hahner, S.; Stuermer, A.; Kreissl, M.; Reiners, C.; Fassnacht, M.; Haenscheid, H.; Beuschlein, F.; Zink, M.; Lang, K.; Allolio, B.; Schirbel, A. [^{123}I]Iodometomidate for Molecular Imaging of Adrenocortical Cytochrome P450 Family 11B Enzymes. *J. Clin. Endocrinol. Metab.* **2008**, *93*, 2358–65. (b) Zolle, I. M.; Berger, M. L.; Hammerschmidt, F.; Hahner, S.; Schirbel, A.; Peric-Simov, B. New selective inhibitors of steroid 11β-hydroxylation in the adrenal cortex. Synthesis and structure–activity relationship of potent etomidate analogues. *J. Med. Chem.* **2008**, *51*, 2244–2253.

(12) Bassett, M. H.; Mayhew, B.; Rehman, K.; White, P. C.; Mantero, F.; Arnaldi, G.; Stewart, P. M.; Bujalska, I.; Rainey, W. E. Expression profiles for steroidogenic enzymes in adrenocortical disease. *J. Clin. Endocrinol. Metab.* **2005**, *90*, 5446–5455.

(13) Taymans, S. E.; Pack, S.; Pak, E.; Torpy, D. J.; Zhuang, Z.; Stratakis, C. A. Human CYP11B2 (aldosterone synthase) maps to chromosome 8q24.3. *J. Clin. Endocrinol. Metab.* **1998**, *83*, 1033–1036.

(14) Ulmschneider, S.; Müller-Vieira, U.; Mitrenga, M.; Hartmann, R. W.; Oberwinkler-Marchais, S.; Klein, C. D.; Bureik, M.; Bernhardt, R.; Antes, I.; Lengauer, T. Synthesis and evaluation of imidazolylmethylenetetrahydronaphthalenes and imidazolylmethyleneindanes: Potent inhibitors of aldosterone synthase. *J. Med. Chem.* **2005**, *48*, 1796–1805.

(15) Ulmschneider, S.; Müller-Vieira, U.; Klein, C. D.; Antes, I.; Lengauer, T.; Hartmann, R. W. Synthesis and evaluation of (pyridylmethylene)tetrahydronaphthalenes/-indanes and structurally modified derivatives: Potent and selective inhibitors of aldosterone synthase. *J. Med. Chem.* **2005**, *48*, 1563–1575.

(16) Voets, M.; Antes, I.; Scherer, C.; Müller-Vieira, U.; Biemel, K.; Barassin, C.; Oberwinkler-Marchais, S.; Hartmann, R. W. Heteroaryl substituted naphthalenes and structurally modified derivatives: Selective inhibitors of CYP11B2 for the treatment of congestive heart failure and myocardial fibrosis. *J. Med. Chem.* **2005**, *48*, 6632–6642.

(17) Lucas, S.; Heim, R.; Negri, M.; Antes, I.; Ries, C.; Schewe, K. E.; Bisi, A.; Gobbi, S.; Hartmann, R. W. Novel aldosterone synthase inhibitors with extended carbocyclic skeleton by a combined ligand-based and structure-based drug design approach. *J. Med. Chem.* **2008**, in press.

(18) Voets, M.; Antes, I.; Scherer, C.; Müller-Vieira, U.; Biemel, K.; Oberwinkler-Marchais, S.; Hartmann, R. W. Synthesis and evaluation of heteroaryl-substituted dihydronaphthalenes and indenes: Potent and selective inhibitors of aldosterone synthase (CYP11B2) for the treatment of congestive heart failure and myocardial fibrosis. *J. Med. Chem.* **2006**, *49*, 2222–2231.

(19) Lucas, S.; Heim, R.; Ries, C.; Schewe, K. E.; Birk, B.; Hartmann, R. W. Nonsteroidal aldosterone synthase inhibitors with improved selectivity: Lead optimization providing a series of pyridine substituted 3,4-dihydro-1*H*-quinolin-2-one derivatives. *J. Med. Chem.* **2008**, submitted.

(20) Heim, R.; Lucas, S.; Grombein, C. M.; Ries, C.; Schewe, K. E.; Negri, M.; Müller-Vieira, U.; Birk, B.; Hartmann, R. W. Overcoming undesirable CYP1A2 inhibition of pyridylnaphthalene type aldosterone synthase inhibitors: Influence of heteroaryl derivatization on potency and selectivity. *J. Med. Chem.* **2008**, *51*, 5064–5074.

(21) Crabb, T. A.; Soilleux, S. L.; Microbiological transformations. Part 9.: Microbiological transformations of 1,2,5,6-tetrahydropyrrolo[3,2,1-*i,j*]-quinolin-4-one and of derivatives of 1,2,3,5,6,7-hexahydropyrido[3,2,1-*i,j*]quinoline with the fungus Cunninghamella elegans. *Tetrahedron* **1986**, *42*, 5407–5413.

(22) Appukkuttan, P.; Orts, A. B.; Chandran, R., P.; Goeman, J. L.; van der Eycken, J.; Dehaen, W.; van der Eycken, E. Generation of a small library of highly electron-rich 2-(hetero)aryl-substituted phenethylamines by the Suzuki-Miyaura reaction: A short synthesis of an apogalanthamine analogue. *Eur. J. Org. Chem.* **2004**, 3277–3285.

(23) Zhu, H.-F.; Zhao, W.; Okamura, T.; Fan, J.; Sun, W.-Y.; Ueyama, N. Syntheses and crystal structures of 1D tubular chains and 2D polycatenanes built from the asymmetric 1-(1-imidazolyl)-4- (imidazol-1-ylmethyl)benzene ligand with metal salts. *New J. Chem.* **2004**, *28*, 1010–1018.

(24) Ishiyama, T.; Murata, M.; Miyaura, N. Palladium(0)-catalyzed cross-coupling reaction of alkoxydiboron with haloarenes: A direct procedure for arylboronic esters. *J. Org. Chem.* **1995**, *60*, 7508–7510.

(25) (a) Denner, K.; Bernhardt, R. Inhibition studies of steroid conversions mediated by human CYP11B1 and CYP11B2 expressed in cell cultures. In *Oxygen Homeostasis and Its Dynamics*, 1st ed.; Ishimura, Y., Shimada, H., Suematsu, M., Eds.; Springer-Verlag: Tokyo, Berlin, Heidelberg, New York, 1998; pp 231–236. (b) Denner, K.; Doehmer, J.; Bernhardt, R. Cloning of CYP11B1 and CYP11B2 from normal human adrenal and their functional expression in COS-7 and V79 chinese hamster cells. *Endocr. Res.* **1995**, *21*, 443–448. (c) Böttner, B.; Denner, K.; Bernhardt, R. Conferring aldosterone synthesis to human CYP11B1 by replacing key amino acid residues with CYP11B2-specific ones. *Eur. J. Biochem.* **1998**, *252*, 458–466.

(26) Lamberts, S. W.; Bruining, H. A.; Marzouk, H.; Zuiderwijk, J.; Uitterlinden, P.; Blijd, J. J.; Hackeng, W. H.; de Jong, F. H. The new aromatase inhibitor CGS-16949A suppresses aldosterone and cortisol production by human adrenal cells *in vitro*. *J. Clin. Endocrinol. Metab.* **1989**, *69*, 896–901.

(27) Demers, L. M.; Melby, J. C.; Wilson, T. E.; Lipton, A.; Harvey, H. A.; Santen, R. J. The effects of CGS 16949A, an aromatase inhibitor on adrenal mineralocorticoid biosynthesis. *J. Clin. Endocrinol. Metab.* **1990**, *70*, 1162–1166.

(28) (a) Ehmer, P. B.; Jose, J.; Hartmann, R. W. Development of a simple and rapid assay for the evaluation of inhibitors of human 17α-hydroxylase-$C_{17,20}$-lyase (P450c17) by coexpression of P450c17 with NADPH-cytochrome-P450-reductase in *Escherichia coli*. *J. Steroid Biochem. Mol. Biol.* **2000**, *75*, 57–63; (b) Hutschenreuter, T. U.; Ehmer, P. B.; Hartmann, R. W. Synthesis of hydroxy derivatives of highly potent nonsteroidal CYP17 inhibitors as potential metabolites and evaluation of their activity by a non cellular assay using recombinant enzyme. *J. Enzyme Inhib. Med. Chem.* **2004**, *19*, 17–32.

(29) Thompson, E. A.; Siiteri, P. K. Utilization of oxygen and reduced nicotinamide adenine dinucleotide phosphate by human placental microsomes during aromatization of androstenedione. *J. Biol. Chem.* **1974**, *249*, 5364–5372.

(30) Hartmann, R. W.; Batzl, C. Aromatase inhibitors. Synthesis and evaluation of mammary tumor inhibiting activity of 3-alkylated 3-(4-aminophenyl)piperidine-2,6-diones. *J. Med. Chem.* **1986**, *29*, 1362–1369.

(31) Belkina, N. V.; Lisurek, M.; Ivanov, A. S.; Bernhardt, R. Modelling of three-dimensional structures of cytochromes P450 11B1 and 11B2. *J. Inorg. Biochem.* **2001**, *87*, 197–207.

(32) Hakki, T.; Bernhardt, R.; CYP17- and CYP11B-dependent steroid hydroxylases as drug development targets. *Pharmacol. Ther.* **2006**, *111*, 27–52.

3.5 Selective Aldosterone Synthase Inhibitors Reduce Aldosterone Formation *in vitro* and *in vivo*

Christina Ries, Simon Lucas, Ralf Heim, Barbara Birk and Rolf W. Hartmann

This manuscript has been published as an article in the

Journal of Steroid Biochemistry and Molecular Biology **2009**, *116*, 121-126

Paper V

Abstract: Aldosterone plays a crucial role in salt and water homeostasis but in case of pathologically increased plasma aldosterone levels it is also involved in the development and the progression of severe cardiovascular diseases like heart failure and myocardial fibrosis. For the treatment of these diseases we propose inhibition of the aldosterone forming enzyme CYP11B2 as a new pharmacological strategy. We recently developed *in vitro* highly potent and selective inhibitors of human CYP11B2, but the evidence of their *in vivo* activity is still missing. For this purpose, rat aldosterone synthase gene was cloned and expressed in V79MZ cells to establish a new screening assay for the identification of "rat-active" substances. Compound **7** from the class of heteroaryl substituted 3,4-dihydro-1*H*-quinolin-2-ones showed a moderate inhibitory effect (65 % at 2 μM) on rat CYP11B2 *in vitro*. Furthermore, it diminished the conversion of deoxycorticosterone to aldosterone in rat adrenals and significantly reduced plasma aldosterone levels *in vivo*.

Introduction

The responsible enzyme for the formation of the major mineralocorticoid aldosterone is aldosterone synthase (CYP11B2). This mitochondrial cytochrome P450 enzyme is localized mainly in the *Zona glomerulosa* in the adrenal cortex and catalyses the terminal three steps in the biosynthesis of aldosterone.[1] This hormone plays a key role in salt and water homeostasis by binding to epithelial mineralocorticoid receptors (MR), regulating sodium and water retention as well as potassium secretion. As a consequence of this it is involved in the regulation of blood volume and blood pressure. Aldosterone release is mainly triggered by angiotensin-II via the renin-angiotensin-aldosterone-system (RAAS) and the extracellular potassium concentration. Pathologically elevated plasma aldosterone levels are associated with severe cardiovascular diseases such as hypertension, heart failure and myocardial fibrosis.[2-4] In these disease states reduction of aldosterone action is indicated. The pharmacological therapies include angiotensin-converting enzyme (ACE) inhibitors or angiotensin-II receptor blockers to prevent the stimulation of aldosterone biosynthesis. However, the limiting factor of these treatments is an iterate increase of plasma aldosterone levels, also referred to as aldosterone escape.[5] Recently, MR antagonists like Spironolactone and Eplerenone decreased in two clinical trials (RALES and EPHESUS) hospitalization and mortality in patients after myocardial infarction and in heart failure patients.[6,7] However, with the use of MR blockers severe side effects such as gynaecomastia or dysmenorrhoea are associated due to their steroidal structure and as a consequence of this affinity to steroid receptors. Another complication is the increased hospitalization rate due to hyperkalemia.[8] Moreover, it was reported that the application of Spironolactone leads to an increase of urinary and plasma aldosterone levels in rats.[9] These facts suggest that a long-term treatment with aldosterone antagonists is not a satisfying therapeutic approach. A novel strategy for the treatment of patients with heart failure, myocardial fibrosis and certain forms of hyperaldosteronism is the reduction of aldosterone biosynthesis by inhibition of CYP11B2. Non-steroidal compounds are to be preferred in order to minimize the risk of side effects caused by interaction with steroid receptors or other steroidogenic enzymes. This approach has been propageted by our group since 1994.[10] In the last decade great efforts were undertaken to develop lead structures from hits discovered by compound library screening.[11-14] Furthermore, a screening system was established to evaluate the potency and the selectivity of the compounds obtained by structural optimization.[15-17] Recently, we succeeded in developing aldosterone synthase inhibitors with improved activity and selectivity against other steroidogenic enzymes such as CYP11B1, CYP17 and CYP19 as well as hepatic cytochrome P450 enzymes (CYP1A2, CYP2B6, CYP2C9, CYP2C19, CYP2D6 and CYP3A4).[18-20] At this stage of preclinical development an *in vivo* proof of concept (POC) should be performed demonstrating that the administration of CYP11B2 inhibitors results in decreased plasma aldosterone concentrations. Consequently, some of these compounds were further tested in rats for their aldosterone lowering activity. However, they were inactive. Subsequent *in vitro* studies showed

that they were not able to inhibit rat aldosterone synthase. This finding can be explained by the fact that the homology between the human and the rat enzyme is only 70 %.

Further pursuing our POC, we describe in the present study the establishment of a new assay to identify a suitable candidate to investigate aldosterone-lowering effects in rats. A new cell line was constituted, that expresses the rat CYP11B2 enzyme to generate an *in vitro* tool for the identification of "rat-active" compounds. Various compounds from diverse substance classes were tested for inhibitory potency toward the rat aldosterone synthase recombinantly expressed in V79MZ cells. Moreover, an additional assay with rat adrenals was carried out to examine the results obtained from the *in vitro* assay. An active compound, which was identified in these assays, was evaluated for its ability to decrease plasma aldosterone levels in rats.

Materials and Methods

1. Chemicals. All chemicals were purchased from Carl Roth (Karlsruhe, Germany) or Sigma-Aldrich (Munich, Germany), unless otherwise stated. Cell culture reagents were obtained from c.c. pro (Oberdorla, Germany). [4-^{14}C]-Deoxycorticosterone (45-60 mCi/mmol) was purchased from NEN Life Science (Boston, USA). **2. Cell culture.** The untransfected V79MZ Chinese hamster cells (provided by Prof. Bernhardt, Saarland University) and the rat CYP11B2 expressing V79MZ cell line were grown as monolayer culture in Dulbecco's modified Eagle medium (DMEM) supplemented with 5 % of fetal calf serum (FCS), penicillin (100 U/ml), streptomycin (100 µg/ml) and sodium pyruvate (1 mM) at 37°C in 5 % CO_2 in air. Transfected cells were maintained in the presence of 750 µg/ml G418 sulfate. **3. Cloning of rat CYP11B2 cDNA and plasmid construction.** The cDNA of rat CYP11B2 was amplified from total RNA extracted from surgically removed rat adrenals after ACTH stimulation (1 mg/kg) of the animals. Total RNA was isolated with the GenElute™ Total Mammalian Miniprep Kit following the manufacturer's instructions. For cDNA synthesis 1 µg total RNA was used with 0.5 µg oligo-$dT_{12\text{-}18}$, 0.5 mM dNTP-mix and 1 µl Improm-II™ Reverse Transcriptase (Promega, Madison, USA) in a synthesis buffer with 3 mM $MgCl_2$ according to Promega's standard reverse transcription protocol. This procedure was followed by a polymerase chain reaction (PCR) to amplify the rat CYP11B2 gene with two specific oligonucleotide primers that contained a cleavage site for *EcoRI* and corresponded to nucleotides 1-29 and 1475-1503 of the rat CYP11B2 cDNA published by Imai *et al.*.[21] The PCR reaction was performed with 2 µM of each primer, 0.2 mM dNTP-mix, 2.5 U of Hifi Taq polymerase (Roche, Mannheim, Germany) and 10 µl cDNA template of RT reaction described above in a reaction buffer containing 7.5 mM $MgCl_2$. The purified PCR-product (1512 bp) was cloned into MCS of pcDNA3.1/V5-His© TOPO® TA expression vector from invitrogen (Carlsbad, USA). The analysis of the nucleotide sequence of the cloned rat CYP11B2 gene was performed by GATC-Biotech (Konstanz, Germany). **4. Transfection procedure.** One day before transfection was performed 2 x 10^5 untransfected V79MZ cells were seeded into 35 mm culture dishes (Nunc, Wiesbaden, Germany) and incubated overnight in complete growth medium. On the following day the

approximately 70 % confluent culture was transfected with the generated plasmid using the liposomal transfecting reagent Roti®-Fect following the manufacturer's recommendations. **5. Selection of stably transfected clones.** Stably transfected clones carrying the Neomycin resistance marker were selected with G418 sulfate. First the killing concentration for the untransfected V79MZ cells was determined by using various concentrations of G418 sulfate (200 µg/ml-1000 µg/ml). After 6 days of incubation at a dose of 500 µg/ml G418 sulfate 50 % of the cells were killed. Transfected cells were grown for 16 h in transfection medium without antibiotics before medium was replaced by complete growth medium. Selection of transfected clones started days later by addition of 750 µg/ml G418 sulfate and was performed for 2 weeks while untransfected cells died. The isolated transfected cells were subsequently separated to create monoclonal cell lines. Therefore single cell clones were seeded into 96-well cell culture plates and grown in selective medium for further analysis. **6. Determination of rat aldosterone synthase activity.** The rat aldosterone synthase activity of several monoclonal cell lines was determined by measuring the conversion of radiolabeled substrate ([4-^{14}C]-deoxycorticosterone) to the three products [4-^{14}C]-corticosterone, [4-^{14}C]-18-OH-corticosterone and [4-^{14}C]-aldosterone. For this purpose, transfected cell lines were seeded one day before into wells of a 24-well culture plate and incubated overnight to allow the attachment of the cells. Before testing growth medium was removed by aspiration and replaced by 500 µl fresh medium containing the substrate deoxycorticosterone

(100 nM, 6 nCi of [4-^{14}C]-deoxycorticosterone in ethanol). After 6 h of incubation enzyme reaction was terminated by extraction of the supernatant with 500 µl ethyl acetate for steroid isolation. The organic solvent was pipetted into fresh cups and evaporated to dryness. The steroids were redissolved in 10 µl chloroform and analyzed by HPTLC (see section 2.8). As a control the untransfected V79MZ cell line was also incubated with [4-^{14}C]-deoxycorticosterone to demonstrate the absence of enzymatic activity concerning this substrate. **7. Screening assay procedure in rat CYP11B2 expressing V79MZ cell line.** For determination of inhibitory effects on the rat CYP11B2, transfected cells were grown in 24-well culture plates (1 x 10^6 cells/well) until confluence. Culture medium was removed by aspiration and replaced by 450 µl fresh medium containing 1 % of the ethanolic dilution of the inhibitor resulting in a final concentration of 2 µM. Controls were treated in the same way without inhibitor but 1 % ethanol. After a preincubation step of 60 min the enzyme reaction was started by addition of 50 µl DMEM in which the radiolabeled substrate (containing 6 nCi of [4-^{14}C]-deoxycorticosterone in ethanol, final concentration 500 nM) was dissolved. After 5 h incubation the steroids were extracted from supernatant with 500 µl ethyl acetate. The organic layer was separated and evaporated to dryness. Subsequently the steroids were redissolved in 10 µl chloroform and subjected to HPTLC analysis as described in section 8. **8. HPTLC analysis and phosphoimaging of radiolabeled steroids.** For analysis of the substrate conversion by rat CYP11B2 expressing V79MZ cell lines the redissolved steroids were transferred on a HPTLC plate (20 x 10 cm, Silicagel 60F_{254} with concentrating zone) from Merck (Darmstadt, Germany) and developed two times

in chloroform:methanol:water (300:20:1) as solvent. Afterwards imaging plates BAS-MS2340 (Raytest, Straubenhardt, Germany) were exposed to the HPTLC plates for 48 h before they were scanned using a FLA3000 scanner (Raytest, Straubenhardt, Germany), substrate and products were quantified by AIDA® software (Raytest, Straubenhardt, Germany). The inhibitory potency of the compounds concerning rat aldosterone synthase activity was calculated from the reduced substrate conversion rate caused by the inhibitor. **9. *In vitro* assay for rat aldosterone synthase inhibitors on rat adrenals.** Adrenals from male Wistar rats (Charles River, Germany) were surgically removed and transferred into wells of a 48-well plate containing 700 µl DMEM per well. After addition of inhibitors in final test concentrations of 50 and 250 µM (ethanol 1 %, v/v) or 1 % ethanol for control organs, preincubation was carried out for 60 min at 37 °C in 5 % CO_2 in air. Further assay procedure was performed with 100 nM [4-^{14}C]-deoxycorticosterone for 6 h as described in section 7. Every determination was performed with five organs. **10. *In vivo* aldosterone lowering.** Animal care and experimental procedures were performed in accordance with the guidelines for the care and use of laboratory animals published by the National Institutes of Health and the German Animal Protection Law as approved by the local government. Male Wistar rats (Charles River, Germany) weighing 251–276 g (day: ACTH stimulation) and 263–281 g (day: test item application) were used in the present study. Animals were housed in a separate temperature-controlled room (20–24 °C) and maintained in a 12 h light/ 12 h dark cycle. Food and water were available ad libitum. At least two days before application, rats were anaesthetized with a ketamine (90 mg/kg)/xylazine (5 mg/kg) mixture, and cannulated with silicone tubing via the right jugular vein. Prior to the first blood sampling, the rats were connected to a counterbalanced system and tubing to perform blood sampling in the freely moving animal. Pre-dose blood samples (400 µl) were taken before application of ACTH, before application of **7**/vehicle followed by sampling 0.25, 0.5, 1, 2, 3, and 6 h post-dose. Blood was collected in tubes, stored at room temperature until coagulation and subsequently centrifuged at 645 g for 10 min at 4 °C. The harvested serum was kept at –20 °C until being assayed. After each blood sample an equal volume of saline (NaCl 0.9 %, ~37°C, 400 µl) was reinjected in order to keep the blood volume stabilized. Subcutaneous application of ACTH: The animals were stimulated by subcutaneous application of ACTH (1 mg/kg; 1 ml/kg) 16 h before test item application. Intravenous application of test item or vehicle: After sampling of 500 µl blood in a heparinized (15 µl, 500 IE/ml) syringe via the catheter, the formulation of **7** (10 mg/ml in 20% ethanol/50% PEG400/30% water) or the vehicle (20% ethanol/50% PEG400/30% water) was applied within 60 sec on the same route to rats with an injection volume of 2 ml/kg. Time zero was registered when the compound was entering the circulation. After that, the 500 µl blood sample taken before was returned via the catheter in order to assure that the entire test compound was administered into the animal. Plasma aldosterone levels were measured using an aldosterone RIA kit from DRG (Marburg, Germany) according to the manufacturer's instructions.

Results

Selection of stably transfected cell clones containing rat CYP11B2 expression plasmid

About 60 h after transfection of V79MZ cells with the generated plasmid selection of clones carrying the Neomycin marker was started by addition of G418 sulfate. After 2 weeks of cultivation untransfected cells had died and resistant clones were separated to achieve monoclonal cell lines. For determination of rat aldosterone synthase activity the conversion rate of [4-^{14}C]-deoxycorticosterone to the three radiolabeled products corticosterone, 18-OH-corticosterone and aldosterone was measured. The untransfected V79MZ cell line was also incubated with the radiolabeled substrate to demonstrate that no substrate was converted. Out of all analyzed monoclonal cell lines the clone with the highest conversion rate was chosen for the development of a new screening assay to identify inhibitors of rat CYP11B2. This monoclonal cell line was named V79/CYP11B2-rat and exhibited a conversion rate of 25.3 % within 6 h, whereas the substrate conversion of untransfected cells was less than 2 %.

Establishment of a cellular screening assay for rat aldosterone synthase inhibitors

For determination of optimal test conditions different parameters were evaluated with the cell line V79/CYP11B2-rat. For this purpose, conversion rates of different numbers of cells were investigated in diverse multi-well cell culture plates at different time points. To reach an ideal substrate conversion of 12-20 % with a confluent cell layer the following test conditions were elaborated: incubation of 1 x 10^6 cells/well in a 24-well plate for 5 h with a substrate concentration of 500 nM.

Screening of selected compounds

For the evaluation of the inhibitory potency toward rat aldosterone synthase, selected compounds were tested at a final concentration of 2 µM as described in section 7. In order to determine a suitable candidate to investigate aldosterone-lowering effects in rats, we evaluated potent and selective inhibitors of human aldosterone synthase[18-20] for their ability to block aldosterone biosynthesis in V79MZ cells expressing rat CYP11B2 prior to *in vivo* experiments. In this screening assay the reference inhibitor **Fadrozole** showed a high inhibition of 73 % at 0.5 µM. As shown in Table 1 only compound **7** (and to a minor degree also the *N*-methyl analogue **9**) showed a moderate inhibitory action (65 % at 2 µM) on rat CYP11B2 *in vitro* within the class of heteroaryl substituted 3,4-dihydro-1*H*-quinolin-2-ones and structurally related substances. Compound **7** is a highly potent inhibitor of human CYP11B2 *in vitro* (IC_{50} = 0.2 nM) and also exhibits a pronounced selectivity versus other CYP enzymes.[20] All other tested compounds, which were in the human enzyme highly active, showed slight or no inhibition (0 – 16 % at 2 µM) of the rat CYP11B2.

Table 1: Percent inhibition at 0.5 µM and IC_{50} values for test compounds in V79MZ cells expressing the human CYP11B2 gene compared to percent inhibition in V79/CYP11B2-rat at 2 µM.

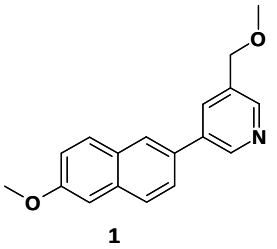

1

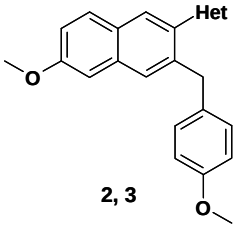

2, 3

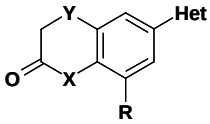

4-11

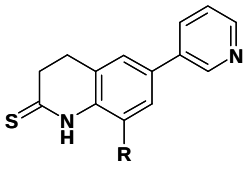

12, 13

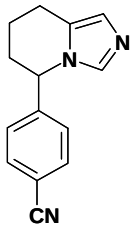

Fadrozole

Compd	R	X	Y	Het	% inhibition[a,f] **human** CYP11B2[c] (V79MZ cells)	IC_{50} [nM][b,f] **human** CYP11B2[c] (V79MZ cells)	% inhibition[d] **rat** CYP11B2[e] (V79MZ cells)
1					96	0.2	2
2				3-pyridine	95	11	16
3				4-isoquinoline	94	5.0	11
4	H	NH	CH_2	3-pyridine	88	28	4
5	H	NMe	CH_2	3-pyridine	92	2.6	0
6	H	NH	CH_2	5-methoxy-3-pyridine	91	2.7	16
7	H	NH	CH_2	4-isoquinoline	94	0.2	65
8	H	NMe	CH_2	5-methoxy-3-pyridine	94	0.2	0
9	H	NMe	CH_2	4-isoquinoline	99	0.1	49
10	Cl	NH	CH_2	3-pyridine	97	3.8	0
11	H	NH	S	3-pyridine	92	12	0
12	H				97	3.1	4
13	Cl				97	4.2	3
Fadrozole						1.0	73 [0.5 µM]

[a]Mean value of at least four experiments, standard deviation less than 10 %. [b]Mean value of at least four experiments, standard deviation usually less than 25 %. [c]Hamster fibroblasts expressing human CYP11B2, substrate deoxycorticosterone, 100 nM. [d]Mean value of at least three experiments, standard deviation less than 15 %. [e]Hamster fibroblasts expressing rat CYP11B2, substrate deoxycorticosterone, 500 nM. [f]Former published data.[18-20]

Inhibition of rat CYP11B2 evaluated in rat adrenals

For examination of the results we achieved by the *in vitro* screening assay compound **7** was also tested for its inhibitory potency against rat aldosterone synthase using rat adrenals, that were surgically removed from male Wistar rats. The CYP11B2 inhibitor SL272 (unpublished data), highly active and selective in human enzyme, but not active in the rat enzyme (0 % inhibition), was taken as a reference (Figure 1a). After preincubation of the organs with the inhibitors at two different concentrations (50 and 250 µM), the reduction of the substrate conversion caused by the substances compared to control organs was measured. In accordance with the results from the cellular inhibition assay the human CYP11B2 inhibitor SL272 did not decrease aldosterone synthase activity in rat adrenals at a concentration of 50 µM and led only to a 30 % reduction of aldosterone formation at 250 µM (Figure 1a). This effect was not significant. For compound **7**, which had shown a moderate inhibition at the rat enzyme (Table 1), the *in vitro* results could also be confirmed. The aldosterone biosynthesis in rat adrenals was significantly reduced by 76 % at 50 µM (P<0.05) and 89 % at 250 µM (P<0.003) (Figure 1b).

Figure 1[a]

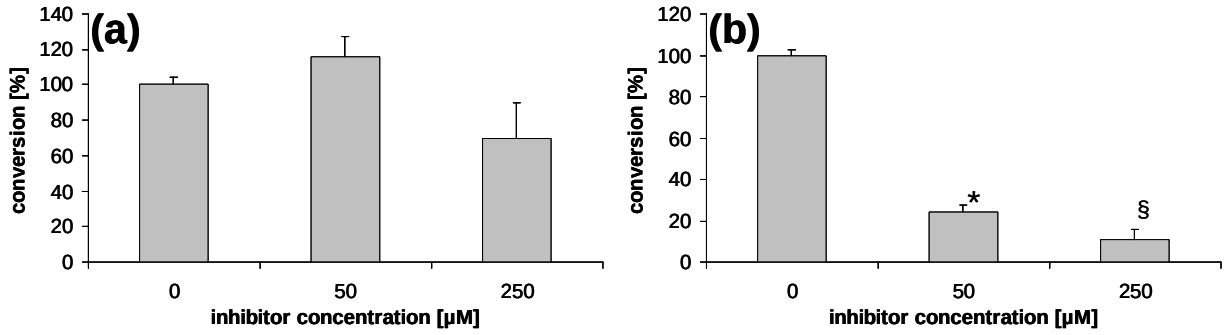

[a] Inhibition of aldosterone biosynthesis in rat adrenals by reference compound SL272 (a) and **7** (b) at 50 and 250 µM. Bars represent mean values (n = 5, ± SD) of relative formation compared to control. [*]P<0.05 versus control; [§]P<0.003 versus control.

Inhibition of aldosterone formation *in vivo*

Two days before application, adult male rats were cannulated with silicone tubing via the right jugular vein. Prior to the first blood sampling, the rats were connected to a counterbalanced system and tubing to perform blood sampling in the freely moving animal. Pre-dose blood samples were taken before application of ACTH and before application of **7** (animals 1–6) or vehicle (animals 7–10), followed by sampling 0.25, 0.5, 1, 2, 3, and 6 h post-dose. The animals received a subcutaneous injection of ACTH (1 mg/kg) 16 h before test item application to stimulate the corticoid biosynthesis. The aldosterone levels were determined using RIA. It becomes apparent that ACTH treatment induced a significant increase of the aldosterone levels. Within the vehicle-treated group (Figure 2b), the concentrations found in the plasma were rather constant over the duration of the experiment (6 h). To six animals,

herein after referred to as compound **7** group, isoquinoline derivative **7** was intravenously applied in a 20 mg/kg dose after 16 h upon ACTH treatment (Figure 2a). As can be seen from the individual curves there are differences in the t_{max} values, course of the curves and maximal reduction values, however, there is no doubt that compound **7** is highly active in reducing aldosterone plasma concentrations. This effect could already be observed after 15 min. Within a timeframe of 0.5–3 h, the aldosterone concentrations were maximally reduced to 36–63 % of the prior ACTH level for the individual animals of the compound **7** group. The aldosterone lowering effect was highly significant (P<0.003) 1 h after the compound **7** administration, and significant (P<0.05) at all other timepoints between 0.25 and 2 h relating to ACTH stimulated plasma aldosterone levels. Furthermore, no obvious sign of toxicity was noted in any animal during the course of treatment. The rats were curious, showed normal behaviour and general conditions (e.g. breathing rate, mobility, normothermia).

Figure 2[a]

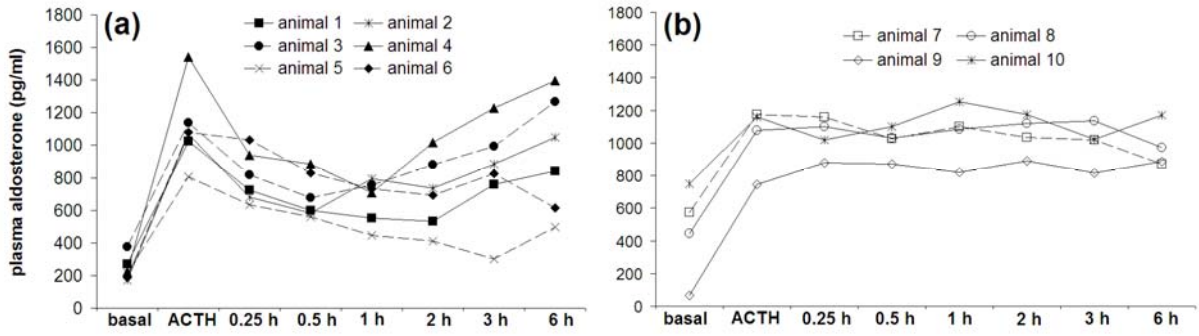

[a] Lowering of aldosterone plasma levels *in vivo*. (a) Compound **7** group (animals 1–6), (b) vehicle group (animals 7–10)

	aldosterone plasma level (pg/ml)			
animal no.	basal[a]	ACTH stimulated[b]	maximally reduced[c] [% reduction[d]]	$t_{max\ red}$ (h)[e]
1	270	1026	531 [48]	2
2	173	1068	585 [45]	0.5
3	375	1139	676 [41]	0.5
4	222	1543	708 [54]	1
5	217	805	302 [63]	3
6	188	1081	694 [36]	2

[a]Pre-dose blood sample taken 0.5 h before application of ACTH. [b]The animals were stimulated by subcutaneous application of ACTH (1 mg/kg) 16 h before test item application; blood sample taken before application of **7**. [c]Lowest aldosterone concentration measured for the individual animal. [d]Maximal reduction of aldosterone level compared to ACTH stimulated level. [e]Time of lowest aldosterone plasma concentration.

Discussion and Conclusion

The involvement of the major mineralocorticoid aldosterone in the development and progression of severe cardiovascular diseases is indisputable. The levels of plasma aldosterone in patients with untreated heart failure are significantly elevated and are strongly associated with mortality.[22] Moreover, high aldosterone levels cause excessive sodium retention with expansion of extracellular volume and loss of potassium. These instances lead to an electrolyte imbalance and increase the sensitivity of cardiac tissue to arrhythmias as well as the risk of sudden death.[23] In this context, it was reported, that aldosterone antagonists reduce the risk of sudden cardiac death in patients with heart failure.[24] Another important complication of chronically elevated plasma aldosterone levels is the development of myocardial fibrosis and as a consequence of this an increasing stiffness of the heart which further impairs the heart in a *circulus vitiosus*. It could be shown, that the activation of the mineralocorticoid receptor in the fibroblasts of the human heart promotes proliferation of these cells and increases production of collagen.[25]

Since the nineties we propose aldosterone synthase (CYP11B2) as a new promising target for the treatment of these cardiovascular diseases and certain forms of hyperaldosteronism. Recently, we improved our lead structures to highly active and selective CYP11B2 inhibitors with ameliorated pharmacological characteristics.[18-20] For the further development of a drug candidate it is necessary to demonstrate its *in vivo* activity. After the evaluation of the *in vitro* profile of the compounds their *in vivo* efficacy had to be shown. Thus, with regard to problems due to species differences we established a further *in vitro* test to examine the activity of various compounds on the rat enzyme. For this purpose, we cloned the rat CYP11B2 encoding cDNA from rat adrenals in an appropriate expression vector and transfected the generated plasmid into V79MZ cells. After selection of stably transfected clones and isolation of monoclonal cell lines, the clone with the highest rat aldosterone synthase activity was chosen. Using the rat CYP11B2 expressing V79MZ cell line a new screening assay was established and our highly selective compounds were tested regarding the reduction of aldosterone formation.

Thereby, it turned out, that only compound **7** showed sufficient activity. All other tested compounds decreased the aldosterone synthesis only to a minor extend. The fact that our highly active compounds (IC_{50} values between 0.1 and 74 nM), show no or just slight inhibition on the rat enzyme is not really surprising as the identity between human and rat enzyme is only 70 %. To verify the results obtained from our new screening assay, an additional *in vitro* assay using whole rat adrenals was performed with compound **7**. Herein, we also found a strong inhibition of aldosterone formation by 76 and 89 % at 50 and 250 μM, respectively. After we had identified **7** to be a suitable candidate for investigation of aldosterone-lowering effects in rats, the *in vivo* assay was performed. A significant lowering of the plasma aldosterone levels in the range of 36-63 % was observed within 0.5–3 h. This result not only supplies POC that inhibition of CYP11B2 leads to a reduction of plasma aldosterone concentration, but also identifies **7** as a scientific tool for general pharmacological studies at the RAAS.

Currently, further experiments in disease-oriented models are underway to determine the potential of our aldosterone synthase inhibitors to prevent or reverse myocardial fibrosis and reduce heart failure induced mortality. Our strategy of aldosterone synthase inhibition is a promising approach for the treatment of certain forms of hyperaldosteronism and might improve the pharmacotherapy of heart failure and myocardial fibrosis. Aldosterone escape as described for ACE inhibitors should not be expected and severe side effects as observed for steroidal MR antagonists are not to be anticipated because of the non-steroidal structures of our compounds. The use of aldosterone synthase inhibitors should not lead to hyperkalemia, which is a common drawback of MR antagonists, as there is still stimulation of the mineralocorticoid receptor by the mineralocorticoids deoxycorticosterone and corticosterone as well as by cortisol.

Acknowledgement

We thank Ms. Gertrud Schmitt and Ms. Jeannine Jung for their help in performing the *in vitro* screening assay. Simon Lucas is grateful to Saarland University for a scholarship (Landesgraduierten-Förderung).

References

(1) T. Kawamoto, Y. Mitsuuchi, K. Toda, Y. Yokoyama, K. Miyahara, S. Miura, T. Ohnishi, Y. Ichikawa, K. Nakao, H. Imura, S. Ulick, Y Shizuta, Role of steroid 11β-hydroxylase and steroid 18-hydroxylase in the biosynthesis of glucocorticoids and mineralocorticoids in humans. *Proc. Natl. Acad. Sci. U. S. A.* **1992,** *89,* 1458-1462.

(2) D. F. Davila, T. J. Nunez, R. Odreman, C. A. de Davila, Mechanisms of neurohormonal activation in chronic congestive heart failure: Pathophysiology and therapeutic implications. *Int. J. Cardiol*. **2005**, *101,* 343-346.

(3) C. G. Brilla, Renin-angiotensin-aldosterone system and myocardial fibrosis. *Cardiovasc. Res.* **2000,** *47,* 1-3.

(4) P. Lijnen, V. Petrov, Induction of cardiac fibrosis by aldosterone. *J. Mol. Cell. Cardiol.* **2000**, *32,* 865-879.

(5) A. Sato, T. Saruta, Aldosterone escape during angiotensin-converting enzyme inhibitor therapy in essential hypertensive patients with left ventricular hypertrophy. *J. Int. Med. Res.* **2001**, *29,* 13-21.

(6) B. Pitt, F. Zannad, W. J. Remme, R. Cody, A. Castaigne, A. Perez, J. Palensky, J. Wittes, The effect of spironolactone on morbidity and mortality in patients with severe heart failure. *N. Engl. J. Med.* **1999**, *341,* 709-717.

(7) B. Pitt, W. Remme, F. Zannad, J. Neaton, F. Martinez, B. Roniker, R. Bittman, S. Hurley, J. Kleiman, M. Gatlin, Eplerenone, a selective aldosterone blocker, in patients with left ventricular dysfunction after myocardial infarction. *N. Engl. J. Med.* **2003,** *348,* 1309-1321.

(8) D. N. Juurlink, M. M. Mamdani, D. S. Lee, A. Kopp, P. C. Austin, A. Laupacis, D. A. Redelmeier, Rates of hyperkalemia after publication of the Randomized Aldactone Evaluation Study. *N. Engl. J. Med.* **2004,** *351,* 543-551.

(9) J. Ménard, M.-F. Gonzalez, T.-T. Guyene, A. Bissery, Investigation of aldosterone-synthase inhibition in rats. *J. Hypertens.* **2006,** *24,* 1147-1155.

(10) R. W. Hartmann, Selective inhibition of steroidogenic P450 enzymes: Current status and future perspectives. *Eur. J. Pharm. Sci.* **1994***, 2,* 15-16.

(11) S. Ulmschneider, U. Müller-Vieira, C. D. Klein, I. Antes, T. Lengauer, R. W. Hartmann, Synthesis and evaluation of (pyridylmethylene)tetrahydronaphthalenes/-indanes and structurally modified derivatives: Potent and selective inhibitors of aldosterone Synthase. *J. Med. Chem.* **2005**, *48,* 1563-1575.

(12) S. Ulmschneider, U. Müller-Vieira, M. Mitrenga, R. W. Hartmann, S. Oberwinkler-Marchais, C. D. Klein, M. Bureik, R. Bernhardt, I. Antes, T. Lengauer, Synthesis and evaluation of imidazolylmethylenetetrahydronaphthalenes and imidazolylmethyleneindanes: Potent inhibitors of aldosterone Synthase. *J. Med. Chem*. **2005**, *48,* 1796-1805.

(13) M. Voets, I. Antes, C. Scherer, U. Müller-Vieira, K. Biemel, C. Barrasin, S. Oberwinkler-Marchais, R. W. Hartmann, Heteroaryl substituted naphthalenes and structurally modified derivatives: Selective inhibitors of CYP11B2 for the treatment of congestive heart failure and myocardial fibrosis. *J. Med. Chem.* **2005,** *48,* 6632-6642.

(14) M. Voets, I. Antes, C. Scherer, U. Müller-Vieira, K. Biemel, S. Oberwinkler-Marchais, R. W. Hartmann, Synthesis and evaluation of heteroaryl-substituted dihydronaphthalenes and indenes: Potent and selective inhibitors of aldosterone synthase (CYP11B2) for the treatment of congestive heart failure and myocardial fibrosis. *J. Med. Chem.* **2006,** *49,* 2222-2231.

(15) P. B. Ehmer, M. Bureik, R. Bernhardt, U. Müller, R. W. Hartmann, Development of a test system for inhibitors of human aldosterone synthase (CYP11B2): Screening in fission yeast and evaluation of selectivity in V79 cells. *J. Steroid Biochem. Mol. Biol.* **2002**, *81,* 173-179.

(16) R. W. Hartmann, U. Müller, P. B. Ehmer, Discovery of selective CYP11B2 (aldosterone synthase) inhibitors for the therapy of congestive heart failure and myocardial fibrosis. *Eur. J. Med. Chem.* **2003,** *38*3, 63-366.

(17) U. Müller-Vieira, M. Angotti, R. W. Hartmann, The adrenocortical tumor cell line NCI-H295R as an *in vitro* screening system for the evaluation of CYP11B2 (aldosterone synthase) and CYP11B1 (steroid-11β-hydroxylase) inhibitors. *J. Steroid. Biochem. Mol. Biol.* **2005**, *96,* 259-270.

(18) R. Heim, S. Lucas, C. M. Grombein, C. Ries, K. E. Schewe, M. Negri, U. Müller-Vieira, B. Birk, R. W. Hartmann, Overcoming undesirable CYP1A2 inhibition of pyridylnaphthalene-type aldosterone synthase inhibitors: Influence of heteroaryl derivatization on potency and selectivity. *J. Med. Chem.* **2008**, *51,* 5064-5074.

(19) S. Lucas, R. Heim, M. Negri, I. Antes, C. Ries, K. E. Schewe, A. Bisi, S. Gobbi, R. W. Hartmann, Novel aldosterone synthase inhibitors with extended carbocyclic skeleton by a combined ligand-based and structure-based drug design approach. *J. Med. Chem.* **2008**, *51,* 6138-6149.

(20) S. Lucas, R. Heim, C. Ries, K. E. Schewe, B. Birk, R. W. Hartmann, *In vivo* active aldosterone synthase inhibitors with improved selectivity: lead optimization providing a series of pyridine substituted 3,4-dihydro-1*H*-quinolin-2-one derivatives. *J. Med. Chem.* **2008**, *51,* 8077-8087.

(21) M. Imai, H. Shimada, Y. Okada, Y. Matsushima-Hibiya, T. Ogishima, Y. Ishimura, Molecular cloning of a cDNA encoding aldosterone synthase cytochrome P-450 in rat adrenal cortex. *FEBS Lett.* **1990**, *263,* 299-302.

(22) K. Swedberg, P. Eneroth, J. Kjekshus, L. Wilhelmsen, Hormones regulating cardiovascular function in patients with severe congestive heart failure and their relation to mortality. CONSENSUS Trial Study Group. *Circulation* **1990**, *82,* 1730-1736.

(23) H. Tsuji, F. J. Venditti Jr., J. C. Evans, M. G. Larson, D. Levy, The association of levels of serum potassium and magnesium with ventricular premature complexes (the Framingham Heart Study). *Am. J. Cardiol*. **1994**, *74*, 232-235.

(24) K. Anand, A. N. Mooss, S. M. Mohiuddin, Aldosterone inhibition reduces the risk of sudden cardiac death in patients with heart failure. *J. Renin Angiotensin Aldosterone Syst.* **2006**, *7,* 15-19.

(25) V. Robert, J.-S. Silvestre, D. Charlemagne, A. Sabri, P. Trouvé, M. Wassef, B. Swynghedauw, C. Delcayre, Biological determinants of aldosterone-induced cardiac fibrosis in rats. *Hypertension* **1995.** *26,* 971-978.

3.6 N-(Pyridin-3-yl)benzamides as Selective Inhibitors of Human Aldosterone Synthase (CYP11B2)

Christina Zimmer, Marieke Hafner, Michael Zender, Dominic Ammann, Rolf W. Hartmann and Carsten A. Vock

This manuscript will be submitted for publication as an article to the

Bioorganic & Medicinal Chemistry Letters **2010**

Paper VI

Abstract: A series of 23 N-(Pyridin-3-yl)benzamides was synthesized and evaluated for their potential to inhibit human steroid-11β-hydroxylase (CYP11B1) and human aldosterone synthase (CYP11B2). The most potent and selective CYP11B2 inhibitors (IC_{50} values 53 – 166 nM) were further evaluated for their potential to inhibit human CYP17 and CYP19, and no inhibition was observed. Clear evidence was shown for N-(Pyridin-3-yl)benzamides to be a highly selective class of CYP11B2 inhibitors *in vitro*.

Aldosterone synthase (CYP11B2) is the key enzyme in the human biosynthesis of mineralocorticoids, catalyzing the three-step interconversion of 11-deoxycorticosterone to aldosterone via corticosterone and 18-hydroxycorticosterone.[1] Due to its pivotal role, CYP11B2 is claimed as useful target for the treatment of hyperaldosteronism, myocardial fibrosis and congestive heart failure.[2] After having successfully developed selective inhibitors of crucial steroidogenic enzymes involved in the endocrine (CYP19[3-5] and CYP17[6-8]) as well as intracrine (5α-reductase[9-11] and 17β-HSD1[12-14]) stimulation of hormone dependent diseases, we more recently have been concerned with the development of selective CYP11B2 inhibitors.[2,15-21] Thus, we have discovered compound **1** to be a highly potent and selective inhibitor of CYP11B2.[15] We were able to verify the lowering of plasma aldosterone levels by **1** in rats, which can be considered as validation of the target and *proof-of-principle*.[22]

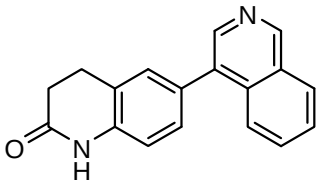

1

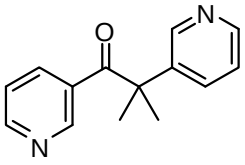

2
Metyrapone

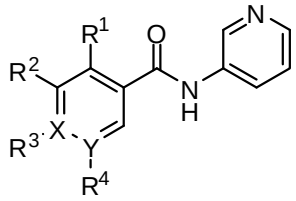

3

In an effort to develop and evaluate new classes of compounds as CYP inhibitors, we based our investigations on the structure of the well-known CYP inhibitor Metyrapone **2**, which has been used for the treatment of hypercortisolism and *Cushing's* syndrome for several decades.[23-27] We decided to substitute the bridging 2,2-dimethylethanone moiety in **2** by a much easier accessible amide linker to generate *N*-(Pyridin-3-yl)benzamides **3**. In addition – and with respect to activity studies carried out with the bovine CYP11B enzyme by *Hays et al.*[28] resp. *Tobes et al.*[29] – we also investigated the exchange of the keto-substituted pyridine system of Metyrapone **2** against substituted phenyl moieties in order to improve the potency of the compounds. We were very pleased by the potency and astonishingly high CYP11B2 selectivity of these small and structurally quite simple compounds *in vitro*, and we would like to communicate our detailed observations in this article.

Compounds of type **3** were prepared by a routine amide coupling procedure using commercially available acid chlorides **4** and 3-aminopyridine **5** in pyridine at room temperature or with application of gentle heating (Scheme 1). The products were obtained as solids in moderate to good yields.

Scheme 1. Synthesis of *N*-(Pyridin-3-yl)benzamides **3**.

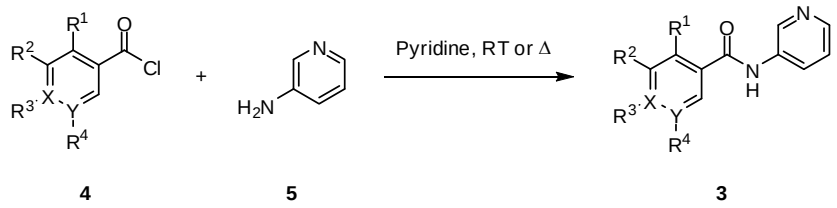

4 **5** **3**

Routinely, all synthesized compounds **3** were evaluated for their potential to inhibit human CYP11B2 and CYP11B1 at an inhibitor concentration of c = 500 nM. Tests were carried out using our established comparative *in-house* test system (V79 chinese hamster cells stably transfected with either human CYP11B2 or CYP11B1; substrate: 11-desoxy-corticosterone for both enzymes; substrate concentration: c = 100 nM).[30] The results are shown in Tab. 1. As can be seen from the data, none of compounds **3** showed significant inhibition of human CYP11B1 at c = 500 nM, while a number of derivatives strongly inhibit human CYP11B2. Concerning the two direct analogues **3a** and **3b** of metyrapone **2**, isonicotinamide **3b** shows weak inhibition of CYP11B2, whereas nicotinamide **3a** is not active. Addition of a bromo substituent in *meta*-position of the nicotinamide moiety leads to the weakly active CYP11B2 inhibitor **3c**, but no improvement is achieved in comparison with **3b**. The unsubstituted benzamide **3d** is of similarly active as **3b**. Introduction of halogeno substituents in *para*-position within the benzamide moiety (**3e**, **3f**, **3g**) leads to strong inhibitors of CYP11B2. Interestingly, similar activities could be observed with strongly electron-withdrawing substituents (-*M*-effect) like cyano derivative **3m** and nitro compound **3n**, whereas trifluoromethoxy-substituted **3i** and trifluoromethyl-substituted **3j** (-*I*-effect) showed no activity at all. Introduction of halogeno substituents in *meta*- (**3o**, **3p**) and *ortho*-position (**3q**) of the benzamide leads to selective CYP11B2 inhibitors with reduced activity in comparison with the *para*-substituted derivatives. The difluoro derivative **3r** shows similar activity to the monohalogenated compounds **3e**, **3f** and **3g**, whereas a slight drop of activity is observed for the trifluoro derivative **3u**. Compound **3t** bearing chloro substituents in *ortho*- and *meta*-position of the benzamide moiety is less active in compared with **3u**.

For the seven most active inhibitors of CYP11B2 (**3e**, **3f**, **3g**, **3m**, **3n**, **3r**, **3u**) IC_{50} values were determined in order to quantify the selectivity toward CYP11B1 (Tab. 2). As can be seen, all compounds are highly selective CYP11B2 inhibitors, the most selective one being **3e** with a selectivity factor of 174. Concerning this parameter, the compounds are comparable with reference compound **1** being developed in our group before.[15,22] However, with regard to activity, the *N*-(Pyridin-3-yl)benzamides **3** turned out to be far less potent inhibitors of CYP11B2. For the most active compound **3r**, an IC_{50} value of 53.5 nM has been determined, which means an approximately 250-fold lower potency in comparison with **1**. However, some of the compounds are exhibiting similar (**3e**, **3m**) or slightly higher (**3f**, **3r**) CYP11B2 inhibitory activity compared to Metyrapone **2**.

For all synthesized compounds **3** and the references **1** and **2**, log P values were calculated (Tab. 1).[31] There is no obvious correlation between the potency as CYP11B2 inhibitors and the lipophilicity of the compounds, which might have been expected due to the location of both CYP11B1 and CYP11B2 enzymes on the inner side of the mitochondrial membrane of adrenal cortex cells. For example, compounds **3e** and **3m** are equally potent inhibitors of CYP11B2, but differ by approximately 0.5 units in log P. However, for almost all compounds log P values of 1.5 – 3.0 have been calculated, showing them to be equally or more lipophilic than Metyrapone **2**, but less lipophilic than reference compound **1**.

In order to obtain a more detailed selectivity profile for compounds **3** toward steroidogenic CYP enzymes, we additionally determined the ability of the seven most active inhibitors of CYP11B2 (**3e**, **3f**, **3g**, **3m**, **3n**, **3r**, **3u**) to inhibit CYP17[32,33] and CYP19[34] (Tab. 3). None of the compounds showed any significant inhibitory effect on these enzymes. Regarding the inhibition of CYP17 and CYP19 as potential unwanted side effect for the application of CYP11B2 inhibitors as drugs, the structural motifs of all seven compounds **3e**, **3f**, **3g**, **3m**, **3n**, **3r** and **3u** can therefore deliver useful informations to overcome residual CYP17 and CYP19 activity, as observed for the highly potent inhibitor FAD286A.[35,36] Interestingly, the latter compound has shown activity in several animal models relevant for heart failure and organ damage caused by elevated plasma aldosterone level, thus demonstrating the importance of the drug target CYP11B2.[37-40]

In summary, we synthesized a panel of 23 *N*-(Pyridin-3-yl)benzamides **3** and evaluated them for their activity as inhibitors of CYP11B1, CYP11B2, CYP17 and CYP19. All compounds did not show any significant inhibition of CYP11B1, and several derivatives (**3e**, **3f**, **3g**, **3m**, **3n**, **3r**, **3u**) turned out to be potent inhibitors of CYP11B2. Those compounds exhibited no inhibitory activity on CYP17 and CYP19. The highest selectivity was observed for **3e** containing a fluoro substituent in *para*-postion of the benzamide moiety, whereas the most active compound was the difluoro compound **3r**. Although the CYP11B2 potency of the compounds is by far lower in comparison to reference **1**, compounds **3** offer a highly interesting selectivity profile. Further investigations concerning metabolic stability and *in vivo* activity are pending.

Tab. 1. Inhibition of human CYP11B2 and CYP11B1 enzymes by compounds **3**.

No.[a]	R^1	R^2	R^3	R^4	X	Y	CYP11B2 Inhibition @ 500 nM[b]	CYP11B1 Inhibition@ 500 nM[b]	log P (calc.)[c]
1	-	-	-	-	-	-	94 ± 2 %	91 ± 4 %	3.03
2	-	-	-	-	-	-	79 ± 4 %	94 ± 1 %	1.78
3a	H	H	H	-	C	N	8 ± 9 %	3 ± 2 %	0.81
3b	H	H	-	H	N	C	39 ± 7 %	4 ± 5 %	0.81
3c	H	Br	H	-	C	N	29 ± 3 %	0.4 ± 0.5 %	1.70
3d	H	H	H	H	C	C	30 ± 2 %	2 ± 2 %	1.98
3e	H	H	F	H	C	C	86 ± 3 %	7 ± 5 %	2.19
3f	H	H	Cl	H	C	C	88 ± 4 %	5 ± 7 %	2.76
3g	H	H	Br	H	C	C	64 ± 8 %	0 %	2.91
3h	H	H	OMe	H	C	C	19 ± 3 %	0 %	2.10
3i	H	H	OCF_3	H	C	C	3 ± 4 %	3 ± 3 %	3.21
3j	H	H	CF_3	H	C	C	1 ± 1 %	1 ± 1 %	2.99
3k	H	H	Me	H	C	C	25 ± 4 %	0 %	1.80
3l	H	H	Ph	H	C	C	6 ± 2 %	0 %	3.87
3m	H	H	CN	H	C	C	81 ± 5 %	9 ± 4 %	1.58
3n	H	H	NO_2	H	C	C	64 ± 3 %	0 %	1.88
3o	H	F	H	H	C	C	47 ± 11 %	1 ± 2 %	2.19
3p	H	Cl	H	H	C	C	26 ± 7 %	0 %	2.76
3q	F	H	H	H	C	C	34 ± 6 %	1 ± 2 %	1.78
3r	H	F	F	H	C	C	83 ± 2 %	6 ± 6 %	2.29
3s	H	OMe	OMe	H	C	C	2 ± 1 %	0.1 ± 0.1 %	1.75
3t	Cl	Cl	H	H	C	C	51 ± 3 %	4 ± 5 %	2.55
3u	F	H	F	F	C	C	70 ± 2 %	2 ± 2 %	2.03

[a] The purity of all tested compounds was ≥ 95 %; [b] Test system: V79 chinese hamster cells stably transfected with either human CYP11B2 or CYP11B1 enzyme; substrate: 11-deoxycorticosterone for both enzymes; substrate concentration: c = 100 nM; [c] log P values were calculated using the add-on *ChemProp* implemented in *ChemDraw Ultra*, *Version 10.0*, CambridgeSoft.

Tab. 2. Inhibition of human CYP11B2 and CYP11B1 enzymes (IC_{50} values) for selected compounds of type **3**.

No.[a]	Structure	CYP11B2 IC_{50}[b]	CYP11B1 IC_{50}[b]	Selectivity Factor IC_{50} (CYP11B1) / IC_{50} (CYP11B2) /
1	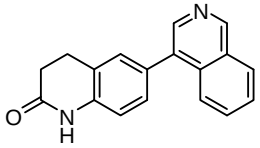	0.20 nM[15]	33 nM[15]	**187**[15]
2	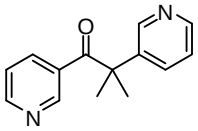	72 ± 17 nM	14.6 ± 2.1 nM	**0.23**
3e	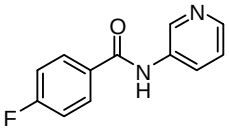	82 ± 11 nM	14.3 ± 3.3 µM	**174**
3f	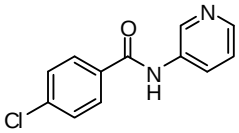	65 ± 12 nM	10.2 ± 2.2 µM	**157**
3g	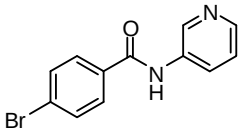	104 ± 20 nM	16.7 ± 2.8 µM	**161**
3m	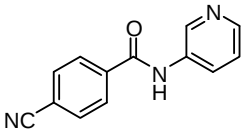	78 ± 20 nM	7.5 ± 1.1 µM	**96**
3n	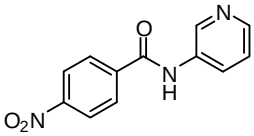	145 ± 24 nM	24.8 ± 3.4 µM	**171**
3r	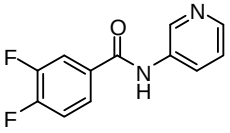	53.5 ± 2.0 nM	5.92 ± 0.89 µM	**111**
3u	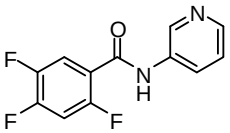	166 ± 23 nM	16.1 ± 2.8 µM	**97**

[a] The purity of all tested compounds was ≥ 95 %; [b] Test system: V79 chinese hamster cells stably transfected with either human CYP11B2 or CYP11B1 enzyme; substrate: 11-deoxycorticosterone for both enzymes; substrate concentration: *c* = 100 nM

Tab. 3. Inhibition of human CYP17 and CYP19 enzymes for selected compounds of type **3**.

No.	Structure	CYP17 Inhibition @ 2000 nM[a]	CYP19 Inhibition @ 500 nM[b]
2	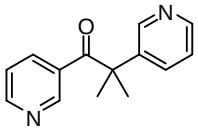	0 %	0 %
3e	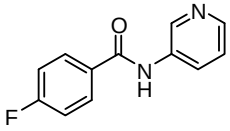	0.3 ± 0.2 %	1.1 ± 1.3 %
3f	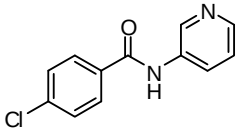	1.3 ± 2.3 %	0 %
3g	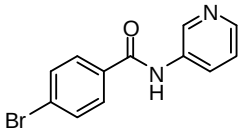	4.3 ± 2.7 %	0.1 ± 0.1 %
3m	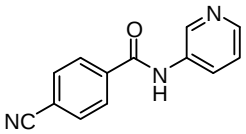	0.2 ± 0.3 %	0.2 ± 0.3 %
3n	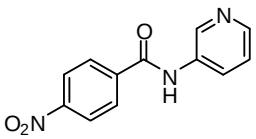	1.0 ± 0.9 %	0 %
3r	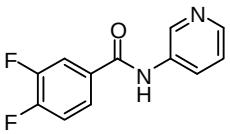	1.0 ± 1.7 %	0.5 ± 0.8 %
3u	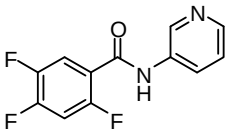	0.6 ± 1.1 %	0 %

[a] CYP17 test system: 50000 g sediment of a homogenate of *E. coli* recombinantly expressing human CYP17, Substrate: Progesterone ($c = 25\ \mu M$), Inhibitor concentration: $c = 2.0\ \mu M$, Ketoconazole, IC_{50} = 2780 nM; [b] CYP19 test system: Human placental CYP19, Substrate: Androstenedione ($c = 500$ nM), Inhibitor concentration: $c = 500$ nM, Fadrozole, $IC_{50} = 30$ nM

Acknowledgement

We are indebted to Jeannine Jung, Gertrud Schmitt and Jannine Ludwig for performing the bioassays. Furthermore, we would like to thank Martina Jankowski and Dr. Stefan Boettcher for the HPLC-MS measurements. We would like to thank Prof. Dr. J. J. Rob Hermans, University of Maastricht, The Netherlands, for generous supply of the V79 CYP11B1 cells and Prof. Dr. Rita Bernhardt, Saarland University, for the V79 CYP11B2 cells.

Supporting Information

Experimental details as well as spectral and HPLC-MS data for all compounds **3** are provided within the Supporting Information.

References

(1) Kawamoto, T.; Mitsuuchi, Y.; Toda, K.; Yokoyama, Y.; Miyahara, K.; Miura, S.; Ohnishi, T.; Ichikawa, Y.; Nakao, K.; Imura, H.; Ulick, S.; Shizuta, Y. *Proc. Natl. Acad. Sci. U.S.A.* **1992**, *89*, 1458.

(2) Hartmann, R. W.; Müller, U.; Ehmer, P. B. *Eur. J. Med. Chem.* **2003**, *38*, 363.

(3) Le Borgne, M.; Marchand, P.; Duflos, M.; Delevoye-Seiller, B.; Piessard-Robert, S.; Le Baut, G.; Hartmann, R. W.; Palzer, M. *Arch. Pharm.* **1997**, *330,* 141.

(4) Leonetti, F.; Favia, A.; Rao, A.; Aliano, R.; Paluszcak, A.; Hartmann, R. W.; Carotti, A. *J. Med. Chem.* **2004**, *47*, 6792.

(5) Gobbi, S.; Cavalli, A.; Rampa, A.; Belluti, F.; Piazzi, L.; Paluszcak, A.; Hartmann, R. W.; Recanatini, M.; Bisi, A. *J. Med. Chem.* **2006**, *49*, 4777.

(6) Pinto-Bazurco Mendieta, M.A.; Negri, M.; Jagusch, C.; Müller-Vieira, U.; Lauterbach, T.; Hartmann, R. W. *J. Med. Chem*. **2008**, *51*, 5009.

(7) Hu, Q.; Negri, M.; Jahn-Hoffmann, K.; Zhuang, Y.; Olgen, S.; Bartels, M.; Müller-Vieira, U.; Lauterbach, T.; Hartmann, R. W. *Bioorg. Med. Chem.* **2008**, *16*, 7715.

(8) Hille, U. E.; Hu, Q.; Vock, C.; Negri, M.; Bartels, M.; Müller-Vieira, U.; Lauterbach, T.; Hartmann, R. W. *Eur. J. Med. Chem.* **2009**, *44*, 2765.

(9) Baston, E.; Hartmann, R. W. *Bioorg. Med. Chem. Lett.* **1999**, *9*, 1601.

(10) Baston, E.; Palusczak, A.; Hartmann, R. W. *Eur. J. Med. Chem.* **2000**, *35*, 931.

(11) Picard, F.; Schulz, T.; Hartmann, R. W. *Bioorg. Med. Chem.* **2002**, *10*, 437.

(12) Frotscher, M.; Ziegler, E.; Marchais-Oberwinkler, S.; Kruchten, P.; Neugebauer, A.; Fetzer, L.; Scherer, C.; Müller-Vieira, U.; Messinger, J.; Thole, H.; Hartmann, R. W. *J. Med. Chem.* **2008**, *51*, 2158.

(13) Bey, E.; Marchais-Oberwinkler, S.; Kruchten, P.; Frotscher, M.; Werth, R.; Oster, A.; Algül, O.; Neugebauer, A.; Hartmann, R. W. *Bioorg. Med. Chem.* **2008**, *16*, 6423.

(14) Marchais-Oberwinkler, S.; Kruchten, P.; Frotscher, M.; Ziegler, E.; Neugebauer, A.; Bhoga, U.; Bey, E.; Müller-Vieira, U.; Messinger, J.; Thole, H.; Hartmann, R. W. *J. Med. Chem.* **2008**, *51*, 4685.

(15) Lucas, S.; Heim, R.; Ries, C.; Schewe, K. E.; Birk, B.; Hartmann, R. W. *J. Med. Chem.* **2008**, *51*, 8077.

(16) Lucas, S.; Heim, R.; Negri, M.; Antes, I.; Ries, C.; Schewe, K. E.; Bisi, A.; Gobbi, S.; Hartmann, R. W. *J. Med. Chem.* **2008**, *51*, 6138.

(17) Heim, R.; Lucas, S.; Grombein, C. M.; Ries, C.; Schewe, K. E.; Negri, M.; Müller-Vieira, U.; Birk, B.; Hartmann, R. W. *J. Med. Chem.* **2008**, *51*, 5064.

(18) Voets, M.; Antes, I.; Scherer, C.; Müller-Vieira, U.; Biemel, K.; Marchais-Oberwinkler, S.; Hartmann, R. W. *J. Med. Chem.* **2006**, *49*, 2222.

(19) Voets, M.; Antes, I.; Scherer, C.; Müller-Vieira, U.; Biemel, K.; Barassin, C.; Marchais-Oberwinkler, S.; Hartmann, R. W. *J. Med. Chem*. **2005**, *48*, 6632.

(20) Ulmschneider, S.; Muller-Vieira, U.; Mitrenga, M.; Hartmann, R. W.; Oberwinkler-Marchais, S.; Klein, C. D.; Bureik, M.; Bernhardt, R.; Antes, I.; Lengauer, T. *J. Med. Chem.* **2005,** *48*, 1796.

(21) Ulmschneider, S.; Muller-Vieira, U.; Klein, C. D.; Antes, I.; Lengauer, T.; Hartmann, R. W. *J. Med. Chem.* **2005,** *48*, 1563.

(22) Ries, C. ; Lucas, S. ; Heim, R.; Birk, B.; Hartmann, R. W. *J. Steroid Biochem. Mol. Biol*. **2009**, *116*, 121.

(23) Diez, J. J.; Iglesias, P. *Mini-Rev. Med. Chem.* **2007**, *7*, 467.

(24) Nieman, L. K. *Pituitary* **2002**, *5*, 77.

(25) Miller, J. W.; Crapo, L. *Endocrine Rev.* **1993**, *14*, 443.

(26) Gower, D. B. *J. Steroid Biochem.* **1974**, *5*, 501.

(27) Daniels, H.; van Amstel, W. J.; Schopman, W.; van Dommelen, C. *Acta Endocrinol. (Copenh)* **1963**, *44*, 346.

(28) Hays, S. J.; Tobes, M. C.; Gildersleeve, D. L.; Wieland, D. M.; Beierwaltes, W. H. *J. Med. Chem.* **1984**, *27*, 15.

(29) Tobes, M. C.; Hays, S. J.; Gildersleeve, D. L.; Wieland, D. M.; Beierwaltes, W. H. *J. Steroid Biochem.* **1985**, *22*, 103.

(30) Ehmer, P. B.; Bureik, M.; Bernhardt, R.; Müller, U.; Hartmann, R. W. *J. Steroid Biochem. Mol. Biol.* **2002**, *81*, 173.

(31) log P values were calculated using the add-on *ChemProp* implemented in *ChemDraw Ultra*, *Version 10.0*, CambridgeSoft.

(32) Ehmer, P. B.; Jose, J.; Hartmann, R. W. *J. Steroid Biochem. Mol. Biol* **2000**, *75*, 57.

(33) Hutschenreuter, T. U.; Ehmer, P. B.; Hartmann, R. W. *J. Enzyme Inhib. Med. Chem*. **2004**, *19*, 17.

(34) Hartmann, R. W.; Batzl, C. *J. Med. Chem.* **1986**, *29*, 1362.

(35) Schieweck, K.; Bhatnagar, A. S.; Matter, A. *Cancer Res.* **1988**, *48*, 834.

(36) Lamberts, S. W.; Bruining, H. A.; Marzouk, H.; Zuiderwijk, J.; Uitterlinden, P.; Blijd, J. J.; Hackeng, W. H.; de Jong, F. H. *J. Clin. Endocrinol. Metab.* **1989**, *69*, 896.

(37) Fiebeler, A.; Nussberger, J.; Shagdarsuren, E.; Rong, S.; Hilfenhaus, G.; Al-Saadi, N.; Dechend, R.; Wellner, M.; Meiners, S.; Maser-Gluth, C.; Jeng, A. Y.; Webb, R. L.; Luft, F. C.; Muller, D. N. *Circulation* **2005,** *111*, 3087.

(38) Menard, J.; Gonzalez, M. F.; Guyene, T. T.; Bissery, A. *J. Hypertens.* **2006,** *24*, 1147.

(39) Minnaard-Huiban, M; Emmen, J. M. A.; Roumen, L.; Beugels, I. P. E.; Cohuet, G. M. S.; van Essen, H.; Ruijters, E.; Pieterse, K.; Hilbers, P. A. J.; Ottenheijm, H. C. J.; Plate, R.; de Gooyer, M. E.; Smits, J. F. M.; Hermans, J. J. R. *Endocrinology* **2008**, *149*, 28.

(40) Mulder, P.; Mellin, V.; Favre, J.; Vercauteren, M.; Remy-Jouet, I.; Monteil, C.; Richard, V.; Renet, S.; Henry, J. P.; Jeng, A. Y.; Webb, R. L.; Thuillez, C. *Eur. Heart J.* **2008,** *29*, 2171.

3.7 First Selective CYP11B1 Inhibitors for the Treatment of Cortisol-Dependent Diseases

Ulrike E. Hille, Christina Zimmer, Carsten A. Vock and Rolf W. Hartmann

This manuscript has been accepted for publication as an article in the

ACS Medicinal Chemistry Letters **2010**

Paper VII

Abstract: Outgoing from an etomidate-based design concept, we succeeded in the development of a series of highly active and selective inhibitors of CYP11B1, the key enzyme of cortisol biosynthesis, as potential drugs for the treatment of Cushing´s syndrome and related diseases. Thus, compound **33** (IC50 = 152 nM) is the first CYP11B1 inhibitor showing a rather good selectivity toward the most important steroidogenic CYP enzymes aldosterone synthase (CYP11B2), the androgen forming CYP17, and aromatase (estrogen synthase, CYP19).

It is well-known that steroid hormones are essential for a large number of vitally important physiological processes. However, they are also associated with life-threatening diseases. Application of hormone receptor antagonists or biosynthesis inhibitors are regarded as therapeutic methods of choice. The biosynthetic pathways contain several established and potential drug targets. In the last decades, aromatase (CYP19) inhibitors were developed and continuously improved.[1-4] Nowadays, second and third generation inhibitors are used as first line therapeutics for hormone-dependent breast cancer.[5] Some 15 years ago, the first selective androgen synthase (CYP17) inhibitors were described,[6-8] and recently, their benefits for the treatment of castration refractory prostate cancer were demonstrated.[9] Research was not only focused on the formation of steroid hormones in their endocrine glands, but also on their activation in the target cell. Inhibition of steroid 5α-reductase is clinically well established for androgen-dependent diseases.[10-13] Experimental results with hydroxysteroid dehydrogenase (HSD) inhibitors are very encouraging for estrogen- and glucocorticoid-dependent diseases.[14-18]

Until some years ago, selective inhibitors of mineralo- and glucocorticoids were not in the focus of research efforts. This was due to the fact that the sequence identity between aldosterone synthase (CYP11B2) and cortisol synthase (steroid-11β-hydroxylase, CYP11B1) is very high (93 %),[19] and it was considered impossible to obtain selective inhibitors of one enzyme versus the other. Recently, however, we have been able to demonstrate that it is possible to selectively inhibit CYP11B2.[20-24] Further structural optimizations resulted in in vivo active compounds with selectivity factors reaching 1000 with regard to CYP11B1.[25,26] They could be candidates for the treatment of hyperaldosteronism, congestive heart failure, and myocardial fibrosis. Although there is a high medical need for drugs interfering with excessive glucocorticoid formation resulting in Cushing´s syndrome, there are only few inhibitors of CYP11B1 described so far.[27] Because of their unselective action, their application is associated with severe side effects: The CYP19 inhibitor aminoglutethimide, metyrapone, the antimycotics ketoconazole and fluconazole, and the hypnotic etomidate are also inhibitors of other adrenal and gonadal Cytochrom P450 (CYP) enzymes, and trilostane is a 3βHSD inhibitor.[28] In the present work, we report about the design, synthesis, and biological evaluation of the first selective (regarding CYP11B2, CYP17, and CYP19) inhibitors of human CYP11B1.

As the lead for the design of the compounds, the highly active CYP11B1 inhibitor *R*-etomidate was used (Scheme 1), in spite of the fact that it shows a stronger inhibition of CYP11B2. Indeed, this compound was one of the starting points recently used for the development of novel CYP11B2 inhibitors.[29] Therein, the authors have shown that modifications of the ester group by conformationally flexible substituents resulted in CYP11B2 selective compounds, while eliminating the ester led to moderate CYP11B1 selectivity. Therefore, we decided to either remove the ethyl-ester or to replace it by a rigid benzene nucleus. The chiral core was abolished by eliminating the methyl group as it has been shown that the alkyl group at the methylene bridge is a prerequisite for the hypnotic activity of etomidate derivatives.[30] As polar substituents at the phenyl moiety were shown to result in poor

CYP11B1 inhibition,[29] methyl, chloro, and additional phenyl substituents were introduced (**2**–**24**). The most selective inhibitor obtained, **11**, was further optimized regarding selectivity versus CYP17 by exchange of one benzene ring by pyridine, furane, or thiophene (**33**–**36**).

Scheme 1. Inhibitor Design Concept

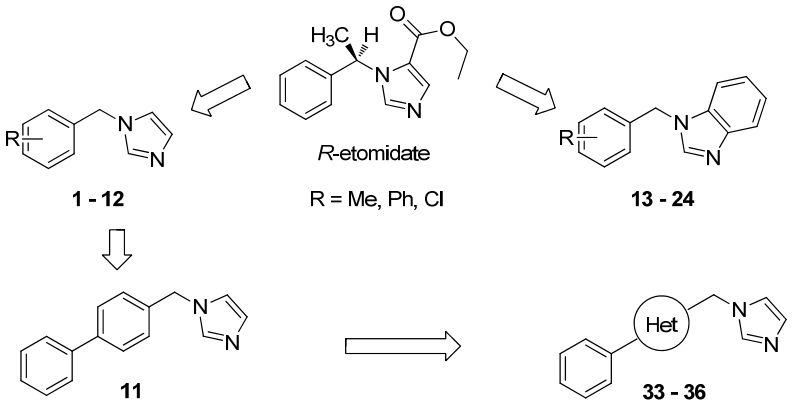

The syntheses of **2**–**36** are shown in Schemes 2 and 3. The starting point was commercially available *N*-benzylimidazole **1**. The preparation of the *N*-benzylimidazoles **2**–**12** and **33** and -benzimidazoles **13**–**24** was carried out via S_N reaction of the corresponding benzyl-halogenides. For the syntheses of **12**, **24,** and **33** palladium catalyzed Suzuki coupling and Wohl–Ziegler bromination were used. Preparation of the adamantanes **25** and **26** included tosylation of adamantan-1-yl-methanol followed by S_N reaction with imidazole or benzimidazole. S_N reaction of tritylchloride with imidazole or benzimidazole afforded **27** and **30**, carrying two additional phenyls at the methylene bridge (not shown). For the synthesis of **28, 29, 31,** and **32**, the corresponding carbonic acids were reduced to the alcohols with $LiAlH_4$ and the products further processed as described above. Compounds **34**–**36** were obtained by reduction of the aldehydes or carbonic acids to the primary alcohols with $NaBH_4$ or $LiAlH_4$ and subsequent CDI-assisted S_Nt reaction.

Scheme 2: Synthesis of Compounds **2**–**26** and **28, 29, 31,** and **32**[a]

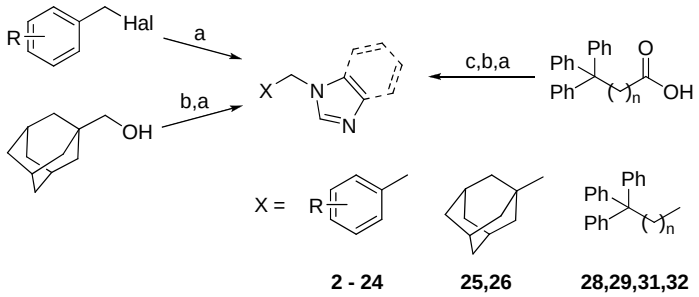

[a]Conditions: (a) Imidazole or benzimidazole, K_2CO_3, DMF, 120°C, 2 h. (b) Trifluoromethanesulfonic anhydride, pyridine, 0°C to room temperature, 3 h. (c) $LiAlH_4$, 0°C to room temperature, overnight.

Scheme 3: Synthesis of Compounds **33–36**[a]

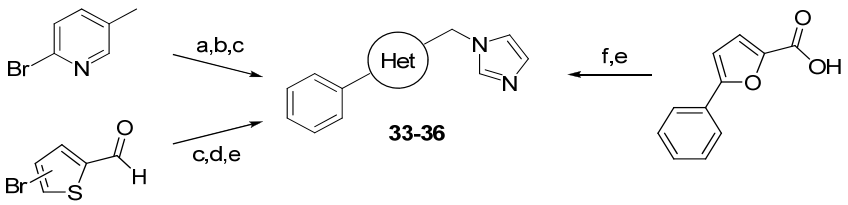

[a]Conditions: (a) NBS, DBPO, CCl_4, 90°C, 12h. (b) Imidazole, K_2CO_3, acetonitrile, 90°C, 2 h. (c) Phenylboronic acid, $Pd(PPh_3)_4$, Na_2CO_3, toluene/ MeOH/ H_2O, reflux, 5 h. (d) $NaBH_4$, MeOH, 2 h, roo temperature. (e) CDI, acetonitrile, reflux, 8 h. (f) $LiAlH_4$, 0°C to room temperature, overnight.

For the determination of CYP11B1 and CYP11B2 inhibition, V79MZ cells expressing either human CYP11B1 or CYP11B2 were used, and [^{3}H]-labelled 11-deoxycorticosterone as the substrate.[31,32] Metyrapone, etomidate, and ketoconazole served as references. The IC_{50} values determined for **1–36** are shown in Tables 1–3. All imidazoles **1–12**, **25**, **27–29,** and **33–36** strongly inhibited CYP11B1, mostly showing IC_{50} values below 100 nM, and compounds **8**, **25**, **27,** and **28** even reached values below 10 nM. Regarding the benzimidazoles, lower CYP11B1 inhibition than for the corresponding imidazoles was observed, some compounds showing IC_{50} values above 1000 nM. Most imidazoles exhibited inhibitory activity toward CYP11B2, while only some benzimidazoles (**14–18**, IC_{50} values: 107 nM–632 nM) showed marked inhibition of this enzyme.

Inhibition of CYP17 was investigated using a homogenate of *Escherichia coli* recombinantly expressing human CYP17 and progesterone as substrate.[8,33] At a concentration of 2000 nM, only **11** and **12** showed a marked inhibition of 40 and 52 %, while **25**, **35,** and **36** exhibited only weak effects with inhibition values around 20 %. All other substances showed no inhibition (data not shown). Inhibitory effects toward CYP19 were determined using human placental microsomes and [1β-^{3}H]androstenedione as substrate.[8] At a concentration of 500 nM, compounds **6, 9, 10, 27–29, 34,** and **36** showed inhibition values above 38 %, while compounds **3**, **4, 8, 12, 25, 26,** and **35** exhibited little activity (12–28 %) and all other substances showed no inhibition (data not shown).

Table 1. Inhibition of CYP11B1 and CYP11B2 by Compounds **1**–**24**

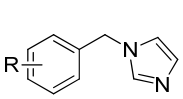

1 - 12

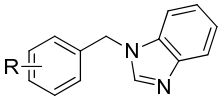

13 - 24

Structure		IC_{50} value (nM)[a,b]		sf[c]		IC_{50} (nM)[a,b]		sf[c]
R	No	CYP11B1	CYP11B2		No	CYP11B1	CYP11B2	
H	**1**[d]	135	456	3.4	**13**	246	865	3.5
4-Cl	**2**[d]	140	46	0.3	**14**	635	107	0.2
2-Me	**3**	61	62	1.0	**15**	779	262	0.3
3-Me	**4**	48	110	2.3	**16**	194	309	1.6
4-Me	**5**	258	320	1.2	**17**	500	520	1.0
3,5-di-Me	**6**	32	77	2.4	**18**	188	632	3.4
2,4,6-tri-Me	**7**	24	30	1.3	**19**	>1000	>1000	
2,3,4,5,6-penta-Me	**8**	5	23	4.6	**20**	>1000	>1000	
2-Ph	**9**	15	39	2.6	**21**	>1000	>1000	
3-Ph	**10**	46	265	5.8	**22**	369	2226	6.0
4-Ph	**11**	32	637	20	**23**	197	1903	10
3,5-di-Ph	**12**	128	332	2.6	**24**	>1000	>1000	
MTP[e]		15	72	4.8				
ETO[e]		0.5	0.1	0.2				
KTZ[e]		127	67	0.5				

[a] Mean value of at least three experiments. The deviations were within < ± 25 %. [b] Hamster fibroblasts expressing human CYP11B1 or CYP11B2; substrate 11-deoxycorticosterone, 100 nM. [c] sf: IC_{50} (CYP11B2)/IC_{50} (CYP11B1). [d] See ref. 29. [e]**MTP**, metyrapone; **ETO**, etomidate; and **KTZ,** ketoconazole.

Table 2. Inhibition of CYP11B2 and CYP11B1 by Compounds **25**–**32**

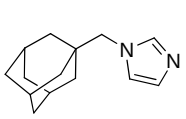

25

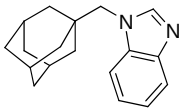

26

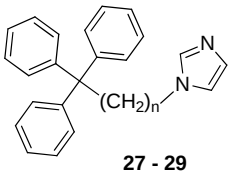

27 - 29

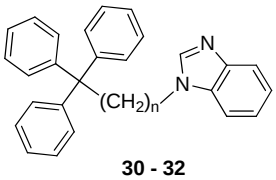

30 - 32

		IC_{50} value (nM)[a,b]		sf[c]		IC_{50} value (nM)[a,b]		sf[c]
n	No	CYP11B1	CYP11B2		No	CYP11B1	CYP11B2	
-	**25**	5	30	5.9	**26**	75	677	9.0
0	**27**	3	11	3.4	**30**	>1000	>1000	
1	**28**	4	8	2.0	**31**	>1000	>1000	
2	**29**	80	290	3.6	**32**	>1000	>1000	
MTP[d]		15	72	4.8				
ETO[d]		0.5	0.1	0.2				
KTZ[d]		127	67	0.5				

[a] Mean value of at least three experiments. The deviations were within < ± 25 %. [b] Hamster fibroblasts expressing human CYP11B1 or CYP11B2; substrate 11-deoxycorticosterone, 100 nM. [c] sf: IC_{50} (CYP11B2)/IC_{50} (CYP11B1). [d] **MTP,** metyrapone; **ETO**, etomidate; and **KTZ,** ketoconazole.

Table 3. Inhibition of CYP11B1, CYP11B2, CYP17, and CYP19 by Compounds **33**–**36**

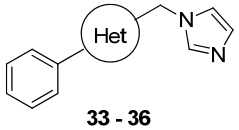

33 - 36

Compound	Structure Het	IC_{50} value (nM)[a,b] CYP11B1	CYP11B2	sf[c]	inhibition (%) CYP17[a,f]	CYP19[a,g]
11	-	32	637	20	40	5
33[d]	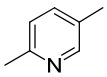	152	2768	18	4	0
34		46	372	8.1	0	51
35		43	353	8.2	21	26
36[d]		19	277	15	21	72
MTP[e]		15	72	4.8		
ETO[e]		0.5	0.1	0.2		
KTZ[e]		127	67	0.5		

[a] Mean value of at least three experiments. The deviations were within < ± 25 %. [b] Hamster fibroblasts expressing human CYP11B1 or CYP11B2; substrate 11-deoxycorticosterone, 100 nM. [c] sf: IC_{50} (CYP11B2)/IC_{50} (CYP11B1). [d] Described in ref. 34. [e] **MTP,** metyrapone; **ETO**, etomidate; and **KTZ**, ketoconazole. [f] *E. coli* expressing human CYP17; substrate progesterone, 25 µM; inhibitor concentration, 2.0 µM. [g] Human placental CYP19; substrate androstenedione, 500 nM; inhibitor concentration, 500 nM.

In the last decades, we and others have demonstrated that the concept of heme complexation is appropriate for the development of highly active inhibitors of CYP enzymes. Furthermore, high selectivity could be obtained by modifying the corresponding molecules using ligand- and structure-based medicinal chemistry strategies. In the present study, etomidate was used as a starting point to develop highly potent and selective CYP11B1 inhibitors that were superior to the currently used drugs ketoconazole, metyrapone, and etomidate. The latter show a broad range of adverse effects, which are mainly due to inhibition of other CYPs. Therefore, selectivity studies regarding the most important steroidogenic CYPs, CYP11B2, CYP17, and CYP19, were performed.

The starting point was the unsubstituted *N*-benzylimidazole **1**[29] and the corresponding benzimidazole **13**. Both showed a good inhibition of the target enzyme (IC_{50} = 135 and 246 nM) and reasonable sfs of 3.4 and 3.5 toward CYP11B2. Interestingly, the introduction of a chloro substituent into the phenyl ring led to an inversion of the selectivity and resulted in CYP11B2 inhibitors (**2** and **14**). As we hypothesized from the results of Roumen et al.,[29] the introduction of apolar substituents increased the inhibitory activity of the imidazoles as can be seen for the methyl-substituted compounds **3**–**8**. The penta methyl compound **8** was the most active compound of this series (IC_{50} = 5 nM). As a similar structure–activity relationship (SAR) was observed for inhibition of CYP11B2, only a slight enhancement of the sf was found for **8**. In contrast, increasing the number of methyl groups at the benzimidazoles was not tolerated (**19** and **20**).

Remarkable SARs were found for the phenyl-substituted compounds. In the case of the *N*-benzylimidazoles, **9**–**11** strongly inhibited cortisol formation (IC_{50} = 15–46 nM). A strong decrease of CYP11B2 inhibition was observed in the order *ortho, meta,* and *para* (**9**, IC_{50} = 39 nM; **10**, 265 nM; and **11**, 637 nM). Further phenyl substituents at the *N*-benzyl moiety of benzimidazole **13** increased activity only in the case of **23,** a fairly selective compound (sf = 10).

Phenyl substitution at the methylene spacer and its elongation resulted in a loss of activity for the benzimidazoles **30**–**32**, while the corresponding imidazoles **27**–**29** showed very high inhibition values, especially **27** (IC_{50} = 3 nM). However, these compounds are also highly potent CYP11B2 inhibitors. The replacement of the phenyl ring of **1** and **13** by an adamantane moiety led to the imidazole **25**, a highly potent (IC_{50} = 5 nM) and moderately selective (sf = 6) compound, and the corresponding benzimidazole **26,** showing a decreased activity (IC_{50} = 75 nM) but higher selectivity (sf = 9).

In the benzimidazole class, a series of highly selective compounds (**22**, **23**, and **26**) was found, demonstrating that this rigidification of the methyl ester group of etomidate was an appropriate optimization strategy. However, the compounds were less active than the imidazoles, especially in case of the bulky core compounds **24** and **30**–**32** or the *ortho*-substituted phenyl compounds **15** and **19**–**21** with hindered rotation around the methylene bridge, presumably as they are not able to properly fit into the binding pocket.

As several compounds were observed to show some residual inhibition of CYP19 and CYP17, the most selective compound regarding CYP11B2, **11** was chosen for further modification, that is, exchange of the central phenyl moiety by different heterocycles.

The compounds obtained were highly potent CYP11B1 inhibitors with selectivity toward CYP11B2. The furan **34** showed no CYP17 but CYP19 inhibition. Both thiophenes **35** and **36** inhibited CYP17 to some extent but showed, especially **36**, enhanced CYP19 inhibition. The best selectivity, comparable to **11**, was achieved by introduction of a pyridine, resulting in **33** (IC_{50} = 152 nM, sf = 18), which, most importantly, did not affect CYP19 and CYP17. Regarding its activity, this compound is comparable to ketoconazole (IC_{50} = 127 nM), which is clinically used for the treatment of Cushing´s syndrome, but highly exceeds ketoconazole (sf = 0.5) and the other clinically used compounds metyrapone (sf = 4.8) and etomidate (sf = 0.2).

Summarizing, we have discovered the first selective CYP11B1 inhibitors described so far. We regard them as novel leads for the development of drugs for the treatment of cortisol-dependent diseases. Thus, the design strategy starting from the CYP11B2 selective etomidate was successful. While Zolle et al. described chiral etomidate derivatives with a high affinity to rat adrenal membranes as well as strong inhibition of cortisol secretion without investigating selectivity issues,[27] the compounds described in this paper were examined for selectivity toward the most crucial steroidogenic CYP enzymes, and several were found to be selective.

Acknowledgement

The assistance of Jeannine Jung and Jannine Ludwig for performing the biological tests and the help of Dr. Marc Bartels for the synthesis of several compounds are highly appreciated. UEH is grateful to the European Postgraduate School 532 (DFG) for a scholarship. We thank Professors Hermans (Maastricht University) and Bernhardt (Saarland University) for providing us with V79MZh11B1 and V79MZh11B2 cells, respectively.

Supporting Information Available: Synthetic experimental details, analytical data of compounds, and biological assay protocols. This material is available free of charge via the Internet at **http://pubs.acs.org.**

References

(1) Le Borgne, M.; Marchand, P.; Duflos, M.; Delevoye-Seiller, B.; Piessard-Robert, S.; Le Baut, G.; Hartmann, R. W.; Palzer, M. Synthesis and in vitro evaluation of 3-(1-Azolylmethyl)-1*H*-indoles and 3-(1-azoly1-1-phenylmethyl)-1*H*-indoles as inhibitors of P450 arom. *Arch. Pharm*. **1997**, *330*, 141-145.

(2) Jacobs, C.; Frotscher, M.; Dannhardt, G.; Hartmann, R. W. 1-Imidazolyl (alkyl) substituted di- and tetrahydroquinolines and analogs. Syntheses and evaluation of dual inhibitors of thromboxane A2 synthase and aromatase. *J. Med. Chem.* **2000**, *43*, 1841-1851.

(3) Leonetti, F.; Favia, A.; Rao, A.; Aliano, R.; Paluszcak, A.; Hartmann, R. W.; Carotti, A. Design, synthesis and 3D QSAR of novel potent and selective aromatase inhibitors. *J. Med. Chem*. **2004**, *47*, 6792-6803.

(4) Gobbi, S.; Cavalli, A.; Rampa, A.; Belluti, F.; Piazzi, L.; Paluszcak, A.; Hartmann, R. W.; Recanatini, M.; Bisi, A. Lead optimization providing a series of flavone derivatives as potent nonsteroidal inhibitors of the cytochrome P450 aromatase enzyme. *J. Med. Chem.* **2006**, *49*, 4777-4780.

(5) Dutta, U.; Pant, K. Aromatase inhibitors: past, present and future in breast cancer therapy. *Med. Oncol*. **2008**, *25*, 113-124.

(6) Zhuang, Y.; Wachall, B. G.; Hartmann, R. W. Novel imidazolyl and triazolyl substituted biphenyl compounds: Synthesis and evaluation as nonsteroidal inhibitors of human 17α-hydroxylase-C17,20-lyase (P450 17). *Bioorg. Med. Chem.* **2000**, *8*, 1245-1252.

(7) Leroux, F.; Hutschenreuter, T.; Charrière, C.; Scopelliti, R.; Hartmann, R. W. *N*-(4-Biphenylmethyl)imidazoles as potential therapeutics for the treatment of prostate cancer: metabolic robustness due to fluorine substition? *Helv. Chim. Act.* **2003**, *86*, 2671-2686.

(8) Hutschenreuter, T. U.; Ehmer, P. B.; Hartmann, R. W. Synthesis of hydroxy derivatives of highly potent non-steroidal CYP 17 inhibitors as potential metabolites and evaluation of their activity by a non cellular assay using recombinant human enzyme. *J. Enz. Inhib. Med. Chem.* **2004**, *19*, 17-32.

(9) Attard, G.; Reid, A. H.; A'Hern, R.; Parker C.; Oommen, N. B.; Folkerd, E.; Messiou, C.; Molife, L. R.; Maier, G.; Thompson, E.; Olmos, D.; Sinha, R.; Lee, G.; Dowsett, M.; Kaye, S. B.; Dearnaley, D.; Kheoh, T.; Molina, A.; de Bono, J. S. Selective inhibition of CYP17 with abiraterone acetate is highly active in the treatment of castration-resistant prostate cancer. *J. Clin. Oncol.* **2009**, *27*, 3742–3748.

(10) Picard, F.; Schulz, T.; Hartmann, R. W. 5-Phenyl substituted 1-methyl-2-pyridones and 4'-substituted biphenyl-4-carboxylic acids. Synthesis and evaluation as inhibitors of steroid-5α-reductase type 1 and 2. *Bioorg. Med. Chem.* **2002**, *10*, 437-448

(11) Picard, F.; Baston, E.; Reichert, W.; Hartmann, R. W. Synthesis of N-substituted piperidine-4-(benzylidene-4-carboxylic acids) and evaluation as inhibitors of steroid-5α-reductase type 1 and 2. *Bioorg. Med. Chem.* **2000**, *8*, 1479-1487.

(12) Baston, E.; Hartmann, R. W. *N*-substituted 4-(5-indolyl)benzoic acids. Synthesis and evaluation of steroid 5α-reductase type I and II inhibitory activity. *Bioorg. Med. Chem. Lett.* **1999**, *9*, 1601-1606.

(13) Aggarwal, S.; Tharejaa, S.; Vermaa, A.; Bhardwaja, T. R.; Kumar, M. An overview on 5α-reductase inhibitors. *Steroids* **2010**, *75*, 109-153.

(14) Bey, E.; Marchais-Oberwinkler, S.; Kruchten, P.; Frotscher, M.; Werth, R.; Oster, A.; Algul, Ö.; Neugebauer, A.; Hartmann, R. W. Design, synthesis and biological evaluation of bis(hydroxyphenyl) azoles as potent and selective non steroidal inhibitors of 17β-hydroxysteroid dehydrogenase type 1 (17β-HSD1) for treatment of estrogen dependent diseases. *Bioorg. Med. Chem.* **2008**, *16*, 6423-6435.

(15) Bey, E.; Marchais-Oberwinkler, S.; Werth, R.; Negri, M.; Al-Soud, Y.; Kruchten, P.; Oster A.; Frotscher, M.; Birk, B.; Hartmann, R. W. Design, synthesis, biological evaluation and pharmacokinetics of bis(hydroxyphenyl)substituted azoles, thiophenes, benzenes and aza-benzenes as potent and selective non-steroidal inhibitors of 17β-hydroxysteroid dehydrogenase type 1 (17β-HSD1). *J. Med. Chem.* **2008,** *51,* 6725-6739.

(16) Frotscher, M.; Ziegler, E.; Marchais-Oberwinkler, S.; Kruchten, P.; Neugebauer, A.; Fetzer, L.; Scherer, C.; Müller-Vieira, U.; Messinger, J.; Thole, H.; Hartmann, R. W. Design, synthesis and biological evaluation of (hydroxyphenyl)naphthalene and -quinoline derivatives: Potent, selective and non-steroidal inhibitors of 17β-hydroxysteroid dehydrogenase type 1 (17β-HSD1) for the treatment of estrogen-dependent diseases. *J. Med. Chem.* **2008**, *51,* 2158-2169.

(17) Marchais-Oberwinkler, S.; Kruchten, P.; Frotscher, M.; Ziegler, E.; Neugebauer, A.; Bhoga, U.; Bey, E.; Müller-Vieira, U.; Messinger, J.; Thole, H.; Hartmann, R. W. Substituted 6-phenyl-2-naphthols. Potent and selective non-steroidal inhibitors of 17β-hydroxysteroid dehydrogenase type 1 (17β-HSD1): Design, synthesis, biological evaluation and pharmacokinetics. *J. Med. Chem.* **2008**, *51*, 4685-4698.

(18) Siu, M.; Johnson, T. O.; Wang, Y.; Nair, S. K.; Taylor, W. D; Cripps, S. J.; Matthews, J. J.; Edwards, M. P.; Pauly, T. A.; Ermolieff, J.; Castro, A.; Hosea, N. A.; LaPaglia, A.; Fanjul, A. N.; Vogel, J. E. *N*-(Pyridin-2-yl) arylsulfonamide inhibitors of 11beta-hydroxysteroid dehydrogenase type 1: Discovery of PF-915275. *Bioorg. Med. Chem. Lett.* **2009**, *19*, 3493-3497.

(19) Mornet, E.; Dupont, J.; Vitek, A.; White, P. C. Characterization of two genes encoding human steroid 11β-hydroxylase [P-450(11)β]. *J. Biol. Chem*. **1989**, *264,* 20961–20967.

(20) Lucas, S.; Heim, R.; Negri, M.; Antes, I.; Ries, C.; Schewe, K. E.; Bisi, A.; Gobbi, S.; Hartmann, R. W. Novel aldosterone synthase inhibitors with extended carbocyclic skeleton by a combined ligand-based and structure-based drug design approach. *J. Med. Chem.* **2008***, 51,* 6138-6149.

(21) Heim, R.; Lucas, S.; Grombein, C. M.; Ries, C.; Schewe, K. E.; Negri, M.; Müller-Vieira, U.; Birk, B.; Hartmann, R. W. Overcoming undesirable CYP1A2 potency of pyridylnaphthalene type aldosterone synthase inhibitors: Influence of heteroaryl substitution on potency and selectivity. *J. Med. Chem.* **2008***, 51,* 5064-5074.

(22) Voets, M.; Antes, I.; Scherer, C.; Müller-Vieira, U.; Biemel, K.; Barassin, C.; Marchais-Oberwinkler, S.; Hartmann, R. W. Heteroaryl substituted naphthalenes and structurally modified derivatives: selective inhibitors of CYP11B2 for the treatment of congestive heart failure and myocardial fibrosis. *J. Med. Chem.* **2005**, *48*, 6632-6642.

(23) Ulmschneider, S.; Müller-Vieira, U.; Mitrenga, M.; Hartmann, R. W.; Marchais-Oberwinkler, S.; Klein, C. D. P.; Bureik, M.; Bernhardt, R.; Antes, I.; Lengauer, T. Synthesis and evaluation of imidazolylmethylenetetrahydronaphthalenes and imidazolylmethyleneindanes: potent inhibitors of aldosterone synthase**.** *J. Med. Chem.* **2005,** *48*, 1796-1805.

(24) Ulmschneider, S.; Müller-Vieira, U.; Klein, C. D. P.; Antes, I.; Lengauer, T.; Hartmann, R. W. Synthesis and evaluation of (pyridylmethylene)tetrahydronaphthalenes/ -indanes and structurally modified derivatives: potent and selective inhibitors of aldosterone synthase. *J. Med. Chem.* **2005**, *48*, 1563-1575.

(25) Ries, C.; Lucas, S.; Heim, R.; Birk, B.; Hartmann, R. W. Selective aldosterone synthase inhibitors reduce aldosterone formation in vitro and in vivo. *J. Steroid Biochem. Mol. Biol.* **2009***, 116*, 121-126.

(26) Lucas, S.; Heim, R.; Ries, C.; Schewe, K. E.; Birk B.; Hartmann, R. W. In vivo active aldosterone synthase inhibitors with improved selectivity: Lead optimization providing a series of pyridine substituted 3,4-dihydro-1*H*-quinolin-2-one derivates. *J. Med. Chem.* **2008**, *51,* 8077-8087.

(27) Zolle, I. M.; Berger, M. L.; Hammerschmidt, F.; Hahner, S.; Schirbel, A.; Peric-Simov, B. New selective inhibitors of steroid 11β-hydroxylation in the adrenal cortex. Synthesis and structure-activity relationship of potent etomidate analogues. *J. Med. Chem*. **2008**, *51*, 2244–2253.

(28) Diez, J. J.; Iglesias, P. Pharmacological therapy of Cushing´s syndrome: Drugs and indications. *Mini Rev. Med. Chem.* **2007***, 7,* 467–480.

(29) Roumen, L.; Peeters, J. W.; Emmen, J. M. A.; Beugels, I. P. E.; Custers, E. M. G.; de Gooyer, M.; Plate, R.; Pieterse, K.; Hilbers, P. A. J.; Smits, J. F. M.; Vekemans, J. A. J.; Leysen, D.; Ottenheijm, H. C. J.; Janssen, H. M.; Hermans, J. J. R. Synthesis, biological evaluation, and molecular modeling of 1-benzyl-1*H*-imidazoles as selective inhibitors of aldosterone synthase (CYP11B2). *J. Med. Chem*. **2010**, *53*, 1712–1725.

(30) Godefroi, E. F.; Janssen, P. A. J.; Van der Eycken, C. A. M.; Van Heertum, A. H. M. T.; Niemegeers, C. J. E. DL-1-(1-Arylalkyl)imidazole-5-carboxylate esters. A novel type of hypnotic agents. *J. Med. Chem*. **1965**, *8*, 220–223.

(31) Ehmer, P. B.; Bureik, M.; Bernhardt, R.; Müller, U.; Hartmann, R. W. Development of a test system for inhibitors of human aldosterone synthase (CYP11B2): Screening in fission yeast and evaluation of selectivity in V79 cells. *J. Steroid Biochem. Mol. Biol.* **2002**, *81*, 173–179.

(32) Denner, K.; Doehmer, J.; Bernhardt, R. Cloning of CYP11B1 and CYP11B2 from normal human adrenal and their functional expression in COS-7 and V79 chinese hamster cells. *Endocr. Res.* **1995**, *21*, 443–448.

(33) Ehmer, P. B.; Jose, J.; Hartmann, R. W. Development of a simple and rapid assay for the evaluation of inhibitors of human 17α-hydroxylase-C(17,20)-lyase (P450c17) by coexpression of P450c17 with NADPH-cytochrome-P450-reductase in *Escherichia coli. J. Steroid Biochem. Mol. Biol.* **2000**, *75*, 57–63.

(34) Jagusch, C.; Negri, M.; Hille, U. E.; Hu, Q.; Bartels, M.; Jahn-Hoffmann, K.; Pinto-Bazurco Mendieta, M. A.; Rodenwaldt, B.; Müller-Vieira, U.; Schmidt, D.; Lauterbach, T.; Recanatini, M.; Cavalli, A.; Hartmann, R. W. Synthesis, biological evaluation and molecular modelling studies of methyleneimidazole substituted biaryls as inhibitors of human 17alpha-hydroxylase-17,20-lyase (CYP17). Part I: Heterocyclic modifications of the core structure. *Bioorg. Med. Chem.* **2008,** *16*, 1992-2010.

4 Zusammenfassende Diskussion

Das Steroidhormon Aldosteron spielt als Hauptmineralocorticoid eine bedeutende Rolle bei der Wasser- und Elektrolythomöostase. Im Falle eines Blutdruckabfalls und einer damit verbundenen Minderperfusion der Niere wird die Aldosteronsekretion unter Kontrolle des RAAS kurzfristig erhöht. Hierdurch werden verschiedene Effekte ausgelöst, die der Aufrechterhaltung des Blutdrucks und der Sicherstellung einer ausreichenden Organdurchblutung dienen. Es kommt zu einer verstärkten Natrium- und Wasserretention bei gleichzeitig vermehrter Ausscheidung von Kalium und Protonen. Bei Patienten mit bestimmten Erkrankungen, wie z.B. Leberzirrhose, Nierenarterienstenosen und Herzinsuffizienz, sowie bei Patienten mit Primärem Hyperaldosteronismus per se, werden chronisch erhöhte Aldosteronspiegel gemessen. Diese pathophysiologischen Aldosteronkonzentrationen führen zu einer Reihe unerwünschter Effekte. Dazu gehört die Gefahr einer Elektrolytverschiebung, die sowohl Arrhythmien als auch eine Veränderung des Blut-pH-Wertes (Alkalose) zur Folge haben kann. Darüber hinaus kommt es zu einer verstärkten Bildung von Kollagen in Herz- und Nierengewebe, was die Funktion dieser Organe in entscheidender Weise beeinträchtigt. Durch die Blockierung der Aldosteronwirkung mit Hilfe von Mineralocorticoidrezeptor-Antagonisten konnte in klinischen Studien bei Patienten mit akutem Myokardinfarkt oder bei bestehender Herzinsuffizienz eine deutliche Verbesserung der Mortalität und der Hospitalisationsrate beobachtet werden.[41] Jedoch ist die Anwendung der MR-Blocker mit diversen, teilweise gravierenden Nebenwirkungen verbunden, die u. a. auf deren steroidale Struktur und die geringe Selektivität gegenüber anderen Steroidrezeptoren zurückzuführen sind.[45] Eine weitere therapeutische Option, um den negativen Effekten erhöhter Aldosteronkonzentrationen entgegenzuwirken, stellt die Reduktion der Plasma-Aldosteronspiegel durch Hemmung der Aldosteronbiosynthese, genauer gesagt ihres Schlüsselenzyms CYP11B2, dar. In vergleichenden Studien mit MR-Antagonisten und dem unselektiven CYP11B2-Inhibitor FAD286A konnte gezeigt werden, dass beide Wirkstoffe gleichermaßen in der Lage waren die jeweils beobachteten Parameter positiv zu beeinflussen.[11,55-58] Somit könnten hoch aktive und selektive Inhibitoren der Aldosteronsynthase innovative und vielversprechende Wirkstoffe zur Behandlung Aldosteron-abhängiger Erkrankungen darstellen, die die zur Zeit verfügbaren Therapiemöglichkeiten entweder ersetzen oder entscheidend verbessern könnten.

Diese Strategie wird bereits seit 1994 von unserer Arbeitsgruppe propagiert.[49-51] Dabei wird die Entwicklung nichtsteroidaler Inhibitoren hinsichtlich potentieller Nebenwirkungen bevorzugt. Hemmstoffe mit einem Pyridin-substituierten Naphthalen-Grundgerüst und strukturell verwandte

Verbindungen konnten als eine Klasse potenter Aldosteronsynthase-Hemmstoffe identifiziert werden, die die Aktivität des hoch homologen CYP11B1-Enzyms deutlich weniger beeinflussen (Selektivitätsfaktoren bis zu 1500). Diese Verbindungen zeigten gute pharmakokinetische Eigenschaften in Ratten nach per oraler Applikation, waren jedoch nicht in der Lage den Plasmaaldosteronspiegel abzusenken. Darüber hinaus wurde eine starke Inhibition des hepatischen CYP1A2-Enzyms festgestellt, was zu unerwünschten Arzneistoff-Wechselwirkungen führen könnte. Im Rahmen dieser Arbeit sollten basierend auf einem bereits etablierten Pharmakophormodell neue Verbindungen entwickelt und bezüglich ihrer biologischen Aktivität evaluiert werden. Dabei war das Ziel hoch potente und selektive Inhibitoren der Aldosteronsynthase (CYP11B2) als potentielle Wirkstoffe zur Behandlung Aldosteron-abhängiger Erkrankungen zu erhalten. Die Selektivität gegenüber anderen CYP-Enzymen, speziell von CYP1A2, sollte durch gezielte Strukturmodifikationen verbessert werden. Zur Validierung neuer Targets ist die Erbringung des *Proof of Principle* und des *Proof of Concept* im geeigneten Tiermodell unerlässlich. Da die gefundenen Leitverbindungen in der Ratte jedoch keinerlei CYP11B2-Aktivität aufwiesen, war die Etablierung neuer Assays zur Beurteilung der Ratten-CYP11B2-Aktivität *in vitro* eine weitere zentrale Fragestellung dieser Arbeit. Darüber hinaus sollte bei fehlender Aktivität am Rattenenzym mit Hilfe eines weiteren *in vitro*-Assays an Nebennieren verschiedener Nager die Auswahl einer geeigneten Spezies ermöglicht werden.

Die Kapitel 3.1-3.6 befassen sich mit der Synthese und der biologischen Testung neuer potentieller CYP11B2-Inhibitoren. Das Designkonzept sowie die Struktur-Wirkungs-Beziehungen der Verbindungen aus den Kapiteln 3.1-3.4 sind in der Dissertation von Simon Lucas (2008) weitreichend beschrieben und diskutiert. Aus diesem Grund wird auf diese Aspekte hier nur kurz eingegangen.

In Kapitel 3.1 sind die Synthese und die biologische Evaluierung einer Serie von 30 Pyridylnaphthalenen und -dihydronaphthalenen **I/1**–**I/30**[†] beschrieben. Im Gegensatz zu früheren Arbeiten, die sich mit Optimierungen des Naphthalengerüstes befassten, wurde in dieser Arbeit der Einfluss verschiedener Substituenten am Häm-komplexierenden Pyridinring bezüglich Aktivität und Selektivität untersucht. Es konnte gezeigt werden, dass die meisten Verbindungen potentere CYP11B2-Hemmstoffe darstellen, als die unsubstituierte Ausgangsverbindung **MV23**. Im Säugerzell-basierten Screening-Assay, bei dem die humanen Enzyme CYP11B2 bzw. CYP11B1 getrennt voneinander rekombinant in V79-Zellen exprimiert werden, konnten für die Aldosteronsynthase IC_{50}-Werte im subnanomolaren Bereich erzielt werden. Die Aktivität der 11β-Hydroxylase wurde in den meisten Fällen weit weniger stark inhibiert, sodass in dieser Serie von Verbindungen Selektivitätsfaktoren bis 442 erreicht werden konnten. Darüber hinaus wirkten sich manche Substituenten des Pyridinrestes positiv auf die unerwünschte CYP1A2-Hemmung aus.

[†] Alle Verbindungen, auf die sich in Kapitel 4 bezogen wird, können durch Nennung der Römischen Ziffer der entsprechenden Publikation zugeordnet werden. Die Arabische Ziffer steht für die jeweilige Verbindung in der entsprechenden Publikation (z.B. **III/8** bezieht sich auf Verbindung Nr. **8** in Publikation Nr. **3**)

Dies konnte mit der Planarität und der Aromatizität der Moleküle korreliert werden. Bei den typischen Substraten (z.B. Koffein[75]) oder Inhibitoren (z.B. Furafyllin[76]) von CYP1A2 handelt es sich um kleine planare Moleküle. Bei den Verbindungen **I/28**–**I/30** wurde durch Substitution am Pyridinring die Planarität aufgehoben, was zu einer Verbesserung der Selektivität gegenüber dem hepatischen CYP-Enzym führte (Tabelle 2). Noch stärker ausgeprägt war dieser Effekt bei den Verbindungen **I/13** und **I/30**, die eine Dihydronaphthalengrundstruktur besitzen und weniger als 20 % Hemmung bei einer Konzentration von 2 µM zeigen. Dieses Ergebnis bestätigt QSAR-Studien, die gezeigt haben, dass die CYP1A2-Inhibition stark von der Anzahl sp^2-hybridisierter Kohlenstoffatome abhängt.[77]

Tabelle 2: ***in vitro*** **Hemmdaten an humanem CYP11B2, CYP11B1 und CYP1A2 durch Heteroaryl-substituierte Naphthalene**

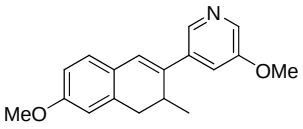

I/13

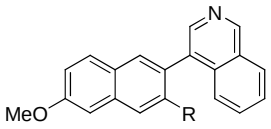

I/28, **I/29**

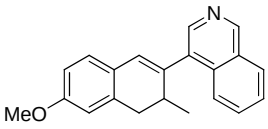

I/30

Verbindung	R	IC_{50}[a] (nM) CYP11B2[b]	IC_{50}[a] (nM) CYP11B1[c]	Selektivitäts-faktor[d]	% Hemmung[e] CYP1A2[f]
I/13		1,2	100	83	18
I/28	H	0,6	67	112	57
I/29	Me	3,1	843	272	45
I/30		0,5	64	128	6

[a] Mittelwert aus mindestens vier Experimenten, Standardabweichung üblicherweise kleiner als 25 %. [b] Hamster Fibroblasten, die humanes CYP11B2 exprimieren; Substrat Deoxycorticosteron, 100 nM. [c] Hamster Fibroblasten, die humanes CYP11B1 exprimieren; Substrat Deoxycorticosteron, 100 nM. [d] IC_{50} CYP11B1/IC_{50} CYP11B2. [e] Mittelwert aus zwei Experimenten, Standardabweichung kleiner als 5 %. [f] Rekombinant exprimierte Enzyme aus Baculovirus infizierten Insektenzell-Mikrosomen (Supersomen); Inhibitor Konzentration, 2,0 μM; Furafyllin, 55 % Hemmung.

Für eine Serie von vier strukturell unterschiedlichen Verbindungen (**I/9**, **I/11**, **I/18** und **I/28**) wurde ein erweitertes Selektivitätsprofil erstellt. Hierbei wurde die Hemmung anderer steroidogener Enzyme, CYP17 und CYP19, sowie die Inhibition anderer bedeutender hepatischer CYP-Enzyme (2B6, 2C9, 2C19, 2D6 und 3A4) untersucht (Tabelle 3). Die ausgewählten Verbindungen weisen bei einer Konzentration von 2,0 µM eine moderate Hemmung der 17α-Hydroxylase-C17,20-lyase auf. Verbindung **I/9** zeigt bei einer Konzentration von 0,5 µM eine vergleichbare Hemmaktivität an Aromatase, während die anderen Verbindungen dieses Enzym praktisch nicht hemmen. Verbindung **I/11** stellte sich mit einem IC_{50}-Wert von 83 nM als sehr potenter CYP1A2-Inhibitor heraus. Bei **I/9** und **I/28** konnte hingegen mit IC_{50}-Werten von ungefähr 1,5 µM eine deutlich bessere Selektivität erzielt werden. Die für die übrigen hepatischen CYP-Enzyme bestimmten IC_{50}-Werte lagen meist deutlich höher und wurden als unkritisch angesehen.

Tabelle 3: *in vitro* Hemmdaten an ausgewählten humanen steroidogenen und hepatischen CYP-Enzymen

	% Hemmung[a]		IC_{50}[b] (nM)					
Verb.	CYP17[c]	CYP19[d]	CYP1A2[e,f]	CYP2B6[e,g]	CYP2C9[e,h]	CYP2C19[e,i]	CYP2D6[e,j]	CYP3A4[e,k]
I/9	42	47	1420	> 50000	48970	45800	11100	21070
I/11	41	14	83	> 25000	1888	> 25000	> 25000	1913
I/18	36	< 5	488	> 50000	> 200000	> 200000	> 200000	9070
I/28	39	7	1619	16540	1270	3540	33110	3540

[a] Mittelwert aus vier Experimenten, Standardabweichung kleiner als 10 %. [b] Mittelwert aus zwei Experimenten, Standardabweichung kleiner als 5 %. [c] Humanes CYP17, rekombinant exprimiert in *E. coli*; Substrat Progesteron, 25 µM; Inhibitor Konzentration 2,0 µM; Ketoconazol, IC_{50} = 2780 nM. [d] Humanes CYP19 aus Plazenta; Substrat Androstendion, 500 nM, Inhibitor Konzentration 500 nM; Fadrozol, IC_{50} = 30 nM. [e] Rekombinant exprimierte Enzyme aus Baculovirus infizierten Insektenzell-Mikrosomen (Supersomen). [f] Furafyllin, IC_{50} = 2419 nM. [g] Tranylcypromin, IC_{50} = 6240 nM. [h] Sulfaphenazol, IC_{50} = 318 nM. [i] Tranylcypromin, IC_{50} = 5950 nM. [j] Quinidine, IC_{50} = 14 nM. [k] Ketoconazol, IC_{50} = 57 nM.

Es konnte gezeigt werden, dass durch Modifikationen der Leitstruktur **MV23** in Form von verschiedenen Substitutionen des Pyridinrestes die Aktivität an CYP11B2 und die Selektivität gegenüber CYP11B1 weitgehend erhalten werden kann. Darüber hinaus wurde die unerwünschte Hemmung des hepatischen CYP1A2 positiv beeinflusst, was zu Verbindungen geführt hat, die insgesamt ein vielversprechendes Selektivitätsprofil aufweisen. Die erhaltenen Ergebnisse lassen den Schluss zu, dass im Bereich des Heterozyklus eine Reihe von Substituenten im aktiven Zentrum des Targetenzyms toleriert werden. Dieser Umstand kann ausgenutzt werden um durch Substitution des Pyridinringes die Selektivität gegenüber anderen CYP-Enzymen und das pharmakokinetische Profil zu optimieren. Diese Strategie wurde weiterverfolgt, was in den folgenden Kapiteln 3.2 - 3.4 beschrieben ist.

In Kapitel 3.2 basiert das Inhibitor-Designkonzept auf der Tatsache, dass Imidazolylmethylen-substituierte Flavone (Abbildung 7) als moderate bis hoch aktive CYP11B2-Inhibitoren aus dem Screening einer Substanzbibliothek hervorgingen. Diese, ursprünglich als Aromatase-Hemmstoffe beschriebenen Verbindungen[78], zeigten bei einer Konzentration von 500 nM 73-94 % Hemmung an CYP11B2, jedoch keinerlei Selektivität gegenüber dem hoch homologen CYP11B1.

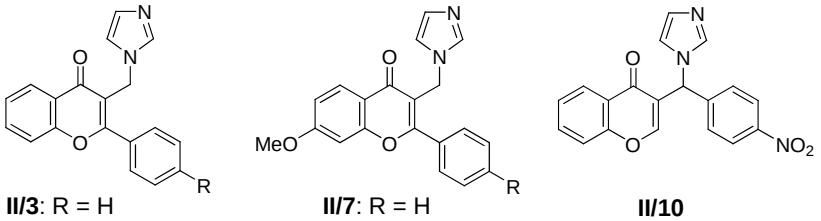

II/3: R = H
II/4: R = NO_2
II/5: R = Br
II/6: R = OMe

II/7: R = H
II/8: R = Br
II/9: R = NO_2

II/10

Abbildung 7: Imidazolylmethylen-substituierte Flavone mit inhibitorischer Aktivität an CYP11B2

Mit Hilfe der potentesten Inhibitoren vom Flavon-Typ, der CYP11B2-aktiven Naphthalene sowie der Methylenindane als Trainingsset wurde mit einem Bestandteil der SYBYL Molecular Modeling Software, dem sogenannten GALAHAD Pharmacophore Generation Module ein erweitertes Pharmakophormodell erstellt.[79] Dabei wurden die bisherigen Pharmakophor-Punkte, nämlich die hydrophoben Bereiche HY0, HY1, HY2a und HY2b als auch die „acceptor atom features" AA1, AA2a und AA2b (Abbildung 8) bestätigt. Darüber hinaus wurde ein weiterer voluminöser hydrophober Bereich HY3 in der Nähe von HY1, zusammen mit den weiteren Akzeptoreigenschaften AA3a and AA3b sowie das zusätzliche „acceptor atom feature" AA4 identifiziert. Abbildung 8 zeigt das erweiterte Pharmakophormodell mit Verbindung **II/1**, der unsubstituierten Pyridylnaphthalen-Grundstruktur. Dabei wird deutlich, dass der hydrophobe Bereich HY3 und die korrespondieren Punkte AA3a und AA3b von Inhibitoren dieses Typs nicht ausgenutzt werden.

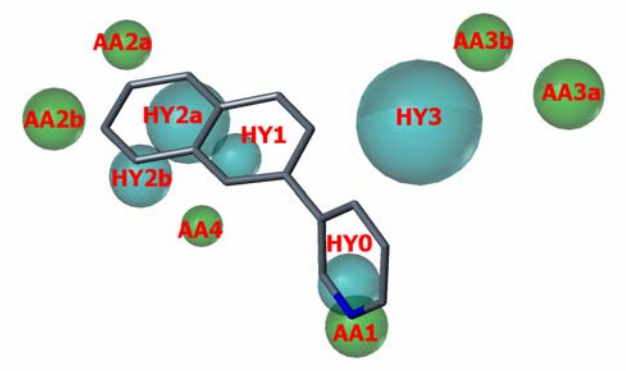

Abbildung 8: Erweitertes Pharmakophormodell mit Verbindung II/1

Die Pharmakophor-Features sind farbig codiert: blaue Punkte stehen für hydrophobe Bereiche (HY0-HY3), grüne Punkte stellen die Akzeptoreigenschaften AA1-AA4 dar.

Um die durch das neue Pharmakophormodell definierten Bereiche in der Bindetasche der Aldosteronsynthase besser auszunutzen, wurden zwei Modellverbindungen **II/11** und **II/12** entworfen (Abbildung 9). Durch Einführung eines hydrophoben Substituenten in Position 3 des Naphthalen-Grundgerüstes sollte der hydrophobe Bereich HY3 des Pharmakophormodells ausgefüllt werden. Hierzu wurde ein Phenylrest ausgewählt (**II/11**), der durch seine direkte Bindung an das Naphthalen wenig konformationelle Freiheit besitzt. Der Benzylrest bei Verbindung **II/12** weist durch die freie Drehbarkeit um die Kohlenstoff-Kohlenstoff-Bindungen und den zusätzlichen Methylenspacer eine größere Flexibilität auf.

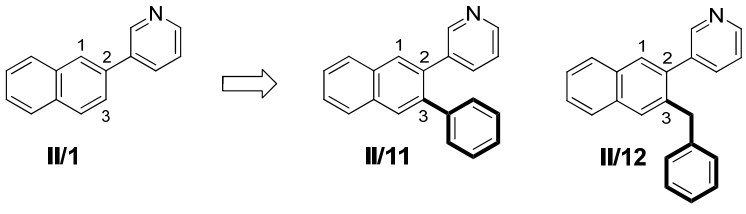

Abbildung 9: Modellverbindungen II/11 und II/12

Vor Synthese der Substanzen wurden Docking-Studien durchgeführt, um die Rolle der konformationellen Flexibilität zu untersuchen. Dabei stellte sich heraus, dass Verbindung **II/11** offensichtlich zu rigide ist und deshalb nicht erfolgreich in die Bindetasche des CYP11B2-Proteinmodells gedockt werden konnte. Unter den gegebenen Einschränkungen des Pharmakophormodells kann der Häm-komplexierende Pyridin-Stickstoff nicht in dem benötigten Winkel mit der prosthetischen Gruppe in Wechselwirkung treten. Im Gegensatz dazu besitzt die 3-Benzyl substituierte Verbindung **II/12** aufgrund ihres zusätzlichen Methylenspacers die nötige Flexibilität und konnte erfolgreich in die Bindetasche gedockt werden. Das Ergebnis dieser *in silico* Experimente wurde durch *in vitro*-Testdaten bestätigt. Während **II/11** bei einer Konzentration von 500 nM keine signifikante CYP11B2-Hemmung aufwies, zeigte die benzylierte Verbindung eine Hemmung von 76 %. Im Einklang mit den Docking-Ergebnissen wurde Verbindung **II/12** mit einem IC_{50}-Wert von 154 nM als moderater CYP11B2-Hemmstoff mit geringer CYP11B1-Selektivität eingestuft. Nachdem **II/12** als vielversprechende Leitstruktur identifiziert werden konnte, wurden 25 weitere Verbindungen dieses Typs synthetisiert, mit dem Ziel das Selektivitätsprofil zu verbessern. Eine Auswahl von *in vitro*-Hemmdaten einiger repräsentativer Beispiele ist in Tabelle 4 dargestellt. Die fehlende Selektivität gegenüber der hoch homologen 11β-Hydroxylase konnte erreicht werden, wobei hier die Verbindungen **II/17** (Selektivitätsfaktor 724) und **II/18** (Selektivitätsfaktor 913) besonders hervorzuheben sind.

Tabelle 4: ***in vitro*** **Hemmdaten ausgewählter 3-Benzylnaphthalenderivate an humanem CYP11B2 und CYP11B1**

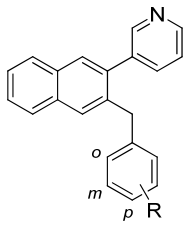

II/12, II/14-II/18

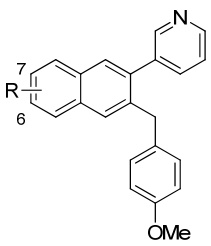

II/19, **II/20**

Verbindung	R	% Hemmung[a] CYP11B2[c]	IC_{50}[b] (nM) CYP11B2[c]	IC_{50}[b] (nM) CYP11B1[d]	Selektivitäts-faktor[e]
II/12	H	76	154	953	6
II/14	*o*-OMe	24	n.d.	n.d.	n.d.
II/15	*m*-OMe	62	n.d.	n.d.	n.d.
II/16	*p*-OMe	89	7,8	2804	359
II/17	*p*-CN	93	2,7	1956	724
II/18	*p*-OCF_3	95	3,9	3559	913
II/19	6-OMe	95	11	4329	394
II/20	7-OMe	35	n.d.	n.d.	n.d.

[a] Mittelwert aus mindestens zwei Experimenten, Standardabweichung üblicherweise kleiner als 10 %; Inhibitor Konzentration, 500 nM. [b] Mittelwert aus mindestens vier Experimenten, Standardabweichung üblicherweise kleiner als 25 %, n.d. = nicht bestimmt. [c] Hamster Fibroblasten, die humanes CYP11B2 exprimieren; Substrat Deoxycorticosteron, 100 nM. [d] Hamster Fibroblasten, die humanes CYP11B1 exprimieren; Substrat Deoxycorticosteron, 100 nM. [e] IC_{50} CYP11B1/IC_{50} CYP11B2, n.d. = nicht bestimmt.

In Abbildung 10 ist die Überlagerung des erweiterten Pharmakophormodells mit Verbindung **II/19** dargestellt. Hierbei wird deutlich, dass Moleküle dieser Substanzklasse sowohl die bereits bekannten (HY0, HY1, HY2a, AA1, AA2a) als auch die neu identifizierten Pharmakophorpunkte (HY3, AA3b) sehr gut ausfüllen, was sich in einer starken CYP11B2-Hemmung widerspiegelt. Die *para*-Methoxygruppe am Benzylrest von Verbindung **II/19**, die zu einer hohen CYP11B2-Aktivität und eine Steigerung der CYP11B1-Selektivität geführt hat, kann dem „acceptor atom feature" AA3b zugeordnet werden, was die Vorhersagekraft des erweiterten Pharmakophormodells unterstreicht. Demnach sollten bei zukünftigen Designstrategien Wechselwirkungen in diesem Bereich der Bindetasche angestrebt werden, um aktive und selektive Aldosteronsynthase-Inhibitoren zu erhalten. Hinsichtlich des Selektivitätsprofils gegenüber anderen CYP-Enzymen muss jedoch beachtet werden, dass Verbindung **II/19** eine mit Fadrozol vergleichbare Aromatase-Hemmung aufweist und darüber hinaus auch starker Inhibitor einiger hepatischer CYP-Enzyme (z. B. CYP2C9, CYP2C19 und CYP3A4) ist.

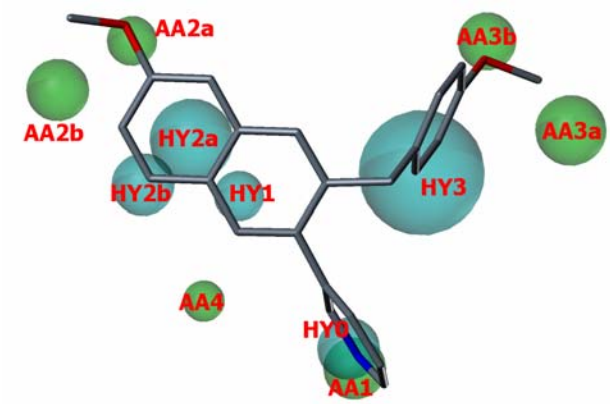

Abbildung 10: Erweitertes Pharmakophormodell mit Verbindung II/19

Die Pharmakophor-Features sind farbig codiert: blaue Punkte stehen für hydrophobe Bereiche (HY0-HY3), grüne Punkte stellen die Akzeptoreigenschaften AA1-AA4 dar.

Kapitel 3.3 befasst sich wie Kapitel 3.1 mit der Überwindung unerwünschter CYP1A2-Hemmaktivität von CYP11B2-Inhibitoren. Wie bereits beschrieben, soll durch Reduzierung der Planarität und der Aromatizität am **MV23**-Grundgerüst ein positiver Einfluss auf die CYP1A2-Hemmung genommen werden. Dabei stellte sich das Tetralon **III/9** (Abbildung 11) als hoch aktiver Aldosteronsynthase-Inhibitor (IC_{50} = 7,8 nM) mit ausgezeichneter Selektivität gegenüber CYP11B1 (IC_{50} = 3,95 μM) und CYP1A2 (IC_{50} = 1,55 μM) heraus. Die Substanz zeigte an fünf weiteren untersuchten hepatischen CYP-Enzymen noch höhere IC_{50}-Werte (zwischen 6,21 µM an CYP3A4 und 171 µM an CYP2D6) und darüber hinaus ein gutes pharmakokinetisches Profil. Obwohl an der Zelllinie U-937 erst ab einer Konzentration von 100 µM zytotoxische Effekte beobachtet wurden (Abbildung 11), erfolgte ein bioisosterer Austausch des zyklischen Ketons von **III/9** durch ein Lactam, was zu Verbindung **III/12**, einem Dihydro-1*H*-chinolin-2-on, führte, die bis zur höchsten getesteten Konzentration (200 µM) keine signifikante Zytotoxizität zeigte.

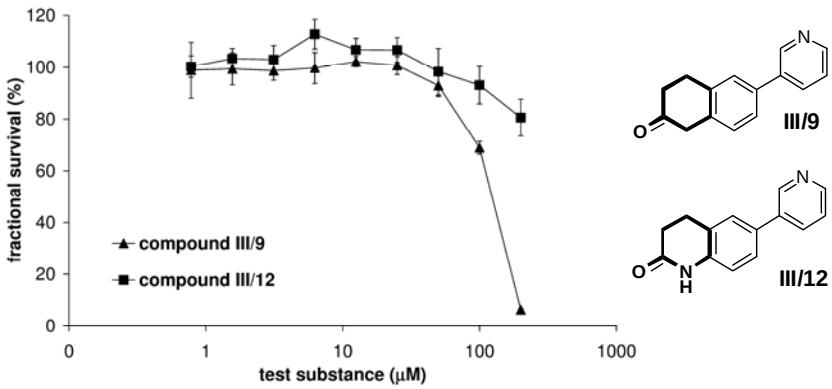

Abbildung 11: Relative Viabilität (%) von humanen U937-Zellen nach Inkubation mit III/9 oder III/12

Darüber hinaus weist **III/12** eine höhere Selektivität gegenüber anderen untersuchten CYP-Enzymen und eine bessere Bioverfügbarkeit als das analoge Tetralon auf. Deshalb wurden, ausgehend von **III/12** als Grundstruktur, diverse strukturell modifizierte Derivate synthetisiert und auf ihre biologische Aktivität getestet. Die Hemmdaten einiger repräsentativer Verbindungen dieser Serie sind in Tabelle 5 zusammengefasst. Hieraus wird ersichtlich, dass Dihydro-1*H*-chinolin-2-one hoch potente CYP11B2-Inhibitoren darstellen mit IC_{50}-Werten im niedrigen nanomolaren Bereich. Bei dem Isochinolinderivat **III/22** handelt es sich um die aktivste bisher bekannte Verbindung mit einem IC_{50} von 90 pM. Darüber hinaus konnten bei den getesteten Substanzen gute Selektivitäten bezüglich CYP11B1 und CYP1A2 erreicht werden. Besonders hervorzuheben ist hierbei Verbindung **III/21**, die praktische keine CYP1A2-Hemmung mehr aufweist (IC_{50} > 150 µM).

Tabelle 5: ***in vitro*** **Hemmdaten ausgewählter Dihydro-1*H*-chinolin-2-one an humanem CYP11B2, CYP11B1 und CYP1A2**

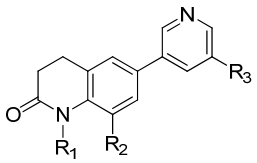

III/12, **III/14**, **III/15**
III/17, **III/19**, **III/20**

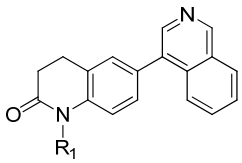

III/21, **III/22**

				IC_{50}[a] (nM)		Selektivitäts-	IC_{50}[e] (nM)
Verbindung	R_1	R_2	R_3	CYP11B2[b]	CYP11B1[c]	faktor[d]	CYP1A2[f]
III/12	H	H	H	28	6746	241	1.95
III/14	Me	H	H	2.6	742	289	1.79
III/15	Et	H	H	22	5177	235	3.48
III/17	H	Cl	H	3.8	1671	440	30.6
III/19	H	H	OMe	2.7	339	126	5.24
III/20	Me	H	OMe	0.18	87	483	16.5
III/21	H			0.18	33	187	> 150
III/22	Me			0.09	6.9	77	n.d.

[a] Mittelwert aus mindestens vier Experimenten, Standardabweichung üblicherweise kleiner als 25 %. [b] Hamster Fibroblasten,die humanes CYP11B2 exprimieren; Substrat Deoxycorticosteron, 100 nM. [c] Hamster Fibroblasten, die humanes CYP11B1 exprimieren; Substrat Deoxycorticosteron, 100 nM. [d] IC_{50} CYP11B1/IC_{50} CYP11B2. [e] Mittelwert aus zwei Experimenten, Standardabweichung kleiner als 5 %. [f] Rekombinant exprimierte Enzyme aus Baculovirus infizierten Insektenzell-Mikrosomen (Supersomen); Furafyllin, IC_{50} = 2.42 μM.

Des Weiteren zeigen die meisten der untersuchten Verbindungen dieser Strukturklasse ein gutes pharmakokinetisches Profil. Nach per oraler Applikation konnten für **III/21** in Ratten annehmbare Plasmaspiegel ($AUC_{0-\infty}$ = 1658 ng·h/ml bei einer Dosis von 25 mg/kg Körpergewicht) und eine Halbwertszeit von 2,9 h bestimmt werden. Da die Verbindungen mit Dihydro-1*H*-chinolin-2-on-Grundgerüst weitaus bessere Eigenschaften aufwiesen als die untersuchten Pyridyl-substituierten Naphthalene vom **MV23**-Typ, wurden sie in einem neu etablierten zellbasierten Enzym-Assay auf ihre

Aktivität am Ratten-CYP11B2-Enzym getestet (siehe Abschnitt zu Kapitel 3.5). Hierbei stellt sich Verbindung **III/21** als potentieller *in vivo*-Kandidat zur Erbringung des *Proof of Principle* heraus und wurde im bereits beschriebenen ACTH-Rattenmodell auf seine Fähigkeit zur Absenkung der Plasma-Aldosteronspiegel untersucht. Dabei konnte nach intravenöser Applikation von 20 mg/kg Körpergewicht eine signifikante Reduzierung der Aldosteronlevel im Vergleich zur Kontrollgruppe beobachtet werden. Diese Ergebnisse werden in einem späteren Abschnitt eingehend diskutiert. Aufgrund der vielversprechenden *in vitro*- und *in vivo*-Daten wurde das Strukturmotiv aus diesem Teilprojekt zur Weiterentwicklung beibehalten.

Die durchgeführten Strukturoptimierungen des Dihydro-1*H*-chinolin-2-on-Grundgerüstes sind in Kapitel 3.4 beschrieben. Zur Rigidisierung der zuletzt beschriebenen Moleküle wurde der Lactam-Stickstoff in einen 5- bzw. 6-Ring eingebunden, wodurch Verbindungen mit einem Pyrrolochinolinon- oder Pyridochinolinon-Grundgerüst erhalten wurden. Die Größe des an den Chinolinonrest kondensierten Rings hat deutlichen Einfluss auf die CYP11B1-Selektivität, die bei den Pyridochinolinonen (**IV/2**, **IV/4** und **IV/11**) höher ist als bei den entsprechenden Pyrrolochinolinonderivaten (**IV/1, IV/3** und **IV/10**). Das Pyridochinolinon **IV/2** ist die selektivste Verbindung dieser Serie (Selektivitätsfaktor = 957). Bezüglich anderer CYP-Enzyme zeigt die Erweiterung zum 6-gliedrigen Kohlenstoffzyklus eine Verschlechterung des Selektivitätsprofils. So konnte für Verbindung **IV/2** eine vergleichsweise starke Inhibition der Aromatase (69 % Hemmung bei 500 nM) beobachtet werden. Die sechs untersuchten hepatischen CYP-Enzyme wurden ebenso stärker von den Pyrido- als von den Pyrrolochinolinonderivaten gehemmt. Darüber hinaus führte die Expansion des Ringes zu einer dramatischen Verschlechterung der pharmakokinetischen Eigenschaften. So konnte für Verbindung **IV/4** ($AUC_{0-\infty}$ = 51 ng·h/ml) im Vergleich zur entsprechenden Pyrroloverbindung **IV/3** ($AUC_{0-\infty}$ = 557 ng·h/ml) eine 10-fach schlechtere Verfügbarkeit im Plasma gemessen werden.

Anhand der ausgewählten Verbindungen in Tabelle 6 wird ersichtlich, dass in dieser Substanzklasse Substituenten am 3-Pyridylrest hauptsächlich die CYP11B1-Aktivität beeinflussen, während die CYP11B2-Aktivität weitgehend unbeeinflusst bleibt. So bewegen sich die IC_{50}-Werte an CYP11B2 für diese Verbindungen in einem sehr kleinen Bereich (0,6-4,6 nM), an CYP11B1 ergeben sich hingegen IC_{50}-Werte von 21 bis 2296 nM, was zu Selektivitäten zwischen 15 und 957 führt. Generell kann festgestellt werden, dass die Mehrheit der kondensierten Heterozyklen aufgrund einer geringeren CYP11B1-Hemmung selektiver sind als die entsprechenden offenkettigen Moleküle.

Tabelle 6: ***in vitro*** **Hemmdaten ausgewählter Pyrrolo- und Pyridochinolinonderivate an humanem CYP11B2 und CYP11B1**

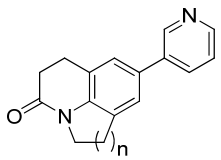

IV/1-IV/2

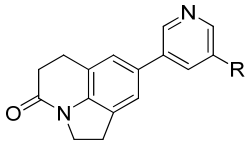

IV/3, IV/5, IV/6

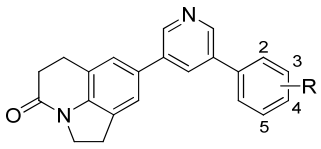

IV/15-IV/18, IV/22-IV/24

Verbindung	n	R	IC_{50}[a] (nM) CYP11B2[b]	IC_{50}[a] (nM) CYP11B1[c]	Selektivitäts-faktor[d]
IV/1	1	H	1.1	715	650
IV/2	2	H	2.4	2296	957
IV/3		OMe	0.6	247	412
IV/5		OEt	1.0	158	158
IV/6		O*i*Pr	2.2	103	47
IV/15		H	1.3	58	45
IV/16		2-F	0.7	43	61
IV/17		3-F	1.4	490	350
IV/18		4-F	0.9	40	44
IV/22		2-OMe	2.4	128	53
IV/23		3-OMe	4.6	1374	299
IV/24		4-OMe	1.4	21	15

[a] Mittelwert aus mindestens vier Experimenten, Standardabweichung üblicherweise kleiner als 25 %.
[b] Hamster Fibroblasten, die humanes CYP11B2 exprimieren; Substrat Deoxycorticosteron, 100 nM.
[c] Hamster Fibroblasten, die humanes CYP11B1 exprimieren; Substrat Deoxycorticosteron, 100 nM.
[d] IC_{50} CYP11B1/IC_{50} CYP11B2.

Wie bereits oben erwähnt zeigten die meisten der untersuchten Pyrrolochinolinon-Verbindungen neben einer niedrigen CYP11B1-Aktivität auch bessere Selektivitäten gegenüber den untersuchten steroidogenen (CYP17 und CYP19) und hepatischen CYP-Enzymen als die entsprechenden Pyridochinolinone. So weist Verbindungen **IV/1** an den sechs wichtigsten hepatischen CYP-Enzymen keine bedeutende Hemmung mit IC_{50}-Werte > 10 µM auf. Darüber hinaus konnte für diese Substanz in Ratten nach per oraler Applikation von 5 mg/kg Körpergewicht eine ausgezeichnete Verfügbarkeit im Plasma gemessen werden (Abbildung 12). Die Plasmaspiegel dieser Verbindung ($AUC_{0-\infty}$ =3464 ng·h/ml) überstiegen in einem *Cassette-Dosing*-Experiment sowohl die der Verbindungen **III/9** und **III/12** als auch die des bereits auf dem Markt befindlichen Aromataseinhibitors Fadrozol ($AUC_{0-\infty}$ = 3207 ng·h/ml). Mit Inhibitor **IV/1** und strukturell ähnlichen Verbindungen konnten hoch aktive CYP11B2-Hemmstoffe identifiziert werden, die neben einem hervorragenden Selektivitätsprofil an ausgewählten CYP-Enzymen auch ausgezeichnete pharmakokinetische Eigenschaften aufweisen.

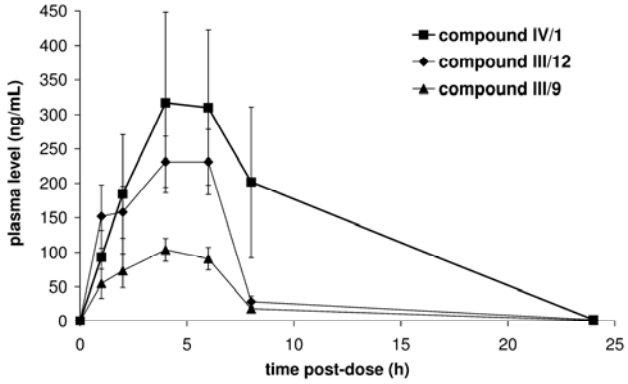

Abbildung 12: ***Cassette-Dosing*-Experiment in Ratten zur Bestimmung der Plasmalevel (ng/ml) der Verbindungen VI/1, III/9 und III/12 nach per oraler Applikation von 5 mg/kg Körpergewicht**

Das auf dem erweiterten Pharmakophormodell basierende Inhibitor-Designkonzept wurde, wie in den Kapiteln 3.1-3.4 beschrieben, innerhalb umfangreicher Syntheseprogramme umgesetzt. Mit Hilfe der durchgeführten Strukturoptimierungen konnten, ausgehend von 3-Pyridyl-substituierten Naphthalenen, Inhibitoren synthetisiert werden, die unter Erhaltung der positiven Eigenschaften der Ausgangsverbindungen (hohe Aktivität an CYP11B2 und gute Selektivität gegen CYP11B1) ein verbessertes pharmakologisches Gesamtprofil besitzen. Besonders hervorzuheben ist hierbei die erreichte Selektivität gegenüber dem Fremdstoff-metabolisierenden CYP1A2. Die starke Hemmung dieses Enzyms durch Verbindungen mit Pyridylnaphthalen-Grundgerüst (> 95 % bei 2 µM) konnte hinsichtlich potentieller Arzneistoff-Wechselwirkungen nicht toleriert werden. Durch Synthese von Molekülen mir reduzierter Planarität und Aromatizität wurden Inhibitoren erhalten, die an CYP1A2 keine bedeutende Hemmung mehr aufweisen. Darüber hinaus zeigten die Verbindungen ausgezeichnete Selektivitäten gegenüber weiteren hepatischen oder steroidogenen CYP-Enzymen und hervorragende pharmakokinetische Eigenschaften.

Die selektive Hemmung der Aldosteronsynthase zur Behandlung Aldosteron-abhängiger Erkrankungen stellt ein neues Target dar, das noch validiert werden muss. Mit diesen bereits weit entwickelten und hoch potenten CYP11B2-Hemmstoffen sollte *in vivo* eine Plasmaaldosteron-Absenkung im Sinne eines *Proof of Principle* gezeigt werden. Die positiven Effekte reduzierter Aldosteronlevel konnten mit dem unselektiven Aromatase-Hemmstoff Fadrozol an verschiedenen Krankheitsmodellen in der Ratte bereits beobachtet werden, das *Proof of Concept* für CYP11B2 mit einem selektiven Inhibitor steht jedoch noch aus. Da das *in vivo*-Modell zur Untersuchung der Corticoid-Biosynthese von Häusler *et al.*[74] und die in Frage kommenden Krankheitsmodelle hauptsächlich an der Ratte etabliert sind, sollten die Versuche an dieser Spezies durchgeführt werden. Mit den Ausgangsverbindungen (z.B. **MV23**) konnte bei vorangegangenen Applikationen in der Ratte jedoch keine signifikante Absenkung der Aldosteronspiegel gemessen werden, obwohl die Substanz im Plasma in hohen Konzentrationen vorlag (Dissertation U. Müller-Vieira, 2005).

Die fehlende CYP11B2-Aktivität in der Ratte wurde auf Speziesunterschiede zurückgeführt, da die Proteinsequenz-Identität zwischen humanem und Ratten-Enzym lediglich 69 % beträgt. Kapitel 3.5 befasst sich mit der Etablierung eines zellbasierten *in vitro*-Assays, der eine zuverlässige Vorhersage bezüglich der Ratten-CYP11B2-Hemmung zulässt, um potentielle Kandidaten zur Erbringung des *Proof of Principle* zu identifizieren. Es erfolgte die Klonierung des Ratten-CYP11B2-Gens, das analog dem entsprechenden humanen Enzym rekombinant in V79MZ-Zellen exprimiert wurde, da sich dieses einfache Testsystem zum Screening von Inhibitoren gut bewährt hat. Nach Isolierung einer monoklonalen Zelllinie mit Aldosteronsynthase-Aktivität wurden die optimalen Testparameter ermittelt und z.B. die Substratkonzentration entsprechend dem bestimmten K_M-Wert angepasst. Für das anschließende Screening auf Ratten-CYP11B2-Aktivität wurden Inhibitoren aus verschiedenen Verbindungsklassen ausgewählt, um die Auswirkung struktureller Unterschiede auf die Hemmung des Ratten-Enzyms zu untersuchen (Abbildung 13). Die ausgewählten Verbindungen stammen aus den in den Kapitel 3.1-3.3 beschriebenen Syntheseprogrammen und mussten neben einer sehr guten inhibitorischen Aktivität am humanen CYP11B2-Enzym (IC_{50}-Wert im nanomolaren Bereich) auch gute Selektivitätsprofile aufweisen, um am Rattenenzym getestet zu werden.

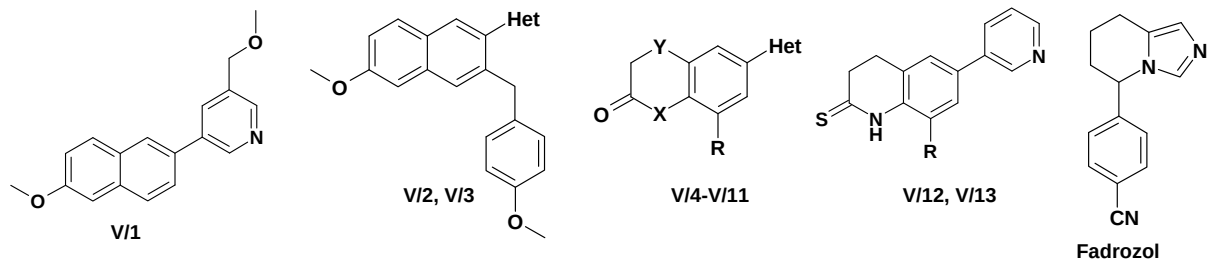

Abbildung 13: Ausgewählte Verbindungen für Aktivitätsscreening am Ratten-CYP11B2-Enzym

Dabei stellten sich lediglich Verbindung **V/7** (entspricht **III/21**; 65 % bei 2 µM) und das *N*-Methyl-Analogon **V/9** (entspricht **III/22**; 49 % bei 2 µM) aus der Klasse der Heteroaryl-substituierten 3,4-Dihydro-1*H*-chinolin-2-one als moderate Inhibitoren des Rattenenzyms heraus. Alle anderen getesteten Verbindungen zeigten keine signifikante Hemmung (0-16 %) bei einer Konzentration von 2 µM. Darüber hinaus wurde die Hemmung von **Fadrozol** als Referenzsubstanz im *in vitro*-Assay untersucht. Wie aufgrund der bereits publizierten *in vivo*-Daten erwartet, zeigte der Aromatase-Hemmstoff eine vergleichsweise starke Inhibition des Ratten-CYP11B2 (73 % bei 0,5 µM). Verbindung **V/7** und **Fadrozol** sind mit IC_{50}-Werten von 0,2 bzw. 1,0 nM vergleichbar gute Inhibitoren der humanen Aldosteronsynthase, hinsichtlich der Selektivität gegenüber CYP11B1 ist **V/7** (Selektivitätsfaktor = 187) dem CYP19-Hemmstoff (Selektivitätsfaktor = 10) allerdings weit überlegen. Bei Betrachtung der erhaltenen Hemmdaten konnte eine hohe Selektivität gegenüber CYP11B1 mit einer schlechten Aktivität am Rattenenzym korreliert werden. Dies zeigt sich eindrucksvoll beim Verhältnis der IC_{50}-Werte zwischen humanem und Ratten-CYP11B2. Während

Fadrozol das Rattenenzym 185 Mal schlechter hemmt als das humane Enzym (berechneter IC_{50}-Wert für Ratten-CYP11B2 = 185 nM), zeigt Verbindung **V/7** eine 5385 mal schwächere Hemmung an der Ratte im Vergleich zum humanen Enzym (berechneter IC_{50}-Wert für Ratten-CYP11B2 = 1077 nM). Dieses Ergebnis konnte in einem weiteren *in vitro*-Assay mit Rattennebennieren bestätigt werden. Im Gegensatz zum V79-Zellassay, bei dem das Ratten-Enzym rekombinant exprimiert wird, liegt es hier in seiner natürlichen Umgebung vor. Nach Inkubation mit Verbindung **V/7** wurde die Aldosteronbiosynthese in den Organen bei einer Konzentration von 50 µM um 76 %, bei 250 µM um 89 % reduziert (Tabelle 7). Eine weitere Verbindung (**IV/1**), die im Screening-Assay keinerlei Ratten-CYP11B2-Hemmung zeigte, und **Fadrozol** wurden ebenfalls an Nebennieren getestet, um die mit V79-Zellen generierten Ergebnisse zu evaluieren. Bei der inaktiven Verbindung konnte erst bei einer Konzentration von 250 µM eine 30 %-ige CYP11B2-Hemmung gemessen werden, die allerdings nicht signifikant war, beim hochaktiven **Fadrozol** hingegen, zeigte sich bereits bei 10 µM eine um 80 % (unpublizierte Daten) verringerte CYP11B2-Aktivität.

Tabelle 7: Hemmung der Ratten-CYP11B2-Aktivität im V79-Zellassay und an Nebennieren-Organkulturen

Verbindung	% Hemmung in V79-Zellen[a]	% Hemmung an Nebennieren[b]
IV/1	0 [2,0 µM]	30 [250 µM]
V/7	65 [2,0 µM]	76 [50 µM]
Fadrozol	73 [0,5 µM]	80 [10 µM][c]

[a] Hamster Fibroblasten, die Ratten-CYP11B2 exprimieren; Substrat Deoxycorticosteron, 500 nM; Mittelwert aus mindestens drei Experimenten, Standardabweichung kleiner als 15 %. [b] Ratten-Nebennieren; Substrat Deoxycorticosteron, 100 nM; n=5. [c] Ratten-Nebennieren; Substrat Deoxycorticosteron, 100 nM; n=3.

Mit diesen Organkultur-Versuchen konnte zum einen der neu entwickelte V79/Ratten-CYP11B2-Assay validiert und zum anderen ein weiterer *in vitro*-Test etabliert werden, der auch mit Nebennieren anderer Spezies (z.B. Hamster oder Meerschweinchen) durchgeführt werden kann, um bei fehlender Aktivität am Rattenenzym eine geeignete Spezies zur Erbringung des *Proof of Principle* zu finden. Dieser einfach und schnell durchzuführende Test ist aufgrund relativ großer Schwankungen zwischen den einzelnen Organen nicht geeignet um geringe Aktivitätsunterschiede zwischen verschiedenen Verbindungen zu quantifizieren, er erlaubt jedoch eine Aussage über das Vorhandensein oder Fehlen von CYP11B2-Hemmaktivität einer Verbindung in der betrachteten Spezies.

Wie bereits beschrieben wurde jedoch aufgrund der etablierten Krankheitsmodelle die Ratte als Versuchstier bevorzugt. Durch die beiden *in vitro*-Assays konnte Verbindung **V/7** als „rattenaktive" Substanz identifiziert werden, die auf ihre Fähigkeit zur Absenkung der Plasma-Aldosteronlevel im von Häusler *et al.* beschriebenen Modell untersucht wurde. Eine subkutane Applikation von ACTH 16 Stunden vor Gabe des Aldosteronsynthase-Inhibitors führt hierbei zu einer deutlichen Erhöhung der Corticoidspiegel, wodurch der zirkadiane Rhythmus dieser Hormone ausgesetzt und die Beobachtung

des Aldosteronspiegels unabhängig von der Tageszeit ermöglicht wird. Dadurch konnte die Aldosteronkonzentration im Blut der Kontrolltiere (Vehikel-Gruppe) über die Dauer des Experimentes konstant gehalten werden (Abbildung 14). Nach intravenöser Applikation von Verbindung **V/7** in einer Dosis von 20 mg/kg Körpergewicht konnte hingegen bereits nach 15 min eine signifikante (P<0,05), nach einer Stunde sogar eine hochsignifikante (P<0,003) Absenkung der Plasma-Aldosteronlevel gemessen werden. In den sechs behandelten Tieren konnten zu Zeitpunkten zwischen 0,5 und 3 Stunden maximale Reduzierungen der Aldosteronkonzentrationen zwischen 36 und 63 % gemessen werden.

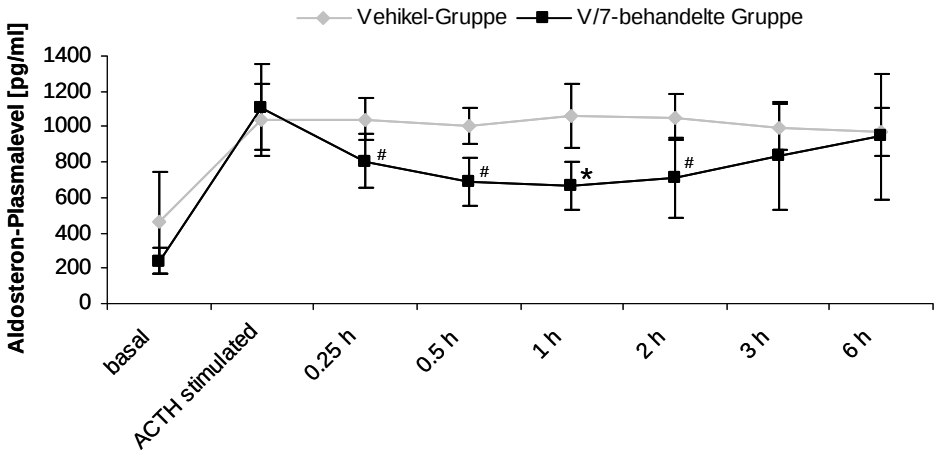

Abbildung 14: *in vivo* Aldosteronabsenkung in Ratten durch Verbindung V/7 im Vergleich zur unbehandelten Kontrollgruppe

Dargestellt sind die gemittelten Profile der Vehikel- bzw. **V/7**-behandelten Gruppe mit den jeweiligen Standardabweichungen. Vehikel-Gruppe: n=4; **V/7**-behandelte Gruppe: n=6. $^{\#}P$<0,05; $^{*}P$<0,003

Die aus dem Screening hervorgegangene „Hit"-Verbindung **V/7** war trotz ihrer um mehrere Größenordnungen schlechteren Rattenaktivität in der Lage den Plasma-Aldosteronspiegel in den behandelten Tieren deutlich abzusenken. Damit konnte das *Proof of Principle* mit einem selektiven Aldosteronsynthase-Inhibitor erbracht werden. Aufgrund der erheblich stärkeren Hemmung des humanen Enzyms kann im Menschen von einem weitaus solideren Effekt ausgegangen werden. Dieses ausgezeichnete Ergebnis unterstreicht die Vorhersagekraft der neu etablierten *in vitro*-Assays in beeindruckender Weise. Mit Hilfe dieser zusätzlichen „Scientific Tools" können zukünftig Designstrategien und Syntheseprogramme verfolgt werden, die eine Verbesserung der Ratten-CYP11B2-Hemmung anstreben. Somit sollen Substanzen generiert werden, die, unter Beibehaltung ihrer positiven Eigenschaften am humanen Enzym, eine stärkere Inhibition des Rattenenzyms zeigen und in einem geeigneten Krankheitsmodell die relevanten Parameter günstig beeinflussen.

Im Hinblick auf die Verbesserung der Ratten-CYP11B2-Aktivität müssen neue Substanzklassen erschlossen werden. Deshalb wurden in einem weiteren Syntheseprojekt Strukturelemente zweier bekannter CYP11B2-Inhibitoren miteinander kombiniert. Die positiven Eigenschaften der Ratten-aktiven Verbindung **VI/1** (entspricht **V/7**) sollten erhalten und mit dem Strukturmotiv des bekannten CYP-Enzym-Inhibitors Metyrapon **VI/2** verknüpft werden. Metyrapon hemmt unspezifisch die Corticoid-bildenden und die Arzneistoff-metabolisierenden CYP-Enzyme und wird sowohl diagnostisch, zur Funktionsprüfung der Hypothalamus-Hypophysen-Nebennierenrinden-Achse, als auch therapeutisch, bei Zuständen die mit einer Überproduktion von Gluco- oder Mineralocorticoiden einhergehen, eingesetzt. In Kapitel 3.6 ist ausgehend von dieser Inhibitor-Designstrategie die Synthese und die biologische Evaluierung einer Serie von 23 *N*-(Pyridin-3-yl)benzamiden **VI/3a-3u** beschrieben. Dabei wurde der verbrückende 2,2-Dimethylethanon-Rest von **VI/2** gegen einen synthetisch leichter zugänglichen Amidlinker und das Keto-substituierte Pyridinsystem gegen einen substituierten Phenylrest ersetzt, um eine höhere Aktivität an CYP11B2 zu erreichen. Während Metyrapon die Steroid-11β-hydroxylase (IC_{50} = 15 nM) etwa fünf Mal stärker hemmt als die Aldosteronsynthase (IC_{50} = 79 nM), zeigten die neu synthetisierten Verbindungen durch Substitution des Phenylrestes eine deutlich verringerte Inhibition von CYP11B1. Da die CYP11B2-Aktivität dabei nahezu unbeeinflusst blieb, führte dies zu sehr guten Selektivitäten zwischen 96 und 174 (Tabelle 8).

Tabelle 8: ***in vitro*-Hemmdaten ausgewählter *N*-(Pyridin-3-yl)benzamid-Derivate an humanem CYP11B2 und CYP11B1**

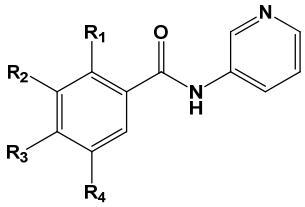

VI/3e-VI/3g, VI/3m, VI/3n, VI/3r, VI/3u

Verb.	R_1	R_2	R_3	R_4	CYP11B2[a] IC_{50}[c]	CYP11B1[b] IC_{50}[c]	Selektivitäts-faktor[d]
VI/1	-	-	-	-	0,2 nM	33 nM	187
VI/2	-	-	-	-	79 nM	15 nM	0.19
VI/3e	H	H	F	H	82 nM	14 µM	174
VI/3f	H	H	Cl	H	65 nM	10 µM	157
VI/3g	H	H	Br	H	104 nM	17 µM	161
VI/3m	H	H	CN	H	78 nM	7,5 µM	96
VI/3n	H	H	NO_2	H	145 nM	25 µM	171
VI/3r	H	F	F	H	54 nM	5,9 µM	111
VI/3u	F	H	F	F	166 nM	16 µM	97

[a] Hamster Fibroblasten, die humanes CYP11B2 exprimieren; Substrat Deoxycorticosteron, 100 nM. [b] Hamster Fibroblasten, die humanes CYP11B1 exprimieren; Substrat Deoxycorticosteron, 100 nM. [c] Mittelwert aus mindestens drei Experimenten, Standardabweichung kleiner als 25 %. [d] IC_{50} CYP11B1/IC_{50} CYP11B2.

Verbindung **VI/3e** mit einem Fluor als Substituent in *para*-Position zum Benzamidrest stellt die selektivste (Selektivitätsfaktor = 174), das difluor-substituierte Analogon **VI/3r** die aktivste Verbindung (IC_{50} = 54 nM) dieser Serie dar. Obwohl mit den *N*-(Pyridin-3-yl)benzamid-Derivaten bezüglich CYP11B2, verglichen mit Metyrapon, keine Steigerung der Aktivität erreicht werden konnte, wurden CYP11B1-Selektivitäten erzielt, die mit der von Verbindung **VI/1** vergleichbar sind. Zur weiteren Charakterisierung wurden die Inhibitoren aus Tabelle 8 auf ihre Selektivität gegenüber anderen steroidogenen CYP-Enzymen (CYP17 und CYP19) untersucht, wobei keinerlei Hemmung festgestellt werden konnte. Diese Substanzklasse stellt trotz etwas schwächerer Aldosteronsynthase-Aktivität einen interessanten Ansatzpunkt für weitere Strukturmodifikationen dar. Untersuchungen bezüglich der für Metyrapon bekannten Hemmung der Arzneistoff-metabolisierenden hepatischen CYP-Enzyme sowie der Aktivität am Ratten-CYP11B2-Enzym stehen allerdings noch aus.

Innerhalb der unter 3.1-3.6 beschriebenen Projekte wurden Verbindungen erhalten, die neben einer exzellenten CYP11B2-Aktivität sehr gute Selektivitäten gegenüber anderen steroidogenen und Fremdstoff-metabolisierenden CYP-Enzymen zeigen. Darüber hinaus weisen einige Verbindungen ausgezeichnete pharmakokinetische und pharmakodynamische Eigenschaften auf, womit für das Target Aldosteronsynthase das *Proof of Principle* mit einem selektiven CYP11B2-Inhibitor erbracht werden konnte. Analog dem beschrieben Konzept zur selektiven Hemmung der Aldosteronbiosynthese könnte bei der Behandlung Cortisol-abhängiger Erkrankungen wie dem *Cushing*-Syndrom die Hemmung der Glucocorticoidbildung durch selektive CYP11B1-Inhibitoren ebenso eine deutliche Verbesserung der zur Zeit verfügbaren Therapiemöglichkeiten bedeuten. In einem weiteren, unter 3.7 beschriebenen, Projekt wurden die Verbindungen **VII/1 - VII/36** synthetisiert, die sich ähnlich der in Kapitel 3.6 dargestellten, von Metyrapon ausgehenden Designstrategie von dem Adrenostatikum *R*-Etomidat (ETO) ableiten. Bei Etomidat handelt es sich um eine substituierte Imidazolverbindung, die in der kurzfristigen Therapie bei Patienten mit schwerem Hypercortisolismus Anwendung findet und neben CYP11B1 auch CYP11B2 und CYP11A1 hemmt. In einer kürzlich erschienen Arbeit von Roumen *et al.*[80] nutzten die Autoren *R*-Etomidat als Leitverbindung für die Entwicklung von neuen Aldosteronsynthase-Inhibitoren. Dabei konnte gezeigt werden, dass die Modifikation der Estergruppe durch konformationell flexible Substituenten zu CYP11B2 selektiven Verbindungen führt, während die Entfernung des Esters die Selektivität eher zu Gunsten von CYP11B1 verschiebt. Deshalb wurde ein Designkonzept erstellt, das entweder die Eliminierung oder den Austausch des Ethylesters gegen einen rigiden Benzolring vorsah. Des Weiteren wurde durch Entfernung der Methylgruppe, welche für die narkotische Wirkung der Ausgangsverbindung verantwortlich ist, das chirale Zentrum beseitigt. So enstand ausgehend vom unsubstituierten *N*-Benzylimidazol **VII/1** bzw. *N*-Benzylbenzimidazole **VII/13** durch Substitution am Phenylrest eine Serie von 24 Verbindungen, die in Tabelle 9 dargestellt sind.

Da die Gruppe um Roumen *et al.* bereits gezeigt hatte, dass polare Substituenten am Phenylring zu einer schlechten CYP11B1-Hemmung führen, wurde hier mit Methyl-, Chloro- und weiteren Phenylresten substituiert (**VII/2-24**). Während Etomidat noch eine schwache CYP11B2-Selektivität (IC_{50} = 0,1 nM; CYP11B1, IC_{50} = 0,5 nM) aufweist, zeigten die meisten neu synthetisierten Substanzen bereits eine leichte bis moderate CYP11B1-Selektivität (Tabelle 9).

Tabelle 9: *in vitro*-Hemmdaten der substituierten *N*-Benzylimidazole und der korrespondierenden Benzimidazole an humanem CYP11B1 und CYP11B2

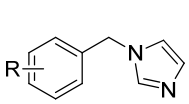

VII/1 - VII/12

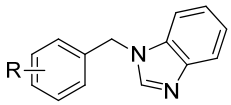

VII/13 - VII/24

Struktur R	Nr.	IC_{50}[a,b] (nM) CYP11B1	IC_{50}[a,b] (nM) CYP11B2	Sf[c]	Nr.	IC_{50}[a,b] (nM) CYP11B1	IC_{50}[a,b] (nM) CYP11B2	Sf[c]
H	**VII/1**	135	456	3.4	**VII/13**	246	865	3.5
4-Cl	**VII/2**	140	46	0.3	**VII/14**	635	107	0.2
2-Me	**VII/3**	61	62	1.0	**VII/15**	779	262	0.3
3-Me	**VII/4**	48	110	2.3	**VII/16**	194	309	1.6
4-Me	**VII/5**	258	320	1.2	**VII/17**	500	520	1.0
3,5-di-Me	**VII/6**	32	77	2.4	**VII/18**	188	632	3.4
2,4,6-tri-Me	**VII/7**	24	30	1.3	**VII/19**	>1000	>1000	
2,3,4,5,6-penta-Me	**VII/8**	5	23	4.6	**VII/20**	>1000	>1000	
2-Ph	**VII/9**	15	39	2.6	**VII/21**	>1000	>1000	
3-Ph	**VII/10**	46	265	5.8	**VII/22**	369	2226	6.0
4-Ph	**VII/11**	32	637	20	**VII/23**	197	1903	10
3,5-di-Ph	**VII/12**	128	332	2.6	**VII/24**	>1000	>1000	
MTP[d]		15	72	4.8				
ETO[d]		0.5	0.1	0.2				
KTZ[d]		127	67	0.5				

[a] Mittelwert aus mindestens drei Experimenten. Standardabweichung < ± 25 %. [b] Hamster Fibroblasten, die humanes CYP11B1 oder CYP11B2 exprimieren; Substrat 11-Deoxycorticosteron, 100 nM. [c] Sf: IC_{50} (CYP11B2)/IC_{50} (CYP11B1). [d]**MTP**, Metyrapon; **ETO**, Etomidat; **KTZ,** Ketoconazol.

Ausgehend vom unsubstituierten *N*-Benzylimidazol **VII/1** konnte die CYP11B1-Aktivität durch Einführung unpolarer Gruppen erhöht werden. Dabei stellte die *penta*-Methylverbindung **VII/8** das aktivste Derivat dieser Serie dar (IC_{50} = 5 nM). Bei den korrespondieren Benzimidazolen führte die Substitution mit Methylgruppen zu keiner Aktivitätssteigerung im Vergleich zur unsubstituierten Verbindung **VII/13**. Darüber hinaus wurde die Erhöhung der Anzahl der Methylgruppen bei den Benzimidazolen nicht toleriert (**VII/19** und **VII/20**). Im Fall der Phenyl-substituierten *N*-Benzylimidazole **VII/9 - VII/11** konnte ebenfalls eine Steigerung der CYP11B1-Aktivität festgestellt werden (IC_{50} = 15 - 46 nM), wobei die Einführung des Phenylrestes in 4-Position zur selektivsten Verbindung **VII/11** (Sf = 20) dieser Serie führte. Dies resultierte aus einer deutlichen Abnahme der Aldosteronsynthase-Hemmung (IC_{50} = 637 nM) in Folge der *para*-Phenylsubstitution. Ein ähnlicher Effekt zeigte sich beim entsprechenden Benzimidazol **VII/23**, wobei es sich zwar um

eine deutlich weniger CYP11B1-aktive, jedoch moderat CYP11B2-selektive Verbindung handelte (Selektivitätsfaktor = 10). Die Einführung von Phenylgruppen am Methylenspacer sowie dessen Verlängerung führte bei den Benzimidazolderivaten **VII/30 - VII/32** zu einem kompletten Aktivitätsverlust an beiden Enzymen (IC_{50}-Werte > 1000 nM). In der Klasse der *N*-Benzylimidazole hingegen resultierten daraus sehr potente CYP11B1-Inhibitoren (**VII/27 - VII/29**) mit IC_{50}-Werten zwischen 3 und 80 nM, allerdings wurde die Aldosteronbiosynthese von diesen Hemmstoffen in ähnlichem Maße gehemmt (Selektivitätsfaktoren = 2,0 - 3,4). In der Klasse der Benzimidazole konnten aktive und leicht selektive Verbindungen identifiziert werden, so dass die Rigidisierung des Ethylesters als geeignete Optimierungsstrategie angesehen werden kann. Jedoch zeigten die entsprechenden Imidazole stets eine höhere CYP11B1-Aktivität.

Da die spezifische Hemmung der Glucocorticoidbiosynthese von zentraler Bedeutung ist, wurden die Inhibitoren aus Tabelle 9 zur weiteren Charakterisierung auf ihre Selektivität gegenüber anderen steroidogenen CYP-Enzymen (CYP17 und CYP19) untersucht. Dabei zeigten einige Verbindungen eine moderate Hemmung dieser Enzyme. Aus diesem Grund wurden ausgehend von der CYP11B2-selektivsten Verbindung **VII/11** weitere Strukturmodifikationen durch Austausch des zentralen Phenylringes gegen verschiedene Heterozyklen vorgenommen. Die erhaltenen Verbindungen sind in Tabelle 10 dargestellt. Es handelt sich hierbei um aktive und selektive Inhibitoren der Steroid-11β-hydroxylase.

Tabelle 10: ***in vitro*-Hemmdaten der Verbindungen VII/33 - VII/36 an humanem CYP11B1, CYP11B2, CYP17 und CYP19**

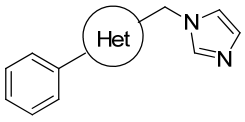

VII/33 - VII/36

Verbindung	Struktur Het	IC_{50}[a,b] (nM) CYP11B1	IC_{50}[a,b] (nM) CYP11B2	Sf[c]	% Hemmung CYP17[a,e]	% Hemmung CYP19[a,f]
VII/11	-	32	637	20	40	5
VII/33	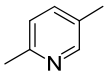	152	2768	18	4	0
VII/34		46	372	8.1	0	51
VII/35	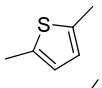	43	353	8.2	21	26
VII/36		19	277	15	21	72
MTP[d]		15	72	4.8		
ETO[d]		0.5	0.1	0.2		
KTZ[d]		127	67	0.5		

[a] Mittelwert aus mindestens drei Experimenten. Standardabweichung < ± 25 %. [b] Hamster Fibroblasten, die humanes CYP11B1 oder CYP11B2 exprimieren; Substrat 11-Deoxycorticosteron, 100 nM. [c] Sf: IC_{50} (CYP11B2)/IC_{50} (CYP11B1). [d]**MTP**, Metyrapon; **ETO**, Etomidat; **KTZ,** Ketoconazol. [e] *E. coli*, die humanes CYP17 exprimieren; Substrat Progesteron, 25 µM; Inhibitor Konzentration, 2.0 µM. [f] Humanes CYP19 aus Plazenta; Substrat Androstendion, 500 nM; Iinhibitor Konzentration, 500 nM.

Während die Einführung von Furan- oder Thiophenringen (**VII/34 - VII/36**) nicht zu einer zufriedenstellenden Abnahme der CYP17- und/oder CYP19-Hemmung führte, wurde durch Einführung eines Pyridinringes der CYP11B1-Inhibitor mit dem vielversprechensten Gesamtprofil erhalten. Die so entstandene Verbindung **VII/33** zeigte bei etwa fünffach schlechterer CYP11B1-Aktivität (IC_{50} = 152 nM) mit einem Selektivitätsfaktor von 18 eine mit **VII/11** vergleichbare CYP11B2-Selektivität und darüber hinaus keine signifikante Hemmung von CYP17 oder CYP19. *In vitro* besitzt diese Substanz somit eine dem klinisch eingesetzten Ketoconazol (IC_{50} = 127 nM) äquivalente Aktivität zur Hemmung der Steroid-11β-hydroxylase bei gleichzeitig deutlich überlegenen Selektivitäten gegenüber CYP11B2 (Selektivitätsfaktor = 0,5) und CYP17.

Innerhalb des unter 3.7 beschriebenen Syntheseprojektes konnten die weltweit ersten selektiven CYP11B1-Inhibitoren identifiziert werden. Sie stellen Leitverbindungen in der Entwicklung neuartiger Wirkstoffe zur Behandlung Cortisol-abhängiger Erkrankungen und einen Ansatzpunkt für weitere Strukturoptimierungen dar. Untersuchungen bezüglich der Hemmung Arzneistoff-metabolisierender hepatischer CYP-Enzyme sowie der Aktivität am Ratten-CYP11B1-Enzym stehen noch aus. Des Weiteren könnte versucht werden in geeigneten humanen Zelllinien (NCI-H295R, HAC15) ein *in vitro Proof of Principle* zu erbringen. Bei NCI-H295R und HAC15 handelt es sich um Nebennierenrinden-Karzinom-Zellen, die, aufgrund der fehlenden natürlichen Zonierung der Nebennierenrinde, das ganze Repertoire der adrenalen steroidogenen CYP-Enzyme exprimieren. Nach der Identifizierung hochaktiver und selektiver CYP11B1-Inhibitoren mit geeignetem PK-Profil und Ratten-CYP11B1-Aktivität sollte im nächsten Schritt in dem von Häusler *et al.* publiziertenTiermodell die Plasma-Corticosteronabsenkung durch einen selektiven Steroid-11β-hydroxylase-Hemmstoff im Sinne eines *in vivo Proof of Principle* gezeigt werden. Im Falle einer signifikanten Reduzierung der Glucocorticoidbiosynthese *in vivo* könnte dann abschließend in einem geeigneten Krankheitsmodell für *Cushing*- oder Metabolisches Syndrom das *Proof of Concept* erbracht werden.

Der Hauptfokus dieser Dissertation lag auf der Erweiterung der Testplattform zur Charakterisierung von Hemmstoffen der Aldosteronbiosynthese. Allerdings stellt die Entwicklung selektiver Inhibitoren der Cortisolbildung eine ebenso große Herausforderung dar. Aufgrund der hohen Sequenzidentität von CYP11B2 und CYP11B1 ist die Bestimmung der Selektivität zwischen diesen beiden Enzymen bereits in einem sehr frühen Stadium des Drug Discovery-Prozesses essentiell. Deshalb wurden stets biologische Testsyteme etabliert, die eine Aktivitätsbestimmung der Substanzen an beiden Enzymen zulassen. Die im Rahmen dieser Arbeit weiter entwickelten und neu etablierten *in vitro*-Assays können deshalb sowohl zur Identifizierung selektiver Inhibitoren der Aldosteronsynthase als auch zur Charakterisierung von potentiellen Steroid-11β-hydroxylase-Hemmstoffen angewendet werden.

5 Referenzen

1 Lieberman, S.; Lin, Y. Y. Reflections on sterol sidechain cleavage process catalyzed by cytochrome P450(scc). *J. Steroid Biochem. Mol. Biol.* **2001**, *78*, 1–14.

2 Kawamoto, T.; Mitsuuchi, Y.; Toda, K.; Yokoyama, Y.; Miyahara, K.; Miura, S.; Ohnishi, T.; Ichikawa, Y.; Nakao, K.; Imura, H.; Ulick, S.; Shizuta, Y. Role of steroid 11β-hydroxylase and steroid 18-hydroxylase in the biosynthesis of glucocorticoids and mineralocorticoids in humans. *Proc. Natl. Acad. Sci. U.S.A.* **1992**, *89*, 1458–1462.

3 Quinn, S. J.; Williams, G. H. Regulation of aldosterone secretion. *Annu. Rev. Physiol.* **1988**, *50*, 409–426.

4 Eaton, D. C.; Malik, B.; Saxena, N. C. Al-Khalili, O. K.; Yue, G. Mechanisms of aldosterone's action on epithelial Na^+ transport. *J. Membrane Biol.* **2001**, *184*, 313–319.

5 Therien, A. G.; Blostein, R. Mechanisms of sodium pump regulation. *Am. J. Physiol. Cell. Physiol.* **2000**, *279*, C541–C566.

6 (a) Reul, J. M. H. M.; de Kloet, E. R. Anatomical resolution of two types of corticosterone receptor sites in rat brain with in vitro autoradiography and computerized image analysis. *J. Steroid Biochem. Mol. Biol.* **1986**, *24*, 269–272. (b) Agarwal, M. K.; Mirshahi, F.; Mirshahi, M.; Rostene, W. Immunochemical detection of the mineralocorticoid receptor in rat brain. *Neuroendocrinology* **1993**, *58*, 575–580.

7 (a) Lombes, M.; Oblin, M. E.; Gasc, J. M.; Baulieu, E. E.; Farman, N.; Bonvalet, J. P. Immunohistochemical and biochemical evidence for a cardiovascular mineralocorticoid receptor. *Circ. Res.* **1992**, *71*, 503–510. (b) Lombes, M.; Alfaidy, N.; Eugene, E.; Lessana, A.; Farman, N.; Bonvalet, J. P. Prerequisite for cardiac aldosterone action. Mineralocorticoid receptor and 11*β*-hydroxysteroid dehydrogenase in the human heart. *Circulation* **1995**, *92*, 175–182.

8 Silvestre, J. S.; Robert, V.; Heymes, C.; Aupetit-Faisant, B.; Mouas, C.; Moalic, J. M.; Swynghedauw, B.; Delcayre, C. Myocardial production of aldosterone and corticosterone in the rat: Physiological regulation. *J. Biol. Chem.* **1998**, *273*, 4883–4891.

9 Delcayre, C.; Silvestre, J. S. Aldosterone and the heart: towards a physiological function? *Cardiovasc. Res.* **1999,** *43*, 7-12.

10 Ye, P.; Kenyon, C. J.; MacKenzie, S. M.; Jong, A. S.; Miller, C.; Gray, G. A.; Wallace, A.; Ryding, A. S.; Mullins, J. J.; McBride, M. W.; Graham, D.; Fraser, R.; Connell, J. M.; Davies, E. The aldosterone synthase (CYP11B2) and 11beta-hydroxylase (CYP11B1) genes are not expressed in the rat heart. *Endocrinology* **2005,** *146*, 5287-5293.

11 Fiebeler, A.; Nussberger, J.; Shagdarsuren, E.; Rong, S.; Hilfenhaus, G.; Al-Saadi, N.; Dechend, R.; Wellner, M.; Meiners, S.; Maser-Gluth, C.; Jeng, A. Y.; Webb, R. L.; Luft, F. C.; Muller, D. N. Aldosterone synthase inhibitor ameliorates angiotensin II-induced organ damage. *Circulation* **2005,** *111*, 3087-3094.

12 (a) Chai, W.; Garrelds, I. M.; de Vries, R.; Danser, A. H. Cardioprotective effects of eplerenone in the rat heart: interaction with locally synthesized or blood-derived aldosterone? *Hypertension* **2006,** *47*, 665-670. (b) Gomez-Sanchez, E. P.; Ahmad, N.; Romero, D. G.; Gomez-Sanchez, C. E. Origin of aldosterone in the rat heart. *Endocrinology* **2004,** *145*, 4796-4802.

13 Tait, S. A.; Tait, J. F.; Coghlan, J. P. The discovery, isolation and identification of aldosterone: reflections on emerging regulation and function. *Mol. Cell. Endocrinol.* **2004**, *217*, 1–21.

14 Moura, A. M.; Worcel, M. Direct action of aldosterone on transmembrane 22Na efflux from arterial smooth muscle. Rapid and delayed effects. *Hypertension* **1984**, *6*, 425-430.

15 Spach, C.; Streeten, D. H. Retardation of sodium exchange in dog erythocytes by physiological concentrations of aldosterone, in vitro. *J. Clin. Invest.* **1964**, *43*, 217–227.

16 Haseroth, K.; Gerdes, D.; Berger, S.; Feuring, M.; Günther, A.; Herbst, C.; Christ, M.; Wehling, M. Rapid nongenomic effects of aldosterone in mineralocorticoid-receptor-knockout mice. *Biochem. Biophys. Res. Commun.* **1999**, *266*, 257–261.

17 (a) Wehling, M.; Armanini, D.; Strasser, T.; Weber, P. C. Effect of aldosterone on sodium and potassium concentrations in human mononuclear leukocytes. *Am. J. Physiol.* **1987**, *252*, E505-508. (b) Wehling, M.; Kasmayr, J.; Theisen, K. Aldosterone influences free intracellular calcium in human mononuclear leukocytes in vitro. *Cell Calcium* **1990**, *11*, 565-571. (c) Wehling, M.; Kuhls, S.; Armanini, D. Volume regulation of human lymphocytes by aldosterone in isotonic media. *Am. J. Physiol.* **1989**, *257*, E170-174.

18 (a) Gekle, M.; Silbernagl, S.; Oberleithner, H. The mineralocorticoid aldosterone activates a proton conductance in cultured kidney cells. *Am. J. Physiol.* **1997,** *273*, C1673-1678. (b) Oberleithner, H.; Weigt, M.; Westphale, H. J.; Wang, W. Aldosterone activates Na+/H+ exchange and raises cytoplasmic pH in target cells of the amphibian kidney. *Proc. Natl. Acad. Sci. U S A* **1987,** *84*, 1464-1468. (c) Alzamora, R.; Michea, L.; Marusic, E. T. Role of 11beta-hydroxysteroid dehydrogenase in nongenomic aldosterone effects in human arteries. *Hypertension* **2000,** *35*, 1099-1104

19 (a) Christ, M.; Douwes, K.; Eisen, C.; Bechtner, G.; Theisen, K; Wehling, M. Rapid Effects of aldosterone on sodium transport in vascular smooth muscle cells. *Hypertension* **1995**, *25*, 117–123. (b) Wehling, M.; Kasmayr, J.; Theisen, K. Rapid effects of mineralocorticoids on sodium-proton exchanger: genomic or nongenomic pathway? *Am. J. Physiol. Endocrinol. Metab.* **1995**, *260*, E719 –E726.

20 Eisen, C.; Meyer, C.; Christ, M.; Theisen, K.; Wehling, M. Novel membrane receptors for aldosterone in human lymphocytes: a 50 kDa protein on SDS-PAGE. *Cell. Mol. Biol.* **1994**, *40*, 351–358.

21 Rupprecht, R.; Reul, J. M.; van Steensel, B.; Spengler, D.; Soder, M.; Berning, B.; Holsboer, F.; Damm, K. Pharmacological and functional characterization of human mineralocorticoid and glucocorticoid receptor ligands. *Eur. J. Pharmacol.* **1993,** *247*, 145-154.

22 Funder, J. W.; Pearce, P. T.; Smith, R.; Smith, A. I. Mineralocorticoid action: target tissue specificity is enzyme, not receptor, mediated. *Science* **1988**, *242*, 583–585.

23 Funder, J. W. Mineralocorticoid receptors: distribution and activation. *Heart Fail. Rev.* **2005,** *10*, 15-22.

24 Taymans, S. E.; Pack, S.; Pak, E.; Torpy, D. J.; Zhuang, Z.; Stratakis, C. A. Human CYP11B2 (aldosterone synthase) maps to chromosome 8q24.3. *J. Clin. Endocrinol. Metab.* **1998,** *83*, 1033-1036.

25 (a) Chua, S. C.; Szabo, P.; Vitek, A.; Grzeschik, K. H.; John, M.; White, P. C. Cloning of cDNA encoding steroid 11 beta-hydroxylase (P450c11). *Proc. Natl. Acad. Sci. U S A* **1987,** *84*, 7193-7197. (b) Wagner, M. J.; Ge, Y.; Siciliano, M.; Wells, D. E. A hybrid cell mapping panel for regional localization of probes to human chromosome 8. *Genomics* **1991,** *10*, 114-125.

26 Mornet, E.; Dupont, J.; Vitek, A.; White, P. C. Characterization of two genes encoding human steroid 11β-hydroxylase (P-450$_{11\beta}$). *J. Biol. Chem.* **1989**, *264*, 20961–20967.

27 Bureik, M.; Lisurek, M.; Bernhardt, R. The human steroid hydroxylases CYP11B1 and CYP11B2. *Chem. Biol.* **2002**, *383*, 1537–1551.

28 (a) Yanagibashi, K.; Haniu, M.; Shively, J. E.; Shen, W. H.; Hall, P. The synthesis of aldosterone by the adrenal cortex. Two zones (fasciculata and glomerulosa) possess one enzyme for 11 beta-, 18-hydroxylation, and aldehyde synthesis. *J. Biol. Chem.* **1986,** *261*, 3556-3562. (b) Nonaka, Y.; Takemori, H.; Halder, S. K.; Sun, T.; Ohta, M.; Hatano, O.; Takakusu, A.; Okamoto, M. Frog cytochrome P-450 (11 beta,aldo), a single enzyme involved in the final steps of glucocorticoid and mineralocorticoid biosynthesis. *Eur. J. Biochem.* **1995,** *229*, 249-256.

29 Boon, W. C.; Coghlan, J. P.; McDougall, J. G. Late steps of aldosterone biosynthesis: sheep are not rats. *Clin. Exp. Pharmacol. Physiol. Suppl.* **1998,** *25*, S21-27.

30 Conn, J. W.; Louis, L. H. Primary aldosteronism, a new clinical entity. *Ann. Intern. Med.* **1956,** *44*, 1-15.

31 (a) Brilla, C. G. Renin-angiotensin-aldosterone system and myocardial fibrosis. *Cardiovasc. Res.* **2000**, *47*, 1–3. (b) Brilla, C. G. Aldosterone and myocardial fibrosis in heart failure. *Herz* **2000**, *25*, 299–306. (c) Lijnen, P.; Petrov, V. Induction of cardiac fibrosis by aldosterone. *J. Mol. Cell. Cardiol.* **2000**, *32*, 865–879.

32 (a) Brilla, C. G.; Zhou, G.; Matsubara, L.; Weber K. T. Collagen metabolism in cultured adult rat cardiac fibroblasts: response to angiotensin II and aldosterone. *J. Mol. Cell. Cardiol*. **1994**, *26*, 809-820. (b) Delcayre, C.; Swynghedauw, B., Molecular mechanisms of myocardial remodeling. The role of aldosterone. *J. Mol. Cell. Cardiol.* **2002,** *34*, 1577-1584.

33 Laragh, J. H. Hormones and the pathogenesis of congestive heart failure: vasopressin, aldosterone, and angiotensin II: further evidence for renal-adrenal interaction from studies in hypertension and in cirrhosis. *Circulation* **1962**, *25*, 1015–1023.

34 Weber, K. T. Aldosterone in congestive heart failure. *N. Engl. J. Med.* **2001**, *345*, 1689–1697.

35 http://www.conn-register.de

36 Cortinovis, M.; Perico, N.; Cattaneo, D.; Remuzzi, G. Aldosterone and progression of kidney disease. *Ther. Adv. Cardiovasc. Dis.* **2009,** *3*, 133-143.

37 (a) Blasi, E. R.; Rocha, R.; Rudolph, A. E.; Blomme, E. A.; Polly, M. L.; McMahon, E. G. Aldosterone/salt induces renal inflammation and fibrosis in hypertensive rats. *Kidney Int.* **2003,** *63*, 1791-1800 (b) Del Vecchio, L.; Procaccio, M.; Vigano, S.; Cusi, D. Mechanisms of disease: The role of aldosterone in kidney damage and clinical benefits of its blockade. *Nat. Clin. Pract. Nephrol.* **2007,** *3*, 42-49.

38 (a) Ho, K. K.; Pinsky, J. L.; Kannel, W. B.; Levy, D. The epidemiology of heart failure: the Framingham Study. *J. Am. Coll. Cardiol.* **1993,** *22*, 6A-13A. (b) Cowie, M. R.; Mosterel, A.; Wood, D. A.; Deckers, J. W.; Poole-Wilson, P. A.; Grobbee, D. E. The epidemiology of heart failure. *Eur. Heart J.* **1997**, *18*, 208–225.

39 (a) The CONSENSUS trial study group. Effects of enalapril on mortality in severe congestive heart failure. Results of the cooperative north scandinavian enalapril survival study (CONSENSUS). *N. Engl. J. Med.* **1987**, *316*, 1429–1435. (b) Kjekshus J, Swedberg K, Snapinn S. Effects of enalapril on long-term mortality in severe congestive heart failure. *Am. J. Cardiol.* **1992**, *69*, 103–107.

40 (a) Struthers, A. D. Aldosterone escape during angiotensin-converting enzyme inhibitor therapy in chronic heart failure. *J. Card. Fail.* **1996**, *2*, 47–54. (b) Sato, A.; Saruta, T. Aldosterone escape during angiotensin-converting enzyme inhibitor therapy in essential hypertensive patients with left ventricular hypertrophy. *J. Int. Med. Res.* **2001**, *29*, 13–21.

41 (a) Pitt, B.; Zannad, F.; Remme, W. J.; Cody, R.; Castaigne, A.; Perez, A.; Palensky, J.; Wittes, J. The effect of spironolactone on morbidity and mortality in patients with severe heart failure. Randomized Aldactone Evaluation Study Investigators. *N. Engl. J. Med.* **1999,** *341*, 709-717. (b) Pitt, B.; Remme, W.; Zannad, F.; Neaton, J.; Martinez, F.; Roniker, B.; Bittman, R.; Hurley, S.; Kleiman, J.; Gatlin, M. Eplerenone, a selective aldosterone blocker, in patients with left ventricular dysfunction after myocardial infarction. *N. Engl. J. Med.* **2003,** *348*, 1309-1321.

42 (a) Zannad, F.; Alla, F.; Dousset, B.; Perez, A.; Pitt, B. Limitation of excessive extracellular matrix turnover may contribute to survival benefit of spironolactone therapy in patients with congestive heart failure: insights from the randomized aldactone evaluation study (RALES). Rales Investigators. *Circulation* **2000**, *102*, 2700–2706. (b) Izawa, H.; Murohara, T.; Nagata, K.; Isobe, S.; Asano, H.; Amano, T.; Ichihara, S.; Kato, T.; Ohshima, S.; Murase, Y.; Iino, S.; Obata, K.; Noda, A.; Okumura, K.; Yokota, M. Mineralocorticoid receptor antagonism ameliorates left ventricular diastolic dysfunction and myocardial fibrosis in mildly symptomatic patients with idiopathic dilated cardiomyopathy: a pilot study. *Circulation* **2005**, *112*, 2940–2945.

43 Young, M.; Funder, J. W. Eplerenone, but not steroid withdrawal, reverses cardiac fibrosis in deoxycorticosterone/salt-treated rats. *Endocrinology* **2004**, *145*, 3153–3157.

44 (a) Rocha, R.; Stier, C. T., Jr.; Kifor, I.; Ochoa-Maya, M. R.; Rennke, H. G.; Williams, G. H.; Adler, G. K. Aldosterone: a mediator of myocardial necrosis and renal arteriopathy. *Endocrinology* **2000,** *141*, 3871-3878. (b) Rudolph, A. E.; Rocha, R.; McMahon, E. G. Aldosterone target organ protection by eplerenone. *Mol. Cell. Endocrinol.* **2004,** *217*, 229-238.

45 Stier, C. T., Jr.; Koenig, S.; Lee, D. Y.; Chawla, M.; Frishman, W. H. Aldosterone and aldosterone antagonism in cardiovascular disease: focus on eplerenone (Inspra). *Heart Dis.* **2003,** *5*, 102-118.

46 Juurlink, D. N.; Mamdani, M. M.; Lee, D. S.; Kopp, A.; Austin, P. C.; Laupacis, A.; Redelmeier, D. A., Rates of hyperkalemia after publication of the Randomized Aldactone Evaluation Study. *N. Engl. J. Med.* **2004,** *351*, 543-551.

47 Rousseau, M. F.; Gurne, O.; Duprez, D.; Van Mieghem, W.; Robert, A.; Ahn, S.; Galanti, L.; Ketelslegers, J. M. Beneficial neurohormonal profile of spironolactone in severe congestive heart failure: results from the RALES neurohormonal substudy. *J. Am. Coll. Cardiol.* **2002,** *40*, 1596-1601.

48 (a) Delcayre, C.; Swynghedauw, B. Molecular mechanisms of myocardial remodeling. The role of aldosterone. *J. Mol. Cell. Cardiol.* **2002**, *34*, 1577–1584. (b) de Resende, M. M.; Kauser, K.; Mill, J. G. Regulation of cardiac and renal mineralocorticoid receptor expression by captopril following myocardial infarction in rats. *Life Sci.* **2006**, *78*, 3066–3073.

49 Hartmann, R. W. Selective inhibition of steroidogenic P450 enzymes: Current status and future perspectives. *Eur. J. Pharm. Sci.* **1994**, *2*, 15–16.

50 Ehmer, P. B.; Bureik, M.; Bernhardt, R.; Müller, U.; Hartmann, R. W. Development of a test system for inhibitors of human aldosterone synthase (CYP11B2): Screening in fission yeast and evaluation of selectivity in V79 cells. *J. Steroid Biochem. Mol. Biol.* **2002**, *81*, 173–179.

51 Hartmann, R. W.; Müller, U.; Ehmer, P. B. Discovery of selective CYP11B2 (aldosterone synthase) inhibitors for the therapy of congestive heart failure and myocardial fibrosis. *Eur. J. Med. Chem.* **2003**, *38*, 363–366.

52 Schieweck, K.; Bhatnagar, A. S.; Matter, A. CGS 16949A, a new nonsteroidal aromatase inhibitor: effects on hormone-dependent and –independent tumors in vivo. *Cancer Res.* **1988**, *48*, 834–838.

53 Lamberts, S. W.; Bruining, H. A.; Marzouk, H.; Zuiderwijk, J.; Uitterlinden, P.; Blijd, J. J.; Hackeng, W. H.; de Jong, F. H. The new aromatase inhibitor CGS-16949A suppresses aldosterone and cortisol production by human adrenal cells in vitro. *J. Clin. Endocrinol. Metab.* **1989**, *69*, 896–901.

54 Demers, L. M.; Melby, J. C.; Wilson, T. E.; Lipton, A.; Harvey, H. A.; Santen, R. J. The effects of CGS 16949A, an aromatase inhibitor on adrenal mineralocorticoid biosynthesis. *J. Clin. Endocrinol. Metab.* **1990**, *70*, 1162–1166.

55 Menard, J.; Gonzalez, M. F.; Guyene, T. T.; Bissery, A. Investigation of aldosterone-synthase inhibition in rats. *J. Hypertens.* **2006,** *24*, 1147-1155.

56 Minnaard-Huiban, M; Emmen, J. M. A.; Roumen, L.; Beugels, I. P. E.; Cohuet, G. M. S.; van Essen, H.; Ruijters, E.; Pieterse, K.; Hilbers, P. A. J.; Ottenheijm, H. C. J.; Plate, R.; de Gooyer, M. E.; Smits, J. F. M.; Hermans, J. J. R. Fadrozole reverses cardiac fibrosis in spontaneously hypertensive heart failure rats: Discordant enantioselectivity versus reduction of plasma aldosterone. *Endocrinology* **2008**, *149*, 28–31.

57 Mulder, P.; Mellin, V.; Favre, J.; Vercauteren, M.; Remy-Jouet, I.; Monteil, C.; Richard, V.; Renet, S.; Henry, J. P.; Jeng, A. Y.; Webb, R. L.; Thuillez, C. Aldosterone synthase inhibition improves cardiovascular function and structure in rats with heart failure: a comparison with spironolactone. *Eur. Heart J.* **2008,** *29*, 2171-2179.

58 Lea, W. B.; Kwak, E. S.; Luther, J. M.; Fowler, S. M.; Wang, Z.; Ma, J.; Fogo, A. B.; Brown, N. J. Aldosterone antagonism or synthase inhibition reduces end-organ damage induced by treatment with angiotensin and high salt. *Kidney Int.* **2009,** *75*, 936-944.

59 Funder, J. W. Aldosterone synthase and mineralocorticoid receptors as targets in cardiovascular disease. *Drug Discov. Today Ther. Strat.* **2005**, *2*, 231–235.

60 Chu, J. W., Matthias, D. F.; Joseph Belanoff, J.; Schatzberg, A.; Hoffman, A. R.; Feldman, D. Successful long-term treatment of refractory Cushing's disease with high-dose mifepristone (RU 486). *J. Clin. Endcrinol. Metab*. **2001**, *86*, 3568–3573.

61 Kolovou, G. D.; Anagnostopoulou, K. K.; Salpea, K. D.; Mikhailidis, D. P. The prevalence of metabolic syndrome in various populations. *Am. J. Med. Sci*. **2007**, *333*, 362-371.

62 Athyros, V. G.; Ganotakis, E. S.; Elisaf, M.; Mikhailidis D. P. The prevalence of the metabolic syndrome using the National Cholesterol Educational Program and International Diabetes Federation definitions. *Curr. Med. Res. Opin*. **2005**, *21*, 1157-1159.

63 Athyros, V. G.; Ganotakis, E. S.; Elisaf, M. S.; Liberopoulos, E. N.; Goudevenos, I. A.; Karagiannis, A; GREECE-METS Collaborative Group. Prevalence of vascular disease in metabolic syndrome using three proposed definitions. *Int. J. Cardiol.* **2007**, *117*, 204-210.

64 Pasquali, R.; Vicennati, V.; Cacciari, M.; Pagotto, U. The hypothalamic-pituitary-adrenal axis activity in obesity and the metabolic syndrome. *Ann. N.Y. Acad. Sci.* **2006**, *1083*, 111-128.

65 Walker, B. R. Cortisol-cause and cure for metabolic syndrome? *Diabet. Med.* **2006**, *23*, 1281-1288.

66 (a) Duclos, M.; Marquez Pereira, P.; Barat, P.; Gatta, B.; Roger, P. Increased cortisol bioavailability, abdominal obesity, and the metabolic syndrome in obese women. *Obes. Res.* **2005**, *13*, 1157-1166. (b) Misra, M.; Bredella, M. A.; Tsai, P.; Mendes, N.; Miller, K. K.; Klibanski, A. Lower growth hormone and higher cortisol are associated with greater visceral adiposity, intramyocellular lipids, and insulin resistance in overweight girls. *Am. J. Physiol. Endocrinol. Metab.* **2008**, *295*, E385-392. (c) Phillips, D. I.; Barker, D. J.; Fall, C. H.; Seckl, J. R.; Whorwood, C. B.; Wood, P. J.; Walker, B. R. Elevated plasma cortisol concentrations: a link between low birth weight and the insulin resistance syndrome? *J. Clin. Endocrinol. Metab.* **1998**, *83*, 757-760. (d) Sen, Y.; Aygun, D.; Yilmaz, E.; Ayar, A. Children and adolescents with obesity and the metabolic syndrome have high circulating cortisol levels. *Neuro. Endocrinol. Lett.* **2008**, *29*, 141-145. (e) Weigensberg, M. J.; Toledo-Corral, C. M.; Goran, M. I. Association between the metabolic syndrome and serum cortisol in overweight Latino youth. *J. Clin. Endocrinol. Metab.* **2008**, *93*, 1372-1378.

67 (a) Rask, E.; Olsson, T.; Soderberg, S.; Andrew, R.; Livingstone, D. E.; Johnson, O.; Walker, B. R. Tissue-specific dysregulation of cortisol metabolism in human obesity. *J. Clin. Endocrinol. Metab.* **2001**, *86*, 1418-1421. (b) Rask, E.; Walker, B. R.; Soderberg, S.; Livingstone, D. E.; Eliasson, M.; Johnson, O.; Andrew, R.; Olsson, T. Tissue-specific changes in peripheral cortisol metabolism in obese women: increased adipose 11beta-hydroxysteroid dehydrogenase type 1 activity. *J. Clin. Endocrinol. Metab.* **2002**, *87*, 3330-3336. (c) Terzolo, M.; Bovio, S.; Pia, A.; Osella, G.; Borretta, G.; Angeli, A.; Reimondo, G. Subclinical Cushing's syndrome. *Arq. Bras. Endocrinol. Metabol.* **2007**, *51*, 1272-1279.

68 (a) Su, X.; Vicker, N.; Trusselle, M.; Halem, H.; Culler, M. D.; Potter, B. V. L. Discovery of novel inhibitors of human 11beta-hydroxysteroid dehydrogenase type 1. *Mol. Cell. Endocrin.* **2009**, *301*, 169-173; (b) Julian, L. D.; Wang, Z.; Bostick, T.; Caille, S.; Choi, R.; DeGraffenreid, M.; Di, Y.; He, X.; Hungate, R. W.; Jaen, J. C.; Liu, J.; Monshouwer, M.; McMinn, D.; Rew, Y.; Sudom, A.; Sun, D.; Tu, H.; Ursu, S.; Walker, N.; Yan, X.; Ye, Q.; Powers, J. P. Discovery of novel, potent benzamide inhibitors of 11beta-hydroxysteroid dehydrogenase type 1 (11beta-HSD1) exhibiting oral activity in an enzyme inhibition ex vivo mode. *J. Med. Chem*. **2008**, *51*, 3953-3960; (c) Xiang, J.; Wan, Z.-K.; Li, H.-Q.; Ipek, M.; Binnun, E.; Nunez, J.; Chen, L.; McKew, J. C.; Mansour, T. S.; Xu, X.; Suri, V.; Tam, M.; Xing, Y.; Li, X.; Hahm, S.; Tobin, J.; Saiah, E. Piperazine Sulfonamides as Potent, Selective, and Orally Available 11β-Hydroxysteroid Dehydrogenase Type 1 Inhibitors with Efficacy in the Rat Cortisone-Induced Hyperinsulinemia Model. *J. Med. Chem.* **2008**, *51*, 4068-4071.

69 (a) Nieman, K. L. Medical therapy of Cushing's disease. *Pituitary* **2002**, *5*, 77–82. (b) Schteingart, D. E., Drugs in the medical treatment of Cushing's syndrome. *Expert Opin Emerg Drugs* **2009**, *14*, 661-671.

70 Zolle, I. M.; Berger, M. L.; Hammerschmidt, F.; Hahner, S.; Schirbel, A.; Peric-Simov, B. New selective inhibitors of steroid 11β-hydroxylation in the adrenal cortex. Synthesis and structure-activity relationship of potent etomidate analogues. *J. Med. Chem*. **2008**, *51*, 2244–2253.

71 Hartmann, R. W.; Bayer, H.; Grun, G.; Sergejew, T.; Bartz, U.; Mitrenga, M. Pyridyl-substituted tetrahydrocyclopropa[a]naphthalenes: highly active and selective inhibitors of P450 arom. *J. Med. Chem.* **1995,** *38*, 2103-2111.

72 Wachter, G. A.; Hartmann, R. W.; Sergejew, T.; Grun, G. L.; Ledergerber, D. Tetrahydronaphthalenes: influence of heterocyclic substituents on inhibition of steroid enzymes P450 arom and P450 17. *J. Med. Chem.* **1996,** *39*, 834-841.

73 (a) Ulmschneider, S.; Muller-Vieira, U.; Klein, C. D.; Antes, I.; Lengauer, T.; Hartmann, R. W. Synthesis and evaluation of (pyridylmethylene)tetrahydronaphthalenes/-indanes and structurally modified derivatives: potent and selective inhibitors of aldosterone synthase. *J. Med. Chem.* **2005,** *48*, 1563-1575. (b) Ulmschneider, S.; Muller-Vieira, U.; Mitrenga, M.; Hartmann, R. W.; Oberwinkler-Marchais, S.; Klein, C. D.; Bureik, M.; Bernhardt, R.; Antes, I.; Lengauer, T. Synthesis and evaluation of imidazolylmethylenetetrahydronaphthalenes and imidazolylmethyleneindanes: potent inhibitors of aldosterone synthase. *J. Med. Chem.* **2005,** *48*, 1796-1805. (c) Voets, M.; Antes, I.; Scherer, C.; Muller-Vieira, U.; Biemel, K.; Barassin, C.; Marchais-Oberwinkler, S.; Hartmann, R. W. Heteroaryl-substituted naphthalenes and structurally modified derivatives: selective inhibitors of CYP11B2 for the treatment of congestive heart failure and myocardial fibrosis. *J. Med. Chem.* **2005,** *48*, 6632-6642. (d) Voets, M.; Antes, I.; Scherer, C.; Muller-Vieira, U.; Biemel, K.; Marchais-Oberwinkler, S.; Hartmann, R. W. Synthesis and evaluation of heteroaryl-substituted dihydronaphthalenes and indenes: potent and selective inhibitors of aldosterone synthase (CYP11B2) for the treatment of congestive heart failure and myocardial fibrosis. *J. Med. Chem.* **2006,** *49*, 2222-2231.

74 Häusler, A.; Monnet, G.; Borer, C.; Bhatnagar, A. S. Evidence that corticosterone is not an obligatory intermediate in aldosterone biosynthesis in the rat adrenal. *J. Steroid Biochem.* **1989**, *34*, 567–570.

75 Butler, M. A.; Iwasaki, M.; Guengerich, F. P.; Kadlubar, F. F., Human cytochrome P-450PA (P-450IA2), the phenacetin O-deethylase, is primarily responsible for the hepatic 3-demethylation of caffeine and N-oxidation of carcinogenic arylamines. *Proc. Natl. Acad. Sci. U S A* **1989,** *86*, 7696-7700.

76 Sesardic, D.; Boobis, A. R.; Murray, B. P.; Murray, S.; Segura, J.; de la Torre, R.; Davies, D. S. Furafylline is a potent and selective inhibitor of cytochrome P450IA2 in man. *Br. J. Clin. Pharmacol.* **1990**, *29*, 651–663.

77 (a) Chohan, K. K.; Paine, S. W.; Mistry, J.; Barton, P.; Davis, A. M. A rapid computational filter for cytochrome P450 1A2 inhibition potential of compound libraries. *J. Med. Chem.* **2005**, *48*, 5154–5161. (b) Korhonen, L. E.; Rahnasto, M.; Mähönen, N. J.; Wittekindt, C.; Poso, A.; Juvonen, R. O.; Raunio, H. Predictive three-dimensional quantitative structure-activity relationship of cytochrome P450 1A2 inhibitors. *J. Med. Chem.* **2005**, *48*, 3808–3815.

78 (a) Cavalli, A.; Bisi, A.; Bertucci, C.; Rosini, C.; Paluszcak, A.; Gobbi, S.; Giorgio, E.; Rampa, A.; Belluti, F.; Piazzi, L.; Valenti, P.; Hartmann, R. W.; Recanatini M. Enantioselective nonsteroidal aromatase inhibitors identified through a multidisciplinary medicinal chemistry approach. *J. Med. Chem.* **2005**, *48*, 7282–7289. (b) Gobbi, S.; Cavalli, A.; Rampa, A.; Belluti, F.; Piazzi, L.; Paluszcak, A.; Hartmann, R. W.; Recanatini, M.; Bisi, A. Lead optimization providing a series of flavone derivatives as potent nonsteroidal inhibitors of the cytochrome P450 aromatase enzyme. *J. Med. Chem.* **2006**, *49*, 4777–4780.

79 (a) Richmond, N. J.; Abrams, C. A.; Wolohan, P. R.; Abrahamian, E.; Willett, P.; Clark, R. D. GALAHAD: 1. Pharmacophore identification by hypermolecular alignment of ligands in 3D. *J. Comput.-Aided Mol. Des.* **2006**, *20*, 567–587. (b) Shepphird, J. K.; Clark, R. D. A marriage made in torsional space: Using GALAHAD models to drive pharmacophore multiplet searches. *J. Comput.-Aided Mol. Des.* **2006**, *20*, 763–771.

80 Roumen, L.; Peeters, J. W.; Emmen, J. M. A.; Beugels, I. P. E.; Custers, E. M. G.; de Gooyer, M.; Plate, R.; Pieterse, K.; Hilbers, P. A. J.; Smits, J. F. M.; Vekemans, J. A. J.; Leysen, D.; Ottenheijm, H. C. J.; Janssen, H. M.; Hermans, J. J. R. Synthesis, biological evaluation, and molecular modeling of 1-benzyl-1*H*-imidazoles as selective inhibitors of aldosterone synthase (CYP11B2). *J. Med. Chem*. **2010**, *53*, 1712–1725.

6 Danksagung

An dieser Stelle möchte ich den Personen, die durch ihre hilfreiche Unterstützung maßgeblich zum Gelingen dieser Dissertation beigetragen haben, meinen herzlichsten Dank aussprechen:

Herrn Prof. Dr. Rolf W. Hartmann für die Vergabe des sehr interessanten Themas, für die wissenschaftlichen Diskussionen, die mich stets voran gebracht haben, für die gute Betreuung, für das entgegen gebrachte Vertrauen und vor allem für die Möglichkeit so viele neue Dinge zu lernen.

Herrn Prof. Dr. Hans H. Maurer für die Übernahme des Koreferates.

Herrn Prof. Dr. Manfred J. Schmitt für die Übernahme des Vorsitzes der Prüfungskommision.

Herrn Dr. Michael Heydel für die Übernahme des Beisitzes der Prüfungskommision.

Dr. Ursula Müller-Vieira und Martina Jankowski für die theoretische und praktische Einführung in die Welt der Aldosteronsynthase. Durch eure nette Betreuung habt ihr mir den Einstieg wirklich sehr erleichtert.

Dr. Martina Streiber und Dr. Patricia Kruchten für die wissenschaftliche Beratung als ich noch unwissend war und für die konstruktiven Diskussionen, wenn nichts mehr weiter ging.

den Mitarbeitern von Pharmacelsus CRO, besonders Dr. Barbara Birk für die gute Zusammenarbeit und Koordination der *in vivo*-Versuche sowie für die Hilfe bei der Interpretation der *in vivo*-Daten und Lionel Hurst für die ausgezeichnete Präparation der benötigten Organe.

Sabrina Rau und Dr. Sigrid Ziegler für die gute Zusammenarbeit bei der Betreuung des Biochemie-Praktikums und der Erstellung scheinbar unlösbarer Klausuraufgaben.

Marieke Hafner für die nette Zusammenarbeit, die schönen Ergebnisse, die im Rahmen ihrer Diplomarbeit erzielt werden konnten und für die Versorgung mit Kaffee und Schokolade während der Praktikumsbetreuung.

Florian Stenger und Nathalie Wagner für die nette Zusammenarbeit während ihres Forschungspraktikums.

Dr. Stefan Boettcher für die Einführung in die Welt der Analytik.

den ehemaligen und derzeitigen Mitstreitern im Aldosteronsynthase-Projekt Sabrina Rau, Cornelia Grombein, Lina Yin, Qingzhong Hu, Matthias Negri, Dr. Simon Lucas, Dr. Michael Heydel und Dr. Ralf Heim für die tolle und überaus erfolgreiche Zusammenarbeit im Kampf gegen Herzinsuffizienz und Myokardfibrose.

Ulrike Hille und Dr. Carsten Vock für die Zusammenarbeit im CYP11B1-Projekt.

Lothar Jager für die prompte Hilfe bei allen technischen Problemen, für das Reparieren von totgeglaubtem Equipment und die schnelle Beschaffung von allen benötigten Materialien.

Martina Schwarz und Corina Pryzbyla für die gute Zusammenarbeit, die offenen Ohren für alle Anliegen und das bereitwillige „dazwischen schieben“ in den stets prall gefüllten Terminkalender von Prof. Dr. Hartmann.

Sabrina Rau, Claudia Henn, Ruth Werth, Alexander Oster, Tobias Klein, Martina Jankowski, Dr. Stefan Boettcher, Dr. Patricia Kruchten und Dr. Martina Streiber für die netten Mittagspausen, die regen Diskussionen, eure Mithilfe im Kampf gegen das Chaos im Labor und für eure Freundschaft.

allen gegenwärtigen und ehemaligen Mitarbeitern des Arbeitskreises für ihre Kollegialität, ihre Unterstützung bei technischen und experimentellen Schwierigkeiten und die nette Arbeitsatmosphäre.

Prof. Dr. J. J. Rob Hermans (Universität Maastricht, Niederlande) für die Zuverfügungstellung der V79*h*CYP11B1-Zelllinie und Prof. Dr. Rita Bernhardt (Universität des Saarlandes) für die Zuverfügungstellung der V79*h*CYP11B2-Zelllinie.

den Arbeitsgruppen von Prof. Dr. Silvia Gobbi, Prof. Dr. Ranju Bansal, Prof. Dr. Mange Ram Yadav, Prof. Dr. Angelo Carotti und Prof. Dr. Bruno Allolio für die gute Zusammenarbeit in zahlreichen Kooperationsprojekten, die zu tollen gemeinsamen Publikationen geführt haben.

meinen Freunden, die während der ganzen Zeit immer mit mir gelitten und die sich mit mir gefreut haben. Danke für die notwendigen Ablenkungen und Aufheiterungen.

mein besonderer Dank gilt meinen Eltern Gerlinde und Harry, meinem Papa Gertram und dem Rest meiner großen Familie für die Unterstützung während meiner Promotion, für das Bedauern nach langen Laborschichten, das stete Antreiben weiterzumachen, wenn es schwierig wurde und dafür, dass ihr immer an mich geglaubt habt.

meinem Mann Pascal danke ich für seine liebevolle Unterstützung und das geduldige Aushalten meiner Launen. Danke, dass Du stets die Nerven behalten hast, wenn ich sie verloren habe. Danke, für Dein großes Interesse an meiner Arbeit und dass Du mich in schwierigen Phasen zum Durchhalten motiviert hast…und Danke für alles was man mit Worten nicht ausdrücken kann.